



Three applications of a geometric approach to conformal field theory

Clement Tauber

► To cite this version:

Clement Tauber. Three applications of a geometric approach to conformal field theory. Mathematical Physics [math-ph]. Ecole normale supérieure de lyon - ENS LYON, 2015. English. NNT : 2015ENSL1047 . tel-01247290

HAL Id: tel-01247290

<https://theses.hal.science/tel-01247290>

Submitted on 4 Jan 2016

HAL is a multi-disciplinary open access archive for the deposit and dissemination of scientific research documents, whether they are published or not. The documents may come from teaching and research institutions in France or abroad, or from public or private research centers.

L'archive ouverte pluridisciplinaire **HAL**, est destinée au dépôt et à la diffusion de documents scientifiques de niveau recherche, publiés ou non, émanant des établissements d'enseignement et de recherche français ou étrangers, des laboratoires publics ou privés.

THÈSE

en vue de l'obtention du grade de

**Docteur de l'Université de Lyon, délivré par
l'École Normale Supérieure de Lyon**

Discipline : Physique

Laboratoire de Physique de l'École Normale Supérieure de Lyon
École doctorale de Physique et d'Astrophysique de Lyon

Trois applications d'une approche géométrique à la théorie conforme des champs

-

THREE APPLICATIONS OF A GEOMETRIC APPROACH TO
CONFORMAL FIELD THEORY

Présentée et soutenue publiquement le mardi 1er décembre 2015 par
M. Clément Tauber

Directeur de thèse :
M. Krzysztof Gawędzki

Après l'avis de
M. Andrea Cappelletti
M. Benjamin Doyon

devant la commission d'examen composée de

M. Denis Bernard,	CNRS et ENS Ulm,	Examineur,
M. Andrea Cappelletti	INFN, Florence,	Rapporteur,
M. Pascal Degiovanni,	CNRS et ENS de Lyon,	Examineur,
M. Benjamin Doyon,	King's College, Londres,	Rapporteur,
M. Krzysztof Gawędzki	CNRS et ENS de Lyon,	Directeur de thèse,
M. Jean Michel Maillet	CNRS et ENS de Lyon,	Co-encadrant.

Remerciements

Parmi les nombreuses personnes qui m'ont accompagné durant cette thèse, la principale est bien sûr mon directeur Krzysztof Gawędzki, que je remercie sincèrement pour ces trois belles années passées ensemble. Sa disponibilité, sa patience, l'incroyable étendue de ses connaissances et sa gentillesse m'ont fait passer d'un simple étudiant à un jeune chercheur. Pour tout ce qu'il m'a appris, sur la théorie conforme mais aussi sur la façon de faire de la recherche, je lui en suis infiniment reconnaissant.

Merci ensuite aux membres du jury qui ont permis de conclure ce travail de thèse : merci à Benjamin Doyon et Andrea Cappelli d'en avoir été rapporteurs, merci à Denis Bernard pour les discussions que l'on a pu avoir à diverses occasions, merci à Jean Michel Maillet pour ses nombreux conseils et enfin merci à Pascal Degiovanni pour ses nombreuses questions, pour les discussions variées durant ces trois années, et aussi pour ses excellentes adresses de restaurants.

Mon travail de thèse a aussi été le résultat d'une collaboration étroite avec Pierre Delplace et Michel Fruchart, que je remercie pour les discussions fructueuses et pour nos différents projets en commun, toujours en cours et qui, je l'espère, continueront. Merci aussi à Gianluca Panati pour son chaleureux accueil lors de ma visite à Rome.

Le bureau a aussi joué un rôle important dans ma vie quotidienne, de part les gens qui s'y sont succédés. Louis-Paul, Thomas, et Étienne quand je suis arrivé et avec qui j'ai passé le plus de temps, mais aussi Irénée, Arnaud et Clément qui sont arrivés ensuite. Je les remercie tous pour la bonne ambiance constante (malgré la clim toujours en panne) et je leur souhaite une bonne continuation dans leurs projets. Le bureau a aussi été un lieu de passage régulier pour certains, entre le fond du couloir et la salle de pause : Arnaud, Marc et un des membres du jury un peu bavard ont contribué par leurs intrusions fréquentes à rendre ce bureau encore plus agréable au quotidien.

Merci aux autres doctorants du laboratoire, qui ont aussi contribué à cette bonne ambiance, que ce soit par leur participation au séminaire de théorie des doctorants, ou par les discussions animées au RU et aux nombreuses pauses café. Ces remerciements s'étendent naturellement à tous les membres du laboratoire, en particulier à Thierry pour ses efforts constants pour entretenir cette bonne ambiance de travail, et son attention particulière à chacun de ses membres. Merci aussi à l'exceptionnelle équipe du secrétariat, et à Laurence en particulier qui s'est occupée avec une grande efficacité de toutes mes missions.

L'enseignement a occupé une part non négligeable de mon travail de thèse, que j'ai beaucoup appréciée et où j'ai appris beaucoup de choses. Je remercie donc les différents collègues avec qui j'ai travaillé et discuté dans ce cadre : Thomas, Dimitrios, Sébastien, François, Stefan, Henning, mais aussi Christoph, Alexandre et Sylvain.

En dehors du travail, de nombreuses personnes m'ont accompagné ces trois dernière années et m'ont permis de continuer à m'épanouir. Merci d'abord à tous les Relous, avec qui j'ai passé de

nombreux sudpers¹ moments, que j'espère revoir le plus souvent possible pour continuer à rigoler autant. En vrac, merci à Sara, Carole, Avelyne, Solenn, Clément, Marlène, Simon, Augustin, Théo, Léonie, Camille, Félix, Arthur, Laura, Guillaume, Guilhem, Richard, Lauren, avec une pensée particulière pour Tomás au moment où j'écris ces lignes.

Merci ensuite à ma famille, à Maman, Julien et Géraldine en particulier qui m'ont soutenu, encouragé et toujours bien conseillé dans mes choix pour que j'en arrive jusque là. Merci bien sûr aussi aux nombreux membres des familles Réquillart et Tauber pour tous leurs encouragements. Je remercie aussi Brigitte et Patrice pour avoir été des fervents supporters de ma thèse, et la famille Pouyet dans son ensemble.

Enfin, un grand merci à Fanny qui pendant tout ce temps (et même avant), m'a accompagné, soutenu, supporté, réconforté, fait rire, et a même accepté de se marier ! J'espère que pendant sa propre thèse elle a autant apprécié notre vie commune que je l'ai appréciée pendant la mienne.

Lyon, le 17 décembre 2015.

¹supers

Contents

1	Introduction	1
1.1	Conformal field theories	1
1.2	Overview of the covered topics	5
I	Nonequilibrium transport across junctions of quantum wires	8
2	Introduction	9
2.1	Quantum wires and conformal field theory	9
2.2	Non equilibrium junctions	12
2.3	Overview of the models	16
3	Free massless bosonic junction	18
3.1	Fermions and bosons in one dimension	18
3.2	Bosonic junction of quantum wires	21
3.3	Quantization	23
3.4	Equilibrium state	30
3.5	Thermodynamic limit	35
3.6	Nonequilibrium stationary state	38
3.7	Full counting statistics	42
3.8	Charge and heat transport, the fluctuation relations	51
3.9	Comparison to the Levitov-Lesovik formulae	52
3.10	Conclusion	53
4	Wess-Zumino-Witten junction with a cyclic brane	54
4.1	Wess-Zumino-Witten models	54
4.2	WZW model on a junction	58
4.3	Equilibrium state	62
4.4	Thermodynamic limit	66
4.5	Nonequilibrium stationary state	69
4.6	Full counting statistics	71
4.7	Conclusion	73
4.A	Modular covariance of correlation functions	74
5	Coset junction	77
5.1	WZW action with a coset brane	77
5.2	Equilibrium state	81
5.3	The $SU(2)$ level 1 coset junction	85

<i>CONTENTS</i>	v
5.4 Conclusion	88
5.A Character formulae	89
6 Conclusions and open questions	90
 II Global gauge anomaly in coset models	 92
7 Global gauge anomalies	93
7.1 Coset models as gauged WZW models	93
7.2 The no-anomaly condition	96
8 Classification of anomalous models	100
8.1 Cases with $\mathfrak{h} = \mathfrak{g}$	100
8.2 Regular subalgebras	106
8.3 Nonregular subalgebras	109
8.4 Twisted case	111
8.5 Conclusions	112
 III Topological insulators with time reversal invariance	 113
9 Topological insulators	114
9.1 Chern insulators	114
9.2 Time-reversal invariance	118
9.3 The tenfold way and beyond	121
9.4 Geometric interpretation of the Kane-Mele invariant	122
10 Geometric formulation of the Kane-Mele invariant	123
10.1 Invariants of 3d families of unitary matrices	123
10.2 Towards the Kane-Mele invariant	126
11 Computation of the Wess-Zumino amplitudes	133
11.1 Case with rank 2 valence bundle	133
11.2 The general case	137
12 Conclusions and perspectives	144
12.1 Floquet systems	144
12.2 Conclusions	147
 13 General conclusion	 148

Chapter 1

Introduction

This thesis is devoted to certain aspects of conformal field theory and related structures. As often in physics, various meanings that can be quite different are hiding behind one name, and the preliminary task is to clarify what we will talk about in the following. After having presented the context of conformal field theories, we specify in which frame the following work takes place, before giving an overview of the covered topics.

1.1 Conformal field theories

1.1.1 Conformal invariance

The conformal transformations are space-time transformations that preserve angles, and not necessarily distances. They basically preserve the local shapes, up to some expansion or contraction. The canonical example is the stereographic projection mapping a sphere onto a plane, due to Ptolemée and used by navigators. Such conformal transformations were then used in the 19th century by mathematicians in the context of potential theory [104], that had various applications in fluid mechanics. For example the Joukowski's transformation allows to compute the airfoil of a plane wing from the one around a cylinder using a conformal transformation [124].

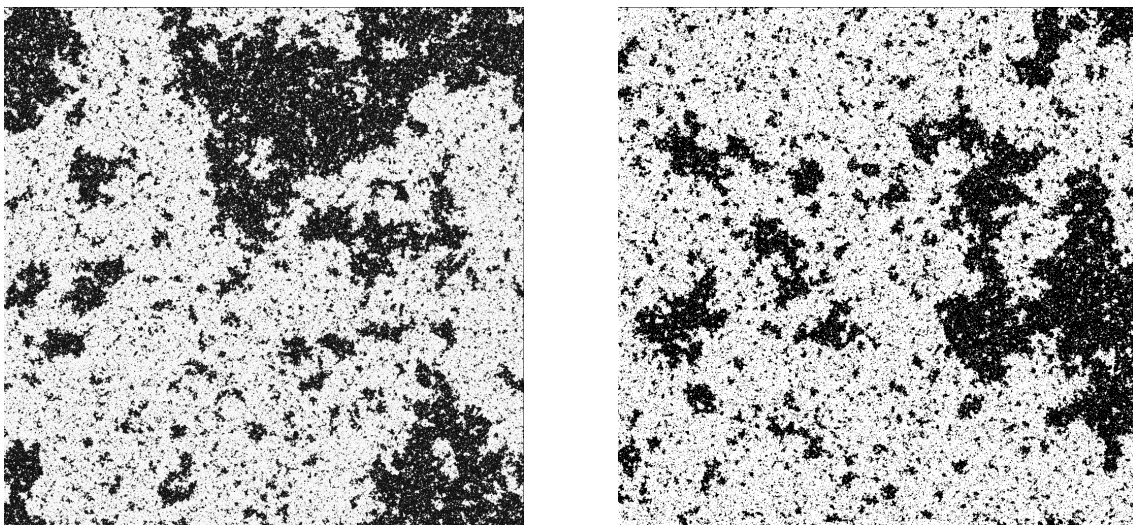


Figure 1.1: *Numerical simulations of Ising model at critical temperature. Regions of spin up (white) and spin down (black) appear at all sizes, with smaller droplets of opposite spin inside. From left to right size of the simulation goes from $L = 2^{11}$ to 2^{17} . The autosimilarity of the patterns illustrates conformal invariance.*

In physics, local dilatation invariance was already introduced by Weyl in [168]. The full conformal invariance appeared more recently as realized in systems that do not have any characteristic length of space and time. Although restrictive, systems with such features actually exist and the canonical example is the celebrated two-dimensional Ising model at critical temperature [98, 134]. At such point, the balance between thermal fluctuations and ferromagnetic interactions between the $1/2$ -spins leads to typical configurations where droplets of all sizes appear, as illustrated on Figure 1.1. The correlation length, ruling the exponential decay of correlation functions outside the critical temperature, becomes infinite here. In other words, correlation functions are algebraic. For example, in $d > 1$ dimensions,

$$\langle \sigma_i \sigma_j \rangle \propto |i - j|^{-d+2-\eta} \quad (1.1)$$

where σ_i is the magnetization at site i . The exponent η , equal to $\frac{1}{4}$ in two dimensions, is just one of many examples and the full system is described by critical exponents for the power laws of different quantities. These exponents are moreover universal: several models with a different microscopic description lead to the same numbers. At critical points of a wide variety of models, only a discrete set of critical exponents exists, corresponding to different realization of scale invariance.

The relation with conformal invariance and critical phenomena was already noticed by Polyakov in [140], but conformal field theory of critical phenomena starts essentially with the work of Belavin, Polyakov and Zamolodchikov [13] where the authors show how conformal invariance allows to construct exactly solvable models, called minimal, that were identified with various two-dimensional statistical systems at their critical points. In the sequel, it was noticed in [69] that the unitarity of the minimal models restricts further the possibility to an even smaller discrete set of universality classes.

Besides, conformal field theory appeared at the same period in string theory [91]. String theory proposes to unify all the fundamental interactions in a quantum field theory by considering particles as one dimensional extended objects (strings) instead of point particles. Here the conformal transformations appear naturally as special reparametrizations of the two-dimensional worldsheet describing the string parameters, with the meaning that the coordinate system on the worldsheet has little physical relevance. Such conformal invariance is manifest in Polyakov's formulation [142, 143] of string theory.

The dimension two is actually very specific. For $d > 2$, the group of conformal transformations has finite dimension and is composed of translations, rotations, global dilatations, and special conformal transformations (composition of translations and inversion). However when $d = 2$ this group contains more and actually becomes infinite. For example in the Euclidean formalism, writing for $(x, y) \in \mathbb{R}^2$

$$z = x + iy, \quad \bar{z} = x - iy \quad (1.2)$$

then any analytic (i.e. holomorphic) function of z leaves the metric unchanged up to a local rescaling, and similarly for any antiholomorphic function. Hence the conformal invariance for $d = 2$ systems is very restrictive since it requires invariance under an infinite number of transformations. As a result, such systems have an infinite number of conserved quantities and may be exactly solvable. At the infinitesimal level, the conformal transformations are encoded in the Virasoro algebra

$$[L_n, L_m] = (n - m)L_{n+m} + \frac{c}{12}(n^3 - n)\delta_{n,-m} \quad (1.3)$$

for the infinite family of generators L_n , $n \in \mathbb{Z}$ corresponding to holomorphic functions, and a similar family \bar{L}_n encodes the antiholomorphic transformations. The number c , whose appearance is due to the projective realization of quantum symmetries, is called the central charge of the theory and is a parameter. It has several physical meanings [43], and it takes different values for different models.

A class of irreducible representations of the Virasoro algebra, called of highest weight, initially studied by Kac [99, 100] and also by Feigin and Fuchs [58], may be constructed in a purely algebraical way defining an infinite series of states from one highest weight state $|\Delta\rangle$, which is an L_0 eigenstate with eigenvalue Δ , see e.g. [73]. The highest weight Δ and the central charge c are then constrained in order to get representations with special properties. From such building blocks, one constructs the space of states of a physical model of conformal field theory described by a collection (eventually infinite) of couples $(\Delta, \bar{\Delta})$ of such representations for fixed c , carrying the action of the holomorphic and antiholomorphic transformations.

Moreover this state description has a field counterpart: each couple of weights corresponds to a field, called primary, that scales with powers $(\Delta, \bar{\Delta})$ under conformal transformations. In particular these weights are related to the critical exponents mentioned before. The fundamental structure of a given conformal field theory is given by the so-called operator product expansion (OPE), introduced by Wilson [171], that encodes the local product of fields as a linear combination of a well-defined family of fields. Schematically

$$\phi_i(x)\phi_j(y) = \sum_k C_{ij}^k(x-y)\phi_k(x) \quad (1.4)$$

for functions C_{ij}^k when x is close to y . This defines an algebra, that, once known, allows to compute any correlation function of the system. One way to construct a conformal field theory is to solve this algebra by requiring a number of rules and symmetries [141]. The minimal models of $d = 2$ theory correspond to the case where the family of primary fields is finite and induces the other (descendent) fields by commutators with the Virasoro generators.

A detailed study of all this structure, in particular for $0 < c \leq 1$, which has been described exhaustively in the book [50], constitutes the basis of $d = 2$ conformal field theory.

1.1.2 Developments of conformal field theory

The initial work [13] induced a wide and fast expansion of conformal field theories. Models with conformal invariance and supplementary infinite-dimensional symmetries have been also developed using the framework of affine Kac-Moody algebras [100, 128] and were also described in a Lagrangian approach as the so-called Wess-Zumino-Witten (WZW) models [173, 110], the conformally invariant $d = 2$ sigma models with group-valued fields. The coset construction proposed by Goddard, Kent and Olive in [89, 88] introduced a method to generate various representation of Virasoro algebra (including unitary minimal models, and, in a different version, the non-unitary ones), and giving on the way their supersymmetric extensions. It was interpreted in the Lagrangian approach in terms of partially gauged WZW models [80].

An important role in $d = 2$ conformal field theory is played by the so called modular invariance (expressing the freedom of choice of spatial and temporal coordinate in the Euclidean formulation of the theory [39]) which led to the so called ADE classification of the minimal models (and of the simplest WZW models with the $SU(2)$ group) [35, 36]. Modular invariance plays also important role in string theory [91]. From a purely algebraic point of view, conformal field theories were reformulated in the language of vertex operator algebras [68, 101, 67], focusing on the state-field correspondence and on the operator product expansion.

Conformal field theory for systems with boundaries was initiated and studied in details by Cardy [40, 37] and, in the context of string theory by [138]. With appropriate boundary conditions, one half the conformal invariance persists, keeping the exactly solvable nature of the models. This was deeply related to the modular invariance in [41]. For the WZW models such boundary conditions were first discussed in [2].

Another extension of conformal field theory called logarithmic appeared more recently [137, 75]. In such theories, the logarithmic scaling accompanies power laws. This topic is still an active subject of research.

From the Lagrangian point of view, a geometric approach to WZW and coset conformal models was further developed in [79, 78], using the underlying theory of geometric quantization. Such point of view led to the application of the geometry of bundle gerbes [131], allowing a deeper understanding of Feynman amplitudes for conformal WZW models with and without boundaries [82]. The geometric approach was also used in [60, 76] to understand the connection between 3-dimensional topological field theories and 2-dimensional conformal field theories living on the boundaries, employed first in the celebrated article [175].

Finally, let us mention the connection of conformal field theory with the stochastic process called SLE (Stochastic Loewner Evolution) developed by in the context of pure mathematics by Lawler, Schramm and Werner but that can be understood in a theoretical physics language [12, 42]. Basically, these are growths process that describe interfaces in two-dimensional conformal field theories.

1.1.3 Applications

Apart from the study of conformal field theory in itself, lots of applications in physics were developed simultaneously, and the incessant dialog between the different formalisms was actually very fruitful both for physics and mathematics [177, 38].

Conformal field theory has been successfully applied in different domains of physics and in different dimensions. For two dimensions of space, it described successfully the scaling limit of statistical models at their critical points, but it turned out that special perturbations of conformal field theory around criticality preserve the integrable nature of the models allowing e.g. to compute the critical exponents associated to the transition [176].

A connection with two-dimensional turbulence was developed in [21] where it was noticed that the statistics of the vorticity clusters presents similarities with the critical phenomenon of percolation, that is described by a $c = 0$ conformal field theory.

With one dimension of space and one dimension of time, conformal field theory (and mostly its supersymmetric version) is at the basis of perturbative formulation of superstring theory, that tries to unify all the interactions including gravitation [139]. The approach of conformal field theory with boundaries has application to the study of branes in this context, that are nonperturbative excitation of string theory.

On a different energy scale, it can also describe one-dimensional quantum systems related to problems of condensed matter. This dimension of space can be genuine as in nanomaterials, or effective through confinement or symmetries, reducing the problem to one space-coordinate. The other dimension can be either the real time to compute the dynamics, or the imaginary time describing the temperature, when the dynamics is stationary. These various possibilities have numerous application in solid state physics [87], among them the boson/fermions correspondence in one dimension, the problem of isolated magnetic impurities (Kondo effect [1]), and more recently the description of bulk and edge states of the quantum Hall effect(s) [166, 129, 34], which is still a booming topic [93, 160].

Finally note that conformal field theory is not restricted to two dimensions, although this is the most fruitful case. Beyond $d = 2$ one famous example is the super Yang-Mills theory at $d = 4$, that, in its highly supersymmetrized version, should be in correspondence with a superstring theory over the Anti-De-Sitter space $\text{AdS}_5 \times S^5$. This is the Maldacena conjecture about the AdS/CFT correspondence that is still under intense research [123]. We also mention here briefly the recent impressive developments of conformal field theory techniques in dimension 3 and beyond. Although the conformal group is finite here, the algebraic approach of conformal field theory and in particular the use of the bootstrap symmetry of the OPE algebra was adapted in order to obtain critical exponents after an amount of computations [156].

1.2 Overview of the covered topics

As we have eluded to, there exist several formalisms for conformal field theory, each one with its advantages and inconveniences, and more or less adapted to a specific problem. Hopefully they are related to each other, so that one can jump from one to another when needed.

1.2.1 Our approach to conformal field theory

In the following, we employ the Lagrangian approach to conformal field theory with heavy geometric flavor. At the classical level, such an approach starts with fields, action and Lagrangian. Upon computing the equation of motion, the symplectic form of the system, and the corresponding Poisson brackets, it is subsequently possible to perform a geometric version of the canonical quantization, ending up with a construction of a representation of the Virasoro algebra or one of its extensions that realizes the conformal symmetry in the space of states. In this approach, boundaries are treated as conditions for the classical fields that preserve conformal invariance. Such a construction was done for Wess-Zumino-Witten and coset models for general worldsheet with boundaries e.g. in [86, 76].

The complementary quantization procedure to the Lagrangian approach is the functional integral, that can be constructed rigorously for such exactly solvable models [78], and produces results consistent with and complementary to the algebraic approach. This language is also convenient to go from the quantum 1+1 world to the Euclidean formalism, by Wick rotation $t \mapsto it$ and analytic continuation. A part of the difficulty in the construction of the functional integral comes from the topological terms in the field-theory action functional. Here, the principal problem is the definition of the Wess-Zumino amplitude, that gives sense to the formal expression

$$\exp \left(\frac{1}{4\pi} \int_{\Sigma} g^* d^{-1} \chi \right) \quad (1.5)$$

where Σ is a two-dimensional worldsheet, g a group valued field and $\chi = 1/3 \text{tr}(g^{-1} dg)^{\wedge 3}$ a closed but not exact 3-form on the target group. This question will appear several times and the precise definition of the above expression will be detailed in the following. Witten proposed in [173] to extend worldsheet Σ and field g on a 3-dimensional manifold M such that $\tilde{\Sigma} = \Sigma$ and to define the amplitude (1.5) by exponentiating the integral of $g^* \chi$ over $\tilde{\Sigma}$. This works for simply connected compact Lie groups leading to functional integrals for the corresponding Wess-Zumino-Witten models. There is however another approach based on the fact that the 3-form χ is locally exact $\chi = dB$ so that the 2-form $d^{-1} \chi$ may be locally defined, resulting in an expression for (1.5) as a product of local terms that must be glued together consistently. This approach in terms of local data was proposed in [5] and pursued in [79], covering also the case of fields with values in non-simply connected groups. The geometric structure of the construction was understood more recently [82] in terms of bundle gerbes of [131], allowing subsequently to tackle the problem of Wess-Zumino amplitudes for worldsheets with boundaries, but also the question of gauge invariance in the gauged versions of WZW models [83] that lead upon functional integration to the coset models [80]. This approach underlies the conformal field theory description adopted in the following, especially for Parts II and III of the present manuscript.

1.2.2 The different topics and their relations

This work is mostly about the use of geometric techniques of conformal field theory to describe certain problems of statistical mechanics and condensed matter physics. The topics, that are mostly independent, will be introduced in details in the respective parts of the manuscript, except that the geometric concepts developed for conformal field theory will be used all along. We only briefly describe the different contexts here.

The first part of the thesis deals with the transport properties in quantum wires. These are one-dimensional devices for which low energy elementary excitations are governed by conformal field theory. For a collection of such wire that are connected at a junction, it is actually possible to construct a nonequilibrium stationary state that describes the wires kept at different temperatures and potentials. For special junctions that preserve the conformal invariance and are described by appropriate boundary conditions, this state remains exactly solvable, and the asymptotic properties of transport of charge and heat may be established. We describe such situations for quantum wires described away from the junctions by free bosonic field modeling Luttinger liquid and, in quite particular cases, when the low energy excitations away from the junction are modeled by WZW theories.

The third part of the thesis deals with two dimensional systems called topological insulators, one of promising new trends in condensed matter physics of the last decade [94]. These are materials whose low energy states exhibit a nontrivial topology that assures the occurrence of protected massless modes localized at the sample edges. We do not discuss here such edge modes that should be described by conformal field theories but show that the formalism of Wess-Zumino amplitudes provides a powerful tool to compute a topological index associated to the insulating bulk ground state of topological insulators. Such an index is used to detect the presence of conducting edge modes. The geometric subtleties of the Wess-Zumino amplitudes play a crucial role in our approach, particularly for time-reversal symmetric systems.

In between, the second part of the thesis answers an important question for the classification of conformal field theories: which are the well defined coset models? It was shown in [83] using the bundle gerbe techniques, that some of the coset models may be inconsistent due to global gauge anomalies induced by the nontrivial topology (in particular, when the target group of the underlying WZW model is not simply connected). The question is reduced here to a purely mathematical one related to the classification of subalgebras of simple Lie algebras. An (almost) complete classification of the anomalous models is obtained by case by case analysis.

Although the main relation between the three topics of the thesis is at the level of the formalism, the first and the third parts are also related by the physical context, since the edges of topological insulators provide particular realizations of quantum wires, although we do not investigate this correspondence in what follows. Finally the gauge symmetry context present in the second and the third part of the thesis shows some similarity. Indeed, we detect the inconsistency of coset models by the global bulk gauge anomaly whereas we reduce the index of the time-reversal invariant topological insulators to a boundary version of the gauge anomaly.

1.2.3 General organization

Since the conformal field theory and its geometric realizations use a quite big machinery, we have chosen to introduce the different concepts only when they need to appear rather than to give a full description of the mathematical tools before the start. In particular, the Wess-Zumino-Witten models will be introduced in Section 4.1 of Chapter 4, with the corresponding highest weight representations of the current algebra discussed in Subsection 4.1.2. The geometrical approach to Wess-Zumino amplitude is introduced briefly in Chapter 7 and then detailed in Chapter 11. The Goddard, Kent, Olive construction of coset models is presented in Subsection 5.2.1 of Chapter 5 whereas the corresponding functional integral approach appears in Chapter 7. The concepts of boundary conformal field theory and of modular invariance are introduced all along the first part, and the theory of semi-simple Lie algebra is summarized in Chapter 7 of the second part.

This work is mostly about constructing explicit models, and the principal results are the detailed calculations for such models. I have tried to put as often as possible figures, schematic descriptions, elementary step decompositions and examples to make the reading more comfortable. Moreover, a few steps have been deliberately omitted to end up with a presentation that is not overburdened with formulae. The following manuscript is still supposed to be self-consistent,

but the most meticulous readers are invited to look at the different appendices and also to the following articles [85, 49, 44] containing the published material closely related to the three parts of the present thesis. *A priori*, however, the reading of these references is not necessary for the understanding of what follows.

Part I

Nonequilibrium transport across junctions of quantum wires

Chapter 2

Introduction

The transport phenomena in quantum wires and, in particular, across their junctions, have attracted a lot of interest in recent times since they are now accessible in experiments. From the theoretical point of view, it is well known that quantum theories in one dimension are very specific because a lot of models are exactly solvable: this is the realm of integrability. Among those models, $1 + 1$ -dimensional conformal field theories (one dimension for space, one for time) are good candidates to describe the low energy excitations appearing in quantum wires. Moreover the ballistic propagation of such excitations, typical in conformal field theory, allows to construct systems driven out of equilibrium while preserving the exactly solvable nature of the model. Thus the conformal invariant junctions of quantum wires appear as a good compromise of systems rich enough to describe different experiments but sufficiently simple in some aspects to tackle nonequilibrium problems, for which no general approach is known up to now [25].

2.1 Quantum wires and conformal field theory

2.1.1 Quantum wires

A quantum wire is a device whose spatial degrees of freedom are effectively reduced to one dimension at the quantum level. They are today realized in a rich spectrum of materials, and we distinguish three general processes to obtain such wires [3], sketched on Figure 2.1.

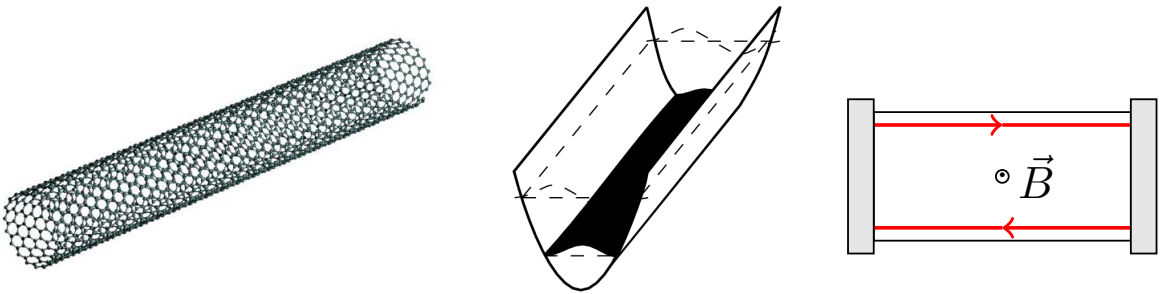


Figure 2.1: *Different realizations of quantum wires: carbon nanotube, steep well potential and quantum Hall effect.*

The first one consists in constructing genuine (quasi) one-dimensional quantum devices, in the context of nanomaterials. The canonical example is the celebrated carbon nanotube, obtained by rolling a graphene sheet into a cylinder [3]. Confinement of the circumferential direction reduce the corresponding degrees of freedom to a finite number, allowing to consider nanotubes as purely one-dimensional systems.

Another way to realize quantum wires is to use a two-dimensional electron gas. Such gas can be obtained at the interface of two well chosen semiconducting devices. By applying external

gates imposing a large gradient potential, it is possible to confine the electrons to a region with very thin transverse direction. The corresponding accessible energies are quantized so that at low temperature, only a few of them can be reached. As for the nanotubes, the transverse degrees of freedom can be reduced to one or a finite number (which can be considered as internal), and only the longitudinal dimension of space remains.

Finally there is another approach to constructing quantum wires grouped under the general name of quantum Hall systems. Consider again a two-dimensional electron gas and apply to it an intense transverse magnetic field. In the bulk of the (2d) material, the electrons are trapped due to their cyclotron orbits and there is no macroscopic transport. However these orbits are broken at the boundaries of the material, forcing the electrons to propagate in one direction, but only for one or a finite number of channels localized at each boundary of the system and giving an effective one dimensional propagation. This semi-classical picture can be established more formally and it can be shown that this geometry induces a macroscopic transport leading to the quantization of the conductivity of such a system. This has been also established experimentally [109].

2.1.2 General features

Whatever the device we consider, the quantum wires obtained share common properties leading to a specific theoretical description.

d=1 The first one is obviously the dimensionality. The case of $d = 1$ is actually specific compared to higher dimensions. Consider free particles on a line: each one is trapped between its two neighbors and cannot avoid or “jump” over it. This situation does not appear in dimension 2 or 3 where the particles are free to avoid any contact by moving around each other. At the quantum level, this picture is manifest in the momentum space, where the Fermi “sphere” is reduced to two points $\{-k_F, k_F\}$, see for example Figure 3.1 in the case of free fermions. This is the only dimension where this is a discrete set that is not connected. Consequently the phase space of the excitations, even with interactions, can be much simpler than in higher dimensional cases. Besides, a lot of quantum field theories become easier when taken to $D = 1 + 1$: one dimension $d = 1$ of space and one of time, and some of them become exactly solvable, also for theories describing interactions.

Linear dispersion The effective reduction to one dimension of the devices depicted above is generally available only in some low energy regime where only a few modes of the transverse direction are attainable. On top of that it appears that in a such regime (or eventually a restriction of it), the dispersion relation of these modes has the following linear form

$$E = vq \quad (2.1)$$

for q small enough around the ground state of the system (e.g. the Fermi sea of free fermions), and v is some characteristic velocity of the system (e.g. the Fermi velocity). This linear dispersion is a sign of conformal invariance, since no typical scale of space and time can be extracted from it. In contrast to massive theories where some typical mass appears, implying some minimal energy or gap for the excitations, the linear dispersion is said to be gapless: excitations can be as small as we want.

Ballistic propagation One of the direct consequence of linear dispersion (2.1) is the fact that the velocity of the excitations, defined by

$$\frac{dE}{dq} = v \quad (2.2)$$

is independent of the momentum q . All the excitations of the particles or quasiparticles involved propagate at the same velocity v and keep their coherence: there is no dispersion or collapse. Such propagation, called ballistic, is crucial for the following because in this case excitations are easy to track.

2.1.3 Conformal field theory description

No characteristic scale, linear dispersion and ballistic propagation are the key ingredients appearing in a conformal field theory description. At the classical level, the low energy excitations in quantum wires that we consider will be described by a field

$$g : \begin{cases} \mathbb{R} \times \mathbb{R} \longrightarrow G \\ (t, x) \longmapsto g(t, x) \end{cases} \quad (2.3)$$

where G is a Lie group. Such field comes with a corresponding classical action $S[g]$ and we consider the case of infinite wire $x \in \mathbb{R}$ to focus on the bulk properties. Appropriate choice of G and S models the kind of quantum wire we want to describe. For example, the case where $G = U(1)$ and S is the action for the free bosonic field describes interacting fermions in the Luttinger regime (see Chapter 3), as well as edge modes in the integer quantum Hall effect ([65], Chap. 15.1). Other theories appear for example when considering fractional quantum Hall effect, where various exotic excitations are propagating along the edges, depending of the filling factor ν of the system. Such excitations involving nonabelian interactions and anyonic statistics are described by Wess-Zumino-Witten models ([65], Chap. 15.5) that would be detailed in Chapter 4.

Whatever the model chosen, the conformal invariance implies that the classical equations of motion are solved by

$$g(t, x) = g^\ell(t + x)g^r(t - x) \quad (2.4)$$

where g^ℓ and g^r are any one-variable functions and we have set the typical velocity v of the theory to 1 identifying the dimensions of space and time. Hence in conformal field theory we always have two opposite chiral propagations, whose product is the general classical solution of the theory. Field g^ℓ and g^r are respectively called left and right movers.

The quantization of the system depends on the model and will be detailed in the next chapters. It turns out that in all the junction considered, the quantum states are described by expectations of the algebra of chiral currents of the theory, which are formally the derivatives of the fields

$$J^\ell \propto g^{-1} \partial g^\ell, \quad J^r \propto g^{-1} \partial g^r \quad (2.5)$$

where ∂ stands for one-variable derivative. These currents are associated to some extra symmetries of the wire dynamics and corresponding conserved quantities, such as the electric charge. On the quantum level, left and right currents induce also a representations of the Virasoro algebra, ensuring conformal invariance and encoding the energy and momentum propagation.

A remark about left and right movers To avoid any ambiguity in the following, we fix once for all the notion of left and right movers: any current (or other field) will be called *left mover*, denoted by subscript ℓ , if its space time dependence is a function of $t + x$. Any current (or other field) will be called *right mover*, denoted by exponent r , if its space time dependence is a function of $t - x$.

This definition comes from the physics of waves: consider an initial profile f at time $t = 0$ for a right moving current $J^r(t, x) = f(t - x)$ (see Figure 2.2, left). For a given time $t' > 0$, the value of J^r at t' and x

$$J^r(t', x) = J^r(0, x - t') \quad (2.6)$$

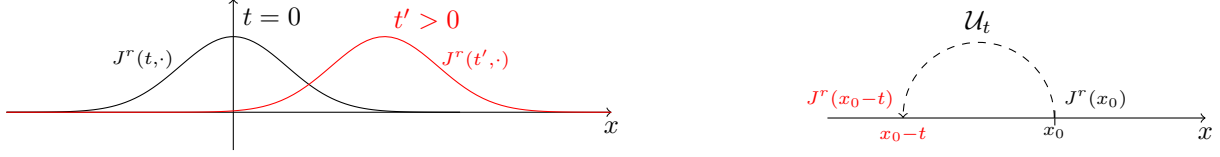


Figure 2.2: Two interpretations of left and right movers

is computed from the profile at $t = 0$ but at position $x - t'$. Hence the profile is effectively moving in the right direction for a right mover, and conversely for the left moving case.

However, there is another interpretation of this fields in the Heisenberg picture, where the state of the quantum system can be seen as expectations of the family of operators $J^r(0, x)$ for $x \in \mathbb{R}$. The choice $t = 0$ is arbitrary and x shall be seen just as a parameter of the family J^r . Dynamics is implemented through time evolution via

$$\mathcal{U}_t J^r(0, x_0) = J^r(t, x_0) = J^r(0, x_0 - t) \quad (2.7)$$

mapping the family $\{J^r(0, x)\}_x$ to itself. In this picture, the field $J^r(0, x_0)$ has been moved to $J^r(0, x_0 - t)$ via time evolution, i.e. to the left if $t > 0$. Hence right movers are moved to the left! Conversely, left movers are moved to the right in that picture.

Note that both pictures are consistent since we are not considering the same objects: the first one focuses on the value of the field whereas the second one focuses on the value of the variable. They are dual to each other and move in converse directions.

2.2 Non equilibrium junctions

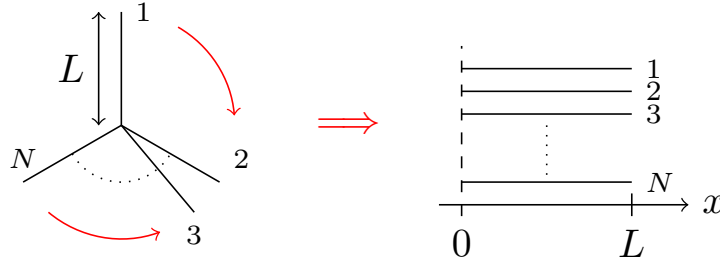
We would like to use ballistic propagation of the fields to construct nonequilibrium state following the proposal of [17, 127]. Note that this propagation is specific in the sense that there is no possible dissipation or collapse of the solution (2.4) and there is no diffusion: wave packets remain coherent while propagating. Hence the corresponding nonequilibrium state will be particular.

2.2.1 The folding trick

Until now we discussed only the case of one infinite wire, but what we have in mind is a collection of N finite quantum wires of length L connected together at one point called the junction, and free at their other end, see Figure 2.3. The junction must allow exchanges between the wires while preserving the conformal invariance of the theory. If this invariance can be preserved for a finite size theory, in general, the contact will break the conformal invariance. However the latter should be restored in the long-distance scaling limit, where the junction can be approximated as a point as compared to the long length of the wires.

One way to construct conformal invariant junctions is to use the “folding trick” of [57] where the junction is folded in a way that the connected ends of the wires can be seen as a boundary condition for a multicomponent field theory $\mathbf{g} = \{g_i\}_{i=1}^N$. Boundary conditions that preserve conformal symmetry lead to consistent field theories that can remain exactly solvable.

It follows that a junction of quantum wires can be described on large scales by a conformal field theory with one field for each wire with an appropriate boundary condition at $x = 0$ mixing the different components and inducing exchanges, whereas the free end $x = L$ requires an independent boundary condition for each wire. The propagation remains ballistic in the bulk of the system as discussed before and the boundary conditions just couple the different degrees of freedom of the theory, which are encoded in the algebra of left and right currents $J_i^{\ell, r}$ on each wire i .

**Figure 2.3:** *The folding trick*

2.2.2 Scattering matrix

In most of the model considered in the following chapters, the boundary conditions for the g_i at $x = 0$ in the folded picture implies the relation

$$J_i^r(t, 0) = \sum_{j=1}^N S_{ij} J_j^\ell(t, 0) \quad (2.8)$$

for some scattering $N \times N$ matrix S . In this picture the right current propagates (to the left) until it hits the junctions, is scattered to all the wires and becomes left currents (which propagate to the right), i.e. away from the junction.

At the free end of the wires $x = L$, we impose boundary conditions on fields g_i in order to have for the corresponding currents the relation

$$J_i^r(t, L) = J_j^\ell(t, L) \quad (2.9)$$

such that the left current “bounces” at the end and comes back to towards the junction as a right mover.

2.2.3 Nonequilibrium stationary state

Consider the thermodynamic limit $L \rightarrow \infty$ of the junction in which the free ends of the wires are sent to infinity and become never reachable so that the bounce just described does not happens. Hence the dynamics for the algebra of currents is reduced to only two simple rules

1. The left currents J_i^ℓ are moved to the right in the folded picture, i.e. away from the junction.
In the thermodynamic limit, left movers never see the junction.
2. The right currents J_i^r are moved to the left in the folded picture, i.e. towards the junction. After some time they reach the junction where they become left currents through the scattering rule (2.8). These currents then propagate according to rule 1, and hence never see the junction anymore.

Rule 1 says that the behavior of the left current is independent of the junction, in particular it remains the same if we consider the disconnected junction where all the wires are independent. On such “non-junction” consider the product state

$$\omega_{\text{in}} = \lim_{L \rightarrow \infty} \bigotimes_{i=1}^N \omega_{\beta_i}^{i,L} \quad (2.10)$$

where on each wire i , $\omega_{\beta_i}^{i,L}$ is the Gibbs equilibrium state of inverse temperature β_i . In particular, the left currents expectations can be computed in that state and we shall keep the same expectations of the currents for any connected junction. This will be not the case for the right currents.

If we wait long enough, however, the right currents will become linear combinations of the left ones and their expectations can be then computed by the previous rule. This suggest to define, at least formally, the following state

$$\omega_{\text{ness}}(A) = \lim_{t \rightarrow \infty} \omega_{\text{in}}(\mathcal{U}_t A) \quad (2.11)$$

where $A \in \mathcal{A}$, the algebra of left and right currents, and \mathcal{U}_t the unitary evolution operator corresponding to the connected junction described by rules 1 and 2. This definition will be developed in the next chapters, depending on the model considered, but at the end one will obtain a nonequilibrium state, stationary under the time evolution of connected wires, as a combination of equilibrium expectations for the disconnected junction.

Note that this state exists and is well defined only because of the ballistic nature of the excitations that assure that the left currents never see the junction. Thus the nonequilibrium physics involved might seem simple compared to diffusive processes, but is still nontrivial since we expect some flow of charge or heat between the different wires. Finally note that the order of the limit is crucial here with first L , then t tending to ∞ to avoid any oscillations due to the possible bounce of the excitations at the free end of the wires.

2.2.4 Hamiltonian reservoirs

Such junction can be seen as driven out of equilibrium via effective reservoirs which actually are restricted parts of the full junction and arising in the following picture proposed in [18]. Consider the finite system where the wires are disconnected and each one is prepared at a different thermal equilibrium, with temperature β_i . Then at initial time $t = 0$ connect the wires, allowing exchanges of energy at characteristic velocity v . When one excitation crosses the junction it is scattered to the other wires and then propagates along them until hitting their free ends. In the regime where $vt \leq L$, the excitations are not scattered back. Then we restrict the observations to a region localized around the junction, delimited by a fixed length ℓ from the contact point. In the regime

$$\ell \ll vt \ll L \quad (2.12)$$

we expect a steady state to appear in the region of observation, whereas far from the junction the wires are still not modified by the contact, such that they should remain in thermal equilibrium. Hence these parts of the system can be considered as effective reservoirs, absorbing the incoming excitations, see Figure 2.4. The dynamics of such reservoirs is deduced from the Hamiltonian dynamics of the junction since they are part of it, hence the name of Hamiltonian reservoirs.

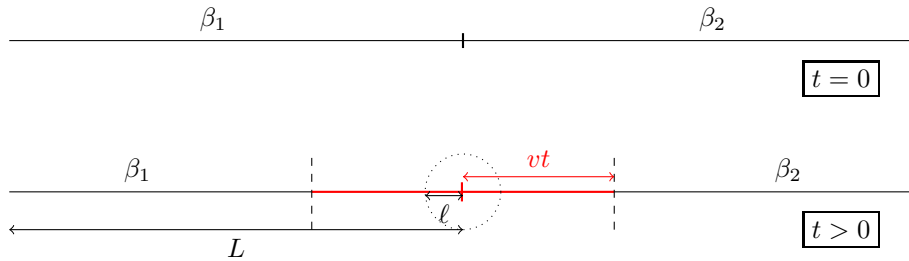


Figure 2.4: *Hamiltonian reservoirs*

For fixed ℓ , take the thermodynamic limit of the system $L \rightarrow \infty$. It ensures that excitations are never scattered back after having crossed the junction. The steady state of energy flow inside the region of observation needs some time to be reached, hence we consider the subsequent limit $t \rightarrow \infty$ (note again the order of the limits). In this limit the region ℓ sees a nonequilibrium flow between the reservoirs that have been sent far away.

2.2.5 Transport properties

Since any measurement perturbs a quantum system, each computed expectation must be related to a specific measurement protocol. We propose the following one, adapted from [18], initially proposed by [119] and illustrated in Figure 2.5.

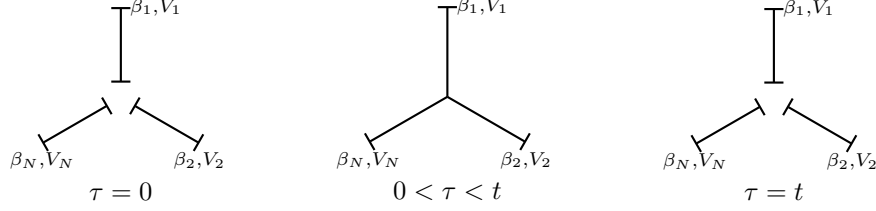


Figure 2.5: A two time measurement protocol.

Consider the disconnected system at $\tau = 0$ prepared in different equilibrium states. In this system we can measure the total energy $\mathbf{e}^0 = (e_i^0)_i$ contained in each wire. This can be done simultaneously since the wires are independent and projects the system on a state relative to the value of the measurement. Then connect the system and let it evolve until time $\tau = t$ where it is again disconnected. Then we proceed to a similar measurement $\mathbf{e}(t) = (e_i(t))_i$ of the total energy in each wire at time t and compare it with the initial one. In this two-time measurement protocol, we compute the probability of a given value of energy change for all wires

$$\mathbb{P}(\Delta \mathbf{e}), \quad \Delta \mathbf{e} \equiv \mathbf{e}(t) - \mathbf{e}^0 \quad (2.13)$$

We compute actually the generating (or characteristic) function of such probability measure

$$F_t^L(\boldsymbol{\lambda}) = \sum_{\Delta \mathbf{e}_i} e^{i \sum_i \lambda_i \Delta \mathbf{e}_i} \mathbb{P}(\Delta \mathbf{e}) \quad (2.14)$$

which contains all the cumulants of \mathbb{P} in its successive derivatives. The variable $\boldsymbol{\lambda}$ is conjugated to the energy and this generating function is called the full counting statistics of energy transport, which can be generalized to any other conserved quantities in the wires, such as the electric charges.

We can extract the asymptotic regime for \mathbb{P} looking at the long time limit of the rescaled logarithm of the full counting statistics, defined as

$$f(\boldsymbol{\lambda}) = \lim_{t \rightarrow \infty} \frac{1}{t} \lim_{L \rightarrow \infty} \ln F_t^L(\boldsymbol{\lambda}). \quad (2.15)$$

Again, we first take the thermodynamic limit before taking the large time one. By a slight abuse of language, we shall call f the large deviations rate function in the following (the genuine large deviations rate function is actually given by the Legendre transform $\mathcal{L}[f(-i \cdot)]$) of the analytic continuation of f to the imaginary values. The function f is in general easier to compute than the full counting statistics and will be the aim of nonequilibrium calculations for the junctions we consider in the next chapters. It encodes the asymptotic properties of the probability distribution \mathbb{P} by the relation

$$\mathbb{P}(\Delta \mathbf{e}) \underset{t \rightarrow \infty}{\sim} e^{-t \mathcal{L}[f(-i \cdot)]\left(\frac{\Delta \mathbf{e}}{t}\right)} \quad (2.16)$$

which will be investigated in more details once f is explicitly computed, see subsections 3.7.1 and 3.7.2 in the next chapter.

The two-time measurement protocol for extracting the full counting statistics described above is not practical because we are interested in the changes of wire energies in time t that are much smaller than the energies themselves if $vt \ll L$. Fortunately, it has been shown in [119] that the same quantity may be extracted by performing more practical indirect measurements on a small gauge coupled appropriately to the junction of wires.

2.3 Overview of the models

Starting with a brief history of the subject, we then describe the general scheme to achieve a nonequilibrium stationary state that will be applied to specific models in the next chapters.

2.3.1 A brief history

The transport properties in quantum wires have attracted a lot of interest in recent times and a large variety of models have been proposed in the last decades, see for example [48, 87]. The first study of transport properties across a junction of such wires goes back to Landauer [115, 114, 113] and Büttiker [31, 32] where they developed a general formalism to compute conductance from scattering of non-interacting electrons on the junction [33]. The computation of the full counting statistics of free electrons was then achieved by Levitov and Lesovik in [120, 119], going deeper in the study of nonequilibrium properties.

The conformal field theory approach is more recent and was initially developed by Affleck and collaborators [57, 135], where the junction is seen as a boundary defect of the multi-wire theory by applying the “folding trick”. Moreover it was realized that such a description gives a direct access to the low energy electric conductance of junctions [146], measuring the small currents induced in a near-to-equilibrium regime. Going beyond the linear response regime, which may be reduced to the equilibrium calculations by the Green-Kubo formula, is not obvious and CFT seems to be also helpful here, although some exact results were already obtained earlier using integrable models of junctions [61].

The conformal field theory description of far from equilibrium junctions has been investigated in details by Bernard, Doyon and collaborators: it was shown in [17, 18, 19, 52] for some simple boundary defects with pure transmission that the long-time asymptotics of the full counting statistics of charge and energy transfers through the junction may be calculated for the wires initially equilibrated at different temperatures and different potentials. Moreover, steady nonequilibrium states obtained at long times from such initial conditions could be explicitly constructed. Physical restrictions for the applicability of the CFT approach in such a nonequilibrium situations were also discussed in some detail in those works, in particular in [18]. Lastly, a generalization of this approach to a larger class of defects was initiated in [20], and a hydrodynamic approach of perturbed nonequilibrium CFT was proposed in [16].

Besides, Mintchev, Sorba and collaborators developed nonequilibrium stationary states for wires described by Luttinger liquids in bosonized description, with scale invariant junctions [14, 127], using the observation that in the thermodynamic limit left movers expectations factorize on individual disconnected wires. The right moving currents were then expressed in term of the left moving ones through a scattering relation (2.8), as sketched above.

Our approach was inspired by the papers of those two groups of authors and our results are complementary to theirs. Indeed, we also use the factorization of the chiral currents in the thermodynamic limit, allowing a simple construction of a nonequilibrium stationary state, and following [18] we show that such a state is obtained if one prepares disconnected wires each in the equilibrium state at different temperature and potential and then one connects the wires instantaneously and lets the initial state evolve for a long time, similarly as in the general construction of nonequilibrium states proposed by Ruelle in [152]. Most importantly, we perform a calculation of the full counting statistics for the transport through the conformally invariant junctions of Luttinger wires with both transmission and reflection.

2.3.2 General strategy

More precisely, the general construction in our approach is the following.

1. Set up the classical theory of a finite size junction by specifying field, action and boundary conditions.
2. Solve the classical equations of motion and give the general solution in terms of Fourier modes.
3. Compute the scattering matrix for such solutions, related to the boundary conditions.
4. Compute the symplectic form of the classical theory and the corresponding Poisson brackets.
5. Perform the canonical quantization of the classical theory.
6. Construct the equilibrium state of the full system at temperature β .
7. Take the thermodynamic limit of such a state: the junction independence of the left currents becomes manifest.
8. Construct the nonequilibrium stationary state as proposed.
9. Compute basic quantities in such state, e.g. mean energy or charge flow.
10. Compute the full counting statistics and the large deviations regime associated to observable such as energy or/and charge.

Of course step 1 is crucial: the starting point is to find clever boundary conditions for the field theory preserving conformal invariance and leading to some scattering relation, with both persisting on the quantum level. At each step the problem is supposed to stay exactly solvable, but that does not mean that the computation is easy and it actually happens that some steps are too complex. The next chapters discuss three distinct models of conformal junction that we have investigated. Here we briefly describe them specifying which steps have been achieved.

The free massless bosonic junction is described in Chapter 3 where the construction is fully achieved, for a large family of boundary conditions leading to various scattering matrices. This model describes free bosons as well as interacting fermions, in the latter case for the Luttinger liquid of electrons. We compute at the end the full counting statistics associated to the transport of electric charge and heat, and extract its asymptotic behavior.

The WZW junction with a cyclic brane generalizes the free bosonic case to a conformal field theory with richer symmetries, but for a specific scattering where the current is fully transmitted to the next wire without any reflection. The large deviations form of the full counting statistics is obtained for heat and charge transport with results similar to those in [52].

The WZW junction with a coset brane tries to generalize the previous model to a richer class of junctions. However the coset decomposition induced by such brane leads to technical problems already for the equilibrium state, that can be solved only in a few cases. Computing the simplest one, we end up with the previous scattering for the cyclic brane.

Finally note that for the construction of the nonequilibrium state, only the thermodynamic limit of step 6 is needed in which the factorization of the left movers occurs. However, due to the exactly solvable nature of the model it is possible to compute the explicit equilibrium state for connected junctions, even at finite size. This is done using the boundary conformal field theory techniques and, in particular, employing the duality between the open and closed string pictures, where the role of space and Euclidean time is exchanged, which leads to a better behavior of the equilibrium expressions in the thermodynamic limit.

Chapter 3

Free massless bosonic junction

This chapter is devoted to the study of the simplest model of quantum wires defined in terms of the free massless bosonic field. The physics described by such a model is simple but not completely trivial, since it also covers interacting electrons in a one-dimensional crystal. It is easy to produce a large family of scale invariant wire junctions for such a theory, and the exactly solvable nature of the model is explicit enough to permit the computation of many interesting quantities, in particular, of the large deviation rate function for nonequilibrium transfers. We first motivate the model by explaining the fermion-boson correspondence in one space dimension, then we construct a class of junctions and proceed from the classical level to the quantum nonequilibrium stationary state. Finally we investigate the nonequilibrium transport properties of the model. The results being already published in [85], we skip the most technical details of the construction to avoid an overloading of the chapter.

3.1 Fermions and bosons in one dimension

Consider the free Fermi field describing a one-dimensional gas of noninteracting nonrelativistic electrons whose spin degree of freedom we ignore for simplicity. Such electrons have a quadratic dispersion relation presented in Figure 3.1. In the ground state all electron states with energies up to the Fermi energy $E_F > 0$ will be filled.

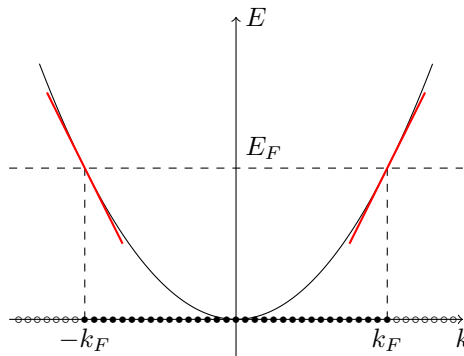


Figure 3.1: Dispersion relation of free nonrelativistic electrons in one dimension. The Fermi surface is reduced to the two points $\pm k_F$, where the dispersion is linear around them.

As announced in the previous chapter, the Fermi surface reduces in this case to two points: $\{k_F, -k_F\}$, a specific property of dimension one. We are interested in low-energy excitations around such Fermi points, for which the dispersion relation becomes linear

$$E(q) \simeq \pm v_F q \quad \text{around} \quad k = \pm k_F \quad |q| < \Gamma \quad (3.1)$$

where v_F is the Fermi velocity and Γ is some momentum cut-off beyond which the linear dispersion is invalid. Similar dispersion relation will characterize low energy excitations for non-interacting electrons in a periodic crystalline potential with the Fermi energy inside an energy band. Such excitations may be as small as we want (at least in the thermodynamic limit) and they do not involve a particular space or time scale, but only a velocity. They are described by relativistic free massless fields, the simplest example of conformal field theory.

The low-energy excitations of the system can be decomposed in terms of elementary particle-hole excitations around the Fermi points, leading to density fluctuations near the Fermi energy. Around k_F , a hole at momentum k and a particle at $k + q$ generate an excitation of energy

$$\epsilon = v_F(k + q - k) = v_F q \quad (3.2)$$

independent of k . Hence all the excitations are propagating at the same velocity: there is no dispersion. Such ballistic propagation is a sign of an underlying conformal field theory description. Since the associated velocity is positive, we call such excitations right movers. The same description applies to $k = -k_F$, where the associated particles have negative velocity, we call them the left movers. Since k_F and $-k_F$ are separated, the two families of excitations are independent.

3.1.1 Free relativistic massless fermions

Relativistic massless free fermions are described by anticommuting fields ψ^ℓ and ψ^r , depending respectively on¹ $t + x$ and $t - x$ and corresponding to the left and right movers mentioned above. For a quantum wire of finite size L , we impose the boundary conditions

$$\psi^\ell(t, 0) = \psi^r(t, 0), \quad \psi^\ell(t, L) = -\psi^r(t, L) \quad (3.3)$$

which couple left and right movers and lead to $2L$ periodic functions, that can be decomposed in terms of Fourier modes c_p for $p \in \mathbb{Z} + 1/2$, which correspond to the elementary excitations (particles and holes). Indeed, once quantized, c_p and $\bar{c}_{-p} = c_p^\dagger$ satisfy the canonical anticommutation relations and act on a Fermionic Fock space \mathcal{F}_f built upon the normalized vacuum state $|0\rangle_f$, corresponding to the ground state where all the states below the Fermi energy are occupied, see Figure 3.1. The Fock space is generated by c_{-p} and c_p^\dagger acting on $|0\rangle_f$ for $p > 0$, corresponding, respectively, to the creation of a hole or a particle of momentum p .

The relevant observables of such a system are the free Hamiltonian H_f for and the $U(1)$ charge Q_f associated to the symmetry $\psi^{\ell,r} \mapsto e^{-i\alpha} \psi^{\ell,r}$. The corresponding Noether current has chiral components J_f^ℓ and J_f^r . The key point is that all the physically relevant operators describing such quantum free fermions can be expressed in terms of the following family

$$\rho_n = \sum_{p \in \mathbb{Z} + \frac{1}{2}} : c_p^\dagger c_{p+n} : \quad (3.4)$$

for $n \in \mathbb{Z}$, see [3]. Such operators, that have bosonic nature and satisfy canonical commutation relations, describe the charge density fluctuations of characteristic momentum n around the Fermi points and correspond to the particle-hole excitations described qualitatively above.

3.1.2 Free relativistic massless bosons

The bosonic modes ρ_n can be obtained by considering a 1+1-dimensional massless free field $\varphi(t, x)$ defined modulo 2π on the space time $\mathbb{R} \times [0, L]$, with the action functional

$$S[\varphi] = \frac{r^2}{4\pi} \int dt \int_0^L [(\partial_t \varphi)^2 - (\partial_x \varphi)^2] dx \quad (3.5)$$

¹To simplify the notations, we use the Fermi velocity v_F to express time in the same units as length.

As for fermions on a finite system, we shall impose on $\varphi(t, x)$ some boundary conditions. It will appear very natural in the following to take the Neumann boundary condition:

$$\partial_x \varphi(t, 0) = 0 = \partial_x \varphi(t, L). \quad (3.6)$$

Such a scalar field will be viewed as having the range of its values compactified to the circle of radius r with metric $r^2(d\varphi)^2$. The classical solutions extremizing the action have the form $\varphi(t, x) = \varphi^\ell(t + x) + \varphi^r(t - x)$, also describing two opposite chiral propagation.

The Neumann boundary conditions couple such chiral fields, and lead to $2L$ -periodic functions allowing the decomposition in terms of Fourier modes α_n for $n \in \mathbb{Z}^*$. Such modes satisfy canonical commutation relations and the corresponding Hilbert space is a bosonic Fock space generated by the $n < 0$ part acting on a vacuum state $|0\rangle_b$. On the top of that, the zero modes φ_0 and α_0 also appear in $\varphi^{\ell, r}$ as affine solutions of the equations of motion. Their Hilbert space of states may be represented as $\mathcal{H}_0 = L^2(U(1))$, with φ_0 viewed as the angle in $U(1)$ and α_0 acts as derivative. In particular, the $U(1)$ symmetry $\varphi \mapsto \varphi + \alpha$ leads to the conserved charge $Q_b = (r^2/2)\alpha_0$ which acts only on \mathcal{H}_0 and has an integer spectrum. The corresponding Noether current has the chiral components J_b^ℓ and J_b^r linear in modes α_n . Finally the bosonic theory comes also with the Hamiltonian H_b that is quadratic in modes α_n .

3.1.3 Bosonization

The correspondence between free fermions and free bosons may be establish precisely, see e.g. [3] or [85] for its realization in the present setup. Consider the free bosonic field described before with compactification radius $r = \sqrt{2}$. There exist a unitary isomorphism $\mathcal{I} : \mathcal{H}_b \rightarrow \mathcal{H}_f$ that maps vacuum to vacuum and intertwines the action of the density fluctuations of fermions ρ_n and the bosonic modes α_n

$$\mathcal{I} |0\rangle_b = |0\rangle_f, \quad \mathcal{I} \alpha_n = \rho_n \mathcal{I} \quad (3.7)$$

Isomorphism \mathcal{I} intertwines also the action of $U(1)$ currents and charges and of the Hamiltonians.

$$\mathcal{I} J_b^{\ell, r} = J_f^{\ell, r} \mathcal{I}, \quad \mathcal{I} Q_b = Q_f \mathcal{I}, \quad \mathcal{I} H_b = H_f \mathcal{I} \quad (3.8)$$

Hence the property of charge, current and energy can be equivalently described in both fermionic and bosonic language. The correspondence between the fields also exists, but has more complicated form:

$$\psi^\ell(t, x) \mathcal{I} = \mathcal{I} \sqrt{\frac{\pi}{2L}} : e^{-2i\varphi^\ell(t, x)} : \quad (3.9)$$

where in left hand side appears the bosonic vertex operator.

3.1.4 Luttinger model

The power of bosonization shows up in the case of interacting fermions, where in some cases much of the previous construction remains valid. In the leading order, the interactions between electrons in a one-dimensional crystal whose momenta are close to the Fermi surface may be described by perturbing the free fermionic Hamiltonian H_f by a combination of quartic terms

$$H^{\text{int}} = \frac{1}{2\pi^2} \int_0^L [2g_2 (: \bar{\psi}^\ell \psi^\ell :)(: \bar{\psi}^r \psi^r :) + g_4 ((: \bar{\psi}^\ell \psi^\ell :)^2 + (: \bar{\psi}^r \psi^r :)^2)] dx + \text{const.} \quad (3.10)$$

where an infinite constant is needed to make the operator well defined in the fermionic Fock space. Such a perturbation defines the Luttinger model of spinless electrons in one-dimensional crystal [164]. Parameter g_2 and g_4 are the coupling constants describing the strength of interaction. They may be related to the Fourier transform of the two-body Coulomb interaction between

the fermions [3]. The crucial fact that enables an exact solution of such a model is that, under the bosonization map, the above perturbation becomes quadratic in the free bosonic field. In the bosonic picture, the total Hamiltonian $H^{\text{tot}} = H_b + \mathcal{I}^{-1}H^{\text{int}}\mathcal{I}$ corresponds to the classical Lagrangian

$$L^{\text{tot}} = \frac{1}{2\pi} \int_0^L \left[\frac{2\pi}{2\pi+g_4+g_2} (\partial_t \varphi)^2 - \frac{2\pi+g_4-g_2}{2\pi} (\partial_x \varphi)^2 \right] dx \quad (3.11)$$

which is close to the one appearing in the original free bosonic action. Indeed, upon the rescaling $x' = \alpha x$, we end up with the same Lagrangian (3.5) of the free massless bosonic theory on a wire of length $L' = \alpha^{-1}L$, with compactification radius r , where

$$\frac{r^2}{2} \equiv K = \sqrt{\frac{2\pi+g_4-g_2}{2\pi+g_4+g_2}}, \quad \alpha \equiv \frac{v_{\text{ren}}}{v_F} = \frac{\sqrt{(2\pi+g_4)^2 - g_2^2}}{2\pi} \quad (3.12)$$

Hence, after the change of the spatial variable, Lagrangian L^{tot} becomes that of the free bosonic field compactified on the radius r that is different from $r = \sqrt{2}$ if $g_2 \neq 0$. The factor α gives the multiplicative renormalization of the wave velocity v_F due to the interactions². The quantization of the free bosonic theory compactified at radius r discussed in Sec. 3.1.2 provides then the exact solution of the Luttinger model on the quantum level.

Summarizing The interacting one dimensional (spinless) fermions described by the Luttinger model can be mapped and solved by a free massless bosonic field, compactified on radius r depending on the strength of the fermionic interactions, with $r = \sqrt{2}$ corresponding to the free fermion cases. The $U(1)$ currents and charges, and the Hamiltonians coincide for the two theories, but the relation at the level of fields is more complicated.

3.2 Bosonic junction of quantum wires

In the spirit of the folding trick described in the previous chapter, see Figure 2.3, we describe a junction of N quantum wires as a compactified field

$$\mathbf{g} : \mathbb{R} \times [0, L] \rightarrow (U(1))^N, \quad (3.13)$$

with N components $g_i(t, x) = e^{i\varphi_i(t, x)} \in U(1)$ whose dynamics is determined by the action functional of the free massless bosonic field

$$S[\mathbf{g}] = \sum_{i=1}^N \frac{r_i^2}{4\pi} \int dt \int_0^L ((\partial_t \varphi_i)^2 - (\partial_x \varphi_i)^2) dx \quad (3.14)$$

and appropriate boundary conditions. The compactification radii r_i play the role of a diagonal metric on $U(1)^N$ and may be different on each wire, corresponding to different couplings g_{2i} and g_{4i} in the Luttinger models describing the electrons in individual wires, see (3.12). Note that here we use the rescaled spatial variables in the wires so that the lengths of the wires in physical variables are fixed to $\alpha_i L$. This will not matter much because the length L will be ultimately sent to infinity.

We shall impose the Neumann reflecting boundary condition at the free extremity of the wires

$$\partial_x \varphi(t, L) = 0 \quad (3.15)$$

²we assume that $|2\pi + g_4| > |g_2|$

where $\varphi = (\varphi_i)_i$. This condition is diagonal: the fields at $x = L$ are independent in the unfolded picture. We also could have chosen the Dirichlet boundary condition, but this one does not preserve the $U(1)$ charge, see below.

On the other hand, the junction is described by a nondiagonal boundary defect at $x = 0$. In order to preserve conformal invariance, the simplest but nontrivial condition at $x = 0$ would be the Neumann or the Dirichlet boundary condition, but involving a linear combination of the components φ_i , so that the wires are coupled together. We can obtain such a combination using a group homomorphism $\kappa : U(1)^M \mapsto U(1)^N$ defined by the map

$$(e^{i\psi_m})_{m=1}^M \xrightarrow{\kappa} (e^{i\sum_m \kappa_i^m \psi_m})_{i=1}^N \quad (3.16)$$

specified by integers κ_i^m . The condition at $x = 0$ will require that the boundary value of field \mathbf{g} belongs to a “brane”:

$$\mathbf{g}(t, 0) \in \mathcal{B} \equiv \text{Im}(\kappa) \subset U(1)^N. \quad (3.17)$$

We assume for the following that κ is an injection³. In particular, $M \leq N$ necessarily and the N -dimensional vectors $\boldsymbol{\kappa}^m = (\kappa_1^m, \dots, \kappa_N^m)$ with $m = 1, \dots, M$ are linearly independent. Consider the projection of rank M in \mathbb{R}^N whose image is spanned by such vectors. Then the boundary condition (3.17) implies

$$P^\perp \partial_t \varphi(t, 0) = 0 \quad (3.18)$$

where $P^\perp = I - P$. To take into account the metric $r_i^2 \delta_{ij}$ on $U(1)^N$, we shall require the projector P to be orthogonal with respect to the corresponding scalar product of \mathbb{R}^N , namely $\mathbf{a} \cdot \mathbf{b} = \sum_i r_i^2 a_i b_i$. Thus the components of the field φ belonging to the image of P^\perp satisfy the Dirichlet boundary condition. Such components are linear combinations of the wires component φ_i .

The stationary points of the action functional (3.14) restricted to fields obeying the boundary conditions satisfy, besides the latter, the equations

$$(\partial_t^2 - \partial_x^2) \varphi(t, x) = 0, \quad (3.19)$$

$$P \partial_x \varphi(t, 0) = 0. \quad (3.20)$$

The second one completes (3.18): at $x = 0$ the components φ in $\text{Im} P$ satisfy the Neumann boundary condition.

Example 3.1

- Consider the case of $N = 2$ wires, $M = 1$, and $\kappa = (1, 1)$. The projector is given by

$$P = \frac{1}{r_1^2 + r_2^2} \begin{pmatrix} r_1^2 & r_2^2 \\ r_1^2 & r_2^2 \end{pmatrix} \quad (3.21)$$

and the corresponding boundary conditions are

$$\partial_x (r_1^2 \varphi_1(x, 0) + r_2^2 \varphi_2(x, 0)) = 0, \quad \partial_t (\varphi_1(x, 0) - \varphi_2(x, 0)) = 0, \quad (3.22)$$

such that the two components of the fields are coupled by the defect at $x = 0$.

- The particular case when κ is the identity mapping of $U(1)^N$, corresponding to the “space-filling” brane $\mathcal{B}_0 = U(1)^N$, describes the disconnected wires. In this case, $P = I$ (i.e. P is the identity matrix) and field φ satisfies the Neumann boundary conditions both at $x = 0$ and $x = L$. One obtains in this case the product of N disconnected theories, already described in Subsection 3.1.2.

³As may be seen from the Smith normal form of matrix (κ_n^m) , such a property is satisfied if and only if the $M \times N$ matrix (κ_n^m) has rank M and the g.c.d. of its $M \times M$ minors is equal to 1, see Proposition 4.3 of [159].

Coming back to the bulk, the general solution of equation of motion (3.19) is

$$\varphi(t, x) = \varphi^\ell(t + x) + \varphi^r(t - x) \quad (3.23)$$

where the fields $\varphi^{\ell/r}$ are function of one variable, defined on the real line, and describe chiral fields propagating to the left and to the right. Boundary conditions (3.18) and (3.20) couple left and right movers by

$$P\partial_x\varphi^\ell(t) = P\partial_x\varphi^r(t), \quad P^\perp\partial_t\varphi^\ell(t) = -P^\perp\partial_t\varphi^r(t), \quad (3.24)$$

Thus with a nontrivial boundary defect (3.17), the left-moving components φ_i^ℓ are related to the right-moving ones φ_j^r in a nondiagonal way, giving a relevant junction of quantum wires.

In order to prepare the quantization of the system, we express left and right movers in terms of modes. Indeed, the boundary conditions (3.18), (3.20) at $x = 0$, (3.15) at $x = L$ and the fact that $P^2 = P$ imply that the fields $\varphi^{\ell/r}$ are necessarily $4L$ -periodic and then can be decomposed as

$$\varphi^{\ell,r}(t \pm x) = \varphi_0^{\ell,r} + \frac{\pi}{2L}\alpha_0^{\ell,r}(t \pm x) + i \sum_{n \neq 0} \frac{1}{n} \alpha_n^{\ell,r} e^{-\frac{\pi i n(t \pm x)}{2L}}, \quad (3.25)$$

with real $\varphi_0 = \varphi_0^\ell + \varphi_0^r$ such that $e^{i\varphi_0} \in \mathcal{B}$. The right modes α_n^r are related to the left ones α_n^ℓ by using P and P^\perp , in order to satisfy (3.24). Moreover, (3.24) also implies

$$P\alpha_{2n+1}^{\ell,r} = 0, \quad P^\perp\alpha_{2n}^{\ell,r} = 0 \quad (3.26)$$

meaning that the odd modes belong to $Im(P^\perp)$ whereas the even ones belong to $Im(P)$. We finally compute the symplectic form Ω on the phase space of the classical solutions in terms of the left movers: only one half of the modes describes the independent degrees of freedom since the remaining half is related to them by the boundary conditions. One obtains:

$$\Omega = \frac{1}{2} \delta\alpha_0^\ell \cdot \wedge \delta\varphi_0 - \frac{i}{2} \sum_{n \neq 0} \frac{1}{n} \delta\alpha_n^\ell \cdot \wedge \delta\alpha_{-n}^\ell. \quad (3.27)$$

The induced Poisson brackets may be extracted from that formula.

3.3 Quantization

We construct the space of states of the theory by canonical quantization. The mode Poisson brackets obtained from symplectic form (3.27) are replaced by $(\frac{1}{i} \times)$ commutators and we represent the algebra obtained this way in the Hilbert space. This part is rather standard but a bit technical. It will allow to define the quantum version of the junction and to investigate the different observables of the system, which will be done in the second step.

3.3.1 Hilbert space

The zero modes φ_0 and α_0^ℓ are completely decoupled from the excited ones α_n^ℓ , thus we can quantize them separately. The boundary conditions $e^{i\varphi_0} \in \mathcal{B}$ and $\alpha_0^\ell \in Im(P)$ mean that N degrees of freedom of zero modes reduce to M , the rank of P . The vectors κ^m are a basis of $Im(P)$. Explicitly,

$$\alpha_0^\ell = \sum_m \beta_m \kappa^m, \quad \varphi_0 = \sum_m \psi_m \kappa^m, \quad (3.28)$$

where (ψ_m) , $m = 1, \dots, M$, are angles parameterizing $U(1)^M$. Rewriting the zero modes part of Ω in terms of ψ_m and β_m , we end up with the commutators

$$[\beta_m, \psi_{m'}] = -2i(T^{-1})_{mm'} \quad (3.29)$$

where the $M \times M$ symmetric matrix $T^{mm'} = \boldsymbol{\kappa}^m \cdot \boldsymbol{\kappa}^{m'}$ encodes the scalar products of vectors $\boldsymbol{\kappa}^m$ and may be seen as defining a metric on \mathbb{R}^M . These are almost canonical commutation relation but nondiagonal. Since angles ψ_m are defined only modulo 2π , the convenient Hilbert space to consider is $\mathcal{H}_0 = L^2[U(1)^M]$ composed of functions of M angles, square integrable in the Haar measure. The action of β_m on this space is defined by setting

$$\beta_m = -2i \sum_{m'} (T^{-1})_{mm'} \frac{\partial}{\partial \psi_{m'}}. \quad (3.30)$$

Since the angular variable ψ_m are multivalued, their action on \mathcal{H}_0 is ill-defined, and only periodic functions of the ψ_m will act as multiplication operators in \mathcal{H}_0 . We will not use these operators in the following focusing only on the momenta β_m , and the corresponding action of $\boldsymbol{\alpha}_0^\ell$. An orthonormal basis of \mathcal{H}_0 is given by the states

$$|k^1 \dots k^M\rangle = \exp\left(i \sum_{m=1}^M k^m \psi_m\right) \quad \text{for } k^m \in \mathbb{Z} \quad (3.31)$$

and it is straightforward to compute the action of the operators β_m , and, subsequently of $\boldsymbol{\alpha}_0^\ell$, which will be sufficient to obtain all the observable considered in the following.

Example 3.2

Consider the previous Example 3.1, with $N = 2$, $M = 1$ and $\kappa = (1, 1)$. Then $T = r_1^2 + r_2^2$ is just a scalar (as a 1 by 1 matrix), and $\mathcal{H}_0 = L^2[U(1)]$ with basis vectors $|k^1\rangle$. We get for the two components of $\boldsymbol{\alpha}_0^\ell$:

$$\alpha_{01}^\ell |k^1\rangle = \alpha_{02}^\ell |k^1\rangle = \frac{2}{r_1^2 + r_2^2} k^1 |k^1\rangle. \quad (3.32)$$

The excited mode part of the symplectic form (3.27) leads to Poisson brackets involving P which are not diagonal in the component α_{ni}^ℓ . Having in mind the canonical quantization of N independent degrees of freedom, we introduce a proper orthonormal basis associated to P and P^\perp , of vectors $\boldsymbol{\Lambda}_j = (\Lambda_{j1}, \dots, \Lambda_{jn})$ for $j = 1, \dots, N$, such that

$$P = \text{diag}(\underbrace{1, \dots, 1}_M, 0, \dots, 0) \quad (3.33)$$

in that basis. Then we consider the excited mode components

$$\tilde{\alpha}_{nj}^\ell = \boldsymbol{\Lambda}_j \cdot \boldsymbol{\alpha}_n^\ell = \sum_i r_i^2 \Lambda_{ji} \alpha_{ni}^\ell \quad (3.34)$$

Such components describe collective oscillations of all N wires. Since this new basis is orthonormal, the excited mode part of the symplectic form (3.27) becomes diagonal in the $\tilde{\alpha}_{nj}^{e/o}$ modes and condition (3.26) becomes much simpler:

$$\tilde{\alpha}_{(2n+1)j} = 0 \quad \text{for } j \leq M, \quad \tilde{\alpha}_{(2n)j} = 0 \quad \text{for } j \geq M + 1. \quad (3.35)$$

This means that the odd modes have M degrees of freedom associated to $\text{Im}(P)$ and the Dirichlet boundary conditions, whereas the even modes have $N - M$ degrees of freedom associated to $\text{Im}(P^\perp)$ and the Neumann boundary conditions. Moreover the corresponding commutators between the non-zero modes take the form

$$[\tilde{\alpha}_{nj}^\ell, \tilde{\alpha}_{nj'}^\ell] = n \delta_{jj'} \delta_{n+n', 0} \quad (3.36)$$

that is a version of the canonical commutation relations. It is straightforward to find a Fock space representation of the resulting algebra. For $j \leq M$, the odd modes vanish, and we consider the (even) Fock space \mathcal{F}_j^e generated from the normalized vacuum $|0\rangle_e$, annihilated by $\tilde{\alpha}_{(2n)j}^\ell$ for $n > 0$ by applying the creation operators $\tilde{\alpha}_{-(2n)j}^\ell = (\tilde{\alpha}_{(2n)j}^\ell)^\dagger$ for $n > 0$. For $j \geq M+1$ we construct the (odd) Fock space \mathcal{F}_j^o in a similar way but considering only the odd modes $\tilde{\alpha}_{(2n+1)j}^\ell$ and the normalized vacuum $|0\rangle_o$. We end up with the full Hilbert space of the theory

$$\mathcal{H} = \mathcal{H}_0 \otimes \left(\bigotimes_{j=1}^M \mathcal{F}_j^e \right) \otimes \left(\bigotimes_{j=M+1}^N \mathcal{F}_j^o \right) \quad (3.37)$$

Example 3.3

Consider the previous Example 3.2 where $N = 2$ and $M = 1$. In that case there is one even and one odd Fock space generated, respectively, by $\tilde{\alpha}_{-(2n)1}^\ell$ acting on $|0\rangle_e$ and by $\tilde{\alpha}_{-(2n+1)2}^\ell$ acting on $|0\rangle_o$, where the modes corresponds to collective oscillations on both wires.

$$\tilde{\alpha}_{(2n)1}^\ell = \frac{1}{r_1^2 + r_2^2} (\alpha_{(2n)1}^\ell + \alpha_{(2n)2}^\ell), \quad \tilde{\alpha}_{(2n+1)2}^\ell = \frac{1}{r_1^2 r_2^4 + r_2^2 r_1^4} (r_2^2 \alpha_{(2n+1)1}^\ell - r_1^2 \alpha_{(2n+1)2}^\ell). \quad (3.38)$$

The total Hilbert space is $\bigoplus_{k_1} \mathbb{C} |k^1\rangle \otimes \mathcal{F}_1^e \otimes \mathcal{F}_2^o$,

3.3.2 $U(1)$ current and charge

Now that the quantum space of states of the junction has been constructed, we would like to understand the operator content of the resulting theory. The simplest operators to understand are the chiral currents associated to the global $U(1)$ -symmetry of the system that acts on the fields by $g_i(t, x) \mapsto u g_i(t, x)$ for $u \in U(1)$. The theory is invariant under this action in the bulk and at $x = L$ since we choose the Neumann boundary condition rather than the Dirichlet ones there. To define a symmetry, this action must also preserve the brane $\mathcal{B} = \kappa(U(1)^M) \subset U(1)^N$, which holds if and only if the vector $\mathbf{1} = (1, \dots, 1)$ belongs to the range of P , i.e.

$$P\mathbf{1} = \mathbf{1} \quad \text{or} \quad \sum_j P_{ij} = 1 \quad \forall i. \quad (3.39)$$

In that case, the components of the Noether current corresponding to this symmetry have the form

$$J^0(t, x) = \sum_{i=1}^N J_i^0(t, x), \quad J^1(t, x) = \sum_{i=1}^N J_i^1(t, x) \quad (3.40)$$

where the contribution of each wire can be computed explicitly. It is however more interesting to look at the chiral components of the currents, since they are directly related to the left and right moving fields (3.23). It turns out that

$$J_i^{\ell, r}(t, x) \equiv \frac{1}{2} (J_i^0 \mp J_i^1)(t, x) = \frac{r_i^2}{2\pi} \partial \varphi_i^{\ell, r}(x \pm t) \quad (3.41)$$

where the derivative on the right hand side acts on the one-variable fields $\varphi_i^{\ell, r}$. This relation defines the left and right currents on each wire, which are at the classical level just functions, respectively, of $t + x$ and $t - x$ for any real t and x . Since only the derivative of the fields $\varphi_i^{\ell, r}$ appears, there is no ambiguity related to the multivaluedness of modes $\varphi_0^{\ell, r}$. One can express J_i^ℓ and J_i^r in terms of the other zero modes and the excited modes. Most importantly, the constraints (3.24) induce the relation

$$J_i^r(t, 0) = \sum_j S_{ij} J_j^\ell(t, 0) \quad \text{where} \quad S \equiv (P - P^\perp)^t \quad (3.42)$$

meaning that the right current of one wire arriving at the junction is scattered to the left currents of all the wires. Hence, to each brane \mathcal{B} one can associate a scattering matrix S , expressing the exchange of chiral currents when they arrive at the junction. Since S is simply related to P , it has real coefficient and the following properties

$$S^t = r^{-2} S r^2, \quad S^2 = I \quad \text{with} \quad r = \text{diag}(r_1, \dots, r_N) \quad (3.43)$$

The first one is due to the fact that the projector is orthogonal only with respect to the non-standard scalar product on \mathbb{R}^N , thus its matrix is not symmetric. The second one expresses the fact that S is actually a reflection with respect to the subspace $\text{Im}(P)$. This second property is specific to our construction and has consequences for the junction. Indeed it means that (3.42) is invariant under the change $\ell \leftrightarrow r$, such that the scattering from left to right is exactly the same as the scattering from right to left. There is actually no underlying physical hypothesis requiring this property and it is an artifact due to our choice of the boundary condition at $x = 0$. Finally, there is one last property satisfied by S , related to the global $U(1)$ -symmetry. Equation (3.39) implies

$$\sum_j S_{ji} = 1 \quad \forall i. \quad (3.44)$$

that was also pointed out in [127]. Note that even if our construction restricts the possible scattering matrices, a large class of them still exists.

Example 3.4

$N = 2$: Consider the previous Example 3.1 of two wires, we get

$$S = \frac{1}{r_1^2 + r_2^2} \begin{pmatrix} r_1^2 - r_2^2 & 2r_1^2 \\ 2r_2^2 & r_2^2 - r_1^2 \end{pmatrix} \xrightarrow{r_1=r_2} \begin{pmatrix} 0 & 1 \\ 1 & 0 \end{pmatrix} \quad (3.45)$$

corresponding in the case of identical wires to the fully transmitting junction.

If we consider the disconnected junction where $N = M$ we get $S = I$ as expected. It turns out that for two wires these are the only possibility for S , if we require (3.39). Thus for a junction of two identical wires, the only possible junctions are the disconnected or the fully transmitting one, so that in our model with $N = 2$, a simultaneous reflection and transmission appears only when the two connected wires are different.

Example 3.5

- *N arbitrary, $M = 1$: it is easy to generate an interesting S -matrix for any number of wires by considering the brane \mathcal{B} diagonally embedded into $U(1)^N$ so that $\kappa = (1, \dots, 1)$. This leads to the S -matrix that for equal radii takes the form*

$$S_{ij} = -\rho \delta_{ij} + \tau(1 - \delta_{ij}), \quad \text{where} \quad \rho = \frac{N-2}{N}, \quad \tau = \frac{2}{N} \quad (3.46)$$

are the reflection and transmission coefficients (note that for $N = 2$ we come back to the fully transmitting junction). Hence for $N \geq 3$ our model is able to generate interesting S matrices, even in the case of the same theory on each wire.

- *$N = 3, M = 2$: Consider*

$$\kappa = \begin{pmatrix} p & -q & 0 \\ 1 & 1 & 1 \end{pmatrix}, \quad p, q \in \mathbb{Z}, \quad p \wedge q = 1. \quad (3.47)$$

The corresponding S -matrix is (again in the case of the same radii)

$$S = \frac{1}{(1+\alpha+\alpha^2)} \begin{pmatrix} 1+\alpha & -\alpha & \alpha(1+\alpha) \\ -\alpha & \alpha(1+\alpha) & 1+\alpha \\ \alpha(1+\alpha) & 1+\alpha & -\alpha \end{pmatrix}, \quad \alpha = \frac{p}{q} \quad (3.48)$$

which is exactly the matrix obtained in the classification in [14], equation (3.16), but with a rational parameter instead of a real one. We see in that example that dealing with integers in our case is not too restrictive since we can approach real cases as close as we want.

Coming back to the chiral currents, the scattering relation (3.42) can be extended to general x and t since we are actually dealing with one-variable functions. Moreover, the Neumann boundary condition (3.20) at $x = L$ implies the full reflection of the current at the free extremity of the wires: $J_i^r(t, L) = J_i^\ell(t, L)$. Note that this relation would have come with a minus sign for the Dirichlet boundary condition, breaking the global $U(1)$ -symmetry. Altogether, using also the property $S^2 = I$, we end up with the relation

$$J_i^r(t, x) = J_i^\ell(t, -x + 2L) \quad (3.49)$$

if we treat the currents as functions of real t and x . This is just the consequence of the relation between the left and the right modes $\alpha_{ni}^{\ell,r}$ coming from (3.24). Indeed we have

$$J_i^{\ell,r}(t, x) = \frac{r_i^2}{4L} \sum_{n \in \mathbb{Z}} \alpha_{ni}^{\ell,r} e^{-\frac{\pi i n(t \pm x)}{2L}}. \quad (3.50)$$

This allows us to define a quantum version of the currents and compute their equal-time commutation relations

$$[J_i^\ell(t, x), J_{i'}^\ell(t, y)] = \frac{ir_i^2}{4\pi} \sum_{n \in \mathbb{Z}} (P_{ii'} + (-1)^n (\delta_{ii'} - P_{ii'})) \delta'(x - y + 2nL) \quad (3.51)$$

and similarly for the right currents but with a global minus sign on the right hand side. The mixed relations read

$$[J_i^\ell(t, x), J_{i'}^r(t, y)] = \frac{ir_i^2}{4\pi} \sum_{n \in \mathbb{Z}} (P_{ii'} - (-1)^n (\delta_{ii'} - P_{ii'})) \delta'(x + y + 2nL). \quad (3.52)$$

In particular, the left-moving currents commute among themselves at equal times if their positions do not coincide modulo $2L$. Similarly for the right-moving currents. The left-moving currents commute with the right-moving ones at equal times if their positions are not opposite modulo $2L$.

Note that for $0 < x, y \leq L$ the only terms that contribute to (3.51) and (3.52) have $n = 0$ or $n = -1$, respectively, so that for such values of x and y the commutation relations of currents do not depend on the choice of brane \mathcal{B} . This permits to identify for different junctions the algebras of observables generated by currents $J_i^{\ell,r}(0, x)$ with $0 < x \leq L$, i.e. localized away from the contact point. In particular, we may identify such observables for disconnected wires with those for connected wires, with the physical meaning that their measurement just before and just after establishing or breaking the connection between the wires should give the same result.

Whatever the junction, the total $U(1)$ -charge

$$Q(t) = \sum_{i=1}^N \int_0^L (J_i^l + J_i^r)(t, x) dx = \sum_{i=1}^N \frac{r_i^2}{2} \alpha_{0i} \quad (3.53)$$

is conserved in time as soon as (3.39) is satisfied. Its modes decomposition tells us that Q acts only on the zero mode Hilbert space \mathcal{H}_0 , with the following spectrum

$$Q |k^1 \dots k^M\rangle = (\mathbf{p}, (T^{-1})\mathbf{k}) |k^1 \dots k^M\rangle \quad (3.54)$$

where \mathbf{p} is a vector in \mathbb{R}^M with components $p^m = \sum_i r_i^2 \kappa_i^m$. Here (\mathbf{x}, \mathbf{y}) denotes the standard scalar product of \mathbb{R}^M , not to be confused with the modified one $\mathbf{a} \cdot \mathbf{b}$ in \mathbb{R}^N introduced before. This is not obvious but it turns out that the spectrum of Q is composed of integers, as must be the case for the generator of a unitary action $U(1)$ -group. This can be shown explicitly using property (3.39) for P ensuring $U(1)$ invariance and the fact that κ is an injective map. However the integrality does not hold for the charges in individual wires, which are not conserved.

Example 3.6

Consider the case $N = 3$ and $M = 2$ discussed in Example 3.5. In the case of different radii, we get

$$T = \begin{pmatrix} p^2 r_1^2 + q^2 r_2^2 & pr_1^2 - qr_2^2 \\ pr_1^2 - qr_2^2 & r_1^2 + r_2^2 + r_3^3 \end{pmatrix} \quad \text{and} \quad \mathbf{p} = \begin{pmatrix} pr_1^2 - qr_2^2 \\ r_1^2 + r_2^2 + r_3^3 \end{pmatrix} \quad (3.55)$$

Of course the vector $T^{-1}\mathbf{k}$ will not have integer coefficients, however we end up with a simple spectrum for Q

$$Q |k^1 k^2\rangle = k^2 |k^1 k^2\rangle \quad (3.56)$$

where $k_2 \in \mathbb{Z}$.

3.3.3 Energy-momentum tensor and Hamiltonian

In addition to the $U(1)$ global charge, energy is always conserved in the system whatever the junction. The classical Hamiltonian of the theory can be expressed in terms of left and right currents

$$H(t) = \sum_{i=1}^N \frac{2\pi}{r_i^2} \int_0^L ((J_i^\ell)^2 + (J_i^r)^2)(x, t) dx \quad (3.57)$$

Its time independence can be shown explicitly and does not require any supplementary condition on P such as (3.39), properties (3.43) being sufficient. In fact, the the boundary conditions with any brane \mathcal{B} preserve conformal invariance of the system, hence the Hamiltonian is nothing but the charge associated to the time components of the total energy momentum tensor of the theory.

At the quantum level, some regularization must be done to avoid infinite quantities. We set

$$H = \sum_{i=1}^N \frac{2\pi}{r_i^2} \int_0^L (:(J_i^\ell)^2: + :(J_i^r)^2:)(x, t) dx + \frac{\pi}{L} \frac{N-3M}{48} \quad (3.58)$$

Indeed H can be decomposed in terms of the zero modes α_{0i}^ℓ and the excited ones $\tilde{\alpha}_{ni}^\ell$ in the proper basis for P (using an inverse relation for (3.34)). The Wick ordering of the modes satisfying canonical commutation relations extracts a zero-point energy which is a diverging sum whose ζ -function regularization leads to the last term on the right hand side of the quantum formula for H .

ζ -function regularization More precisely, the contributions to the zero-point energy from each of the Fock spaces $\mathcal{F}_j^{e/o}$ is the infinite sum

$$\sum_{\substack{n=1 \\ n \text{ even/odd}}}^{\infty} \frac{n}{2} \quad (3.59)$$

This infinite sum is regularized by the Riemann zeta function $\zeta(s) = \sum_{n=1}^{\infty} n^{-s}$ for s where the sum converges and defined by analytic continuation for other values. In particular $\zeta(-1) = -1/12$ which gives a finite result for the sum $\sum_{n=1}^{\infty} \frac{n}{2}$. Actually we have M sums over even number and $N - M$ sums over odd numbers, resulting in

$$M \sum_{p=1}^{+\infty} \frac{2p}{2} + (N - M) \sum_{p=1}^{+\infty} \frac{2p+1}{2} = M\zeta(-1) + (N - M) \left(\frac{\zeta(-1)}{2} - \zeta(-1) \right) = \frac{3M-N}{2} \zeta(-1) \quad (3.60)$$

where we have written the odd sum as a difference between the sum over all and even positive integers. Of course this term is somewhat arbitrary and does not contribute to physical quantities such as the thermal expectations of observables, see below, but the above regularization is consistent with the functional integral approach to the theory.

Using the mode decomposition of H , we compute its spectrum: the basis vector of \mathcal{H}_0 and states generating the different Fock spaces discussed in subsection 3.3.1 are actually eigenstates of H . On \mathcal{H}_0 , we get

$$H |k^1 \dots k^M\rangle = \frac{\pi}{2L} \left(2(\mathbf{k}, T^{-1}\mathbf{k}) + \frac{N-3M}{24} \right) |k^1 \dots k^M\rangle \quad (3.61)$$

whereas the action on the excited Fock-space states is longer to write but simple: consider for example the basis vectors of one Fock space $\mathcal{F}_j^{e/o}$

$$\tilde{\alpha}_{(-n_1)j} \dots \tilde{\alpha}_{(-n_l)j} |0\rangle_{e/o}, \quad l \geq 0 \quad n_1 \geq \dots \geq n_l > 0 \quad (3.62)$$

where the n_s will be even or odd, depending on j . The action of creation modes raises the eigenvalue of H by

$$\frac{\pi}{2L} n \quad \text{where} \quad n = n_1 + \dots + n_l \quad (3.63)$$

and the generalization to the full Hilbert space is immediate, resulting in the sum of such contributions from the N Fock spaces. The degeneracy of this spectrum will be investigated in the next section.

As for the charge, the total Hamiltonian can be decomposed as the sum of contributions from different wires

$$H = \sum_{i=1}^N H_i = \sum_{i=1}^N \int_0^L K_i^0(t, x) dx \quad (3.64)$$

with the energy density $K_i^0 = T_i^r + T_i^\ell$ and the energy current $K_i^0 = T_i^r - T_i^\ell$ in each wires, where

$$T_i^{\ell/r}(t, x) = \frac{2\pi}{r_i^2} : J_i^{\ell/r}(t, x)^2 : - \frac{\pi}{48L^2} P_{ii} + \frac{\pi}{96L^2} P_{ii}^\perp \quad (3.65)$$

are the left- and right-moving energy momentum tensor components (again, constant terms are the zero point energy contributions). The individual wire Hamiltonians H_i are not conserved but their total sum H is. Moreover, we can compute the relation between the chiral components of the individual wire contributions to the energy-momentum tensor, similarly to (3.42) for the currents:

$$T_i^r(t, 0) = \sum_{j=1}^N S_{ij} T_j^\ell(t, 0) S_{ji} + \frac{2\pi}{r_i^2} \sum_{j \neq k} S_{ij} J_j^\ell(t, 0) S_{ik} J_k^\ell(t, 0) \quad (3.66)$$

which tells us how the energy from the right moving part is scattered to the left moving one at the junction. Hence the scattering matrix for the $U(1)$ currents induces a transfer of energy at the junction. The latter relation, however, does not close on the $T_i^{\ell,r}$ components and also involves the currents.

3.4 Equilibrium state

In previous sections, we quantized the bosonic model of the junction. The Hilbert space has M zero modes degrees of freedom and N infinite series of excited Fock space states divided into to M even and $N - M$ odd series. The two conserved quantities are the total $U(1)$ (electric) charge and the total energy of the system represented by observables Q and H , and the first one is present only for specific branes \mathcal{B} preserving the global $U(1)$ -symmetry. Before constructing a nonequilibrium state of the system, we first focus on its equilibrium properties, since nonequilibrium expectations will be expressed as a combination of appropriate equilibrium ones. The equilibrium state where the full system of all the wires is at inverse temperature β and electric potential V is given by the following density matrix

$$\rho_{\beta,V} = \frac{1}{Z_{\beta,V}} e^{-\beta(H-VQ)} \quad (3.67)$$

where $Z_{\beta,V}$ is the the partition function. Note that with our conventions, positive V plays the role of a positive chemical potential for electrons and of a negative one for holes. The partition function is exactly computable from the spectra (3.54) of Q and the H (with the multiplicities). The spectrum of H is given by (3.61) on \mathcal{H}_0 . For the excited modes, each Fock space leads to degenerate energy levels involving the partition number $p(n)$, counting all the different ways of writing an integer n as a sum of ordered smaller integers, see (3.63). The numbers of partitions are encoded in the Dedekind function [50], which is the partition function for one free boson:

$$\eta(\tau) = e^{\frac{\pi i \tau}{12}} \prod_{n=1}^{\infty} (1 - e^{2\pi i \tau n}) \quad (3.68)$$

and has the modular property $\eta(\tau) = (-i\tau)^{-1/2} \eta(-\tau^{-1})$. Here we have N copies of such functions, but we have to take care of the odd or even parity of the numbers in the partitions, and express the corresponding generating functions in terms of standard Dedekind functions. The \mathcal{H}_0 sector leads to k -sums that can be improved by the Poisson resummation formula and some Gaussian integration. Putting all together we end up with

$$Z_{\beta,V} = 2^{-N} \sqrt{\det(T)} e^{\frac{L\beta V^2}{4\pi}(\mathbf{p}, T^{-1}\mathbf{p})} \left(\sum_{\mathbf{k} \in \mathbb{Z}^M} e^{-iLV(\mathbf{p}, \mathbf{k}) - \frac{\pi L}{\beta}(\mathbf{k}, T\mathbf{k})} \right) \left[\eta\left(\frac{2iL}{\beta}\right) \right]^{N-2M} \left[\eta\left(\frac{4iL}{\beta}\right) \right]^{M-N} \quad (3.69)$$

where the Dedekind functions come from the excited states, whereas the remaining factor is related to the zero modes. In the \mathbf{k} -sum, one term in the exponential corresponds to the action of Q and the other to the action of H (compare with the spectrum (3.54) and (3.61)). The modular property of η and the Poisson resummation allowed to have coefficients proportional to L instead of $1/L$ in the exponential terms, which will be more tractable when considering the thermodynamic limit, see section 3.5.

Once the density matrix defined and the partition function computed, let us focus on the algebra \mathcal{A} of observables generated by the currents $J_i^{\ell,r}$ and on the corresponding equilibrium state expectations

$$\omega_{\beta,V}^L(A) = \text{Tr}(\rho_{\beta,V} A), \quad A \in \mathcal{A}. \quad (3.70)$$

The superscript L stresses that the state concerns the junction of wires of finite length L . Due to relation (3.49) it is enough to consider only the currents $J^\ell(t, x)$ at fixed t and real x . We shall decompose such currents into the contributions from the zero modes and the excited modes:

$$J_i^\ell(t, x) = \frac{r_i^2}{4L} \alpha_{0i}^\ell + \hat{J}_i^\ell(t, x), \quad (3.71)$$

see (3.50). In the equilibrium state expectation of products of currents, the contributions from the zero modes and from the excited modes factorize. Since Q is proportional to the zero modes

α_{0i}^ℓ , it is possible to extract the zero-modes expectations by successive derivatives of $\log Z$, with respect to the (formal) coordinates p^m in (3.69). For one zero mode we get,

$$\omega_{\beta,V}^L \left(\frac{r_i^2}{4L} \alpha_{0i}^\ell \right) = \frac{r_i^2 V}{4\pi} - \frac{r_i^2}{2\beta} \sum_m \kappa_i^m \frac{\sum_{\mathbf{k} \in \mathbb{Z}^M} k^m e^{-iLV(\mathbf{p},\mathbf{k}) - \frac{\pi L}{\beta}(\mathbf{k},T\mathbf{k})}}{\sum_{\mathbf{k} \in \mathbb{Z}^M} e^{-iLV(\mathbf{p},\mathbf{k}) - \frac{\pi L}{\beta}(\mathbf{k},T\mathbf{k})}}, \quad (3.72)$$

where the first term has been simplified using the condition (3.39) on P ensuring charge conservation. This formula is already quite heavy, and the general formula for an arbitrary number of zero modes expectation is straightforward to obtain, involving more terms with \mathbf{k} -sums. We actually do not need it for the following hence we don't write it here but it can be found in [85]. Moreover, in the one point case, we see that the second term involving the sum will vanish in the thermodynamic limit, and the general zero modes expectations will just become a product involving the first term on the right hand side of (3.72).

The expectations of products of $\hat{J}_i^\ell(t, x)$ can be computed with the Wick rule since the Hamiltonian H is quadratic in the $\tilde{\alpha}_{ni}^\ell$. Hence we just need to compute the one and two point correlation function. Knowing explicitly the Hilbert space and the action of H , Q and $\hat{J}_i^\ell(t, x)$, one shows easily that $\omega_{\beta,V}^L(\hat{J}_i^\ell(t, x)) = 0$. For the two point function one end up after some algebra with the result

$$\omega_{\beta,V}^L(\hat{J}_i^\ell(t, x) \hat{J}_j^\ell(t, y)) = -\frac{1}{2} \left(\frac{r_i}{2\pi} \right)^2 \left(P_{ij} f_e(x-y) + (\delta_{ij} - P_{ij}) f_o(x-y) \right) \quad (3.73)$$

where

$$\begin{aligned} f_e(x-y) &= \wp(x-y; -i\beta, 2L) + C_e \\ f_o(x-y) &= 2\wp(x-y; -i\beta, 4L) - \wp(x-y; -i\beta, 2L) + C_o \end{aligned} \quad (3.74)$$

involve the Weierstrass function $\wp(z; \omega_1, \omega_2)$ on the real line $z = x-y$ and with periods $\omega_1 = -i\beta$ and $\omega_2 = 2L$ or $4L$. Such a function is uniquely defined (up to a constant) on the complex torus of period ω_1 and ω_2 by a pole of order 2 at $z = 0$ with coefficient 1, and its analyticity on the rest of the torus [169]. One explicit formula for \wp , actually the one arising in the previous calculation is

$$\wp(z; \omega_1, \omega_2) = \left(\frac{\pi}{\omega_2} \right)^2 \left[-\frac{1}{3} + \sum_n \sin^{-2} \left(\frac{\pi(z-n\omega_1)}{\omega_2} \right) - \sum_{n \neq 0} \sin^{-2} \left(\frac{\pi n \omega_1}{\omega_2} \right) \right]. \quad (3.75)$$

The terms in the first sum imply that the two-point function (3.73) is singular when the insertion points x and y coincide modulo $2L$, which is related to the contact terms appearing in the commutators of the currents, see (3.51). The uniqueness of \wp allows us to permute ω_1 and ω_2 since it defines the same torus. This will be convenient when taking the thermodynamic limit. Indeed with $\omega_1 = 2L \rightarrow \infty$, only the singular $n = 0$ term will survive in (3.75) when $L \rightarrow \infty$. However, not only \wp comes out from our calculation, but also two constant terms, which are

$$C_e = \left(\frac{\pi}{2L} \right)^2 \left(\frac{1}{3} - \sum_{n \neq 0} \sinh^{-2} \left(\frac{\pi n \beta}{2L} \right) \right), \quad (3.76)$$

$$C_o = \left(\frac{\pi}{2L} \right)^2 \left(-\frac{1}{6} - \frac{1}{2} \sum_{n \neq 0} \sinh^{-2} \left(\frac{\pi n \beta}{4L} \right) + \sum_{n \neq 0} \sinh^{-2} \left(\frac{\pi n \beta}{2L} \right) \right). \quad (3.77)$$

These terms are not really easy to handle in the thermodynamic limit and some work with the theory of the Weierstrass function is necessary in order to express these constants in a more convenient way, see below.

We have collected all the ingredients to compute any current correlation function expressing the expectation of $A \in \mathcal{A}$ in the state $\omega_{\beta,V}^L$. The left moving currents factorize between zero and excited modes, and the correlation functions of the latter ones are computed by the Wick formula so that (3.73) is all one need to know. Correlation functions involving the right currents are reduced to those of the left currents only using relation (3.49). Since the one point function is time and space invariant, it follows that $\omega_{\beta,V}^L(J_i^r(t, x))$ is also given by (3.72) so that

$$\omega_{\beta,V}^L(J_i^0(t, x)) = 2\omega_{\beta,V}^L(J_i^\ell(t, x)), \quad \omega_{\beta,V}^L(J_i^1(t, x)) = 0. \quad (3.78)$$

Hence, in the equilibrium state, the mean charge density is constant in each wire, whereas the mean current vanishes. The state $\omega_{\beta,V}^L$ is stationary in the sense that all the equal-time t expectations do not depend on t . Computing the two point correlation functions for the right currents, it is easy to see that we end up with exactly the same formula as for the left currents. It follows that the equilibrium state we constructed is invariant under the exchange $J^\ell \leftrightarrow J^r$, the property related to the time-reversal invariance of the system. This symmetry will be broken in the stationary nonequilibrium state constructed below.

The equilibrium expectations of the components of the energy-momentum tensor may be extracted from the two point function for left and for right currents, respectively, using the operator product expansion (OPE)

$$\omega_{\beta,V}^L(T_i^\ell(t, x)) = \lim_{\epsilon \rightarrow 0} \omega_{\beta,V}^L\left(\frac{2\pi}{\epsilon^2} J_i^\ell(t, x + \epsilon) J_i^\ell(t, x) + \frac{1}{4\pi\epsilon^2}\right) = \omega_{\beta,V}^L(T_i^\ell(t, x)). \quad (3.79)$$

The result is given in [85].

3.4.1 Functional integral representation

The equilibrium expectations at inverse temperature β may be reproduced by a functional integral over classical fields defined on the cylindrical worldsheet $(x, \tilde{t}) \in [0, L] \times [0, \beta]$, see Figure 3.2, where \tilde{t} is the Euclidean time related to the Minkowskian time t by the Wick rotation $\tilde{t} = it$. In particular, The partition function $Z_{\beta,V}$ can be represented as

$$Z_{\beta,V} = \int e^{iS^E[g]} \mathcal{D}g \quad (3.80)$$

where the functional integral is over the maps $\mathbf{g}(t, x) = (e^{i\varphi_i(\tilde{t}, x)})$ from $\mathbb{R} \times [0, L]$ to $U(1)^N$ which are twisted β -periodic in \tilde{t} ,

$$\mathbf{g}(\tilde{t} + \beta, x) = \mathbf{g}(\tilde{t}, x) e^{-\beta V} \quad (3.81)$$

where V is assumed imaginary here (the real values of V will be accessible by analytic continuation). Field \mathbf{g} satisfies the boundary conditions

$$\mathbf{g}(\tilde{t}, 0) \in \mathcal{B}, \quad P(\mathbf{g}^{-1} \partial_x \mathbf{g})(\tilde{t}, 0) = 0, \quad (\mathbf{g}^{-1} \partial_x \mathbf{g})(\tilde{t}, L) = 0 \quad (3.82)$$

In this picture, the field \mathbf{g} represents an open string of size L in $(U(1))^N$ with specified boundary conditions at $x = 0$ and L , which propagates (twisted) periodically in Euclidean time \tilde{t} from 0 to β . Hence the name of open string picture. The Euclidean action functional $S^E(\mathbf{g})$ (purely imaginary in our convention) is obtained by the replacement $t \mapsto -i\tilde{t}$ in the initial action (3.14) with the time integration from 0 to β .

The functional integral for the partition function may be calculated explicitly by decomposing fields on the infinite basis of the Laplacian operator with the appropriate boundary conditions, and the final result matches with (3.69) (see [85]). On the top of that, using the Green functions of the Laplacian (also depending on boundary conditions), one can show that the the thermal

equilibrium expectations of products of currents coincide with the functional integral expectations. Namely,

$$\omega_{\beta,V}^L \left(\prod_{k=1}^K J_{i_k}^\ell(t, x_k) \prod_{k'=1}^{K'} J_{i_{k'}}^r(t, y_{k'}) \right) = \frac{1}{Z_{\beta,V}} \int \prod_k j_{i_k}^\ell(0, x_k) \prod_{k'} j_{i_{k'}}^r(0, y_{k'}) e^{iS^E(\mathbf{g})} \mathcal{D}\mathbf{g}, \quad (3.83)$$

where the j_i are given by derivatives of fields φ_i associated to \mathbf{g} , see [85].

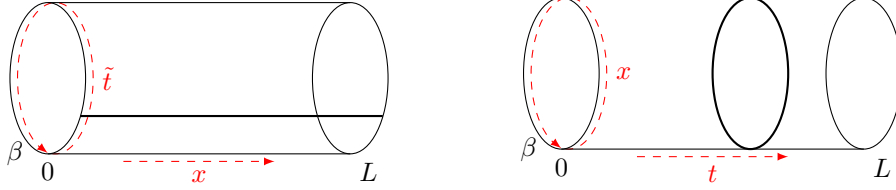


Figure 3.2: Left: the open string picture where the spatial coordinate x is in a finite interval of length L whereas the Euclidean time \tilde{t} is in a circle of length β . Right: the roles of space and time are reversed in the closed string picture.

3.4.2 Closed-string picture

In the previous Euclidean functional integral formalism, the role of “space” and “time” is completely arbitrary and indistinguishable, they are only two orthogonal direction and their roles can be exchanged. Consequently, there should exist a representation of the thermal state $\omega_{\beta,V}^L$ where $[0, \beta]$ plays the role of space and $[0, L]$ the role of time. In the cylindrical geometry, we then have a space-(twisted)-periodic string (hence closed), propagating during “time” L , which corresponds to the closed-string worldsheet depicted on the right of Figure 3.2, to be contrasted with the open-string worldsheet on the left.

Since the space direction is closed, no boundary conditions are needed here. Here the previous boundary conditions from the open-string picture will be encoded here as initial (and final) conditions in the time direction. At the quantum level, this means that the closed string will propagate between two boundary states, that have to be constructed in order to reproduce the equilibrium expectations of $\omega_{\beta,V}^L$. Apart from these states, the closed string is easier to quantize than the open one.

A collection of N closed strings of length β , is described by fields $g_i(t, x) = e^{i\varphi_i(x,t)}$ defined for real t and x and twisted-periodic in the x direction:

$$g_i(t, x + \beta) = g_i(t, x) e^{-\beta V}, \quad (3.84)$$

where V is again taken imaginary, compare to (3.81). For Minkowski time, such fields are governed by the action functional

$$S[\mathbf{g}] = \frac{1}{4\pi} \sum_{i=1}^N \int dt \int_0^\beta r_i^2 ((\partial_t \varphi_i)^2 - (\partial_x \varphi_i)^2) dx. \quad (3.85)$$

The twist in the periodicity condition may be absorbed by setting

$$\varphi_i(t, x) \equiv \hat{\varphi}_i(t, x) + iVx, \quad \text{where} \quad \hat{\varphi}_i(t, x + \beta) = \hat{\varphi}_i(t, x) + 2\pi m_i, \quad (3.86)$$

and $m_i \in \mathbb{Z}$ is the winding number of the field $\hat{\varphi}_i$ when x goes from 0 to β , ($\hat{\varphi}_i$ is only defined modulo 2π). The equations of motions minimizing the action lead to the d’Alembertian acting

on $\hat{\varphi}$, which has again for general solution a sum of two chiral components $\hat{\varphi}_i = \hat{\varphi}_i^\ell + \hat{\varphi}_i^r$ but this time the left and right fields are independent since we have periodic boundary conditions in space for fields $e^{i\hat{\varphi}_i}$. The left and right movers can be decomposed in terms of modes, similarly as for the open string case. We have:

$$\hat{\varphi}^{\ell,r}(t \pm x) = \hat{\varphi}_0^{\ell,r} + \frac{\sqrt{2}\pi}{\beta} \alpha_0^{\ell,r}(t \pm x) + \frac{i}{\sqrt{2}} \sum_{n \neq 0} \frac{1}{n} \alpha_n^{\ell,r} e^{-\frac{2\pi i n(t \pm x)}{\beta}} \quad (3.87)$$

There is no particular relation between the left and right modes, except that

$$\frac{1}{\sqrt{2}}(\alpha_0^\ell - \alpha_0^r) = \mathbf{m} \quad (3.88)$$

where \mathbf{m} is the vector of N winding numbers $m_i \in \mathbb{Z}$, already discrete at the classical level. The zero modes involve $\varphi_0^{\ell,r}$ and $\mathbf{p}_0 \equiv 1/\sqrt{2}(\alpha_0^\ell + \alpha_0^r)$ which is the momentum vector of N closed strings. The quantization of these modes leads to the states

$$|\mathbf{m}, \mathbf{k}\rangle \in \mathcal{H}_0 = \bigoplus_{\mathbf{m} \in \mathbb{Z}} L^2(U(1)^N), \quad (3.89)$$

where \mathbf{k} is the momentum eigenvalue. The quantization of the excited modes is done independently for left and right movers and leads to the independent canonical commutation relation for both. They are represented in the tensor product of two standard Fock spaces $\mathcal{F}^{\ell,r}$ generated by the $\alpha_{ni}^{\ell,r}$ with negative n acting on the vacuum vector $|0\rangle^{\ell,r}$. The Hilbert space of the full theory is $\mathcal{H} = \mathcal{H}_0 \otimes \mathcal{F}^\ell \otimes \mathcal{F}^r$.

The quantized closed string propagates between boundary states in (a completion of) \mathcal{H} that encode the information on the junction and the reflection at the free ends of the wires. Such a propagation will reproduce the thermal expectations in the state $\omega_{\beta,V}^L$. Let us start with the free ends of the wires, characterized by the diagonal Neumann boundary condition. Thus in the closed string picture, we want to build a state satisfying

$$\partial_t \varphi_i(0, x) ||\mathcal{N}\rangle\rangle = 0 \quad (3.90)$$

(recall that time and space have been exchanged so that the Neumann condition now corresponds to time derivative). This equation relates the chiral components of the field φ_i in the action on such state. Using the mode decomposition (3.87) and looking at the different parts of the Hilbert space, we first see that state $||\mathcal{N}\rangle\rangle$ necessarily has no momentum: $\mathbf{k} = \mathbf{0}$, whereas \mathbf{m} can be any integer vector. On the excited part, the relation between left and right modes reads

$$(\alpha_{ni}^\ell + \alpha_{(-n)i}^r) ||\mathcal{N}\rangle\rangle = 0 \quad (3.91)$$

The most general solution for such states, together with the zero mode part, is given by [74, 135]

$$||\mathcal{N}\rangle\rangle = A_{\mathcal{N}} \sum_{\mathbf{m} \in \mathbb{Z}^N} e^{-\sum_{n=1}^{\infty} \frac{1}{n} \alpha_{-n}^\ell \cdot \alpha_{-n}^r} |\mathbf{0}, \mathbf{m}\rangle \quad (3.92)$$

where $A_{\mathcal{N}}$ is a normalization constant. Note that this state belongs only to the completion of the Hilbert space \mathcal{H} since it involves infinite sums. Similarly, a diagonal Dirichlet state $||D\rangle\rangle$ is easy to construct [74, 135]: it will require $\mathbf{m} = 0$ and \mathbf{k} arbitrary in the zero modes, whereas the plus sign in (3.91) will become a minus sign, removing the one in the exponential coefficient of (3.92). Finally, the junction of the wires mixes the Neumann and the Dirichlet boundary conditions, see (3.18) and (3.20). In the closed string picture, the boundary state $||\mathcal{B}\rangle\rangle$ corresponding to the brane \mathcal{B} satisfies the relations

$$P \partial_x \varphi(0, x) ||\mathcal{B}\rangle\rangle = 0, \quad P^\perp \varphi(0, x) ||\mathcal{B}\rangle\rangle = 0 \quad (3.93)$$

where $\varphi = (\varphi_i)$. Using decomposition (3.87) for φ we get constraints for the zero modes and for the excited part taking a simple form if we decompose the modes in the eigen-basis of P . In such a basis, we end up with M Neumann boundary conditions and $(N - M)$ Dirichlet ones. It is then possible to write an explicit expression for $||\mathcal{B}\rangle\rangle$ that was given in [85].

3.4.3 Equivalence between open and closed string

The thermal equilibrium state expectations are represented in the closed string picture by the ratios of the transition amplitudes by

$$\mathcal{E}_{cs}^L(A) = \frac{\langle\langle \mathcal{N} | e^{-LH} A | \mathcal{B} \rangle\rangle}{\langle\langle \mathcal{N} | e^{-LH} | \mathcal{B} \rangle\rangle} \quad (3.94)$$

for $A \in \mathcal{A}_{cs}$, the algebra of currents defined by

$$\mathcal{J}_i^{\ell,r}(t, x) = \frac{r_i^2}{2\pi} \partial \varphi_i^{\ell,r}(t \pm x), \quad (3.95)$$

and for the closed-string Hamiltonian given by

$$H = H_{cs} + iVQ_{cs}^m - \frac{V^2\beta}{4\pi} \quad (3.96)$$

where H_{cs} is the standard Hamiltonian of N closed string and the two extra terms come from (3.86) due to the twisted periodicity (Q_{cs}^m is the magnetic charge related to the winding numbers \mathbf{m}).

The ratios (3.94) are not always well defined and need some precisions. The equivalence between open and closed string picture is established by the following relation:

$$\omega_{\beta,V}^L \left(\prod_{k=1}^K J_{i_k}^{\ell}(0, x_k) \prod_{k'=1}^{K'} J_{i_{k'}}^r(0, y_{k'}) \right) = (-i)^{K+K'} \mathcal{E}_{cs}^L \left(\mathcal{T} \prod_{k=1}^K \mathcal{J}_{i_k}^{\ell}(-ix_k, 0) \prod_{k'=1}^{K'} \mathcal{J}_{i_{k'}}^r(-iy_{k'}, 0) \right) \quad (3.97)$$

where the Euclidean time ordering \mathcal{T} puts the operators at bigger x_k or $y_{k'}$ to the left. The powers of $-i$ and i represent the derivatives of the Euclidean conformal change of variables that reverses the roles of time and space. The proof of this statement is based on the explicit computation of the one and two point functions in the closed string picture. It is shown in [85] that they match with the open string thermal expectations, using non trivial identities involving the Weierstrass function. Moreover one shows that boundary states $||B\rangle\rangle$ also reproduce the scattering rule (3.42) in the closed string language.

Summarizing The equilibrium state $\omega_{\beta,V}^L$ in the open string picture can be represented by the closed string propagating in Euclidean time of duration L between the boundary states $||B\rangle\rangle$ and $||N\rangle\rangle$. These are two different representation of the same Euclidean functional integral corresponding to different choice of space and time directions. The equivalence of two representations was proved by showing that the expectation values on the algebra of currents are identical in the two pictures. Hence we may use whichever descriptions of the equilibrium state is more convenient.

3.5 Thermodynamic limit

Having in mind the construction of a nonequilibrium state, we would like to consider the case where the wires are semi-infinite, so that far from the junction they can be considered as reservoirs. This corresponds to the thermodynamic limit $L \rightarrow \infty$, that can be taken now explicitly after the work we have done. The general idea is the following: in the closed string picture, L appears only in front of the Hamiltonian H in the expectation \mathcal{E}_{cs}^L , see (3.94), and nowhere else. Hence in the thermodynamic limit, only the state with lowest eigenvalues of H will contribute and the Neumann state can be replaced by the closed string vacuum $|\mathbf{0}, \mathbf{0}\rangle$ so that \mathcal{E}_{cs}^L tends to the limit

$$\mathcal{E}_{cs}(A) = \frac{\langle\langle \mathbf{0}, \mathbf{0} | e^{-LH} A | \mathbf{0}, \mathbf{0} \rangle\rangle}{\langle\langle \mathbf{0}, \mathbf{0} | e^{-LH} | \mathbf{0}, \mathbf{0} \rangle\rangle} \quad (3.98)$$

which is much simpler to compute. In fact, our formulae in the open string picture have been already improved so that $L \rightarrow \infty$ limit may be obtained for them directly and shown to be represented in the closed string picture by the corresponding ratios (3.98).

The partition function $Z_{\beta,V}$ diverges when $L \rightarrow \infty$ but the free energy per unit length has a limit:

$$f_{\beta,V}^L = -\frac{1}{L\beta} \ln Z_{\beta,V} \xrightarrow{L \rightarrow \infty} -\frac{V^2}{4\pi} \sum_{i=1}^N r_i^2 - \frac{\pi N}{6\beta^2} \equiv f_{\beta,V} \quad (3.99)$$

as easily follows from (3.69).

In the limiting zero mode expectations for one left current obtained from (3.72), only the first term does not vanish and the generalization for several zero mode left currents is just the product of such terms (this was not true in the finite size case).

$$\lim_{L \rightarrow \infty} \omega_{\beta,V}^L \left(\prod_{k=1}^K \frac{r_{i_k}^2}{4L} \alpha_{0i_k}^\ell \right) = \prod_{k=1}^K \frac{r_{i_k}^2 V}{4\pi} \quad (3.100)$$

Then we look at the two point function of the excited part (3.73). The periods of the Weierstrass function can be exchanged so that most of the terms vanish in (3.75) with $\omega_1 = 2L \rightarrow \infty$. Finally, a nontrivial identity for the Weierstrass functions [169] basically says that β and L can be exchanged in the constants C_e and C_o (up to a term that vanishes in the limit). Only a few terms survive and we end up with

$$\lim_{L \rightarrow \infty} \omega_{\beta,V}^L (\hat{J}_{i_1}^\ell(t, x_1) \hat{J}_{i_2}^\ell(t, x_2)) = -\delta_{i_1 i_2} \frac{r_{i_1}^2}{8\beta^2} \sinh^{-2} \left(\frac{\pi(x_1 - x_2)}{\beta} \right) \quad (3.101)$$

and the mean of one $\hat{J}_{i_1}^\ell$ still vanishes. Equations (3.100), (3.101) together with the Wick rule, and finally the scattering relation (3.42) between left and right currents define the $L \rightarrow \infty$ limit $\omega_{\beta,V}$ of the states $\omega_{\beta,V}^L$. Unlike for finite L , that limit is not represented by the trace with a density matrix⁴.

Let us look at some interesting quantities in the infinite size system. The one point function reads

$$\omega_{\beta,V} (J_i^\ell(t, x)) = \frac{r_i^2 V}{4\pi} = \omega_{\beta,V} (J_i^r(t, x)) \quad (3.102)$$

meaning that the mean of the charge current J_i^1 still vanishes whereas the mean of the charge density J_i^0 is constant in each wire and equal to $(r_i^2 V)/(2\pi)$. Note that the latter may be different in different wires. This is similar to the finite size case but the explicit formula is simpler.

The two point function is also very simple:

$$\omega_{\beta,V} (J_i^\ell(t, x) J_j^\ell(t, y)) = \frac{r_i^2 r_j^2 V^2}{16\pi^2} - \delta_{ij} \frac{r_i^2}{8\beta^2} \sinh^{-2} \left(\frac{\pi(x_1 - x_2)}{\beta} \right), \quad (3.103)$$

with the same expression for the right current two point function. The first term comes from the non vanishing zero mode part (3.100) and the second one is just the standard conformal correlation two point function on the infinite cylinder. This might look somewhat surprising: the presence of the junction has completely disappeared in the chiral two point functions, and due to the δ_{ij} factor, the expectations of left currents factorizes on each wire, and similarly for the right currents, as if the wires were disconnected. Actually the influence of the junction is still present but only in the mixed left-right expectations involving the scattering rule (3.42) relating left and right currents.

This observation can be generalized, using (3.100), (3.101) and the Wick rule: when restricted to the products of left-moving currents, the limiting $L = \infty$ equilibrium expectations do not

⁴For $L = \infty$, the open string Hamiltonian has a continuous spectrum and the operator $e^{-\beta(H-VQ)}$ is not traceclass.

depend on the choice of the brane \mathcal{B} describing the contact of wires and completely factorize on each wire

$$\omega_{\beta,V} \left(\prod_{k=1}^K J_{i_k}^\ell(t, x_k) \right) = \prod_{i=1}^N \omega_{\beta,V} \left(\prod_{\substack{k \\ i_k=i}} J_i^\ell(t, x_k) \right), \quad (3.104)$$

meaning that a general expectation of left currents just has to be computed wire by wire, with the product of all contribution taken at the end. We get a similar formula when we restrict the expectations to the right currents only. In particular, such expectations are the same as for the space-filling brane \mathcal{B}_0 with $S = I$ corresponding to the disconnected wires for which $J_i^r(t, x) = J_i^\ell(t, -x)$ and $|\mathcal{B}_0\rangle\rangle = |\mathcal{N}\rangle\rangle$. In addition to factorization, we have for such (finite) junction

$$\omega_{\beta,V}^L \left(\prod_{k'=1}^{K'} J_{i_{k'}}^r(t, y_{k'}) \right) = \prod_{i=1}^N \omega_{\beta,V}^L \left(\prod_{\substack{k' \\ i_{k'}=i}} J_i^\ell(t, -y_{k'}) \right). \quad (3.105)$$

relating left and right expectations, and it is easy to check using the scattering rule (3.42) and its properties (3.43) that the latter factorization holds in the limit $L \rightarrow \infty$ also for any nontrivial branes $\mathcal{B} = \kappa(U(1)^M)$.

Hence in the thermodynamic limit the equilibrium state is very simple: the expectations of left currents are just computed as products wire by wire, whatever the junction. Similarly for the expectations of the right currents. The latter are equal to the expectations of the left currents. The symmetry $\ell \leftrightarrow r$ is a sign of time reversal invariance of the system. The junction enters only through the scattering rule (3.42), needed to compute mixed left-right currents correlations functions. For example,

$$\omega_{\beta,V} (J_i^\ell(t, x) J_j^r(t, y)) = \sum_k S_{jk} \omega_{\beta,V} (J_i^\ell(t, x) J_i^\ell(t, -y)) \quad (3.106)$$

requiring again only the factorized left-current expectations. A general formula for any correlation function is straightforward: expressing the right movers in terms of the left ones, we get a complete expression in terms of the left movers only that factorizes over different wires. Thus, up to some combinations with the scattering matrix coefficients, the expectations are the same as for the disconnected junction. This observations are essential for the construction of nonequilibrium stationary state where the individual wires are kept at different temperatures and at different potentials.

The equilibrium expectation values of the components of the energy-momentum tensor in the thermodynamic limit may again be obtained from the current two point functions by the OPE (3.79). The result is

$$\omega_{\beta,V} (T_i^\ell(t, x)) = \frac{r_i^2 V^2}{8\pi} + \frac{\pi}{12\beta^2} = \omega_{\beta,V} (T_i^r(t, x)). \quad (3.107)$$

In particular,

$$\omega_{\beta,V}^L (\omega_{\beta,V} (K_i^0(t, x))) = \frac{r_i^2 V^2}{4\pi} + \frac{\pi}{6\beta^2}, \quad \omega_{\beta,V}^L (\omega_{\beta,V} (K_i^1(t, x))) = 0 \quad (3.108)$$

for $K_i^{0,1} = T_i^r \pm T_i^\ell$ representing the energy density and energy current in wire i . Thus the equilibrium mean energy density is positive and constant in each wire whereas the mean energy current vanishes. Note that the mean energy density in equilibrium summed over wires is equal to the negative of the free energy density (3.99). We shall recover the same relation for other conformal junctions.

3.6 Nonequilibrium stationary state

3.6.1 One algebra, several dynamics

In order to construct the nonequilibrium stationary state as proposed in Subsection 2.2.3, we adopt the following description of the system. Consider the algebra of observables generated by $J_i^\ell(0, x)$ and $J_i^r(0, x)$ for $x > 0$. Such an algebra is independent of the brane \mathcal{B} and thus can be identified with the one of the disconnected junction for any choice of brane \mathcal{B} . Hence we identify the operator content of the theory with the algebra \mathcal{A} generated by of currents $J_i^{\ell,r}(0, x)$ at $t = 0$ and $x > 0$ corresponding to the disconnected junction.

The Heisenberg dynamics on such an algebra depends, however, on the junction we are considering. Let \mathcal{U}_t for $t > 0$ describe the forward in time Heisenberg-picture evolution of the currents $J_i^{\ell,r}(0, x)$ with $x > 0$, and in the presence of a brane \mathcal{B} . First consider the left movers, the evolution is simple:

$$\mathcal{U}_t J_i^\ell(0, x) = J_i^\ell(0, x + t) \quad (3.109)$$

since $x + t > 0$ in this case. As argued in Subsection 2.1.3 this equation means that the operator $J_i^\ell(0, x)$ is sent to the operator $J_i^\ell(0, x + t)$ during time evolution of duration t . Thus in this formalism, the left movers are “moved” to the right, or far away from the junction. The right current evolution is different on \mathcal{A} since x is sent to $x - t$ with forward time evolution, which can become negative. Hence when $x - t = 0$ we shall use the scattering rule (3.42), expressing the right current in terms of the left ones, whose further time evolution is simple, as just described. We end up with the relations

$$\mathcal{U}_t J_i^r(0, x) = \begin{cases} J_i^r(0, x - t) & \text{for } t \leq x \\ \sum_j S_{ij} J_j^\ell(0, t - x) & \text{for } t \geq x \end{cases} \quad (3.110)$$

This relation is continuous at $t = x$ by the scattering rule (3.42). Such dynamics is illustrated in Figure 3.3

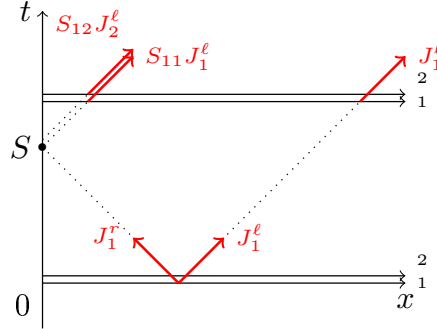


Figure 3.3: Dynamics for the connected junction. The positive x half-axis is a parameter for the family of currents, and time evolution moves the current along this half line. At $x = 0$ the right current is scattered to a combination of left ones with S -matrix coefficients.

On product of currents, \mathcal{U}_t acts multiplicatively. In this picture, the right movers are moved closer to the junction until they reach it, where they are scattered into left currents, which are moved away from the junction from time $t = x$ on. Finally note that this dynamics is also available for the disconnected junction where $S = I$ and hence a right mover is just reflected to left mover on the same wire. We denote \mathcal{U}_t^0 the evolution of such particular dynamics, and compute the corresponding backward evolution that will be needed in the following, namely for $x, t > 0$

$$\mathcal{U}_{-t}^0 J_i^\ell(0, x) = \begin{cases} J_i^\ell(0, x - t) & \text{for } t \leq x \\ J_i^r(0, t - x) & \text{for } t \geq x \end{cases} \quad (3.111)$$

$$\mathcal{U}_{-t}^0 J_i^r(0, x) = J_i^r(0, x + t). \quad (3.112)$$

3.6.2 Nonequilibrium state

We are now able to construct a nonequilibrium stationary state (NESS), denoted ω_{neq} , describing the situation when different semi-infinite wires are kept at different temperatures and different potentials. Such state can be constructed as follows: for each disconnected semi-infinite wire, one considers the algebra \mathcal{A}_i generated by products of currents $J_i^{\ell,r}(0, x)$ for $x > 0$, together with a state ω_{β_i, V_i}^i given by the restriction to \mathcal{A}_i of the $L = \infty$ equilibrium state ω_{β_i, V_i} for the space-filling brane \mathcal{B}_0 . The product state

$$\omega_{\text{in}} \equiv \bigotimes_{i=1}^N \omega_{\beta_i, V_i}^i, \quad (3.113)$$

on algebra $\mathcal{A} = \bigotimes_i \mathcal{A}_i$, describes the disconnected wires with each prepared in its own equilibrium state ω_{β_i, V_i}^i . Now consider time evolution on \mathcal{A} given by (3.109) and (3.110) and notice that when waiting long enough all the currents are sent to the left ones. Then for $A \in \mathcal{A}$, we define

$$\omega_{\text{neq}}(A) = \lim_{t \rightarrow \infty} \omega_{\text{in}}(\mathcal{U}_t A). \quad (3.114)$$

If the limit exists, the limiting state will be invariant under the Heisenberg evolution \mathcal{U}_t , so that its stationarity will follow. The existence of the infinite time limit will be tackled using the backward Heisenberg evolution (3.111) and (3.112) of the decoupled wires which preserves the product state ω_{in} , and allows to rewrite

$$\lim_{t \rightarrow \infty} \omega_{\text{in}}(\mathcal{U}_t A) = \omega_{\text{in}}(\mathcal{S}A), \quad \text{where} \quad \mathcal{S} = \lim_{t \rightarrow \infty} \mathcal{U}_{-t}^0 \mathcal{U}_t \quad (3.115)$$

is the scattering operator acting on algebra \mathcal{A} . The action of $\mathcal{U}_{-t}^0 \mathcal{U}_t$ on the currents is obtained by combining equations (3.109), (3.110), (3.111) and (3.112). The action of \mathcal{U}_t for some t large enough is to express the right currents in terms of the left ones after the former ones pass through the junction. The subsequent \mathcal{U}_{-t}^0 evolution allows to “come back” to $t = 0$, expressing the left movers in terms of the right ones by a simple reflection. The existence of the infinite time limit in the definition of \mathcal{S} follows easily by observing that $\mathcal{U}_{-t}^0 \mathcal{U}_t(A)$ stabilizes for large enough time. In particular,

$$\mathcal{S}J_i^\ell(0, x) = J_i^\ell(0, x), \quad \mathcal{S}J_i^r(0, x) = \sum_{i'} S_{ii'} J_{i'}^r(0, x) \quad (3.116)$$

The identity (3.115) gives then rise to the following explicit formula:

$$\omega_{\text{neq}} \left(\prod_{k=1}^K J_{i_k}^\ell(0, x_k) \prod_{k'=1}^{K'} J_{i_{k'}}^r(0, y_{k'}) \right) = \prod_{k'=1}^{K'} \sum_{i_{k'}} S_{i_{k'} i_{k'}} \prod_{i=1}^N \omega_{\beta_i, V_i}^i \left(\prod_{i_k=i} J_i^\ell(0, x_k) \prod_{i_{k'}=i} J_i^r(0, y_{k'}) \right) \quad (3.117)$$

This means that the nonequilibrium state expectations are expressed as combinations of expectations in disconnected wire states at different inverse temperatures β_i and electric potentials V_i . The coefficients of such combinations are given by products of the entries of the scattering matrix S . In particular, if we restrict formula (3.117) to products of left currents only, the expectation in ω_{neq} and in ω_{in} are identical. As discussed in the previous section, the left movers do not feel the influence of the junction.

Formula (3.117) still holds if the time zero currents are replaced by time t if on the left hand side the currents correspond to connected wires and on the right hand side to the disconnected ones. The values x_k and $y_{k'}$ may be taken arbitrary positive (with noncoincident points $x_i, -y_j$ to avoid singularities).

3.6.3 Some nonequilibrium expectations

We first specify (3.117) to the one point expectations, and deduce the mean electric charge density and mean current in the wires

$$\omega_{\text{neq}}(J_i^0(t, x)) = \sum_j^N (S_{ij} + \delta_{ij}) \frac{r_j^2 V_j}{4\pi}, \quad \omega_{\text{neq}}(J_i^1(t, x)) = \sum_{j=1}^N (S_{ij} - \delta_{ij}) \frac{r_j^2 V_j}{4\pi}, \quad (3.118)$$

respectively. They are constant in each wire and the mean current does not vanish, in general, at difference with the equilibrium state. The electric conductance tensor of the junction (in the units e^2/\hbar) is the linear response of the theory for small perturbation of the electric potentials V_i around equilibrium

$$^{\text{el}}G_{ij} \equiv \left. \frac{\partial}{\partial V_j} \omega_{\text{neq}}(J_i^1(0, x)) \right|_{\substack{\beta_k = \beta \\ V_k = V}} = \frac{1}{4\pi} (S_{ij} - \delta_{ij}) r_j^2. \quad (3.119)$$

This agrees with the calculation of [147, 146] based on the combination of the Green-Kubo formula with the conformal field theory representation of the equilibrium state. Note that the conductance vanishes for the decoupled wires.

The nonequilibrium 2-point functions are also computable from (3.117) that gives:

$$\omega_{\text{neq}}(J_i^\ell(t, x) J_j^\ell(t, y)) = \frac{r_i^2 r_j^2 V_i V_j}{16\pi^2} - \delta_{ij} \frac{r_i^2}{8\beta_i^2} \sinh^{-2} \left(\frac{\pi(x-y)}{\beta_i} \right), \quad (3.120)$$

$$\omega_{\text{neq}}(J_i^\ell(t, x) J_j^r(t, y)) = \sum_{i=1}^N S_{ji} \frac{r_i^2 r_j^2 V_i V_j}{16\pi^2} - S_{ji} \frac{r_i^2}{8\beta_i^2} \sinh^{-2} \left(\frac{\pi(x+y)}{\beta_i} \right), \quad (3.121)$$

$$\omega_{\text{neq}}(J_i^r(t, x) J_j^r(t, y)) = \sum_{k,l}^N S_{ik} S_{jl} \frac{r_k^2 r_l^2 V_k V_l}{16\pi^2} - \sum_{i=1}^N S_{ik} S_{jk} \frac{r_k^2}{8\beta_k^2} \sinh^{-2} \left(\frac{\pi(x-y)}{\beta_k} \right). \quad (3.122)$$

Note that the nonequilibrium state ω_{neq} breaks the symmetry $J^\ell \leftrightarrow J^r$ related to the time reversal invariance that is absent in the nonequilibrium state (except for disconnected wires with $S = I$).

It is also possible to compute expectations of the chiral components of energy-momentum tensor $T_i^{\ell,r}$ by taking a (regularized) limit $y \rightarrow x$ of the two point functions, and deduce the mean energy density and mean energy current giving by the expectations of $K_i^{0,1} = T_i^r \pm T_i^\ell$. One obtains:

$$\omega_{\text{neq}}(K_i^{0,1}(t, x)) = \frac{1}{8\pi r_i^2} \left(\sum_j^N S_{ij} r_j^2 V_j \right)^2 \pm \frac{r_i^2 V_i^2}{8\pi} + \frac{\pi}{12 r_i^2} \sum_{j=1}^N \left(S_{ij} \frac{r_j}{\beta_j} \right)^2 \pm \frac{\pi}{12 \beta_j^2}, \quad (3.123)$$

Similar as for the $U(1)$ charge, we can define and compute the thermal conductance:

$$^{\text{th}}G_{ij} = -\beta_j^2 \frac{\partial}{\partial \beta_j} \omega_{\text{neq}}(K_i^1(t, x)) \Big|_{\substack{\beta_j = \beta \\ V_j = V}} = \frac{\pi}{6\beta} ((S_{ij})^2 \frac{r_j^2}{r_i^2} - \delta_{ij}). \quad (3.124)$$

Note that the right hand sides of (3.118) and (3.123) reduce the the equilibrium expressions when $V_i = V$ and $\beta_i = \beta$.

Example 3.7

Take $N = 2$, $M = 1$, $\kappa = (1, 1)$, as already discussed in Example 3.4. Recall the scattering matrix

$$S = \frac{1}{r_1^2 + r_2^2} \begin{pmatrix} r_1^2 - r_2^2 & 2r_1^2 \\ 2r_2^2 & r_2^2 - r_1^2 \end{pmatrix}. \quad (3.125)$$

The mean $U(1)$ current in the first wire is

$$\omega_{\text{neq}}(J_1^1(t, x)) = a(r_1, r_2) \frac{V_2 - V_1}{4\pi} \quad \text{for} \quad a(r_1, r_2) = \frac{2r_1^2 r_2^2}{r_1^2 + r_2^2} \quad (3.126)$$

Note that charge conservation for the two-wire junction implies that the expectation of $J_2^1(t, x)$ is opposite to that of $J_2^1(t, x)$. In the case of the same radii $r_1 = r_2$, the scattering matrix S is fully transmitting and the mean electric current just becomes $(4\pi)^{-1}r^2(V_2 - V_1)$. Hence the difference of radii, inducing some reflection at the junction, tunes by a factor $a(r_1, r_2)$ the value of the mean current given in the fully transmitting case. Moreover note that the current in the first wire is positive if $V_2 > V_1$, and since we are measuring the charge in unit $-e$, the electrons are effectively moving from smaller to greater electric potential. The mean energy current in the first wire is

$$\omega_{\text{neq}}(K_1^1(t, x)) = \frac{4r_1^2 r_2^2}{(r_1^2 + r_2^2)^2} \left(\frac{V_2 - V_1}{8\pi} (r_1^2 V_1 + r_2^2 V_2) + \frac{\pi}{12} \left(\frac{1}{\beta_2^2} - \frac{1}{\beta_1^2} \right) \right) \quad (3.127)$$

which is also opposite to the energy current in the second wire $\omega_{\text{neq}}(K_2^1(t, x))$ by conservation of the total energy. Energy transfer is due to different electric potentials and different temperatures. Moreover, the β_i dependance of such current is proportional to the difference of squared temperatures $T_2^2 - T_1^2$ so that, for equal potentials, the energy is going from the wire with higher temperature to the one with lower one.

The black body interpretation Consider the mean energy current (3.127) in the previous example of two wires in the case where $r_1 = r_2$, $V_1 = V_2 = 0$ and $T_1 = 0$ so that the first wire feels only the reservoir of energy from the second wire. Restoring the fundamental constants, we get

$$\omega_{\text{neq}}(K_1^1(t, x)) = \frac{\pi}{12\hbar} k_B T_2^2 \quad (3.128)$$

As was pointed out in [18] this formula is similar to the Stefan-Boltzmann law for the energy radiated by a thermal black body in one dimension [43]. Thus if we look only at the mean energy current, the junction of N wires can be seen as N black bodies exchanging energy carried in a ballistic way by massless free bosons and the boundary defect is just a beamsplitter. This picture is available for this particular mean current (linear terms can also appear for other junctions) and we will see below that the energy transfer is not a Gaussian process, but it helps anyway to have a simple picture of the nonequilibrium state that was constructed.

Example 3.8

- $N = 3$, $M = 1$, $\kappa = (1, 1, 1)$ and the same radii $r_i = r$. To go beyond two wires, we consider the simple example already mentioned in Example 3.5, where $S_{ij} = -1/3\delta_{ij} + 2/3(1 - \delta_{ij})$, see (3.46). In this case, for the mean charge and energy current in the first wire, we obtain:

$$\begin{aligned} \omega_{\text{neq}}(J_1^1) &= \frac{r^2}{4\pi} \frac{2}{3} (V_2 + V_3 - V_1) \\ \omega_{\text{neq}}(K_1^1) &= \frac{r^2}{8\pi} \frac{4}{9} (V_2 + V_3 - 2V_1)(V_1 + V_2 + V_3) + \frac{\pi}{12} \frac{4}{9} \left(\frac{1}{\beta_2^2} + \frac{1}{\beta_3^2} - \frac{2}{\beta_1^2} \right) \end{aligned} \quad (3.129)$$

and similarly for the other wires, cyclically permuting the indexes. The sum of the the currents in three wires vanishes. Thus for the charge the first wire sees the other ones as one effective wire at potential $V_2 + V_3$, whereas for the energy we get two distinct contribution from wire 2 and wire 3, respectively proportional to $V_2 - V_1$ and $V_3 - V_1$, and to $\beta_2^{-2} - \beta_1^{-2}$ and $\beta_3^{-2} - \beta_1^{-2}$. Taking into account different radii will just modulate those different contributions and also change the total amplitude of the current.

- $N = 3, M = 2$. Consider the last matrix proposed in Example 3.5, where the symmetry between the three wires is broken through the rational parameter α . The mean charge current is driven by differences of electric potentials, weighted by α :

$$\omega_{\text{neq}}(J_1^1) = \frac{r^2}{4\pi} \frac{1}{1+\alpha+\alpha^2} (\alpha(V_3 - V_2) + \alpha^2(V_3 - V_1)), \quad (3.130)$$

but the mean current for energy involves term linear in the differences of temperatures, in addition to the quadratic one proportional to the differences of temperatures squared (we took $V_i = 0$ for simplicity):

$$\begin{aligned} \omega_{\text{neq}}(K_1^1) = \frac{\pi}{12} \frac{1}{(1+\alpha+\alpha^2)^2} & \left(2\alpha(1+\alpha)[\beta_1^{-1}(\beta_3^{-1} - \beta_2^{-1}) + \alpha\beta_3^{-1}(\beta_1^{-1} - \beta_2^{-1})] \right. \\ & \left. + \alpha^2[(\beta_2^{-2} - \beta_1^{-2}) + (1+\alpha)^2(\beta_3^{-2} - \beta_1^{-2})] \right), \end{aligned} \quad (3.131)$$

where again α weights different contributions.

Looking at the previous examples, we make the following conjecture about the nonequilibrium state ω_{neq} . The mean charge and energy currents are driven by three kind of terms, proportional to the difference of electric potential and the difference of temperatures at powers one and two. Each contribution is weighted by the scattering coefficients of the matrix S and the radii r_i . The general formulae (3.118) and (3.123) suggests that no other kind of contributions should appear in expectations of mean charge and energy currents.

3.7 Full counting statistics

We follow the measurement protocol illustrated in Figure 2.5. First consider the finite system of disconnected wires of length L , each with Hamiltonian H_i^0 and charge operator Q_i^0 . Prepare the system in the product state $\omega_0^L = \otimes_{i=1}^N \omega_{\beta_i, V_i}^{i, L}$, given by the density matrix

$$\rho_0 \equiv \bigotimes_{i=1}^N \rho_{\beta_i, V_i}^i \quad \text{where} \quad \rho_{\beta_i, V_i}^i = \frac{1}{Z_{\beta_i, V_i}^i} e^{-\beta_i(H_i^0 - V_i Q_i^0)}, \quad (3.132)$$

such that each wire is initially prepared at β_i, V_i . In such a system, it is possible to measure the total charge or energy in each wire simultaneously, since the wires are disconnected. At $t = 0$, connect the wires instantaneously and let the system evolve. Then at time t disconnect the wires. It is now possible to measure again the total charge or total energy in each wire and compare the result with the initial measurement. We would like to compute the probability of different results of such two-time measurements for our junction. Since the charge operators and the Hamiltonians commute, we can measure both charge and energy simultaneously. For pedagogical reasons, however, we shall focus first on the transfer of charge, then of energy, before considering both together.

3.7.1 Charge transport

For each wire i , we measure the charge associated to operator Q_i^0 at $t = 0$ and $Q_i(t)$ at time t . By spectral decomposition,

$$Q_i^0 = \sum_{q^0} q^0 P_{i, q^0}^0, \quad Q_i(t) = \sum_q q P_{i, q}(t). \quad (3.133)$$

The probability that the first measurement gives the values of charges $(q_i^0) \equiv \mathbf{q}^0$ and that the second ones gives $(q_i) \equiv \mathbf{q}$ is obtained by the standard quantum mechanics rules and leads to the

expression

$$\mathbb{P}_t(\mathbf{q}^0, \mathbf{q}) = \omega_0^L \left(\prod_i P_{i, q_i^0} \prod_i P_{i, q_i}(t) \right), \quad (3.134)$$

where we used the fact that $P_{i, q}^0$ commute with ρ_{β_i, V_i}^i . We are more interested in the probability $\mathbb{P}_t(\Delta \mathbf{q})$ of the charge variations $\Delta q_i = q_i - q_i^0$, easily extractable from the previous probability, and instead of computing such probability directly, we compute its characteristic function called the generating function of full counting statistics (FCS) for the electric charge transfers, defined by

$$\text{el}F_t^L(\boldsymbol{\nu}) = \sum_{\Delta \mathbf{q}} e^{i \sum_i \nu_i \Delta q_i} \mathbb{P}_t(\Delta \mathbf{q}) = \sum_{(\mathbf{q}^0, \mathbf{q})} e^{i \sum_i (q_i - q_i^0) \nu_i} \mathbb{P}_t(\mathbf{q}^0, \mathbf{q}) \quad (3.135)$$

We call $\boldsymbol{\nu}$ the conjugated variable to $\Delta \mathbf{q}$. Function $\text{el}F_t^L(\boldsymbol{\nu})$ contains full information about probability distribution $P_t(\Delta \mathbf{q})$. In particular, the moments of the latter may be computed by successive derivation of $\text{el}F_t^L$ around $\boldsymbol{\nu} = 0$. Moreover the generating function will be more tractable to investigate the asymptotic transfer properties, see below. It can be expressed as an expectation in the initial state ω_0^L , namely

$$\text{el}F_t^L(\boldsymbol{\nu}) = \omega_0^L \left(e^{-i \sum_i \nu_i Q_i^0} e^{i \sum_i \nu_i Q_i(t)} \right). \quad (3.136)$$

Note that, by construction of the protocol, the properties of charge transfers are computed in the state ω_0^L corresponding to the disconnected wire, but they keep track of the junction through the operators $Q_i(t)$. It is actually more natural to work with the operator $\Delta Q_i \equiv Q_i(t) - Q_i^0$ encoding the variation of the charge. The latter operators may be decomposed in terms of the chiral currents evolving during period $]0, t[$ and related by the scattering rule (3.42). One ends up with the expression

$$\Delta Q_i(t) = - \int_0^t (J_i^\ell(0, s) - \sum_j S_{ij} J_j^\ell(0, s)) ds, \quad (3.137)$$

where we assumed $t < L$ so that the left currents do not reach the free end of the wires. Note that observables ΔQ_i have been written in term of currents at $t = 0$ that correspond to disconnected wires. The crucial fact about such observables is that they are extensive in time but not in the wire length, unlike the total charges. Moreover they commute with the initial charges: $[\Delta Q_i(t), Q_i^0] = 0$ so that the FCS generating function has the simpler form

$$\text{el}F_t^L(\boldsymbol{\nu}) = \omega_0^L \left(e^{i \sum_i \nu_i \Delta Q_i(t)} \right). \quad (3.138)$$

In the thermodynamic limit $L \rightarrow \infty$, the initial state ω_0^L becomes the product state ω_{in} for semi-infinite wires given by (3.113). Moreover, expression (3.137) for ΔQ_i involves only left currents, so that the expectations in ω_{in} and in the nonequilibrium state ω_{neq} are identical. Hence the relation between the FCS and the previous nonequilibrium stationary state:

$$\lim_{L \rightarrow \infty} \text{el}F_t^L(\boldsymbol{\nu}) = \omega_{\text{neq}} \left(e^{i \sum_i \nu_i \Delta Q_i(t)} \right) \quad (3.139)$$

We would like to study the asymptotic properties of the probability distribution \mathbb{P}_t , which are encoded in the large deviation form of the FCS generating function. For this purpose we define the following rate function⁵

$$\text{el}f(\boldsymbol{\nu}) = \lim_{t \rightarrow \infty} t^{-1} \ln \text{el}F_t(\boldsymbol{\nu}). \quad (3.140)$$

⁵As already mentioned, the name is slightly abusive here: what we are actually computing is the analytic continuation of the Legendre transform of the large deviation rate function.

The calculation of the above rate function can be done in several ways. The first one is to look at ${}^{\text{el}}F_t(\boldsymbol{\nu})$ using the explicit expression (3.137) of ΔQ_i , allowing to factorize on each wire

$${}^{\text{el}}F_t(\boldsymbol{\nu}) = \prod_{i=1}^N \omega_{\beta_i, V_i}^i \left(e^{-i\tilde{\nu}_i \int_0^t J_i^\ell(0,s) ds} \right) \quad \text{where} \quad \tilde{\nu}_i \equiv \nu_i - \sum_j S_{ji} \nu_j \quad (3.141)$$

Then, using the translation invariance of the states ω_{β_i, V_i}^i , we can rewrite the integral term in the exponential factor such that in the long time limit $t \rightarrow \infty$, the corresponding integral becomes close to the charge Q_i^0 of the wire i and the coefficients $\tilde{\nu}_i$ becomes some effective imaginary electric potentials. In this case

$$\omega_{\beta_i, V_i}^i \left(e^{-i\sum_i \tilde{\nu}_i Q_i^0} \right) = \frac{Z_{\beta_i, V_i - i\beta_i^{-1}\tilde{\nu}_i}^i}{Z_{\beta_i, V_i}^i} \quad (3.142)$$

is nothing but a quotient of two partition functions of the wire i at different electric potentials, one requiring analytic continuation. Hence its logarithm will give for ${}^{\text{el}}f(\boldsymbol{\nu})$ a difference of equilibrium free energy densities computed in (3.99).

The above limit performed formally here was actually proposed and investigated more closely in [18] in the case of a purely transmitting junction, by focusing on first derivatives of ${}^{\text{el}}f$. At large time the exponential factors are identified with the addition of an imaginary potential proportional to coefficient $\tilde{\nu}_i$ and each current is finally computed in its corresponding wire. Following this approach, one can treat the case with any matrix S and not only with the fully transmitting one. We end up (see [85]) with differences of free energy density for different potentials

$${}^{\text{el}}f(\boldsymbol{\nu}) = \frac{1}{2} \sum_{i=1}^N \beta_i \left(f_i(\beta_i, V_i) - f_i(\beta_i, V_i - i\beta_i^{-1}\tilde{\nu}_i) \right), \quad (3.143)$$

where $f_i(\beta, V)$ is the equilibrium free energy per unit length in a single decoupled semi-infinite wire with the Neumann boundary conditions, see (3.99). One can make the above approximate calculation more more rigorous by extending (formally) the definition of ${}^{\text{el}}F_t^L(\boldsymbol{\nu})$ to $t > L$ by

$${}^{\text{el}}F_t^L(\boldsymbol{\nu}) = \prod_{i=1}^N \omega_{\beta_i, V_i}^i \left(e^{-i\tilde{\nu}_i \int_0^{t/2} J_i^\ell(0,s) + J_i^r(0,s) ds} \right). \quad (3.144)$$

In the very specific case where $t = 2L$, the generating function ${}^{\text{el}}F_{2L}^L(\boldsymbol{\nu})$ is exactly the product over all the wires of partitions functions from the right hand side of (3.142), even for finite size. We get immediately for this specific case

$$\lim_{t=2L \rightarrow \infty} t^{-1} \ln {}^{\text{el}}F_t^L(\boldsymbol{\nu}) = {}^{\text{el}}f(\boldsymbol{\nu}) \quad (3.145)$$

with ${}^{\text{el}}f(\boldsymbol{\nu})$ on the right hand side given by (3.143) in terms of free energy densities. *A priori*, it is not clear that the same result for ${}^{\text{el}}f(\boldsymbol{\nu})$ arises in the physically different limit that takes the thermodynamic limit $L \rightarrow \infty$ before sending $t \rightarrow \infty$. The calculation of [18] amounts to the claim that both limits are equal. Moreover, setting $t = 2L$, although unphysical, will be also very convenient to compute the generating function associated to energy transport, see below.

An exact formula The exactly soluble nature of the model considered here allows to examine closer the distribution of charge transfers for finite L and t and to see in more details how its large-deviations form arises. A direct calculation performed in [85] gives the result

$${}^{\text{el}}F_t^L(\boldsymbol{\nu})_{\text{reg}} = \exp \left[- \sum_{i=1}^N \frac{\tilde{\nu}_i^2 r_i^2}{8\pi^2} \left(C_{\Lambda L} + \ln \frac{2\pi \theta_1(\frac{i\beta_i}{2L}; \frac{t}{2L})}{\partial_z \theta_1(\frac{i\beta_i}{2L}; 0)} \right) \right] \frac{\sum_{\mathbf{k} \in \mathbb{Z}^N} \exp \left[\sum_{i=1}^N \left(-\frac{\pi\beta_i}{Lr_i^2} k_i^2 + \beta_i V_i k_i - i\frac{\tilde{\nu}_i t}{2L} k_i \right) \right]}{\sum_{\mathbf{k} \in \mathbb{Z}^N} \exp \left[\sum_{i=1}^N \left(-\frac{\pi\beta_i}{Lr_i^2} k_i^2 + \beta_i V_i k_i \right) \right]} \quad (3.146)$$

where the subscript “reg” refers to a necessary ultraviolet regularization, that replaces the divergent constant $C_\infty = \sum_{n>0} \frac{1}{n}$ by

$$C_{\Lambda L} = \sum_{n=1}^{\Lambda L} \frac{1}{n} = \ln(\Lambda L) + C + O\left(\frac{1}{\Lambda L}\right) \quad (3.147)$$

with the ultraviolet cutoff Λ . Variables $\tilde{\nu}_i$ are as before, see (3.141), and θ_1 is one of the Jacobi theta-functions [50].

In order to study the behavior of the charge-transfer distribution for large L and large t , we proceed as for the correlation functions in the equilibrium state: discrete \mathbf{k} -sums are rewritten using Poisson resummation formula, and as for the Dedekind function before, we use the modular property of the Jacobi theta function. After such a transformation of the right hand side of (3.146), we extract the asymptotic behavior

$${}^{\text{el}}F_t^L(\boldsymbol{\nu})_{\text{reg}} = \prod_{i=1}^N \left((e^C \Lambda \beta_i \sinh \frac{\pi t}{\beta_i})^{-\frac{\tilde{\nu}_i^2 r_i^2}{8\pi^2}} e^{-\frac{i\tilde{\nu}_i V_i r_i^2 t}{4\pi}} \right) \left(1 + O\left(\frac{1}{\Lambda L}\right) + O\left(\frac{t^2}{L}\right) + O(e^{-cL}) \right) \quad (3.148)$$

where $c > 0$ is some β_i - and r_i -dependent constant. Hence

$${}^{\text{el}}f(\boldsymbol{\nu})_{\text{reg}} \equiv \lim_{t \rightarrow \infty} \frac{1}{t} \lim_{L \rightarrow \infty} \ln {}^{\text{el}}F_t^L(\boldsymbol{\nu})_{\text{reg}} = - \sum_{i=1}^N \left(\frac{\tilde{\nu}_i^2 r_i^2}{8\pi\beta_i} + i \frac{\tilde{\nu}_i V_i r_i^2}{4\pi} \right) \quad (3.149)$$

reproducing the large deviations result (3.143), up to the ultraviolet regularization. Note that it follows from relation (3.148) that the same result is obtained for the limit of $\frac{1}{t} \ln {}^{\text{el}}F_t^L(\boldsymbol{\nu})_{\text{reg}}$ obtained by sending simultaneously Λ , L and t to infinity in such a way that the ratios $\frac{\ln \Lambda}{t}$ and $\frac{t}{L}$ tend to zero. This specifies more precisely the region where the distribution of charge transfers takes the quadratic large deviation form (3.143) described previously. The above analysis does not cover, however, the case (3.145) with $t = 2L \rightarrow \infty$ which, although giving the same limit, is somewhat special. In particular, no ultraviolet regularization of is required for ${}^{\text{el}}F_{2L}^L(\boldsymbol{\nu})$.

Summarizing, the different calculations of the rate function ${}^{\text{el}}f(\boldsymbol{\nu})$ lead to the same result, given for example by the right hand side of (3.149). The existence of such a limit means that at long times the probability density of charge transfers takes asymptotically the large-deviations form

$$\mathbb{P}_t(\Delta \mathbf{q}) \sim e^{-t {}^{\text{el}}I(\frac{1}{t} \Delta \mathbf{q})} \quad (3.150)$$

where the rate function

$${}^{\text{el}}I(\boldsymbol{\rho}) = \max_{\boldsymbol{\nu}} \left(\sum_{i=1}^N \rho_i \nu_i - {}^{\text{el}}f(-i\boldsymbol{\nu}) \right) \quad (3.151)$$

is the Legendre transform of ${}^{\text{el}}f(-i\boldsymbol{\nu})$. For ${}^{\text{el}}f(\boldsymbol{\nu})$ given by (3.149), ${}^{\text{el}}I(\boldsymbol{\rho})$ is a quadratic polynomial on the subspace where it is finite. In other words, the large deviations of charge transfers per unit time have the Gaussian distribution with mean and covariance given by the expressions

$$\langle \frac{\Delta q_i}{t} \rangle = \sum_{j=1}^N (S_{ij} - \delta_{ij}) \frac{V_j r_j^2}{4\pi}, \quad C_{ij} = \frac{1}{t} \sum_{k=1}^N \frac{r_k^2}{4\pi\beta_k} (\delta_{ki} - S_{ik})(\delta_{kj} - S_{jk}). \quad (3.152)$$

driven by, respectively, electric potentials and temperatures and both weighted by the scattering matrix S of the junction.

Example 3.9

$N = 2$, $M = 1$. Consider the same matrix S as in the first example of 3.7. For two wires, charge conservation implies that ν_1 and ν_2 are redundant, only their difference is relevant. Here the rate function is

$$\text{elf}(\nu) = -\frac{1}{4\pi} \frac{2r_1^2 r_2^2}{(r_1^2 + r_2^2)^2} \left(\frac{r_2^2}{\beta_1} + \frac{r_1^2}{\beta_2} \right) \nu^2 + \frac{i}{2\pi} \frac{r_1^2 r_2^2}{r_1^2 + r_2^2} (V_2 - V_1) \nu, \quad (3.153)$$

where $\nu = \nu_1 - \nu_2$. In the special case $r_1 = r_2 = r$ of a fully transmitting junction,

$$\text{elf}(\nu) = -\frac{r^2}{8\pi} \left(\frac{1}{\beta_1} + \frac{1}{\beta_2} \right) \nu^2 + \frac{ir^2}{4\pi} (V_2 - V_1) \nu \quad (3.154)$$

which is compatible with Eq. (86) of [18]. As discussed, the quadratic dependence of $\text{elf}(\nu)$ on ν implies that for large time the charge transfers per unit time become Gaussian random variables with mean and covariance equal, respectively, to

$$\left\langle \frac{\Delta q_1}{t} \right\rangle = -\left\langle \frac{\Delta q_2}{t} \right\rangle = \frac{2r_1^2 r_2^2}{r_1^2 + r_2^2} \frac{V_2 - V_1}{4\pi} \quad \text{and} \quad \mathcal{C} = \frac{1}{4\pi t} \frac{4r_1^2 r_2^2}{(r_1^2 + r_2^2)^2} \left(\frac{r_2^2}{\beta_1} + \frac{r_1^2}{\beta_2} \right) \begin{pmatrix} 1 & -1 \\ -1 & 1 \end{pmatrix}. \quad (3.155)$$

3.7.2 Heat transport

For the energy (or heat) transfer, the measurement protocol is the same. It consists in preparing the system of wires of length L in the initial product state ω_0^L given by the density matrix (3.132) and performing the measurements of the energies $H_i(0) = H_i^0$ and $H_i(t)$ in the disconnected wires at two times in between which the wires were connected. Denoting the results, respectively, $(e_i^0) \equiv \mathbf{e}^0$ and $(e_i) \equiv \mathbf{e}$, we encode the probability of the change of energies $\Delta e_i = e_i - e_i^0$ in the characteristic function

$$\text{th}F_t^L(\boldsymbol{\lambda}) = \sum_{\Delta \mathbf{e}} e^{i \sum_i \lambda_i \Delta e_i} \mathbb{P}_t(\Delta \mathbf{e}) = \omega_0^L \left(e^{-i \sum_i \lambda_i H_i(0)} e^{i \sum_i \lambda_i H_i(t)} \right), \quad (3.156)$$

the generating function of FCS for heat transfers. The change of energy of the wires connected between times 0 and t is, as for the charge, $\Delta H_i(t) = H_i(t) - H_i(0)$. This time, however, its expression in terms of chiral components is more complicated, because the scattering rule for the energy momentum tensor also involves currents, see (3.66). We end up with the expression

$$\Delta H_i(t) = -\frac{1}{r_i^2} \int_0^t \left(\sum_j (\delta_{ij} - (S_{ij})^2) r_j^2 T_j^\ell(0, s) - 2\pi \sum_{j \neq k} S_{ij} J_j^\ell(0, s) S_{ik} J_k^\ell(0, s) \right) ds. \quad (3.157)$$

In particular this observables do not commute with the initial Hamiltonians: $[H_j^0, \Delta H_i(t)] \neq 0$, hence we only have

$$\text{th}F_t^L(\boldsymbol{\lambda}) = \omega_0^L \left(e^{-i \sum_i \lambda_i H_i^0} e^{i \sum_i \lambda_i (H_i^0 + \Delta H_i(t))} \right) \neq \omega_0^L \left(e^{i \sum_i \lambda_i \Delta H_i(t)} \right) \quad (3.158)$$

The first exponential factor $\exp(-i \sum_i \lambda_i H_i^0)$ can be immediately seen as imaginary contributions to the inverse temperature β_i , but the second one has to be computed explicitly, in terms of the mode decomposition of T_i^ℓ and J_i^ℓ . Looking at (3.157) this calculation seems to require quite an amount of work which, however, can be considerably simplified if we take time $t = 2L$, an effect that has already appeared in the case of charge transfers. Here the simplification is purely technical and comes from the fact that a lot of terms in the mode decomposition of (3.157) carry the factors

$$e^{\frac{\pi i m t}{L}} - 1 \quad (3.159)$$

with various integers m . They all drop out when $t = 2L$ leaving us with the relatively simple expectation of $\exp(iA)$, with

$$A \equiv \sum_i \lambda_i (H_i^0 + \Delta H_i(2L)) = \frac{\pi}{2L} \sum_{i,j} (O\lambda O)_{ij} \left(\alpha_{0i} \alpha_{0j} + 2 \sum_{n>0} \alpha_{-2n,i} \alpha_{2n,j} \right), \quad (3.160)$$

where O is the orthogonal matrix related to matrix S by $O = r^{-1} S r$. The expectation of $\exp(iA)$ factors into the contribution from the zero and excited modes upon decomposing $A = A_0 + A_{\text{ex}}$ accordingly. The expectation of e^{iA_0} leads to a \mathbf{k} -sum that, after Poisson resummation in order to see better the behavior at $L \rightarrow \infty$, reads

$$\omega_0^L \left(e^{-i \sum_i \lambda_i H_i^0} e^{iA_0} \right) = \det(I + i\beta^{-1}C)^{-1/2} \frac{h_0^L(r, \mathbf{V}, \beta, \beta + iC)}{h_0^L(r, \mathbf{V}, \beta, \beta)}, \quad (3.161)$$

where r and β stand for the diagonal matrices with entries (r_i) and (β_i) , respectively, \mathbf{V} denotes the vector of potentials V_i , and

$$C = \lambda - O\lambda O \quad (3.162)$$

is a symmetric matrix (we identified the vector λ of variables conjugate to energy with the corresponding diagonal matrix). Function h_0^L contains the \mathbf{k} -sums:

$$h_0(r, \mathbf{V}, \beta, \tilde{\beta}) = e^{\frac{L}{4\pi}(r\beta\mathbf{V}, \tilde{\beta}^{-1}r\beta\mathbf{V})} \sum_{\mathbf{k} \in \mathbb{Z}^N} e^{-\pi L(r\mathbf{k}, \tilde{\beta}^{-1}r\mathbf{k}) - iL(r\beta\mathbf{V}, \tilde{\beta}^{-1}r\mathbf{k})} \quad (3.163)$$

Naively, matrix C plays the role of imaginary inverse temperatures, but is not necessarily diagonal, meaning that the energy transfers between the wires are more complex than for the charge.

The excited mode expectation of $e^{iA_{\text{ex}}}$ is less direct to compute. One way is to translate it to a vacuum expectation of an exponential of a Bogoliubov type of operator quadratic in creation and annihilation operators by using the Araki-Woods representation of canonical commutation relations [7]. The general idea is to construct new operators from the $\alpha_{2n,i}$, doubling the corresponding Fock space in such a way that the initial thermal expectation just becomes a vacuum matrix element on this double Fock space. The end result is

$$\omega_0^L \left(e^{-i \sum_i \lambda_i H_i^0} e^{iA_{\text{ex}}} \right) = \prod_{n>0} \det \left(I + (I - e^{-\frac{\pi i}{L} n \lambda} O e^{\frac{\pi i}{L} n \lambda} O) (e^{\frac{\pi n}{L} \beta} - I)^{-1} \right)^{-1}, \quad (3.164)$$

see [85]. Finally, the generating function of the FCS for energy transfer ${}^{\text{th}}F_{2L}^L(\boldsymbol{\lambda})$ is given by the product of the contributions of the zero modes (3.161) and of the excited ones (3.164).

In the asymptotic limit, which sends here both time $t = 2L$ and the length L to infinity, the ratio of \mathbf{k} -sums h_0^L is reduced for sufficiently small $|\lambda_i|$ to the contribution from $\mathbf{k} = 0$. The infinite discrete product for the excited states becomes an exponential of a continuous integral. Hence,

$${}^{\text{th}}f(\boldsymbol{\lambda}) \equiv \lim_{L \rightarrow \infty} \frac{1}{2L} {}^{\text{th}}F_{2L}^L(\boldsymbol{\lambda}) = f_0(r, \beta, C(\boldsymbol{\lambda}), \mathbf{V}) + f_{\text{ex}}(\lambda, \beta, O) \quad (3.165)$$

where the asymptotic contribution from the zero modes is

$$f_0(r, \beta, C(\lambda), \mathbf{V}) = \frac{1}{8\pi} \left((r\beta\mathbf{V}, (\beta + iC(\lambda))^{-1}r\beta\mathbf{V}) - (r\mathbf{V}, \beta r\mathbf{V}) \right) \quad (3.166)$$

encoding the energy transfer driven by electric potentials. It vanishes at $\mathbf{V} = 0$ but remains in the case of same potentials $V_i = V$. The asymptotic part from the excited states contribution reads

$$f_{\text{ex}}(\lambda, \beta, O) = - \int_0^\infty \ln \det \left(I + (I - e^{-2\pi i x \lambda} O e^{2\pi i x \lambda} O) (e^{2\pi x \beta} - I)^{-1} \right) dx \quad (3.167)$$

which encodes the transfer due purely to temperatures.

An explicit calculation of ${}^{\text{th}}F_t^L(\boldsymbol{\lambda})$ for $t \neq 2L$ is also possible along similar lines of [85], using the expansion of $H_i^0 + \Delta H_i(t)$ in terms of the modes, which is more involved without the simplification obtained for $t = 2L$. We expect that the same large-deviations rate function for energy transfers would result if we sent L to infinity before t , as suggested by the analysis of [18, 52]. In particular, Ref. [52] developed a perturbative calculation for the generating function of heat transfers in the case of junctions with circular full transmission of the heat current and handled the large L limit for fixed t order by order in $\boldsymbol{\lambda}$. A similar strategy could be applied in our case leading to a perturbative analysis of the exact formula for ${}^{\text{th}}F_t^L(\boldsymbol{\lambda})$, but applying it requires technical work that we postponed to the future.

Finally the function f_{ex} is similar to the one occurring in the Levitov-Lesovik approach, see section 3.9 below for more details. Together with the fact that the calculation for $t = 2L$ coincides with the exact asymptotic formula in the case of charge transfers, we have good hope that the formula obtained in (3.165) for the large deviation rate function of energy transfers is correct.

3.7.3 Examples

The rate function ${}^{\text{th}}f(\boldsymbol{\lambda})$ obtained in (3.165) involves several parameters. We would like to understand better the asymptotic properties of energy transfers by studying some examples.

Two wires : $N = 2, M = 1$. Again we take the first matrix S considered in example 3.7. By energy conservation, the dependence of ${}^{\text{th}}f$ is reduced to one variable $\lambda = \lambda_1 - \lambda_2$. We get for the zero modes part a ratio of two quadratic polynomial in λ , whose contribution to asymptotic form of the FCS is not Gaussian, unlike for the charge transfers. The excited modes part takes the form

$$f_{\text{ex}} = - \int_0^\infty \ln \frac{(1 + e^{-2\pi x(\beta_1 + \beta_2)}) - (O_{11})^2 (e^{-2\pi x\beta_1} + e^{-2\pi x\beta_2}) - (O_{12})^2 (e^{-2\pi x(\beta_1 + i\lambda)} + e^{-2\pi x(\beta_2 - i\lambda)})}{(1 - e^{-2\pi x\beta_1})(1 - e^{-2\pi x\beta_2})} dx, \quad (3.168)$$

where in this case

$$O = \frac{1}{r_1^2 + r_2^2} \begin{pmatrix} r_1^2 - r_2^2 & 2r_1 r_2 \\ 2r_1 r_2 & r_2^2 - r_1^2 \end{pmatrix} \xrightarrow{r_1 = r_2} \begin{pmatrix} 0 & 1 \\ 1 & 0 \end{pmatrix} \quad (3.169)$$

In general, the above integral is not computable explicitly, except in the case of the fully transmitting junction where $r_1 = r_2$ where the full rate function reads

$${}^{\text{th}}f(\lambda) = -\frac{r^2}{8\pi} \frac{(\beta_1 V_1^2 + \beta_2 V_2^2)\lambda^2 + i\beta_1\beta_2(V_1^2 - V_2^2)\lambda}{(\beta_1 + i\lambda)(\beta_2 - i\lambda)} + \frac{\pi}{12} \left(\frac{1}{\beta_1 + i\lambda} - \frac{1}{\beta_1} + \frac{1}{\beta_2 - i\lambda} - \frac{1}{\beta_2} \right), \quad (3.170)$$

which agrees with Eq. (90) of [18] taken at $\nu = 0$. Note that the second part is diverging at $\lambda = -i\beta_i$. This is also true in the general case (3.168) and has consequences for the corresponding asymptotic probability density, see below.

In the case of a general matrix O given by (3.169), we focus on the excited part (3.168) of ${}^{\text{th}}f$ by setting $V_1 = V_2 = 0$ so that f_0 vanishes. Let us look more closely at the analytic continuation ${}^{\text{th}}f(-i\lambda) \equiv f(\lambda)$ of the rate function. There is no analytic expression for the integral, but it can be computed numerically. First note that it is actually finite only for $-\beta_1 < \lambda < \beta_2$. Outside this interval, the dominant exponential factor does not vanish when $x \rightarrow \infty$ so that the value of f becomes $+\infty$. Moreover, $f(\lambda)$ is symmetric around $(\beta_2 - \beta_1)/2$. Finally, it is invariant under exchange of radii $r_1 \leftrightarrow r_2$. The left part of Figure 3.4 presents the graphs of $f(\lambda)$ for $\beta_1 = 1$ and $\beta_2 = 5$ for different values of the parameter $\rho = r_2/r_1 = 1, 2, 3$.

Note that for $\rho = 1$ we recover the analytic expression obtained in (3.170). When ρ increases, the graph of f becomes flatter around 0 inside the interval of definition and highly diverges at

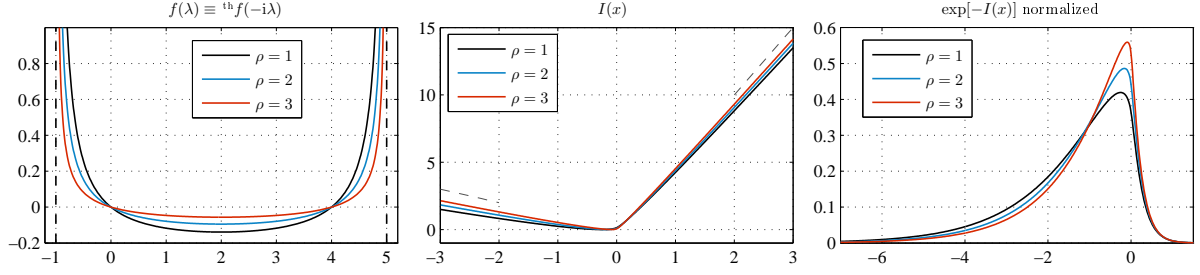


Figure 3.4: Large deviation rate function $f(\lambda)$, its Legendre transform $I(x)$ and probability density $\propto e^{-I(x)}$ for heat transfer in the case of two wires for different values of $\rho = r_2/r_1$. Here $\beta_1 = 1$ and $\beta_2 = 5$.

its boundaries. In the limit $\rho \rightarrow \infty$, function $f(\lambda)$ vanishes in the interval $]-\beta_1, \beta_2[$ and stays infinite outside of it.

The divergence of f at the boundaries $\lambda = \beta_i$ does not present a problem in the calculation of its Legendre transform, it just restricts the maximization interval:

$$I(x) = \max_{\lambda \in]-\beta_1, \beta_2[} \{\lambda x - f(\lambda)\} \quad (3.171)$$

since outside the interval the quantity to maximize is equal to $-\infty$. The graph of I is plotted in the middle part of Figure 3.4. The divergence of f implies that the corresponding large deviation rate function I has linear asymptotes, with the slope $-\beta_1$ and β_2 on the left and right, respectively.

The large deviations rate function $I(x)$ is that of the probability distribution of the energy change in the first wire per unit time $\Delta H_1(t)/t$, so that the linear asymptotes indicate an exponential decay of the probability density arising at long time. We represented in the right part of Figure 3.4 the graphs of normalized distribution functions $\propto \exp[-I(x)]$ which, as expected, exponentially decrease. The probability density is asymmetric and its maximum value is not zero. When ρ increases, the density seems to be tightened around this value. Finally, one can compute the mean value and check that it is negative, meaning that the energy is going from the lower inverse temperature $\beta_1 = 1$ to the higher one $\beta_2 = 5$.

The influence of temperature on the rate function $f(\lambda)$, its Legendre transform $I(x)$ and on the probability distribution $\propto \exp[-I(x)]$ is illustrated in Figure 3.5, showing the influence of β_2 on the asymptotic slope of $I(x)$ and on the asymmetry of the probability distribution.

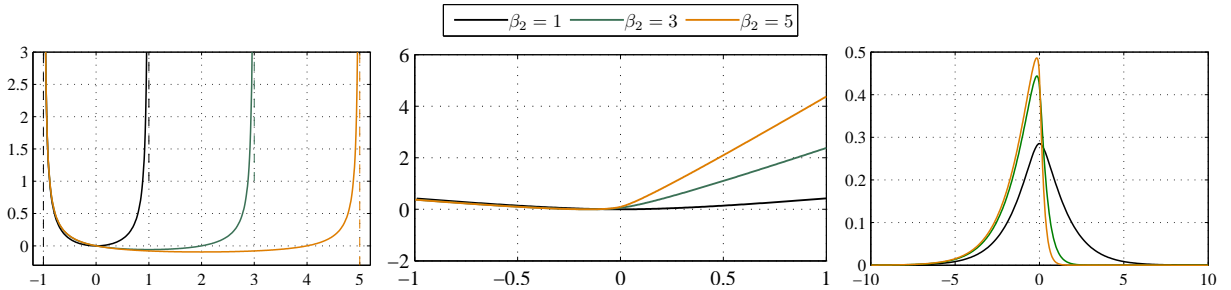


Figure 3.5: Large deviations rate function $f(\lambda)$, its Legendre transform $I(x)$, and probability density $\propto \exp[-I(x)]$ for different β_2 ($N = 2$, $\beta_1 = 1$, $r_2 = 2r_1$, and $V_1 = V_2 = 0$)

Three wires : $N = 3$, $M = 1$. The case of three wires can also be investigated, but formulas and graphs become more complicated, hence we focus on the simplest example already considered before of three identical wires ($r_i = r$) with $S_{ij} = \rho\delta_{ij} + \tau(1 - \delta_{ij})$ for $\rho = 1/3$ and $\tau = 2/3$, see

Example 3.7. The large deviation rate function for FCS of energy transfers is quite complicated even for $V_i = 0$. The formula can be found in [85]. Upon the analytic continuation, ${}^{\text{th}}f(-i\boldsymbol{\lambda}) \equiv f(\lambda_{12}, \lambda_{13})$ for $\lambda_{12} = \lambda_1 - \lambda_2$ and $\lambda_{13} = \lambda_1 - \lambda_3$ is finite only in the region

$$-\beta_1 < \lambda_{12} < \beta_2, \quad -\beta_1 < \lambda_{13} < \beta_3, \quad -\beta_2 < \lambda_{13} - \lambda_{12} < \beta_3. \quad (3.172)$$

This conditions generalize the restriction of the two wire case. The S matrix we consider here is symmetric under the exchange of wires since reflection and transmission coefficients are identical for each wire. Exploiting this symmetry, we plot function f in the coordinate system with axes at 120° so that the counter-clockwise rotation of the graph by 120° corresponds to the cyclic permutation $(\lambda_1, \lambda_2, \lambda_3) \mapsto (\lambda_3, \lambda_1, \lambda_2)$. We compare in Figure 3.6 the equilibrium case where $(\beta_1, \beta_2, \beta_3) = (1, 1, 1)$ to the case where $(\beta_1, \beta_2, \beta_3) = (1, 2, 3)$.

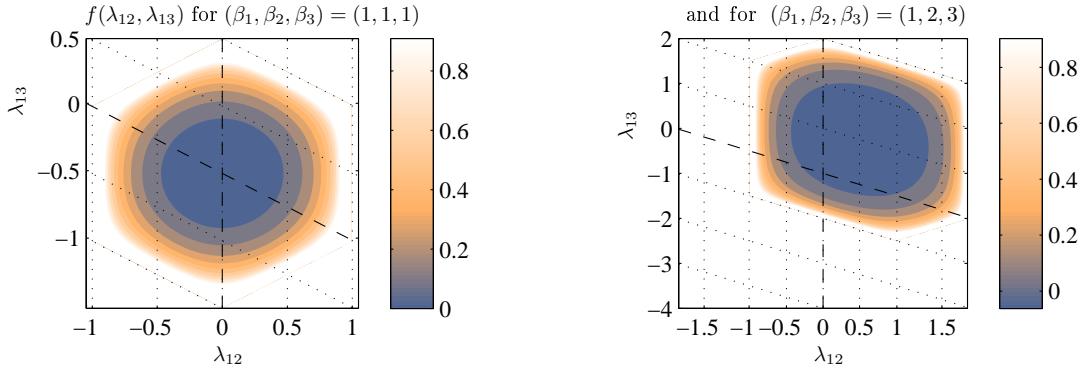


Figure 3.6: Rate function $f(\lambda_{12}, \lambda_{13})$ for 3 wires

In equilibrium, f is symmetric under 120° rotations but out of equilibrium, the above \mathbf{Z}_3 symmetry is broken to a degree that may be used as a measure of the distance from equilibrium. The Legendre transform of ${}^{\text{th}}f(-i\boldsymbol{\lambda})$ is infinite out of the plane $x_1 + x_2 + x_3 = 0$ and on that plane, it may be regarded as a function

$$I(x_{12}, x_{13}) = \max_{\lambda_{12}, \lambda_{13}} \left\{ \frac{1}{3}(2x_{12}\lambda_{12} - x_{12}\lambda_{13} - x_{13}\lambda_{12} + 2x_{13}\lambda_{13}) - f(\lambda_{12}, \lambda_{13}) \right\}. \quad (3.173)$$

Figure 3.7 presents the plot of $I(x_{12}, x_{13})$ for the equilibrium and nonequilibrium choice of

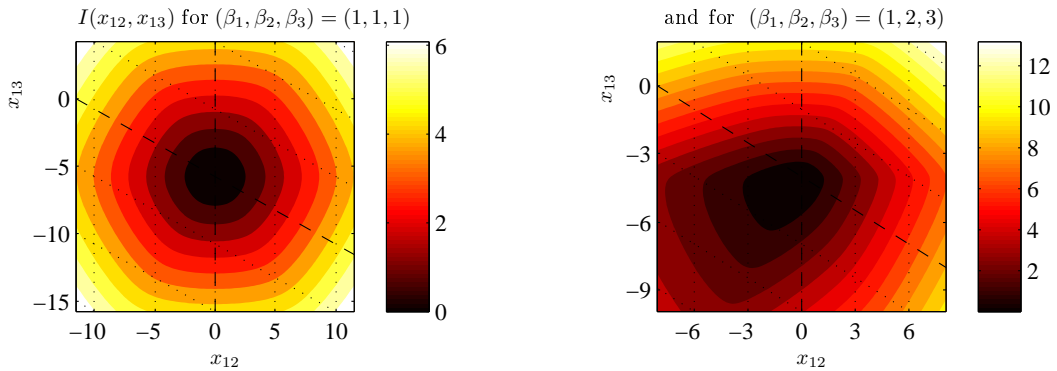


Figure 3.7: Legendre transform $I(x_{12}, x_{13})$ for 3 wires

temperatures. The level lines of I are equally spaced in various direction far from the origin, indicating the asymptotic linear increase of the function, as in the two wire case. The similar breaking of \mathbf{Z}_3 symmetry as for f may be observed.

Finally, Figure 3.8 plots for illustration the probability densities $\propto \exp[-I(x_{12}, x_{13})]$. Note that most mass of the distribution is in the negative quadrant indicating the heat transfer from the hotter 1st and 2nd wires to the colder 3rd one.

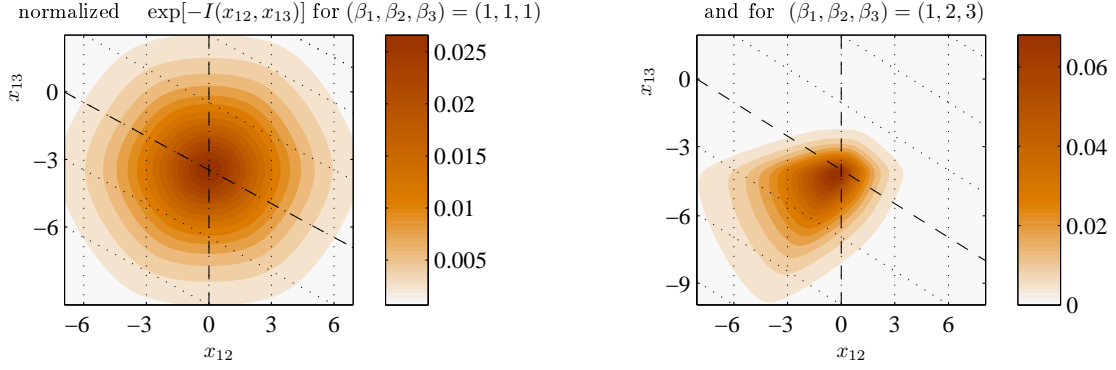


Figure 3.8: Probability density $\propto \exp[-I(x_{12}, x_{13})]$ for 3 wires

3.8 Charge and heat transport, the fluctuation relations

As mentioned before, charges Q_i and Hamiltonians H_j in the disconnected wires are commuting operators, so that the two measurement protocols can be adapted to a joint measurement. The generating function for FCS of both charge and heat transfers is defined as

$$F_t^L(\boldsymbol{\nu}, \boldsymbol{\lambda}) = \sum_{\Delta \mathbf{q}, \Delta \mathbf{e}} e^{i \sum_i \nu_i \Delta q_i + \lambda_i \Delta e_i} \mathbb{P}_t(\Delta \mathbf{q}, \Delta \mathbf{e}). \quad (3.174)$$

It is given by the expectation

$$F_t^L(\boldsymbol{\nu}, \boldsymbol{\lambda}) = \omega_0^L \left(e^{-i \sum_i (\nu_i Q_i(0) + \lambda_i H_i(0))} e^{i \sum_i (\nu_i Q_i(t) + \lambda_i H_i(t))} \right). \quad (3.175)$$

Proceeding as before and computing this function at time $t = 2L$, the exponential factors involving charge effectively become $-i \sum_i \tilde{\nu}_i Q_i^0$ with $\tilde{\nu}_i$ defined in (3.141), so that their only effect is the change of \mathbf{V} to $\mathbf{V} - i\beta^{-1} \tilde{\boldsymbol{\nu}}$, and we are left with a calculation of energy transfer as in (3.158), with this shifted electric potential. The zero mode contribution leads to the \mathbf{k} -sums appearing in (3.161) and the excited modes result in the infinite product (3.164). The long time limit gives immediately

$$f(\boldsymbol{\nu}, \boldsymbol{\lambda}) \equiv \lim_{L \rightarrow \infty} \frac{1}{2L} F_{2L}^L(\boldsymbol{\nu}, \boldsymbol{\lambda}) = f_0(r, \beta, C(\boldsymbol{\lambda}), \mathbf{V} - i\beta^{-1} \tilde{\boldsymbol{\nu}}) + f_{\text{ex}}(\boldsymbol{\lambda}, \beta, O) \quad (3.176)$$

similarly as for the large deviations of heat transfers (3.165), with f_0 and f_{ex} given by (3.166) and (3.167).

Beyond encoding both charge and heat transfers in a single rate function, giving a more compact solution of the problem, $f(\boldsymbol{\nu}, \boldsymbol{\lambda})$ satisfies the fluctuation relation [6]

$$f(\boldsymbol{\nu}, \boldsymbol{\lambda}) = f(-\boldsymbol{\nu} - i\beta \mathbf{V}, -\boldsymbol{\lambda} + i\beta) \quad (3.177)$$

that reflects the time reversal invariance of dynamics, as argued in [19]. Such a fluctuation relation imposes constraints on “mixed” transfers, such as the heat transfer induced due to difference of electric potentials, for example. Hence the interest in considering rate function $f(\boldsymbol{\nu}, \boldsymbol{\lambda})$ taking into account all kinds of exchanges.

The fluctuation relation (3.177) leads after taking a Legendre transform to an asymptotic symmetry

$$\mathbb{P}_t(-\Delta \mathbf{q}, -\Delta \mathbf{e}) \sim e^{-\sum_i \beta_i (\Delta e_i - V_i \Delta q_i)} \mathbb{P}_t(\Delta \mathbf{q}, \Delta \mathbf{e}) \quad (3.178)$$

for the probability density of tranfers holding for large L and t . Since charge and energy are conserved, the probability density $P_t(\Delta \mathbf{q}, \Delta \mathbf{e})$ does not vanish only if the sums of Δe_i and Δq_i

vanish. This allows to rewrite the latter relation in terms of differences of potentials V_i and of products $\beta_i V_i$. In the equilibrium case, the probability density recovers then its symmetry around zero transfers.

Again, we established the above relations considering the particular case where $t = 2L$, but we expect the result (3.176) for f to be the same in the physical limit $L \rightarrow \infty$ then $t \rightarrow \infty$.

3.9 Comparison to the Levitov-Lesovik formulae

The computation of the full counting statistics of charge transfers between N free fermionic system was originally proposed by L.S. Levitov and G.B. Lesovik in [120]. Such systems are assumed to be initially in different equilibrium states and to interact subsequently during a period of time t . Their interaction is described by an $N \times N$ unitary mode-dependent matrix $\mathbb{S}_t(p)$ accounting for the scattering between the fermions of different systems, see also [119]. The Levitov-Lesovik formula for the generating function of charge FCS has the form of a product over the free fermionic modes of determinants:

$$\Phi_t(\boldsymbol{\nu}) = \prod_p \det (I - f(p) + f(p)e^{-is(p)\nu} \mathbb{S}_t(p)^\dagger e^{is(p)\nu} \mathbb{S}_t(p)), \quad (3.179)$$

where $s(p)$ is the sign function representing the charge of modes, ν is the diagonal $N \times N$ matrix of coefficients ν_i and $f(p)$ that of Fermi functions $f_i(p) = (e^{\beta_i(\epsilon(p)-s(p)V_i)} + 1)^{-1}$, with $\epsilon(p)$ representing the energy of modes.

We would like to see if there is a relation between the FCS of charge transfers $^{\text{el}}f$ and the above Levitov-Lesovik formula. Of course, in spite of similarities, the coupling between free fermions realized by the bosonic junction induces a scattering of the currents, which is different than the fermion scattering assumed in the Levitov-Lesovik approach, so there is no *a priori* reason for the two systems to lead to the same FCS⁶. It appears, however, that in a (very) particular case the two formulae may be related. Under the following assumption: $\mathbb{S}_t(p) = \mathbb{S}$ is mode and time independent, with linear dispersion for fermions $\epsilon(p) = \frac{\pi}{L}|p|$, upon setting $t = 2L$, at radius $r_i = \sqrt{2}$ and in the case of same temperatures $\beta_i = \beta$, we have

$$^{\text{el}}f(\boldsymbol{\nu}) = \lim_{\theta \rightarrow \infty} \theta^2 \lim_{t=2L \rightarrow \infty} \frac{1}{2L} \ln \Phi_t(\theta^{-1}\boldsymbol{\nu}) \Big|_{\beta, \theta^{-1}\mathbf{V}} \quad (3.180)$$

if we identify $|\mathbb{S}_{ij}|^2 = S_{ij}$. In that case, the fluctuations of charge transfers induced by different electric potentials at the same ambient temperature agree in the two setups at the level of the Gaussian central limit contributions. One should remark, however, that the scaling limit on the right hand side of (3.180) removes from the Levitov-Lesovik rate function the term linear in \mathbf{V} and quadratic in $\boldsymbol{\nu}$ that is responsible for the zero-temperature shot noise given by the Khlus-Lesovik-Büttiker formula [26]. Note that this quantity has been investigated in details for other models of scale invariant junctions in [126, 53] and should be, in principle, accessible in our model too through the current correlation functions.

There is another relation of the FCS statistics that we have obtained for the junction of wires and the Levitov-Lesovik type formulae, this time for the energy transfers. Indeed, the contribution (3.167) of the excited modes to the generating function $^{\text{th}}F_{2L}^L(\boldsymbol{\lambda})$ of energy FCS coincides directly with the version of the Levitov-Lesovik formula for N free bosons with the dispersion relation $\epsilon_n = \frac{\pi n}{L}$ and the interaction described by the scattering matrix $\mathbb{S} = O$, without any supplementary assumption. Such bosonic version of the Levitov-Lesovik formula was obtained in [108].

⁶The scattering of the fermionic modes corresponding to the bosonic junction is actually highly nontrivial, see [62] for example.

3.10 Conclusion

We described a detailed investigation of a free massless bosonic field model of a junction of quantum wires. We constructed a nonequilibrium stationary state describing wires kept at different temperatures and electric potentials and computed the corresponding mean charge and energy flows in each wire. Our results are consistent with those of [127] and cover also the linear response regime considered in [147]. We also obtained the full counting statistics for charge and energy transport associated to a two-time measurement protocol, and the corresponding large deviation rate function giving the long time asymptotics of FCS. Our results overlap with those in [18, 52], generalizing the latter ones beyond the case of fully transmitting junctions, but only for a system modeled by free fields.

Our model describes a large class of junctions with various possibilities of reflection and transmission, and the free field nature of the theory allows to calculate explicitly a variety of interesting quantities. It may be applied to study charge and energy flows through point contacts of one-dimensional systems of free massless bosons, free or interacting electrons, the latter in the Luttinger regime, and also edge modes in the integer quantum Hall effect [65].

The fermionic systems were described using the fermion-boson correspondence and the junctions modeled here induce scattering of fermions through their currents, as a consequence of the bosonic boundary conditions imposed at the junction. Such conditions do not lead to a simple scattering of fermions that was assumed in the Levitov-Lesovik approach, hence the difficulty to match our result with theirs.

One of the things that remains to be done is the calculation of FCS for heat transport outside the specific case $t = 2L$, but it should be expected that this would not change the result for the large deviations rate function obtained here. We could also try to modify the model in order to obtain a more general class of scattering matrices S , since the results should be the same if we consider any orthogonal matrix S . The subclass that appeared here is only an artifact due to our choice of boundary conditions. Finally, another direction would be to consider nonequilibrium states with same boundary conditions but in other wire geometries than the star graph, such as N wires joining and then separating, or a loop between two wires (for which we have preliminary results) or, ultimately, a general graph. Such nonequilibrium states seem technically reachable and should have interesting properties.

Chapter 4

Wess-Zumino-Witten junction with a cyclic brane

The successful results obtained in the previous chapter suggest that our approach should be generalizable to models involving other conformal field theories than the free massless bosonic field compactified on a circle. Wess-Zumino-Witten models come as the most natural candidate for generalization: classically, they describe fields taking values in compact nonabelian groups rather than in $U(1)$ but are conformal invariant, preserving the ballistic propagation of excitations. The latter can be described exactly due to a rich infinite-dimensional symmetry of the theory. The exact solvability of WZW models does not mean, however, that all calculations may be explicitly done in practice. In particular, the exact solutions are reachable only for rather special boundary conditions. This will lead to few possible junctions. In this chapter, we present only one of them where the current from one wire arriving at the junction is fully transmitted to the next wire, in a cyclic way. This simple case will allow us to introduce WZW models in details and to carry explicit calculations almost to the very end. The final results described in this chapter are similar to those in [52] although they were obtained largely independently.

4.1 Wess-Zumino-Witten models

4.1.1 Lagrangian approach

Wess-Zumino-Witten models arise naturally in trying to extend the massless free field theory to a nonabelian case. Consider a general field

$$g : \Sigma \rightarrow G, \quad (t, x) \mapsto g(t, x), \quad (4.1)$$

where Σ is a two dimensional Minkowskian worldsheet and G a compact Lie group. Let \mathfrak{g} be the Lie algebra of G , assumed to be simple, and consider the corresponding Killing form $k/2 \operatorname{tr}(XY)$ for $X, Y \in \mathfrak{g}$ normalized so that the long roots have length squared 2. For $g \in G$, the 1-form $g^{-1}dg$ is \mathfrak{g} -valued. We define the classical sigma-model action

$$S_0[g] = \frac{k}{8\pi} \int_{\Sigma} \operatorname{tr} [- (g^{-1} \partial_t g)^2 + (g^{-1} \partial_x g)^2] dt dx \quad (4.2)$$

This action is invariant under conformal transformations and the equations of motion are, in the light cone coordinates $x_{\pm} = t \pm x$

$$2\partial_+(g^{-1}\partial_-g) + [g^{-1}\partial_+g, g^{-1}\partial_-g] = 0 \quad (4.3)$$

where $[\cdot, \cdot]$ is the Lie bracket on \mathfrak{g} . This equation is simple only in the case where G is Abelian since the second term vanishes and we are back in the case of Chapter 3, otherwise the solutions are

not easy to describe. On the top of that the quantized version of such a theory (and in particular its renormalization) breaks conformal invariance. To overcome these problems, Witten proposed in [173] to add to action S_0 the following topological term

$$S_{\text{WZ}}[g] = \frac{k'}{4\pi} \int_{\tilde{\Sigma}} \tilde{g}^* \chi, \quad (4.4)$$

which is known as the Wess-Zumino term [167]. It requires an extension of the worldsheet Σ to a three dimensional manifold $\hat{\Sigma}$ such that $\partial\hat{\Sigma} = \Sigma$, and of field g to $\tilde{g} : \tilde{\Sigma} \rightarrow G$ such that its restriction to $\partial\hat{\Sigma}$ coincides with g . χ is a closed 3-form on group G given by

$$\chi = \frac{1}{3} (g^{-1} dg)^{\wedge 3}. \quad (4.5)$$

Finally the constant k' has to be an integer so that the Feynman amplitudes $\exp[iS_{\text{WZ}}]$ be well defined on closed worldsheets Σ : if two extensions (1 and 2) of Σ and g exist, the ambiguity $S_{\text{WZ}}^1 - S_{\text{WZ}}^2$ is $2\pi k'$ valued. Hence if $k' \in \mathbb{Z}$ the corresponding Feynman amplitude is the same whatever the extension. We will assume the existence of such extension, and the case where it does not exist will be discussed later, see the next Part of the thesis. Note that if field g takes values in the subset of G on which $\chi = dB$ then the Wess-Zumino action is reduced to

$$S_{\text{WZ}}[g] = \frac{k'}{4\pi} \int_{\Sigma} g^* B. \quad (4.6)$$

χ , however, is not an exact form globally. Taking both actions S_0 and S_{WZ} together, the new equations of motion are computed using for the topological term the geometric identity $\delta \int f^* \alpha = \int \mathcal{L}_{\delta f} \alpha$, where $\mathcal{L}_X = \iota_X d + d\iota_X$ is the Lie derivative, and the Stokes theorem. At the end, one gets the classical equations

$$2k\partial_+(g^{-1}\partial_-g) + (k - k')[g^{-1}\partial_+g, g^{-1}\partial_-g] = 0. \quad (4.7)$$

For $k = k'$ the last term vanishes and the equations simplify. The Wess-Zumino-Witten action is then defined by $S_{\text{WZW}} = S_0 + S_{\text{WZ}}$ where we have taken $k = k' \in \mathbb{Z}$. The equations of motion have the simple form

$$\partial_+(g^{-1}\partial_-g) = 0 \quad \Rightarrow \quad g(t, x) = g_\ell(t+x)g_r^{-1}(t-x) \quad (4.8)$$

where in the general solution g_ℓ and g_r are any G -valued functions (the order matters since G is nonabelian). This factorization indicates that this model is very much like a free field theory, involving ballistic propagation of left and right movers, as already discussed in the previous chapter. The equation of motion (4.8) is actually nothing but the conservation of the currents

$$J_r \equiv -ikg^{-1}\partial_-g = ik(\partial_-g_r)g_r^{-1} \quad (4.9)$$

Moreover, equation of motion (4.8) can be written equivalently as

$$\partial_-((\partial_+g)g^{-1}) = 0 \quad \text{such that} \quad J_\ell \equiv ik(\partial_+g)g^{-1} = ik(\partial_+g_\ell)g_\ell^{-1} \quad (4.10)$$

is another conserved current. As for the free field, the model contains two independent conserved currents that propagate in a ballistic way in opposite directions. Indeed, J_ℓ depends only on $t+x$ so is a left mover in the previous terminology and J_r only on $t-x$ so it is a right mover. However the underlying symmetry is nonabelian. The WZW action is invariant under the transformations

$$g(t, x) \mapsto h_\ell(t+x)g(t, x)h_r(t-x)^{-1} \quad (4.11)$$

for any G -valued one variable functions $h_{\ell,r}$. The current J_ℓ and J_r are the chiral component of the Noether current associated to the rigid adjoint symmetry $g \mapsto hgh^{-1}$ for $h \in G$. They generate transformations (4.11) in the phase space of the theory.

The WZW action remains conformal invariant since the topological term S_{WZ} is independent of the worldsheet metric. The conformal transformations are generated in the phase space by the chiral components of the energy momentum tensor, which take the form

$$T_{i,\ell/r} = \frac{1}{4\pi k} \text{tr}((J_{\ell,r})^2) \quad (4.12)$$

They inherit the coordinate dependence from the currents and hence propagate ballistically.

4.1.2 Quantization

Assume that the previous worldsheet is space periodic: $g(t, x + L) = g(t, x)$, then the left and right currents can be decomposed in Fourier modes

$$J_\ell^a(t, x) = \frac{2\pi}{L} \sum_{n \in \mathbb{Z}} J_n^a e^{-\frac{2\pi i n(t+x)}{R}} \quad J_r^a(t, x) = \frac{2\pi}{L} \sum_{n \in \mathbb{Z}} \bar{J}_n^a e^{-\frac{2\pi i n(t-x)}{R}} \quad (4.13)$$

where a denotes the component of J in the basis (t^a) of the Lie algebra \mathfrak{g} , satisfying $[t^a, t^b] = if^{abc}t^c$ and $\text{tr}(t^a t^b) = \frac{1}{2}\delta^{ab}$. The quantization of the WZW model (see [50] or below for a specific example) leads to the commutation relations

$$[J_n^a, J_m^b] = if^{abc} J_{n+m}^c + \frac{kn}{2} \delta^{ab} \delta_{n,-m} \quad (4.14)$$

and similarly for the \bar{J}_n^a . This corresponds to the current (or affine) algebra $\widehat{\mathfrak{g}}$ [73]. The Hilbert space of the WZW theory is constructed from highest weight representations of $\widehat{\mathfrak{g}}$ defined as follows:

1. Consider an irreducible representation of Lie algebra \mathfrak{g} , denoted by its corresponding highest weight λ (e.g., if $\mathfrak{g} = su(2)$, $\lambda = 0, \frac{1}{2}, 1, \frac{3}{2}, \dots$ is the spin of representation). Denote by M_λ the corresponding representation space.
2. Such space is invariant under the action of the zero modes J_0^a corresponding to the irreducible representation λ .
3. Assume that for any $|v\rangle \in M_\lambda$ and $n > 0$ $J_n^a |v\rangle = 0$.
4. Vectors

$$J_{-n_1}^{a_1} \dots J_{-n_s}^{a_s} |v\rangle, \quad s \geq 0, \quad n_1 \geq \dots n_s \geq 1, \quad |v\rangle \in M_\lambda \quad (4.15)$$

generate the space $\widehat{M}_{k,\lambda}$ of the highest weight representation of $\widehat{\mathfrak{g}}$.

For given λ , there may exist different such representations. We shall be interested in unitary highest weight representations for which there exists a hermitian scalar product on $\widehat{M}_{k,\lambda}$ with respect to which $(J_p^a)^\dagger = J_{-p}^a$ (so that the currents become symmetric operators). They exist only for $k = 0, 1, \dots$ and, for each such “level” k , for a finite number of weights λ , and are irreducible and unique (up to equivalence) [73, 50]. Such λ are called integrable and the corresponding unitary irreducible representations of $\widehat{\mathfrak{g}}$ are denoted $\widehat{V}_{k,\lambda}$ and also called integrable [100]. We do not need to describe in details the conditions for λ but just will mention that in the case where $\mathfrak{g} = su(2)$, the integrable weights correspond to spins $\lambda = 0, \frac{1}{2}, 1, \dots, \frac{k}{2}$, i.e. there are $k + 1$ possibilities.

The action of affine algebra $\widehat{\mathfrak{g}}$ in $\widehat{V}_{k,\lambda}$ induces the one of the Virasoro algebra via the Sugawara construction:

$$L_n = \frac{1}{k+h^\vee} \sum_{m \in \mathbb{Z}} \sum_a : J_m^a J_{n-m}^a :, \quad (4.16)$$

where h^\vee is the dual Coxeter number of \mathfrak{g} [73] and the Wick ordering resets the modes J_p^a with positive p to the right of those with negative p . The Virasoro generators L_n satisfy the commutation relations

$$[L_n, L_m] = (n-m)L_{n+m} + \frac{1}{12}c_k n(n^2-1)\delta_{n,-m} \quad (4.17)$$

with the Virasoro central charge

$$c_k = \frac{k \dim(\mathfrak{g})}{k+h^\vee} \quad (4.18)$$

and the unitarity conditions $L_n^\dagger = L_{-n}$. We also have the relation $[L_n, J_m^a] = -mJ_{n+m}^a$ between current and Virasoro generators.

The quantization of the right current modes \bar{J}_p^a similarly leads to unitary highest weight representations and Virasoro operators \bar{L}_n . The full Hilbert space of the theory will be a (the completion in norm) of a consistent combination over all the possible λ of tensor product of left and right representations. The simplest combination is the “diagonal” one

$$\mathcal{H} = \bigoplus_{\lambda} \widehat{V}_{k,\lambda} \otimes \widehat{V}_{k,\bar{\lambda}}, \quad (4.19)$$

where the direct sum is performed over all the integrable weights λ for a given k and $\bar{\lambda}$ denotes the highest weight corresponding to the representation of \mathfrak{g} complex conjugate to that in M_λ . Such space of state corresponds to the WZW model with simply connected target group G . For non-simply connected target groups, other nondiagonal combinations occur (see Part II). In the case of boundary WZW model, the chiral and antichiral currents are related and the corresponding Hilbert space of states is a combination of unitary representations of a single affine algebra, as we shall see in the next example.

4.1.3 Disconnected wires

Consider the case where the worldsheet has finite spatial size: $x \in [0, L]$ and is infinite in time: $t \in \mathbb{R}$. Such a band worldsheet has boundaries that require supplementary conditions to define the corresponding WZW model. The simplest ones are

$$g(t, 0) = 1 = g(t, L) \quad (4.20)$$

for all $t \in \mathbb{R}$ and where 1 is the unit element of G . We say that at the boundaries the field g belongs to the trivial brane \mathcal{C}_0 (the notation will be explained below). The action is defined similarly and the equations of motion are identical to (4.8), except that the left and right currents are now related by the boundary conditions. Indeed the previous equation relates the left and right functions g_ℓ and g_r appearing in (4.8) at $x = 0$ and $x = L$. Consequently, the corresponding left and right currents are related by $J_\ell(t, 0) = J_r(t, 0)$ and similarly at $x = L$, meaning that the left current is reflected to the right one at each boundary and corresponds to the case of one disconnected wire with a full reflection condition at each end. The relations between left and right currents can be rewritten as

$$J_r(t, x) = J_\ell(t, -x), \quad J_\ell(t, x + 2L) = J_\ell(t, x) \quad (4.21)$$

such that right current is fully expressed in terms of the left one, which becomes a periodic field on a worldsheet of size $2L$. The quantization of J_ℓ is done as in the previous subsection, leading

to a highest weight irreducible representations $\widehat{V}_{k,0}$ corresponding to the trivial representation of \mathfrak{g} [86]. Since the right current is expressed through the left one, it also acts on $\widehat{V}_{k,0}$ and there is no freedom remaining for its quantization. Thus the boundary theory on the strip $\mathbb{R} \times [0, L]$ with the boundary conditions that we chose contains only one irreducible highest weight representation, i.e. just a piece of the chiral part of the bulk theory on the cylinder.

4.1.4 WZW models and quantum wires

Wess-Zumino-Witten models on quantum wires are motivated from the theoretical point of view as a natural generalization of the free massless bosonic field developed in the previous chapter. The ballistic propagation of the excitations is preserved and more internal degrees of freedom are allowed through the choice of the group G , leading to a description of richer collective excitations. Such models were actually introduced by Witten in [173] to generalize the scheme of bosonization to collections of free massless fermi fields in 1+1 dimensions. Thus a WZW model for a quantum wire should describe an effective low energy behavior of some fermionic theory, and G should reflect the initial symmetries of the system. For example, such models appear explicitly in the description of the edge states of the fractional quantum Hall effect [65].

The biggest difference of the collective chiral excitations in WZW models as compared to the free bosons is their nonabelian statistics: chiral fields may mix with each other in a nonabelian way when exchanged, instead of picking a phase (+1 for bosons or -1 for fermions, or a more general one for anyons). It was pointed out in [129] that such a nonabelian statistics can be realized in a fractional quantum Hall effect at the filling factor $\nu = 5/2$, and its experimental evidence is still in progress [170].

4.2 WZW model on a junction

4.2.1 Classical action and equations of motion

In the spirit of the folding trick explained in 2.2.1, we consider the model of an N -component field:

$$\begin{aligned} \mathbf{g} : \mathbb{R} \times I &\rightarrow (G)^N, \\ \mathbf{g}(t, x) &= (g_1(t, x), \dots, g_N(t, x)). \end{aligned} \quad (4.22)$$

where $I = [0, L]$ for L the length of the wire. Each component g_i will be ruled by a WZW action presented above, but in order to set the full action of the system, we first work out the boundary conditions. At the free end of the wires, the condition has to be independent on each wire. We set the simplest one

$$\forall i = 1, \dots, n, \quad \forall t \in \mathbb{R} \quad g_i(t, L) \in \mathcal{C}_0 = \{1\} \quad (4.23)$$

where 1 is the neutral element of G , as in the previous example of the disconnected wire. This leads to the bouncing of the corresponding currents at $x = L$, see below. At the junction we propose the following boundary condition involving the product of all wire components:

$$\forall t \in \mathbb{R}, \quad (g_1 g_2 \cdots g_n)(t, 0) \in \mathcal{C}_\tau \equiv \{h e^{2\pi i \tau} h^{-1} | h \in G\} \quad (4.24)$$

for a given τ in the positive Weyl alcove in \mathfrak{t} , the Cartan subalgebra of $\mathfrak{g} = \text{Lie}(G)$. Subset \mathcal{C}_τ is a conjugacy class in the group G . Such conjugacy classes are invariant under the adjoint action and appear naturally when considering boundary conditions for WZW model that preserve the adjoint symmetry: they were already considered in [2, 56, 76]. Moreover, the 3-form χ involved in the topological term S_{WZ} is exact on such classes

$$\chi|_{\mathcal{C}_\tau} = d\omega_\tau, \quad \omega_\tau(g) = \text{tr}((h^{-1}dh) \wedge e^{2\pi i \tau} (h^{-1}dh) e^{-2\pi i \tau}) \quad (4.25)$$

The 3-form χ also has the multiplicative property $\chi(g_1 g_2) = \chi(g_1) + \chi(g_2) - \text{dtr}(g_1^{-1} dg_1 \wedge (dg_2) g_2^{-1})$ that can be generalized on any product by induction, and such that at least locally we have

$$\omega_\tau(g_1 \cdots g_n) + \sum_{i=2}^n \text{tr} \left((g_1 \cdots g_{i-1})^{-1} d(g_1 \cdots g_{i-1}) \wedge (dg_i) g_i^{-1} \right) = \sum_{i=1}^n \omega(g_i) + d\eta(g_1, \dots, g_n). \quad (4.26)$$

for $g_1 \cdots g_N \in \mathcal{C}_\tau$, and where η is a 1-form. We consequently define the action of the model:

$$S[g] = \frac{k}{8\pi} \sum_{i=1}^N \int_{\mathbb{R} \times I} \left(\text{tr} \left[-(g_i^{-1} \partial_t g_i)^2 + (g_i^{-1} \partial_x g_i)^2 \right] dt dx + 2\omega(g_i) \right) + \frac{k}{4\pi} \int_{\mathbb{R}} \eta(g_1, \dots, g_n)(t, 0) \quad (4.27)$$

The first integral is the standard WZW action on G^N , where ω should be seen as a formal notation for $d^{-1}H$, and the integral of η is a supplementary term taking into account the specific boundary condition at $x = 0$.

The equations of motions are computed as in the case developed in the previous section, except that the boundaries give extra terms in the integration by parts (however note that $\delta g_i = 0$ at $x = L$), and the presence of η allows to use (4.26) during the computation. We end up with $\delta S = \delta S_{\text{bulk}} + \delta S_{\text{bdry}}$ that can be treated separately for dimensional reasons. The Bulk term is a sum over the wires of computations similar to the previous section so that $\delta S_{\text{bulk}} = 0$ gives the standard equation of motion on each wire i

$$\partial_+(g_i^{-1} \partial_- g_i) = 0 \quad \Rightarrow \quad g_i(t, x) = g_{i,\ell}(t+x) g_{i,r}^{-1}(t-x), \quad (4.28)$$

solved by the general formula with one-variable functions $g_{i,\ell}$ and $g_{i,r}$. Moreover the left and right currents on each wire, defined by

$$J_{i,\ell} \equiv ik(\partial_+ g_i) g_i^{-1} = ik g'_{i,\ell} g_{i,\ell}^{-1}, \quad J_{i,r} \equiv -ik g_i^{-1} \partial_- g_i = ik g'_{i,r} g_{i,r}^{-1} \quad (4.29)$$

are conserved in the bulk, as in the case without boundaries (the primes stands for the single variable derivatives).

The boundary term localized at $x = 0$, is somewhat more complicated,

$$\begin{aligned} \delta S_{\text{bdry}} &= \frac{k}{4\pi} \int_{\mathbb{R}} \iota_{(\delta g_1, \dots, \delta g_n)}(\cdot, 0) \left(\omega_\tau(g_1 \cdots g_n) + \sum_{i=2}^n \text{tr} \left((g_1 \cdots g_{i-1})^{-1} d(g_1 \cdots g_{i-1}) (dg_i) g_i^{-1} \right) \right) \\ &\quad - \frac{k}{4\pi} \sum_{i=1}^n \int_{\mathbb{R}} \text{tr} \left((g_i^{-1} \delta g_i) (g_i^{-1} \partial_x g_i)(\cdot, 0) \right) dt, \end{aligned} \quad (4.30)$$

and has to be investigated. At $x = 0$ the degrees of freedom are encoded in the $g_i(t, 0)$ and $h(t, 0)$, all related by Eq. (4.24). The above boundary variation has to be decomposed as a combination of N independent among the $N+1$ available group-valued fields, then each coefficient has to vanish independently. After some algebra, equations of motion $\delta S_{\text{bdry}} = 0$ actually simplify, leading to the relations

$$g_i^{-1} \partial_- g_i = -(\partial_+ g_{i+1}) g_{i+1}^{-1} \quad \Leftrightarrow \quad J_{i,r}(t, 0) = J_{i+1,\ell}(t, 0) \quad (4.31)$$

for $i = 1, \dots, n$ (where $n+1$ is identified with 1). Thus at the junction, the right current is fully transmitted to the left one in the next wire. Hence the previous equation is a very simple scattering rule where $S_{ij} = \delta_{(i+1)j}$ (compare with the bosonic case (3.42)) and reproduces the star graph junction of N wires studied in [52]. Note that this rule is invariant under the cyclic permutation $i \mapsto i+1$, reflecting the symmetry of boundary condition (4.24), so that we call such model the cyclic brane junction. Finally note that in the particular case where $N = 2$ the

current from one wire is fully transmitted in the other part of the system. This corresponds to the configuration proposed in [18].

The equation of motion $\delta S = 0$ does not involve $x = L$ term, however boundary condition (4.23) has to be satisfied, relating the left and right g fields

$$g_{i,\ell}(t+L) = g_{i,r}(t-L) \quad \Rightarrow \quad J_{i,\ell}(t, L) = J_{i,r}(t, L) \quad (4.32)$$

At the free end of the wire, the left current is fully reflected to the right one, as in the bosonic case discussed in the previous chapter.

4.2.2 Phase space

The classical solutions of the equations of motion forms the phase space of the system whose structure we should understand better. The consistency between the bulk and boundary properties of the fields and the corresponding currents leads to a simplification of the degrees of freedom. Starting with the fields g_i , boundary conditions (4.31) at $x = 0$ together with (4.32) at $x = L$ give:

$$g_{i,r}(t) = g_{i+1,\ell}(t)g_{i,0}^{-1}, \quad g_{i,\ell}(t+2L) = g_{i+1,\ell}(t)g_{i,0}^{-1} \quad (4.33)$$

where the $g_{i,0}$ may be set to 1 except $g_{n,0} = e^{2\pi i\tau}$ by redefining the chiral fields $g_{i,\ell/r}$. After such a redefinition, any left mover can be expressed in terms of the first one by transitivity leading to

$$g_{i,\ell}(t) = g_{1,\ell}(t + (i-1)2L) \quad (4.34)$$

for all $i = 1, \dots, n$, and the twisted-periodic field on the first wire

$$g_{1,\ell}(t+2nL) = g_{1,\ell}(t) e^{2\pi i\tau}. \quad (4.35)$$

Thus the phase space is reduced the maps $\mathbb{R} \ni x \mapsto g_{1,\ell}(x) \in G$ that are twisted-periodic of period $R \equiv 2NL$ with monodromy $e^{2\pi i\tau}$.

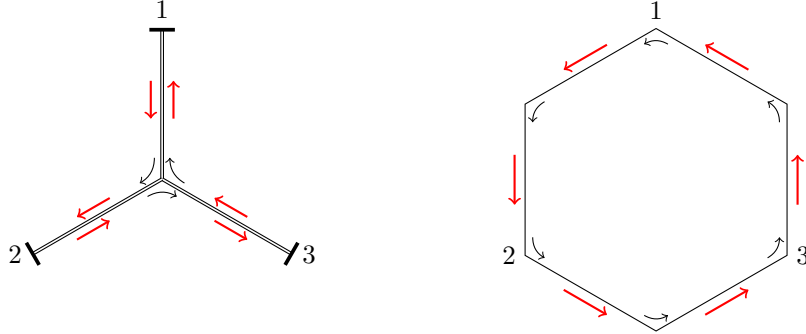


Figure 4.1: In the initial picture (left figure), the right moving currents are fully transmitted at the junction and the left moving ones are fully reflected at the end of wires. However, in an equivalent picture (right figure) the phase space can be also described by only one periodic left moving current J on a closed wire of length $2NL \equiv R$.

The corresponding left current $J_1^\ell(t, x)$ is $2NL$ -periodic without monodromy and will be denoted $J(t, x)$ in the following to make notations lighter. All the currents of the junctions are given by the dictionary

$$J_{i,\ell}(t, x) = J(t, (i-1)2L + x), \quad J_{i,r}(t, x) = J(t, i2L - x), \quad (4.36)$$

for $x \in [0, L]$. This phase space is actually easy to understand : a left mover propagates away from the junction then is reflected to a right mover, going to the junction and scattered to a left mover on the next wire, etc. Starting with $J_{1,\ell}$, we see that, after the distance $R = 2NL$, it has come back to the same point, hence the periodicity. The situation is illustrated on Figure 4.1.

4.2.3 Symplectic structure

The canonical symplectic form on the space of classical solutions is computed by differentiating twice the action. It gives boundary and bulk terms that have to be worked out. Moreover on the space of solution we have decomposition (4.28) for the g_i in terms of left and right movers. After a calculation, due to compensations between different terms, the symplectic form is reduced to

$$\Omega[\mathbf{g}] = \frac{k}{4\pi} \int_0^R \text{tr} \left[(g_{1,\ell}^{-1} \delta g_{1,\ell}) \partial (g_{1,\ell}^{-1} \delta g_{1,\ell}) \right] dx, \quad (4.37)$$

where $g_{1,\ell}$ is the twisted $N(2L)$ -periodic field introduced above with fixed monodromy $e^{2\pi i \tau}$. This confirms that the effective worldsheet of the theory is an infinite cylinder of diameter $R \equiv 2NL$, as depicted on the right of Figure 4.1.

From the symplectic form, we deduce the corresponding Poisson brackets for the field $g_{1,\ell}$ and the corresponding current $J(t, x) = ik \partial (g_{1,\ell}) g_{1,\ell}^{-1}$, both depending only on $t + x$. The current is \mathfrak{g} -valued and we decompose it in the Lie algebra basis $(t^a)_a$ defining $J^a(t, x) = \text{tr } t^a J(t, x)$. The equal-time Poisson brackets are

$$\{J^a(t, x), J^b(t, y)\} = 2\pi \delta(x - y) f^{abc} J^c(t, y) + \pi k \delta^{ab} \delta'(x - y), \quad (4.38)$$

$$\{J^a(t, x), g_{1,\ell}(t, y)\} = 2\pi i \delta(x - y) t^a g_{1,\ell}(t, y) \quad (4.39)$$

with the periodic δ -functions with period R .

4.2.4 Conserved charge and energy

With the scattering rule (4.31) at $x = 0$, the sum over all the wires of the left currents is equal to the sum of the right one and the same at $x = L$ due to (4.32), ensuring that the \mathfrak{g} -valued total charge inducing the symmetry $g_i(t, x) \mapsto h g_i(t, x) h^{-1}$ and the total energy

$$Q(t) = \sum_{i=1}^n \int_0^L (J_{i,\ell} + J_{i,r})(t, x) dx, \quad E(t) = \sum_{i=1}^n \int_0^L (T_{i,\ell} + T_{i,r})(t, x) dx \quad (4.40)$$

are conserved by the junction, where $T_i^{L/R} = \frac{1}{4\pi k} \text{tr}(J_{i,\ell/r})^2$. In terms of the periodic field J , these conserved quantities become

$$Q(t) = \int_0^R J(t, x) dx, \quad E(t) = \int_0^R T(t, x) dx \quad (4.41)$$

where $T = \frac{1}{4\pi k} \text{tr}(J)^2$.

4.2.5 Cyclic permutation brane interpretation

The boundary condition considered above may be rewritten as a (twisted)-conjugacy-class boundary conditions [60] for the WZW theory with group G^N . Consider a general Lie group \mathcal{G} and a cyclic permutation automorphism $\alpha : \mathcal{G} \rightarrow \mathcal{G}$. As before, consider a WZW theory for \mathcal{G} on $\mathbb{R} \times I = [0, L]$ with the following boundary conditions:

$$g(\cdot, 0) \in C_{\gamma, \alpha} = \{g \in \mathcal{G} \mid g = h \gamma \alpha(h^{-1}), \quad h \in \mathcal{G}\}, \quad g(\cdot, L) = 1 \quad (4.42)$$

Instead of treating each component of G separately, we may consider a single component WZW theory for group $\mathcal{G} = G^N$ and consider a cyclic permutation automorphism $\alpha(g_1, \dots, g_n) = (g_2, \dots, g_n, g_1)$, setting $\gamma = (1, \dots, 1, e^{2\pi i \tau})$. Note that for those specific choices,

$$C_{\gamma, \alpha}(G^{\times n}) = \{(g_1, \dots, g_n) \in G^{\times n} \mid g_1 \dots g_n \in C_\tau(G)\} \quad (4.43)$$

Hence the boundary condition (4.24) at $x = 0$. The action of such model can be constructed as above, together with its phase space and symplectic form and it reproduces our junction. For example, one recovers the fully transmitting scattering rule (4.31).

$$J_r = \alpha(J_\ell) \quad (4.44)$$

Note that our boundary condition at $x = L$ may be viewed as corresponding to the one-element untwisted conjugacy $C_{1,Id}$ of $1 \in G^N$. In general, one considers in WZW theories with group G^N boundary conditions forcing the fields to take values in the “permutation branes” $C_{\gamma,\alpha}$ where α is generated by a permutation of components [148]. Our boundary condition at $x = 0$ corresponds to a permutation brane with a cyclic permutation. Hence our name of the cyclic brane junction.

4.2.6 Quantization

The data of the classical phase space can be canonically quantized by replacing $(i \times)$ Poisson brackets by commutators. We focus only on the quantification of the current J . One obtains the current algebra associated to \mathfrak{g}

$$[J^a(t, x), J^b(t, y)] = 2\pi i f^{abc} \delta(x - y) J^c(t, y) + \pi k i \delta^{ab} \delta'(x - y). \quad (4.45)$$

In terms of the Fourier modes,

$$J^a(t, x) = \frac{2\pi}{R} \sum_{n \in \mathbb{Z}} J_n^a e^{-\frac{2\pi i p(t+x)}{R}}, \quad (4.46)$$

one obtains the commutation relation (4.14) of the affine Lie algebra $\hat{\mathfrak{g}}$. The (geometric) quantization of the phase space of fields g_i, ℓ is possible when $\tau = \lambda/k$ with λ running through the weights integrable on level k [86]. The corresponding space of states becomes the irreducible unitary representation $\hat{V}_{k,\lambda}$ of level k and highest weight λ described in Subsection 4.1.2 of the affine algebra $\hat{\mathfrak{g}}$ whose generators J_n satisfy the algebra (4.14).

As mentioned in Subsection 4.1.2, representation $\hat{V}_{k,\lambda}$ carries also a representation of the Virasoro algebra obtained through the Sugawara construction (4.16). The operator L_n satisfy commutation relations (4.17) with central charge c_k , see (4.18). The classical conserved quantities Q and E given by (4.41) have both quantum versions. The quantum charge and the quantum Hamiltonian become respectively

$$Q = 2\pi J_0, \quad H \equiv \frac{2\pi}{R} \left(L_0 - \frac{c_k}{24} \right) \quad (4.47)$$

Both are time independent and commute together: $[Q, H] = 0$. Note, however, that the components of $Q \in \mathfrak{g}$ satisfy the commutation relations of that algebra, so only the components of Q corresponding to the Cartan subalgebra $\mathfrak{t} \subset \mathfrak{g}$ commute with each other. Below, we shall also use the relation

$$[H, J(t, x)] = i \partial_t J(t, x) = i \partial_x J(t, x) \quad (4.48)$$

following from the fact that H induces the time translation.

4.3 Equilibrium state

As in the previous chapter we would like to investigate the thermal equilibrium of the junction before to switch on nonequilibrium problems. Hence we shall be interested in quantum expectations

$$\text{Tr}_{\mathcal{H}} e^{-\beta H} \prod_{i=1}^n \left(\prod_{p_i=1}^{P_i} J_{i,\ell}^{a_{p_i}}(t, x_{p_i}^i) \prod_{q_i=1}^{Q_i} J_{i,r}^{a_{q_i}}(t, x_{q_i}^i) \right) \quad (4.49)$$

of any product of left and right currents on the different wires. The Hilbert space of the theory is the highest weight representation $\mathcal{H} = \widehat{V}_{k,\lambda}$, the Hamiltonian is given by (4.47) and the currents are expressed in terms of the R -periodic quantized current J via the dictionary (4.36). Thus the general expectation we want to compute has the following form

$$\mathrm{Tr}_{\widehat{V}_{k,\lambda}} e^{-\frac{2\pi\beta}{R}(L_0 - \frac{c_k}{24})} \prod_{s=1}^S J^{a_s}(x_s), \quad (4.50)$$

where we dropped t -dependence since every expectation is computed at equal (Minkovskian) time. Note that the order of operators $J^{a_s}(x_s)$ does not count since they commute at noncoinciding points, see (4.45). Of course what we really want to compute is the normalized version such expectation, divided by the partition function Z_β corresponding to $S = 0$ in the previous equation. To make computations simpler, we forget this factor for a while.

The above expectation is involved and depends on the highest weight representation $\widehat{V}_{k,\lambda}$, depending itself on the group G considered. However in the thermodynamic limit $R \rightarrow \infty$ we could expect some simplifications. The aim of the following section is to rewrite expectation (4.50) to exhibit its asymptotic behavior when $R \rightarrow \infty$.

4.3.1 Modular covariance

We first start with the partition function Z_β , corresponding to (4.50) with $S = 0$ current expectation. We recognize the character

$$Z_\beta = \widehat{\mathrm{ch}}_\lambda\left(\frac{i\beta}{R}\right), \quad \text{where} \quad \widehat{\mathrm{ch}}_\lambda(\tau) = \mathrm{Tr}_{\widehat{V}_{k,\lambda}} e^{2\pi i\tau(L_0 - \frac{c_k}{24})} \quad (4.51)$$

of the WZW model on a torus. Since J is R -periodic and thermal expectations corresponds to propagation in Euclidean time $i\beta$, the boundary theory of the junction actually becomes a chiral theory on a torus. In particular, the role of space and time can be exchanged leaving the torus invariant: this is the celebrated modular invariance in conformal field theory, which translates to a formula for the characters [50]

$$\widehat{\mathrm{ch}}_\lambda\left(-\frac{1}{\tau}\right) = \sum_{\sigma} S_{\lambda}^{\sigma} \widehat{\mathrm{ch}}_{\sigma}(\tau), \quad (4.52)$$

where the sum is performed over all the highest weight representations of $\widehat{\mathfrak{g}}$ integrable at level k labeled by σ (in particular it is finite). The elements of the modular matrix S_{λ}^{σ} satisfy $S_0^0 = 1$ and $S_{\lambda}^{\sigma} = S_{\lambda}^{\bar{\sigma}} = \overline{S_{\lambda}^{\sigma}}$. In our case, Eq. (4.52) implies that

$$Z_\beta = \sum_{\sigma} S_{\lambda}^{\sigma} \mathrm{Tr}_{\widehat{V}_{k,\sigma}} e^{-\frac{2\pi R}{\beta}(L_0 - \frac{c_k}{24})}. \quad (4.53)$$

The analogue of such formula for the current expectations (4.50) is obtained by considering the dual picture, where the role of space and time are reversed. This is analogous to the closed string picture developed in the previous chapter for the bosonic field. The thermal expectations of the system describing string of length R with fully reflecting boundary conditions, such that it becomes $2R$ periodic, as explained in the disconnected wire example, see 4.1.3, have a corresponding closed string description. Consider the closed string Hilbert space

$$\mathcal{H}^{\mathrm{cs}} = \bigoplus_{\sigma} \widehat{V}_{k,\sigma} \otimes \widehat{V}_{k,\bar{\sigma}}, \quad (4.54)$$

a diagonal sum of the tensor products of two copies over the integrable representations $\widehat{V}_{k,\sigma}$. On such space we define the currents

$$\mathcal{J}_{\ell}^a(z) = \frac{2\pi}{\beta} \sum_{n \in \mathbb{Z}} \mathcal{J}_n^a e^{-\frac{2\pi i n z}{\beta}} \quad \text{and} \quad \mathcal{J}_r^a(\bar{z}) = -\frac{2\pi}{\beta} \sum_{n \in \mathbb{Z}} \bar{\mathcal{J}}_n^a e^{\frac{2\pi i n \bar{z}}{\beta}} \quad (4.55)$$

with \mathcal{J}_n^a satisfying commutation relation (4.14) and generating the representations of $\widehat{\mathfrak{g}}$ in the highest weight modules $\widehat{V}_{k,\sigma}$ and $\widehat{\mathcal{J}}_p^a$ the same operators viewed as acting in $\widehat{V}_{k,\bar{\sigma}}$. We denote L_0 and \bar{L}_0 are the corresponding Sugawara generators. The “space” is now of length β , and such current will propagate in the Euclidean time during a period R between two boundary states defined as follows. Consider an abstract orthonormal basis of $\widehat{V}_{k,\sigma}$ denoted $\{e_j^\sigma\}_j$ and consider the following states belonging to the completion of the space \mathcal{H}^{cs}

$$|\mathcal{D}_\lambda\rangle = \bigoplus_\sigma \frac{S_\lambda^\sigma}{\sqrt{S_0^\sigma}} |\sigma\rangle \quad \text{where} \quad |\sigma\rangle = \sum_j e_j^\sigma \otimes \bar{e}_j^\sigma \quad (4.56)$$

are called the Ishibashi states [50]. Boundary states $|\mathcal{D}_\lambda\rangle$ were already considered in [145] and reproduce the expectation (4.50) in such dual picture through the formula

$$\begin{aligned} \text{Tr}_{\widehat{V}_{k,\lambda}} e^{-\beta H} \prod_{s=1}^S J^{a_s}(x_s) &= (-i)^{2m-S} \langle \mathcal{D}_0 | e^{-\frac{2\pi}{\beta} (L_0 + \bar{L}_0 - \frac{c_k}{12}) \frac{R}{2}} \prod_{s=m}^1 \mathcal{J}_\ell^{a_s}(-ix_s) \\ &\quad \prod_{s=m+1}^S \mathcal{J}_r^{a_s}(i(R-x_s)) |\mathcal{D}_\lambda\rangle \end{aligned} \quad (4.57)$$

for $0 < x_1 < \dots < x_m < \frac{R}{2} < x_{m+1} < \dots < x_S$. On the left hand side the order of the current insertions does not matter, but on the right hand side is assumed to go from left to right with decreasing imaginary parts. Forgetting about the junction, the left hand side expectation can be seen as an effective one for an open string of length $R/2$ in G with the boundary conditions $g(t, 0) \in \mathcal{C}_\tau$ and $g(t, \frac{R}{2}) = 1$. Then the right moving current with $0 < x < \frac{R}{2}$ may be represented by the left one at $R - x$ and the left current becomes R periodic, as in the case of decoupled wires. In the dual picture, a closed string of length β propagates between two boundary states that couple left and right movers $\mathcal{J}_{\ell/r}$ in order to reproduce the open string expectation. The prefactor takes into account the change of variable $z \mapsto -iz$ between the two pictures. The last equality is nothing but two different operator representations of the same functional integral.

We are in a case very similar to the previous chapter, except that here the field are (twisted) periodic in both directions, so that the previous formula should reflect the modular covariance on the torus. Indeed a bit of algebra shows that the boundary states actually perform traces, leading to the identity

$$\text{Tr}_{\widehat{V}_{k,\lambda}} e^{-\beta H} \prod_{s=1}^S J^{a_s}(x_s) = (-i)^S \sum_\sigma S_\lambda^\sigma \text{Tr}_{\widehat{V}_{k,\sigma}} e^{-\frac{2\pi}{\beta} (L_0 - \frac{c_k}{12}) R} \prod_{s=S}^1 \mathcal{J}_\ell^{a_s}(-ix_s) \quad (4.58)$$

where the right movers have been expressed in terms of the left ones when acting on the boundary states. Again the imaginary parts of the insertion points on the right hand side arise in the increasing order. This formula generalizes modular invariance (4.53) for the partition function to any current expectation. It is difficult to compute explicitly the two expectations to show that they coincide as in the bosonic case, but still a partial proof of this formula in a generalized version with chemical potentials will be given in the next subsection.

4.3.2 Adding chemical potential

The interest of adding a chemical potential is double: first because in the perspective of nonequilibrium systems it leads to a richer transport, but also because it allows to prove formula (4.58), at least partially. What we have in mind is to compute the expectations

$$\text{Tr}_{\widehat{V}_{k,\lambda}} e^{-\beta(H - \text{tr} \mu Q)} \prod_{s=1}^S J^{a_s}(x_s) \quad (4.59)$$

where H is related to L_0 by (4.47), $Q = 2\pi J_0$ is the conserved charge, and μ is the \mathfrak{g} -valued chemical potential which will be eventual restricted to the Cartan subalgebra \mathfrak{t} of \mathfrak{g} (the Gibbs state is defined for commuting conserved observables). With dictionary (4.36), this reproduce the equilibrium expectations of products of currents in different wires.

Looking first at the partition function $Z_{\beta,\mu}$ with no current insertions, we get the unrestricted version of the affine characters, namely

$$Z_{\beta,\mu} = \widehat{\text{ch}}_\lambda\left(\frac{i\beta}{R}, -2\pi i\beta\mu\right), \quad \widehat{\text{ch}}_\lambda(\tau, u) = \text{Tr}_{\widehat{V}_{k,\lambda}} \left(e^{2\pi i(L_0 - \frac{c_k}{24}) + iu^a J_0^a} \right) \quad (4.60)$$

for $u = u^a t^a$. Note that we have set the following normalization: $\text{tr}(t^a t^b) = \frac{1}{2}\delta^{ab}$ and defined $J_0^a = \text{tr} t^a J_0$ so that $J_0 = 2J_0^a t^a$, however, we take $\mu = \mu^a t^a$, or $\mu^a = 2 \text{tr} t^a \mu$. The unrestricted affine characters also have a modular covariance property:

$$\widehat{\text{ch}}_\lambda(\tau, u) = \exp\left[-\frac{ik\text{tr}u^2}{4\pi\tau}\right] \sum_\sigma S_\lambda^\sigma \widehat{\text{ch}}_{k,\sigma}\left(-\frac{1}{\tau}, \frac{u}{\tau}\right) \quad (4.61)$$

which implies for the partition function the identity

$$Z_{\beta,\mu} = e^{\pi k R \beta \text{tr} \mu^2} \sum_\sigma S_\lambda^\sigma \text{Tr}_{\widehat{V}_{k,\sigma}} \left(e^{-\frac{2\pi}{\beta}(L_0 - \frac{c_k}{24})R} e^{-2\pi i R \text{tr} \mu J_0} \right) \quad (4.62)$$

which coincides with (4.53) when $\mu = 0$. Note that such formula involves the mean J_0 of the current J , so that by successive derivatives with respect to μ we can try to get some current expectations in equilibrium state.

Consider the simplest case $S = 1$ of one current insertion. Using commutation relation (4.48) one easily sees that one point expectations (4.59) are independent of the insertion point, so that $J(x_1)$ may be replaced by its mean value $Q = 2\pi J_0$. Moreover, from the current algebra (4.45) we deduce that

$$[Q, J^a(x)] = 4\pi i f^{abc} t^b J^c(x) \quad (4.63)$$

such that in (4.59) with $\mu \in \mathfrak{t}$, the one point expectations do not vanish only for the Cartan components of J . Then the expectation of J_0 is obtained by taking first order derivative of (4.61) with respect to μ^a , making a J_0^a mode appear, which can be also interpreted as the mean of the closed string current. Putting all together, we end up with the one point correspondence between the open and closed string picture

$$\text{Tr}_{\widehat{V}_{k,\lambda}} \left(e^{-\beta(H - \text{tr} \mu Q)} J^a(x) \right) = e^{\pi k R \beta \text{tr} \mu^2} \sum_\sigma S_\lambda^\sigma \text{Tr}_{\widehat{V}_{k,\sigma}} \left(e^{-\frac{2\pi}{\beta}(L_0 - \frac{c_k}{24})R} e^{-2\pi i R \text{tr} \mu J_0} (\pi k \mu^a - i \mathcal{J}_\ell^a(-ix)) \right) \quad (4.64)$$

where a is restricted to the Cartan components. Note that the point $-ix$ is arbitrary here since it does not change the expectation. It is, however, consistent with the general formula that we shall write below. Again, Eq. (4.64) coincides with (4.58) when $\mu = 0$.

We immediately guess a general formula for expectations in presence of a chemical potential

$$\begin{aligned} \text{Tr}_{\widehat{V}_{k,\lambda}} e^{-\beta(H - \text{tr} \mu Q)} \prod_{s=1}^S J^{a_s}(x_s) = \\ e^{\pi k R \beta \text{tr} \mu^2} \sum_\sigma S_\lambda^\sigma \text{Tr}_{\widehat{V}_{k,\sigma}} \left(e^{-\frac{2\pi}{\beta}(L_0 - \frac{c_k}{24})R} e^{-2\pi i R \text{tr} \mu J_0} \mathcal{T} \prod_{s=1}^S (k\pi \mu^{a_s} - i \mathcal{J}_\ell^{a_s}(-ix_s)) \right) \end{aligned} \quad (4.65)$$

extending (4.58) when $\mu \neq 0$, but only for the Cartan components of J . \mathcal{T} time orders the insertions as before. The above formula may be proven explicitly. We give the general idea of

the proof here deferring the technical details to Appendix 4.A. Consider each side of the previous equation as complex function of the variables z_1, \dots, z_s by analytic continuation. Fixing all the z_i except one, we end up with an equality between two meromorphic functions, defined on the complex torus since we have periodicity in β and R for the Cartan components of the currents. Such functions are almost unique since meromorphic function are fully characterized by their singularities coefficients, up to a constant [169]. Here the singularity comes from the operator product expansion (OPE) of the currents

$$J^a(w+z)J^b(z) = -\frac{k}{2} \frac{\delta^{ab}}{w^2} + \frac{f^{abc}}{w} J^c(z) + \dots \quad (4.66)$$

where the dots stand for a regular part, and similarly for \mathcal{J} . This is obtained by standard conformal field theory computation. Hence both side of (4.65) are meromorphic functions on the torus with poles of order one and two and can be identified by computing each singular coefficient. This is done in Appendix 4.A for Cartan components of J where the second term in the previous OPE vanishes.

We use the formalism of Abelian differential [116] and show that both sides of (4.65) have the same values when integrated over the cycles of the torus. This is in some sense the generalization of the arguments for the Weierstrass function developed in the previous chapter for the free bosonic field, except that here we do not write explicitly the regular part and only focus on singularities and on contour integrals along cycles, which is enough to show that the functions coincide.

A general formula for the modular covariance of the current expectations, beyond their Cartan components, seems more difficult to establish (except for the one point expectations).

4.4 Thermodynamic limit

The thermodynamic limit equilibrium expectations for the junction are defined as

$$\omega_{\beta,\mu}(A) = \lim_{L \rightarrow \infty} \frac{\text{Tr}_{\widehat{V}_{k,\lambda}} e^{-\beta(H - \text{tr} \mu Q)} A}{Z_{\beta,\mu}} \quad \text{where} \quad A = \prod_{i=1}^n \left(\prod_{p_i=1}^{P_i} J_{i,\ell}^{a_{p_i}}(x_{p_i}^i) \prod_{q_i=1}^{Q_i} J_{i,r}^{a_{q_i}}(x_{q_i}^i) \right) \quad (4.67)$$

is a product of currents and $Z_{\beta,\mu}$ is the partition function of the theory. We shall be able to compute such limits for the expectations of products of components of currents for which we have the dual closed-string picture expression. The formula that will be used is equation (4.65), which has been proven only in the following cases: no insertions (modular covariance of the partition function (4.62)), one insertion (equation (4.64) for a for the Cartan-subalgebra component and zero otherwise) and for more than one insertions with all a_s corresponding to Cartan-subalgebra generators.

4.4.1 Partition function

From its dual version (4.62), we see that $Z_{\beta,\mu}$ behaves exponentially when $R = 2NL \rightarrow \infty$. However the free energy density

$$f_{\beta,\mu} \equiv - \lim_{L \rightarrow \infty} \frac{1}{\beta L} \ln Z_{\beta,\mu} \quad (4.68)$$

has a finite limit. We have:

$$f_{\beta,\mu} = -2\pi k N \text{tr} \mu^2 - \frac{1}{\beta L} \lim_{L \rightarrow \infty} \ln \sum_{\sigma} S_{\lambda}^{\sigma} \text{Tr}_{\widehat{V}_{k,\sigma}} \left(e^{-\frac{2\pi}{\beta} (L_0 - \frac{c_k}{24}) R} e^{-2\pi i R \text{tr} \mu J_0} \right). \quad (4.69)$$

The last trace is a sum over all the states of $\widehat{V}_{k,\sigma}$. Let $\{e_j^\sigma\}_j$ be the basis of the highest weight representation $\widehat{V}_{k,\sigma}$ composed of eigenvectors of L_0 with eigenvalues $\Delta(\sigma) + n_j$, where $\Delta(\sigma)$ is the conformal weight corresponding to the representation σ and n_j is a nonnegative integer. Only the vacuum state $|0\rangle = e_0^0$ of representation $\sigma = 0$ has L_0 eigenvalue 0 and all the other states of $\widehat{V}_{k,0}$, but also of $\widehat{V}_{k,\sigma}$ for $\sigma \neq 0$ have strictly positive L_0 eigenvalues. Hence

$$\sum_{\sigma} S_{\lambda}^{\sigma} \operatorname{Tr}_{\widehat{V}_{k,\sigma}} \left(e^{-\frac{2\pi}{\beta}(L_0 - \frac{c_k}{24})R} e^{-2\pi i R \operatorname{tr} \mu J_0} \right) = e^{\frac{2\pi}{\beta} \frac{c_k}{24} 2NL} S_{\lambda}^0 (1 + O(e^{-\delta L})) \quad (4.70)$$

when $L \rightarrow \infty$ for some $\delta > 0$. That implies that

$$f_{\beta,\mu} = -2\pi k N \operatorname{tr} \mu^2 - \frac{\pi N c_k}{6\beta^2} \quad (4.71)$$

which is analogue to the free massless bosonic formula (3.99).

4.4.2 One point expectations

Using the dual formulae (4.64) for one point (4.62) and for the partition function, the exponential factors with $\operatorname{tr} \mu^2$ cancel in the normalized one point expectation and we are left with a similar behavior at $R \rightarrow \infty$ of both the numerator and the denominator to which the leading contributions come the lowest L_0 eigenvalue, i.e. the vacuum state $|0\rangle \in \widehat{V}_{k,0}$. Hence

$$\omega_{\beta,\mu}(J^a(x)) = \frac{\langle 0 | \pi k \mu^a - i \mathcal{J}_{\ell}^a(-ix) | 0 \rangle}{\langle 0 | 0 \rangle} \quad (4.72)$$

is reduced to a vacuum expectation. With the highest weight representation construction, a one point expectation on the vacuum state always vanish, such that finally

$$\omega_{\beta,\mu}(\operatorname{tr} \nu J(x)) = 2\pi k \operatorname{tr}(\nu \mu) \quad (4.73)$$

for $\nu \in \mathfrak{g}$. Because of the independence of x , we can come back easily to the expectations on different wires. Using dictionary (4.36), we conclude that the previous equation is also true for any $J_{i,\ell/r}(x)$. Thus at the equilibrium state

$$\omega_{\beta,\mu}(\operatorname{tr} \nu (J_{i,r} - J_{i,\ell})) = 0, \quad \omega_{\beta,\mu}(\operatorname{tr} \nu (J_{i,r} + J_{i,\ell})) = 4\pi k \operatorname{tr}(\nu \mu). \quad (4.74)$$

The mean currents vanish in each wire whereas the mean charge density is constant and nonzero for $\mu \neq 0$. This is similar to the result for the bosonic case of the previous chapter, see (3.102).

It is also possible to compute the one point function associated to the energy. Let us define for the current J , the corresponding energy-momentum component

$$T(x) = \frac{1}{4\pi(k+h^{\vee})} : \operatorname{tr} J^2(x) : \quad (4.75)$$

Its expectation value $\omega_{\beta,\mu}(T(x))$ is also x -independent since $[H, T(x)] = i\partial_x T(x)$ and then can be replaced by its mean value, which is the Hamiltonian (up to a central charge term that will not contribute in the thermodynamic limit):

$$\omega_{\beta,\mu}(T(x)) = \lim_{R \rightarrow \infty} \frac{1}{R} \omega_{\beta,\mu}(H). \quad (4.76)$$

The expectation under the limit can be expressed by the first order derivative of the partition function. Indeed,

$$\omega_{\beta,\mu}(H) = -\frac{d}{d\beta} \ln \operatorname{Tr} e^{-\beta(H - \operatorname{tr} \mu Q)} + \omega_{\beta,\mu}(\operatorname{tr} \mu Q). \quad (4.77)$$

Again we recognize in the first term the affine character of the theory whose large R behavior may be controlled using modular covariance: we extract the few dominant terms that will not vanish when derivated by β . The second term appearing in the expectation of H has been already computed since Q can be replaced by $RJ(x)$ and the x -independent expectation has been already computed. Putting all together, we obtain

$$\omega_{\beta,\mu}(T(x)) = \frac{\pi c_k}{12\beta^2} + \pi k \operatorname{tr} \mu^2 \quad (4.78)$$

again this expectation is x -independent and allows to come back to the initial model of the different wires through the dictionary (4.36). We deduce that

$$\omega_{\beta,\mu}(T_{i,r} - T_{i,\ell}) = 0, \quad \omega_{\beta,\mu}(T_{i,r} + T_{i,\ell}) = \frac{\pi c_k}{6\beta^2} + 2\pi k \operatorname{tr} \mu^2 = -\frac{1}{N} f_{\beta,\mu} \quad (4.79)$$

At equilibrium, the mean energy current vanishes and the mean energy density is positive and, summed over wires, is equal to the negative of the free energy density per wire, similarly as for the bosonic junction.

4.4.3 Higher point expectations

It is easy to obtain the thermodynamic limit of higher-point current Cartan-components expectations from Eq. (4.65) if the points x_s correspond to fixed locations of insertions of left- and right-moving currents on the wires that become longer and longer. From the dictionary (4.36), it follows that such points x_s separate into groups that contain right moving insertions on wire $i-1$ and left moving insertions on wire i separated by averaged distance of order $2L$. Such separations will lead to insertions of the projections on the vacuum state in the expectation on the right hand side of (4.65) in the dominant contribution with the trace over the $\widehat{V}_{k,0}$ representation. At the end, one obtains the relation

$$\omega_{\beta,\mu} \left(\prod_{i=1}^N \left(\prod_{p_i=1}^{P_i} J_{i,\ell}^{a_{p_i}^i}(0, x_{p_i}^i) \prod_{q_i=1}^{Q_i} J_{i,r}^{a_{q_i}^i}(0, x_{q_i}^i) \right) \right) \quad (4.80)$$

$$= \prod_{i=1}^N \left\langle \Omega \left| \tau \prod_{p_i=1}^{P_i} (\pi k \mu^{a_{p_i}^i} - i \mathcal{J}_\ell^{a_{p_i}^i}(-i x_{p_i}^i)) \prod_{q_{i-1}=1}^{Q_{i-1}} (\pi k \mu^{a_{q_{i-1}}^{i-1}} - i \mathcal{J}_\ell^{a_{q_{i-1}}^{i-1}}(i x_{q_{i-1}}^{i-1})) \right| \Omega \right\rangle. \quad (4.81)$$

Note that for left movers only, the equilibrium expectation factorizes over different wires:

$$\omega_{\beta,\mu} \left(\prod_{i=1}^N \prod_{p_i=1}^{P_i} J_{i,\ell}^{a_{p_i}^i}(0, x_{p_i}^i) \right) = \prod_{i=1}^N \omega_{\beta,\mu} \left(\prod_{p_i=1}^{P_i} J_{i,\ell}^{a_{p_i}^i}(0, x_{p_i}^i) \right) \quad (4.82)$$

(and similarly for the right-movers only).

4.4.4 The case of the disconnected junction

The previous computations for one point expectations and partition function of the connected junction were done using one left periodic current J on $[0, R]$ where $R = 2NL$ and the correspondence with the initial current, through the dictionary (4.36). Now consider the disconnected junction, which is a collection of independent disconnected wires described in Subsection 4.1.3. For each wire i , right current is expressed in terms of the left one $J_{i,\ell}$, which is now $2L$ periodic, see (4.21). Hence $J_{i,\ell}$ and J are formally the same objects except that the size of the space differs, which will not matter in the thermodynamic limit.

Consequently, the previous computation are also available for each wire of the disconnected junction. Moreover for such junction each wire may be considered independently, and then in different equilibrium states. We deduce that for disconnected junction

$$f_{\beta_i, \mu_i} = -2\pi k \text{tr}(\mu_i^2) - \frac{\pi c_k}{6\beta_i}, \quad (4.83)$$

$$\omega_{\beta_i, \mu_i}(\text{tr } \nu J_{i, \ell}(x)) = 2\pi k \text{tr}(\nu \mu_i) \quad (4.84)$$

$$\omega_{\beta_i, \mu_i}(T_{i, \ell}(x)) = \frac{\pi c_k}{12\beta_i^2} + k\pi \text{tr} \mu_i^2 \quad (4.85)$$

that will be used in the following. Similarly, the higher correlations for the disconnected junctions take the form

$$\begin{aligned} & \omega_{\beta_i, \mu_i} \left(\prod_{p_i=1}^{P_i} J_{i, \ell}^{a_{p_i}^i}(0, x_{p_i}^i) \prod_{q_i=1}^{Q_i} J_{i, r}^{a_{q_i}^i}(0, x_{q_i}^i) \right) \\ &= \left\langle \Omega \left| \mathcal{T} \prod_{p_i=1}^{P_i} (\pi k \mu^{a_{p_i}^i} - i \mathcal{J}_\ell^{a_{p_i}^i}(-i x_{p_i}^i)) \prod_{q_i=1}^{Q_i} (\pi k \mu^{a_{q_i}^i} - i \mathcal{J}_\ell^{a_{q_i}^i}(i x_{q_i}^i)) \right| \Omega \right\rangle. \end{aligned} \quad (4.86)$$

Note now that (4.80) may be rewritten as the identity

$$\omega_{\beta, \mu} \left(\prod_{i=1}^N \left(\prod_{p_i=1}^{P_i} J_{i, \ell}^{a_{p_i}^i}(0, x_{p_i}^i) \prod_{q_i=1}^{Q_i} J_{i, r}^{a_{q_i}^i}(0, x_{q_i}^i) \right) \right) \quad (4.87)$$

$$= \prod_{i=1}^N \omega_{\beta_i, \mu_i} \left(\prod_{p_i=1}^{P_i} J_{i, \ell}^{a_{p_i}^i}(0, x_{p_i}^i) \prod_{q_{i-1}=1}^{Q_{i-1}} J_{i, r}^{a_{q_{i-1}}^{i-1}}(0, x_{q_{i-1}}^{i-1}) \right) \Big|_{\substack{\beta_i = \beta \\ \mu_i = \mu}} \quad (4.88)$$

that on the right hand side we have a product of expectations for the disconnected wires.

4.5 Nonequilibrium stationary state

The nonequilibrium stationary state is constructed as in the previous chapter. In the Heisenberg picture, consider the algebra \mathcal{A} of currents generated by the left and right movers $J_{i, \ell}(0, x)$ and $J_{i, r}(0, x)$ for $x > 0$. This algebra is the same for the connected and the disconnected junction and these two systems are distinguished through their dynamics. For both we have chiral propagation $J_{i, \ell/r}(t, x) = J_{i, \ell/r}(0, x \pm t)$, but $J_{i, \ell/r}(0, x)$ for $x < 0$ are expressed differently in terms of the currents with $x > 0$, according to the junction. Namely, for the connected junction where $J_{i, r}(t, 0) = J_{i+1, \ell}(t, 0)$ the forward time evolution on \mathcal{A} reads

$$\begin{aligned} \mathcal{U}_t J_{i, r}(0, x) &= \begin{cases} J_{i, r}(0, x - t) & \text{if } 0 \leq t \leq x \\ J_{i+1, \ell}(0, t - x) & \text{if } 0 \leq x \leq t \end{cases} \\ \mathcal{U}_t J_{i, \ell}(0, x) &= J_{i, \ell}(0, x + t) \quad \text{for } 0 \leq t, x \end{aligned} \quad (4.89)$$

so that right currents are moved to the junction and then sent as left currents on the next wire, whereas left currents are moved away from the junctions and never come back in such an infinite system. On the other hand, the disconnected junction is characterized by $J_{i, r}(t, 0) = J_{i, \ell}(t, 0)$ and we can write the corresponding dynamics defined by \mathcal{U}_t^0 . For convenience we write the backward time evolution, given by

$$\mathcal{U}_{-t}^0 J_{i, r}(0, x) = J_{i, \ell}(0, x + t) \quad \text{for } 0 \leq t, x \quad (4.90)$$

$$\mathcal{U}_{-t}^0 J_{i, \ell}(0, x) = \begin{cases} J_{i, \ell}(0, x - t) & \text{if } 0 \leq t \leq x \\ J_{i, r}(0, t - x) & \text{if } 0 \leq x \leq t \end{cases} \quad (4.91)$$

and we define the corresponding S -matrix of the junction by $\mathcal{S} = \lim_{t \rightarrow \infty} \mathcal{U}_{-t}^0 \mathcal{U}_t$, so that for $x > 0$

$$\mathcal{S}J_{i,r}(0, x) = J_{i+1,r}(0, x), \quad \mathcal{S}J_{i,\ell}(0, x) = J_{i,\ell}(0, x), \quad (4.92)$$

which extends to an algebra homomorphism on \mathcal{A} . One can check by direct computation that the action of \mathcal{U}_t and \mathcal{U}_t^0 are intertwined by \mathcal{S} , namely

$$\mathcal{S}\mathcal{U}_t = \mathcal{U}_t^0 \mathcal{S} \quad (4.93)$$

The nonequilibrium state is then constructed as before, by considering on the disconnected junction the product state

$$\omega_{\text{in}} \equiv \bigotimes_{i=1}^N \omega_{\beta_i, \mu_i} \quad (4.94)$$

where ω_{β_i, μ_i} are the equilibrium states on disconnected wires. Then for a general product of currents $A \in \mathcal{A}$

$$A = \prod_i \left(\prod_{p_i}^{P_i} J_{i,\ell}^{a_{p_i}^i}(0, x_{p_i}^i) \prod_{q_i=1}^{Q_i} J_{i,r}^{a_{q_i}^i}(0, x_{q_i}^i) \right), \quad (4.95)$$

The nonequilibrium state expectation is defined by

$$\omega_{\text{neq}}(A) \equiv \omega_{\text{in}}(\mathcal{S}A) \quad (4.96)$$

Such state is explicitly stationary using the intertwining property (4.93) of \mathcal{S} and the fact that ω_{in} is invariant under disconnected evolution \mathcal{U}_t^0 . More explicitly,

$$\omega_{\text{neq}}(A) = \omega_{\text{in}} \left(\prod_{i=1}^N \left(\prod_{p_i}^{P_i} J_{i,\ell}^{a_{p_i}^i}(0, x_{p_i}^i) \prod_{q_i=1}^{Q_i} J_{i+1,r}^{a_{q_i}^i}(0, x_{q_i}^i) \right) \right) \quad (4.97)$$

$$= \prod_{i=1}^N \omega_{\beta_i, \mu_i} \left(\prod_{p_i=1}^{P_i} J_{i,\ell}^{a_{p_i}^i}(0, x_{p_i}^i) \prod_{q_{i-1}=1}^{Q_{i-1}} J_{i,r}^{a_{q_{i-1}}^{i-1}}(0, x_{q_{i-1}}^{i-1}) \right) \quad (4.98)$$

in terms of the equilibrium expectations in disconnected wires. Note that ω_{neq} coincides with ω_{in} when restricted to left-moving currents. Comparison of relations (4.97) and (4.80) also shows that the nonequilibrium expectations reduce to the equilibrium ones for equal temperatures and chemical potentials.

4.5.1 Some particular expectations

For convenience we express the right currents of the disconnected wires in terms of the left ones for $x < 0$ via equation (4.21) and the left currents then are defined for $x \in \mathbb{R}$. The S -matrix action becomes

$$\mathcal{S}J_{i,r}(0, x) = J_{i+1,\ell}(0, -x), \quad \mathcal{S}J_{i,\ell}(0, x) = J_{i,\ell}(0, x). \quad (4.99)$$

The one point expectations can be easily computed since we already have the one point expectation for the disconnected junction, see (4.84). Consider for the connected junction the charge current $J_i^1(0, x) = J_{i,r}(0, x) - J_{i,\ell}(0, x)$. Its expectation reads

$$\omega_{\text{neq}}(J_{i,1}(0, x)) = \omega_{\beta_{i+1}, \mu_{i+1}}(J_{i+1,\ell}(0, -x)) - \omega_{\beta_i, \mu_i}(J_{i,\ell}(0, x)) \quad (4.100)$$

and thus we only need the equilibrium expectations $\omega_{\beta_i, \mu_i}(J_{i,\ell}(0, x))$ for the disconnected system. Using (4.84), we obtain:

$$\omega_{\text{neq}}(J_i^1(0, x)) = 2\pi k(\mu_{i+1} - \mu_i) \quad (4.101)$$

which is non vanishing for different chemical potentials on the wires. Note that this expectation is independent from the temperature, so that the charge current is driven only by different chemical potentials and vanishes in the equilibrium state, as already seen in the previous section. The corresponding linear response conductance is

$${}^{\text{el}}G_{ij}\nu \equiv \lim_{\epsilon \rightarrow 0} \frac{1}{\epsilon} \omega(J_{i,1}(0, x)) \Big|_{\mu_l = \mu + \epsilon \delta_{ij}\nu} = 2\pi k(\delta_{(i+1)j} - \delta_{ij})\nu \quad (4.102)$$

The expectation of the mean energy current in each wire $K_{i,1}(0, x) = T_{i,r}(0, x) - T_{i,\ell}(0, x)$ is also computable in the nonequilibrium state. Using the S -matrix and the disconnected equilibrium expectations (4.85), one ends up with the expression

$$\omega_{\text{neq}}(K_{i,1}(0, x)) = \frac{\pi c_k}{12}(\beta_{i+1}^{-2} - \beta_i^{-2}) + \pi k \text{tr}(\mu_{i+1}^2 - \text{tr} \mu_i). \quad (4.103)$$

The heat flow is driven by both the difference of temperatures and the difference of chemical potentials, and again it vanishes in the equilibrium. The corresponding thermal conductance reads:

$${}^{\text{th}}G_{ij} \equiv -\beta_j^2 \frac{\partial}{\partial \beta_j} \omega_{\text{neq}}(K_{i,1}(0, x)) \Big|_{\beta_r = \beta} = \frac{\pi c_k}{6\beta}(\delta_{(i+1),j} - \delta_{i,j}). \quad (4.104)$$

These expressions coincide with the result of [18] (that uses a different normalization), and with the one for free massless bosonic case with the specific S -matrix $S_{ij} = \delta_{(i+1),j}$, compare to (3.119), except that here the potential is \mathfrak{t} -valued instead of being a scalar.

4.6 Full counting statistics

As in the previous chapter we define the following measurement protocol: the disconnected system is prepared with each wire in equilibrium state at different temperature and chemical potential and the charge or/and the energy in each wire are measured; then the wires are connected for time t ; after that time the wires are disconnected and their charge or/and energy are measured again. We are interested in the characteristic function associated to the probability measure of charge and energy transfers, called the full counting statistics (FCS).

4.6.1 Charge transfer

Following subsection 3.7.1 for charge transport in the bosonic case, measure the Cartan components of $Q_i(0)$ in each wire, for the disconnected junction prepared in the product state $\omega_0^L = \otimes_i \omega_{\beta_i, \mu_i}^i$. Then measure after time t and disconnection the Cartan components of charge $Q_i(t)$, which have evolved via the connected dynamics. The generating function of FCS of charge transfers Δq_i is

$${}^{\text{el}}F_t^L(\boldsymbol{\nu}) \equiv \sum_{\Delta q_i} e^{i \sum_i \text{tr} \nu_i \Delta q_i} \mathbb{P}_t(\Delta q_i) \quad (4.105)$$

where $\boldsymbol{\nu}$ is a vector with N \mathfrak{t} -valued components. Such function can be rewritten as an expectation

$${}^{\text{el}}F_t^L(\boldsymbol{\nu}) = \omega_0^L \left(e^{-i \sum_i \text{tr} \nu_i Q_i(0)} e^{i \sum_i \text{tr} \nu_i Q_i(t)} \right) \quad (4.106)$$

involving operators $Q_i(0)$ and $Q_i(t)$. The difference of the latter may be rewritten in terms of an integral over the left currents, via the scattering rule (4.31), namely

$$\Delta Q_i(t) \equiv Q_i(t) - Q_i(0) = - \int_0^t (J_{i,\ell}(0, s) - J_{i+1,\ell}(0, s)) ds, \quad (4.107)$$

similarly to the bosonic case (3.137). Note that this calculation is valid only for $t < L$ to avoid the bouncing back of the left currents at the free end of the wires. Moreover, such operator

commutes with the initial charge operator $Q_i(0)$ if we project both to the Cartan components, as follows from the commutation relation (4.45):

$$[\text{tr } \nu_i Q_i(0), \text{tr } \nu_j \Delta Q_j(t)] = 0. \quad (4.108)$$

Thus the full counting statistics can be rewritten in the simpler form

$${}^{\text{el}}F_t^L(\boldsymbol{\nu}) = \omega_0^L \left(e^{i \sum_i \text{tr } \nu_i \Delta Q_i(t)} \right), \quad (4.109)$$

as in the bosonic case. We are interested in the long-time large-volume behavior of such function and, consequently, want to compute the rate function

$${}^{\text{el}}f(\boldsymbol{\nu}) = \lim_{t \rightarrow \infty} t^{-1} \lim_{L \rightarrow \infty} \ln F_t^L \quad (4.110)$$

which, continued to imaginary ν , is the Legendre transform of the large deviation rate function for the probability of charge transfers. Following the previous chapter, we propose a computation of such function by the most effective, although not the most natural, way. We extend formally the definition of F_t^L to $t \geq L$ by equation (4.109) and consider the specific case where $t = 2L$, implying a simple form for $\Delta Q_i = Q_{i+1} - Q_i$, that can be seen from (4.107). Then the expectation on the right hand side of (4.109) involves just a shift by imaginary chemical potentials leading to a product of quotients of disconnected wire partition functions:

$${}^{\text{el}}F_{2L}^L(\boldsymbol{\nu}) = \prod_i \frac{Z_{\beta_i, \mu_i + i\beta_i^{-1}(\nu_i - \nu_{i-1})}}{Z_{\beta_i, \nu_i}}. \quad (4.111)$$

The corresponding rate function can be expressed by differences of free energies f_{β_i, μ_i} of the disconnected wires under an imaginary change of the chemical potential. From the explicit expression (4.83) for f_{β_i, μ_i} we deduce that

$${}^{\text{el}}f(\boldsymbol{\nu}) = \sum_i \pi k \beta_i \text{tr} (\mu_i - i\beta_i^{-1}(\nu_i - \nu_{i+1}))^2 - \sum_i \pi k \beta_i \text{tr } \mu_i^2 \quad (4.112)$$

Note that expression (4.112) is similar to that for the charge transfer in the free bosonic case given by (3.149): function ${}^{\text{el}}f$ is quadratic in $\boldsymbol{\nu}$ meaning that the probability measure of charge transfers is asymptotically Gaussian. We have obtained the above result only in the specific limit $t = 2L$, as, here, there is no explicit formula for F_t^L outside that regime. Formula (4.112) coincides, however, with the result for two wires obtained previously in [18], where a detailed perturbative analysis of the $L \rightarrow \infty$, $t \rightarrow \infty$ asymptotics of the one point current expectation representing the $\boldsymbol{\nu}$ -derivative of $\ln {}^{\text{el}}F_t^L(\boldsymbol{\nu})$ was performed.

4.6.2 Energy transfer

The same reasoning can be applied to the two time measurement of energy transfer Δe_i in each wire i via observables $H_i(0)$ and $H_i(t)$. The corresponding full counting statistics is

$${}^{\text{th}}F_t^L(\boldsymbol{\lambda}) \equiv \sum_{\Delta q_i} e^{i \sum_i \lambda_i \Delta e_i} \mathbb{P}_t(\Delta e_i) = \omega_0^L \left(e^{-i \sum_i \lambda_i H_i(0)} e^{i \sum_i \text{tr } \lambda_i H_i(t)} \right) \quad (4.113)$$

and the corresponding difference operator is also simple here because of the particularly simple S -matrix,

$$\Delta H_i(t) \equiv H_i(t) - H_i(0) = - \int_0^t (K_{i,\ell}(0, s) - K_{i+1,\ell}(0, s)) ds. \quad (4.114)$$

In this junction, the energy is transmitted with the same scattering rule that the current: $K_{i,r}(t, 0) = K_{i+1,r}(t, 0)$. However since $[H_i, K_{i,\ell}] = i\partial_x K_{i,\ell}$, the commutator

$$[H_i, \Delta H_j(t)] = i(\delta_{i,j+1} - \delta_{i,j})(K_{i,\ell}(0, t) - K_{i,\ell}(0, 0)) \quad (4.115)$$

does not vanish in general, so that it is not obvious that the two exponential factors appearing in the left hand side of (4.113) can be regrouped in a simple one. It was actually proved in [52] that the simpler functional

$${}^{\text{th}}\tilde{F}_t^L(\boldsymbol{\lambda}) = \omega_0^L \left(e^{i \sum_i \text{tr} \lambda_i \Delta H_i(t)} \right) \quad (4.116)$$

corresponds to the same asymptotic rate function that ${}^{\text{th}}F_t^L$. The proof used an exhaustive diagrammatic expansion, and was done in the case without chemical potential. Here we take again the same shortcut as before by considering the specific case where $t = 2L$. The commutator (4.115) vanishes in this case so that we can use the simpler formula for ${}^{\text{th}}\tilde{F}_{2L}^L$ that factorizes over the wires (this would not be the case for more general matrices S). As for the charge, ${}^{\text{th}}\tilde{F}_{2L}^L$ appears as a quotient of partition functions with temperature and potential shifted by imaginary terms:

$${}^{\text{th}}F_{2L}^L(\boldsymbol{\lambda}) = {}^{\text{th}}\tilde{F}_{2L}^L(\boldsymbol{\lambda}) = \prod_i \frac{Z_{\beta'_i, \mu'_i}}{Z_{\beta_i, \mu_i}}, \quad (4.117)$$

where $\beta'_i = \beta_i + i(\lambda_i - \lambda_{i-1})$ and $\mu'_i = \beta_i(\beta_i + i(\lambda_i - \lambda_{i-1}))^{-1}\mu_i$, so that we get

$${}^{\text{th}}f(\boldsymbol{\lambda}) = \lim_{L \rightarrow \infty} \frac{1}{2L} {}^{\text{th}}F_{2L}^L(\boldsymbol{\lambda}) \quad (4.118)$$

as a difference of free energy densities for disconnected wires, see (4.83). The final result is

$${}^{\text{th}}f(\boldsymbol{\lambda}) = \sum_{i=1}^N \frac{\pi c_k}{12} \left(\frac{1}{\beta_i + i(\lambda_i - \lambda_{i-1})} - \frac{1}{\beta_i} \right) + k\pi \beta_i \left(\frac{\beta_i}{\beta_i + i(\lambda_i - \lambda_{i-1})} - 1 \right) \text{tr} \mu_i^2 \quad (4.119)$$

This expression coincides with the one obtained in [18] in the case of two wires and in [52] for the full star graph when taking $\mu_i = 0$. It generalizes the latter results to the case of nonvanishing chemical potential. With the particular limit $t = 2L \rightarrow \infty$, our computation is almost immediate and does not require any regularization, as it was already noticed in the free bosonic case. The result from [52] was obtained more carefully for $t < L$ using a diagrammatic expansion of expression (4.113), involving a regularization procedure. At the end, however, one obtains the same expression for the large deviations rate function of the thermal FCS.

4.7 Conclusion

The analysis of a WZW model of a junction of quantum wires performed here shows that it is possible to generalize the nonequilibrium description developed in the free bosonic case to more involved conformal field theories. However the computations become more complicated and hence the results are less explicit, even in the simplest case of a fully transmitting junction that we considered here. We only computed few expectations in equilibrium and in the nonequilibrium states. However this was enough to get the large deviations associated to the full counting statistics of charge and energy transfer. Although we used a mathematical trick which simplified considerably the computation of the latter, the final results matched with other approaches.

As already noticed in the bosonic case, the computation of large deviations for charge transfer can be done for any scattering matrix, and since the calculations were similar here it should be possible to generalize formula (4.112) to WZW junctions with reflection and transmission. It is however not obvious to construct an explicit WZW junction leading to a nontrivial scattering. The next chapter is an attempt to describe such a junction.

4.A Modular covariance of correlation functions

Here we prove formula (4.65) for the case $S = 2$. The case of general S follows by induction. We restrict J^a to Cartan components, which simplifies the operator product expansion and gives correlators periodic in both directions (this would not be true for other current components).

Two insertions For $S = 2$, we want to prove the formula

$$\begin{aligned} & \text{Tr}_{\widehat{V}_{k,\lambda}} e^{-\beta(H - \text{tr}\mu Q)} J^{a_1}(x_1) J^{a_2}(x_2) \\ &= e^{\pi k R \beta \text{tr}\mu^2} \sum_{\sigma} S_{\lambda}^{\sigma} \text{Tr}_{\widehat{V}_{k,\sigma}} \left(e^{-\frac{2\pi}{\beta}(L_0 - \frac{c_k}{24})R} e^{-2\pi i R \text{tr}\mu J_0} \mathcal{T}(\pi k \mu^{a_1} - i \mathcal{J}_{\ell}^{a_1}(-ix_1)) \right. \\ & \quad \left. (\pi k \mu^{a_2} - i \mathcal{J}_{\ell}^{a_2}(-ix_2)) \right). \end{aligned} \quad (4.120)$$

Let us consider the following meromorphic functions

$$f(z) = \text{Tr}_{\widehat{V}_{k,\lambda}} e^{-\beta(H - \text{tr}\mu Q)} J^{a_1}(z_2 + z) J^{a_2}(z_2) \quad (4.121)$$

$$\begin{aligned} g(z) = e^{\pi k R \beta \text{tr}\mu^2} \sum_{\sigma} S_{\lambda}^{\sigma} \text{Tr}_{\widehat{V}_{k,\sigma}} & \left(e^{-\frac{2\pi}{\beta}(L_0 - \frac{c_k}{24})R} e^{-2\pi i R \text{tr}\mu J_0} (\pi k \mu^{a_1} - i \mathcal{J}_{\ell}^{a_1}(-i(z_2 + z))) \right. \\ & \left. (\pi k \mu^{a_2} - i \mathcal{J}_{\ell}^{a_2}(-iz_2)) \right) \end{aligned} \quad (4.122)$$

so that the formula to establish is reduced to the identity $f(z) = g(z)$ for $z_1 = x_1$, $z_2 = x_2$ and $z = z_1 - z_2$.

We now want to prove the equality between two meromorphic functions on the complex torus. It is then enough to show that they have the same singular parts and that their integrals along the cocycles of a homology basis of the torus are equal. For such cycles, we shall take the closed straight paths $a = (0 \rightarrow R)$ and $b = (0 \rightarrow i\beta)$. Let us consider the Abelian differential of the first kind [116, 47] $\omega = cdz$ that is the only holomorphic 1-form such that its period over cycle a is 1. This gives $c = \frac{1}{R}$ and one can write $\omega = \omega(z)dz$ with

$$\omega(z) = - \sum_{r=1}^{\infty} A_r z^{r-1}, \quad A_r = -\frac{1}{R} \delta_{r,1}, \quad (4.123)$$

which will be used in the following. Then we look for the singularities of f and g . By operator product expansion given in (4.66) we have

$$J^{a_1}(z_2 + z) J^{a_2}(z_2) = -\frac{k}{2} \frac{\delta^{a_1 a_2}}{z^2} + \dots \quad (4.124)$$

$$\mathcal{J}_{\ell}^{a_1}(-i(z_2 + z)) \mathcal{J}_{\ell}^{a_2}(-iz_2) = +\frac{k}{2} \frac{\delta^{a_1 a_2}}{z^2} + \dots \quad (4.125)$$

where the dots mean a regular expression. Note that here we consider only Cartan components of the current, such that the z^{-1} term vanishes in the OPE. Thus, we extract the second order poles of f and g :

$$f(z) = -\frac{k}{2} \frac{\delta^{a_1 a_2}}{z^2} \text{Tr}_{\widehat{V}_{k,\lambda}} e^{-\beta(H - \text{tr}\mu Q)} + \tilde{f}(z) = -\frac{\alpha}{z^2} + \tilde{f}(z) \quad (4.126)$$

$$g(z) = -\frac{k}{2} \frac{\delta^{a_1 a_2}}{z^2} e^{\pi k R \beta \text{tr}\mu^2} \sum_{\sigma} S_{\lambda}^{\sigma} \text{Tr}_{\widehat{V}_{k,\sigma}} e^{-\frac{2\pi}{\beta}(L_0 - \frac{c_k}{24})R} e^{-2\pi i R \text{tr}\mu J_0} + \tilde{g}(z) = -\frac{\alpha}{z^2} + \tilde{g}(z) \quad (4.127)$$

Because of the result at $S = 0$ (4.62), these two functions then have the same coefficient at second order pole, that we denoted α in the following. Thus f and g are two function on the torus with

the same singularity, of order 2. They are then related to the Abelian differential of second kind $\eta_r = \eta_r(z)dz$ where

$$\eta_r(z) = -rz^{-(r+1)} + \dots \quad (4.128)$$

with the following properties

$$\int_a \eta_r = 0 \quad \int_b \eta_r = 2\pi i A_r \quad (4.129)$$

where the A_r are the previous coefficients appearing in ω . Since $f(z)$ and $\alpha\eta_1(z)$ are two meromorphic functions defined on the torus with the same singularity, they only differ by a holomorphic function on the torus, which is a constant, that we will denote C_f . From that we get for f :

$$\int_a f(z)dz = RC_f \quad \int_b f(z)dz = \alpha 2\pi i A_1 + i\beta C_f \quad (4.130)$$

which leads to

$$\frac{1}{R} \int_a f(z)dz = \frac{1}{i\beta} \int_b f(z)dz + \frac{2\pi}{R\beta} \alpha \quad (4.131)$$

and, similarly replacing f by g . Coming back to the explicit expression of f and g , we compute right hand side of (4.131), getting

$$\frac{1}{R} \int_a f(z)dz = \left(\frac{2\pi}{R}\right)^2 \text{Tr}_{\widehat{V}_{k,\lambda}} e^{-\beta(H - \text{tr}\mu Q)} J_0^{a_1} J_0^{a_2} \quad (4.132)$$

where we have considered the z_2 dependence of $J^{a_2}(z_2)$ as an holomorphic function on the torus, i.e. a constant that can be computed through its mean around the contour a . Then we compute the left hand side of (4.131) where we have replaced f by g :

$$\begin{aligned} \frac{1}{i\beta} \int_b g(z)dz + \frac{2\pi}{R\beta} \alpha &= \left(\frac{2\pi}{R}\right)^2 e^{\pi k R \beta \text{tr}\mu^2} \sum_{\sigma} S_{\lambda}^{\sigma} \text{Tr}_{\widehat{V}_{k,\sigma}} \left(e^{-\frac{2\pi}{\beta}(L_0 - \frac{c_k}{24})R} e^{-2\pi i R \text{tr}\mu J_0} \right. \\ &\quad \left. \left[\left(\frac{kR}{2}\mu^{a_1} - i\frac{R}{\beta}J_0^{a_1}\right) \left(\frac{kR}{2}\mu^{a_2} - i\frac{R}{\beta}J_0^{a_2}\right) + \frac{kR}{4\pi\beta}\delta^{a_1 a_2} \right] \right) \end{aligned} \quad (4.133)$$

where again, we have replaced the z_2 holomorphic function by its mean value. To compare the two previous quantities, we compute the second derivative of the modular covariance formula (4.61). Left hand side gives

$$\left. \frac{d^2}{d\varepsilon_2 d\varepsilon_1} \right|_{\varepsilon_{1,2}=0} \text{Tr}_{\widehat{V}_{k,\lambda}} e^{-\beta(H - \text{tr}(\mu + \varepsilon_1 \tilde{\mu}_1 + \varepsilon_2 \tilde{\mu}_2)Q)} = (2\pi\beta)^2 \text{Tr}_{\widehat{V}_{k,\lambda}} \left(e^{-\beta(H - \text{tr}\mu Q)} \text{tr}(\tilde{\mu}_1 J_0) \text{tr}(\tilde{\mu}_2 J_0) \right) \quad (4.134)$$

and, on the other side,

$$\begin{aligned} \left. \frac{d^2}{d\varepsilon_2 d\varepsilon_1} \right|_{\varepsilon_{1,2}=0} \text{Tr}_{\widehat{V}_{k,\lambda}} e^{-\beta(H - \text{tr}(\mu + \varepsilon_1 \tilde{\mu}_1 + \varepsilon_2 \tilde{\mu}_2)Q)} &= e^{\pi k R \beta \text{tr}\mu^2} \sum_{\sigma} S_{\lambda}^{\sigma} \text{Tr}_{\widehat{V}_{k,\sigma}} \left(e^{-\frac{2\pi}{\beta}(L_0 - \frac{c_k}{24})R} e^{-2\pi i R \text{tr}\mu J_0} \right. \\ &\quad \left. \left[\text{tr} \tilde{\mu}_1 (2k\pi R \beta \mu - 2\pi i R J_0) \text{tr} \tilde{\mu}_2 (2k\pi R \beta \mu - 2\pi i R J_0) + 2\pi k n R \beta \text{tr} \tilde{\mu}_1 \tilde{\mu}_2 \right] \right) \end{aligned} \quad (4.135)$$

so that in the component notations, setting $\tilde{\mu}_1 = t^{a_1}$, $\tilde{\mu}_2 = t^{a_2}$,

$$\begin{aligned} \text{Tr}_{\widehat{V}_{k,\lambda}} \left(e^{-\beta(H - \text{tr}\mu Q)} J_0^{a_1} J_0^{a_2} \right) &= e^{\pi k R \beta \text{tr}\mu^2} \sum_{\sigma} S_{\lambda}^{\sigma} \text{Tr}_{\widehat{V}_{k,\sigma}} \left(e^{-\frac{2\pi}{\beta}(L_0 - \frac{c_k}{24})R} e^{-2\pi i R \text{tr}\mu J_0} \right. \\ &\quad \left. \left[\left(\frac{kR}{2}\mu^{a_1} - i\frac{R}{\beta}J_0^{a_1}\right) \left(\frac{kR}{2}\mu^{a_2} - i\frac{R}{\beta}J_0^{a_2}\right) + \frac{1}{2} \frac{k n R}{2\pi\beta} \delta^{a_1 a_2} \right] \right). \end{aligned} \quad (4.136)$$

This equation proves that

$$\frac{1}{R} \int_a f(z) dz = \frac{1}{i\beta} \int_b g(z) dz + \frac{2\pi}{R\beta} \alpha \quad (4.137)$$

which means, together with (4.131) and its version with g , that

$$\int_a f(z) dz = \int_a g(z) dz \quad \text{and} \quad \int_b f(z) dz = \int_b g(z) dz. \quad (4.138)$$

This implies that $f = g$ completing the proof of formula (4.65) for $S = 2$.

Chapter 5

Coset junction

The model developed in the previous chapter suggests that other junctions of quantum wires ruled by WZW models should exist in principle, with a richer scattering than pure transmission to the next wire. We try to realize such scattering in the following model with a boundary condition inducing a coset decomposition of the theory. This coset junction seems promising but even the equilibrium state requires explicit expression of operators that are not known in general. Nevertheless, we compute it on a simple example, involving already some nontrivial calculations.

5.1 WZW action with a coset brane

5.1.1 Classical action and equations of motion

As for the permutation brane junction, we start with a multicomponent field

$$\mathbf{g} : \mathbb{R} \times I \rightarrow (G)^N, \quad (t, x) \mapsto (g_1(t, x), \dots, g_N(t, x)) \quad (5.1)$$

with components taking values in Lie group G , where $I = [0, L]$ for L the size of the wires. At the free end of the wires we impose, as before, the simplest reflecting boundary condition

$$g_i(t, L) = 1, \quad \forall t \in \mathbb{R}, \quad \forall i = 1, \dots, N \quad (5.2)$$

where 1 is the neutral element of G . In the spirit of the folding trick, the junction is defined by a boundary condition for \mathbf{g} at $x = 0$. Again we use the conjugacy classes of G ,

$$\mathcal{C}_\tau = \{g e^{2\pi i \tau} g^{-1} \mid g \in G\} \quad (5.3)$$

for τ in the positive Weyl alcove of $\mathfrak{t} \subset \mathfrak{g}$. The previous junction was defined by a conjugacy class involving the product of all the wire components g_i . Here we propose instead to impose the condition

$$g_i(t, 0) = h_i(t) \gamma(t), \quad h_i(t) \in \mathcal{C}_{\tau_i}, \quad \gamma(t) \in \mathcal{C}_\tau \quad (5.4)$$

for each $i = 1, \dots, N$. At the boundary we have N independent degrees of freedom h_i , one for each wire, and one field γ common to all the wires and ensuring that they are all connected. Such boundary conditions were already considered in [76, 56] in the context of the G/H coset models. In our case we consider them for the WZW model with group G^N and for $H = G_{\text{diag}} \subset G^N$ the diagonal subgroup. The action of such model is given by

$$S[\mathbf{g}] = \frac{k}{8\pi} \sum_{i=1}^N \int_{\mathbb{R} \times I} (\text{tr} [-(g_i^{-1} \partial_t g_i)^2 + (g_i^{-1} \partial_x g_i)^2]) dt dx + 2\omega(g_i) + \frac{k}{4\pi} \sum_{i=1}^N \int_{\mathbb{R}} \eta_i(g_i)(t, 0) dt \quad (5.5)$$

where, as before, ω denotes a local 2-form on G such that $d\omega = \chi$ for $\chi = \frac{1}{3} \text{tr}(g^{-1}dg)^{\wedge 3}$ the closed 3-form on G . 3-form χ becomes exact over each conjugacy class \mathcal{C}_τ : $\chi|_{\mathcal{C}_\tau} = d\omega_\tau$, where 2-forms ω_τ on \mathcal{C}_τ are given by formula (4.25) in Section 4.2. One has a multiplicative property stating that there exist locally 1-forms η_i such that

$$d\eta_i(g_i) = -\omega(g_i) + \omega_{\tau_i}(h_i) + \omega_\tau(\gamma) - \text{tr}(h_i^{-1}dh_i) \wedge (d\gamma)\gamma^{-1} \quad (5.6)$$

for $g_i = h_i\gamma$ as in the boundary condition (5.4). Indeed, one may check that the right hand side of (5.6) is a closed 2-form.

The classical equations of motion are extracted from the variational principle $\delta S = \delta S_{\text{bulk}} + \delta S_{\text{bound}} = 0$ with a bulk and a boundary terms that can be investigated separately. The bulk term leads to the standard WZW equation of motion on each wire i

$$\partial_+(g_i^{-1}\partial_-g_i) = 0 \quad \Rightarrow \quad g_i(t, x) = g_{i,\ell}(t+x)g_{i,r}^{-1}(t-x), \quad (5.7)$$

solved by the general formula for any one-variable functions $g_{i,\ell}$ and $g_{i,r}$. Moreover the left and right currents on each wire, defined by

$$J_{i,\ell} \equiv ik(\partial_+g_i)g_i^{-1}, \quad J_{i,r} \equiv -ikg_i^{-1}\partial_-g_i \quad (5.8)$$

are conserved in the bulk, as in the case without boundaries.

In the boundary term, the variation δg_i are decomposed in terms of the $N+1$ boundary degrees of freedom $h_i(t)$ and $\gamma(t)$, that can be expressed in terms of the parameters of different conjugacy classes. Since such degrees are independent, all coefficients of the boundary variation must vanish independently, leading after some algebra to the relations

$$-\partial_+g_i g_i^{-1}(t, 0) - Ad_{\gamma(t)}(g_i^{-1}\partial_-g_i)(t, 0) + (\partial_t\gamma)\gamma^{-1} = 0, \quad (5.9)$$

$$N(\partial_t\gamma)\gamma^{-1} + \sum_{i=1}^N (1 - Ad_{\gamma(t)})(g_i^{-1}\partial_-g_i)(t, 0) = 0, \quad (5.10)$$

where the first line corresponds to N equation for $i = 1, \dots, N$ and $Ad_u(X) = uXu^{-1}$ is the adjoint action of G on \mathfrak{g} . Such equations can be written in terms of left and right currents (5.8), and the second equation can be used to remove the last factor of the first one, leading to the scattering rule

$$J_{i,\ell}(t, 0) = Ad_{\gamma(t)}J_{i,r}(t, 0) + \frac{1}{N} \sum_{j=1}^N (1 - Ad_{\gamma(t)})J_{j,r}(t, 0) \quad (5.11)$$

which is both reflecting and transmitting and where Ad_γ and $1 - Ad_\gamma$ can be seen as reflection and transmission coefficients respectively. Note that in this case the transmission coefficient is the same in all the wires. Moreover, the scattering matrix is now depending on the boundary field $\gamma(t)$ and not on static coefficients as in the previous models. Hence we built this way a junction with a dynamical defect, at least at the classical level. Finally such scattering rule can be inverted to compare with the previous models (3.42) and (4.31) where right movers were expressed in terms of the left ones. Indeed the previous equation is invariant under the change $\ell \leftrightarrow r$ and $\gamma \rightarrow \gamma^{-1}$, due to the fact that

$$\sum_{i=1}^N J_{i,\ell}(t, 0) = \sum_{i=1}^N J_{i,r}(t, 0) \quad (5.12)$$

obtained by summing (5.11) over i .

As in the previous model, the free end of the wires relates simply left and right currents by a fully reflecting condition

$$J_{i,\ell}(t, L) = J_{i,r}(t, L). \quad (5.13)$$

5.1.2 Conserved charge and energy

Because of the two previous equations, the classical \mathfrak{g} -valued charge

$$Q(t) = \sum_{i=1}^N \int_I (J_{i,\ell} + J_{i,r})(t, x) dx \quad (5.14)$$

is conserved. It induces the diagonal adjoint symmetry $g_i \mapsto h g_i h^{-1}$, which is preserved by the junction. Moreover the total energy of the system, expressed in term of the energy-momentum tensors of each wire,

$$E(t) = \sum_i \int_I (T_{i,\ell} + T_{i,r})(t, x) dx, \quad T_{i,\ell/r} = \frac{1}{4\pi k} \text{tr}(J_{i,\ell/r})^2 \quad (5.15)$$

is also conserved in such a junction due to the relation

$$\sum_{i=1}^N (J_{i,\ell})^2(t, 0) = \sum_{i=1}^N (J_{i,r})^2(t, 0) \quad (5.16)$$

obtained using (5.11), and a similar one at $x = L$ following from (5.13).

5.1.3 Phase space

The compatibility condition between the different boundary conditions relates left and right movers in such a way that only one half of the degrees of freedom remains and becomes periodic. Namely, in terms of the one-variable fields $g_{i,\ell/r}$,

$$g_{i,r}(-t) = \gamma(t)^{-1} g_{i,\ell}(t) e^{-2\pi i \tau_i} = g_{i,\ell}(t + 2L). \quad (5.17)$$

Hence $g_{i,\ell}$ are $2L$ -twisted-periodic functions with monodromy related to the defect through γ and τ_i and is enough to describe the phase space of the system.

For the currents, the scattering rule (5.11) relating left and right is not sufficient since both (5.9) and (5.10) must be satisfied. Let us divide the current in terms of its diagonal and off-diagonal part

$$J_{i,\ell} = J_{i,\ell}^\perp + \frac{1}{N} J_\ell^\parallel, \quad \text{where} \quad J_\ell^\parallel = \sum_{i=1}^N J_{i,\ell}, \quad (5.18)$$

so that

$$\sum_{i=1}^N J_{i,\ell}^\perp = 0, \quad (5.19)$$

and similarly for the right currents. Then the full relations between left and right movers in terms of the currents read

$$J_\ell^\parallel(t, 0) = J_r^\parallel(t, 0), \quad J_{i,\ell}^\perp = \text{Ad}_\gamma J_{i,r}^\perp, \quad (5.20)$$

and

$$(1 - \text{Ad}_{\gamma(t)}) J_\ell^\parallel(t, 0) = iNk(\partial_t \gamma) \gamma^{-1} \quad (5.21)$$

The parallel and perpendicular currents are independent. Each perpendicular component is fully reflected (up to a conjugation by γ), and the parallel part is responsible for the transmission in the junction since it is equal in each wire. The situation is summarized in Figure 5.1

Finally the relation between $J_{\ell/r}^\parallel$ and γ allows to rewrite

$$J_\ell^\parallel(t, 0) = iNk \zeta' \zeta(t) \quad \text{with} \quad \gamma(t) = \zeta(t) e^{2\pi i \tau} \zeta(t)^{-1}. \quad (5.22)$$

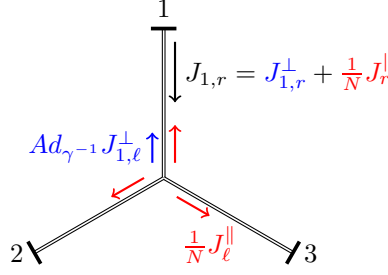


Figure 5.1: The right current from the first wire is scattered at the junction. The perpendicular part is reflected and the parallel one is common to all the wires and allows for equal transmission into each wire.

Then we can decompose the corresponding fields in terms of a diagonal and a nondiagonal part, writing

$$g_{i,\ell}(t) = \zeta(t) \tilde{g}_i(t) \quad (5.23)$$

for ζ and \tilde{g}_i that are G valued fields with the following periodicity

$$\tilde{g}_i(t + 2L) = \alpha_0 e^{-2\pi i \tau} \tilde{g}_i(t) e^{-2\pi i \tau_i}, \quad \zeta(t + 2L) = \zeta(t) \alpha_0^{-1} \quad (5.24)$$

where $\alpha_0 \in G$ is a remaining constant ambiguity that disappears in $g_{i,\ell}$. Finally one has

$$ik \tilde{g}'_i \tilde{g}_i^{-1}(t) = \zeta^{-1}(t) J_{i,\ell}^{\perp}(t, 0) \zeta(t) \quad \Rightarrow \quad \sum_{i=1}^N \tilde{g}'_i \tilde{g}_i^{-1}(t) = 0 \quad (5.25)$$

5.1.4 Symplectic structure

It is possible to compute the symplectic form of the system in terms of the degrees of freedom \tilde{g}_i and ζ by differentiating twice the action on the space of solutions and expressing every fields in terms of the last ones. A bit of algebra leads then to the expression

$$\begin{aligned} \Omega[g] = & \frac{k}{4\pi} \sum_{i=1}^N \int_{-L}^L \text{tr}(\tilde{g}_i^{-1} \delta \tilde{g}_i \partial(\tilde{g}_i^{-1} \delta \tilde{g}_i)) dx + \frac{Nk}{4\pi} \int_{-L}^L \text{tr}(\zeta^{-1} \delta \zeta \partial(\zeta^{-1} \delta \zeta)) dx \\ & + \frac{k}{4\pi} \sum_{i=1}^N [\text{tr}((\delta \alpha_0) \alpha_0^{-1} (\delta \tilde{g}_i) \tilde{g}_i^{-1})]_{x=L} + \frac{Nk}{4\pi} \sum_{i=1}^N [\text{tr}((\delta \alpha_0) \alpha_0^{-1} \zeta^{-1} \delta \zeta)]_{x=L} \end{aligned} \quad (5.26)$$

which seems to have a nice form: up to the extra α_0 terms, it looks like $N+1$ independent degrees of freedom. However the computation of the corresponding Poisson Brackets reveals a nontrivial structure that is not easily tractable for canonical quantization. First it is not too hard to see that

$$\{J_{\ell}^{\parallel}(t, x), J_{i,\ell}^{\perp}(t, y)\} = 0 \quad (5.27)$$

so that parallel and perpendicular currents will commute once quantized. Moreover the calculation of the Poisson brackets for the parallel current leads to

$$\{J_{\ell}^{a\parallel}(t, x), J_{\ell}^{b\parallel}(t, y)\} = 2\pi \delta(x - y) f^{abc} J_{\ell}^{c\parallel}(t, y) + \pi N k \delta^{ab} \delta'(x - y) \quad (5.28)$$

where the components are given by $J^{a\parallel}(t, x) = \text{tr } t^a J^{\parallel}(t, x)$, with normalization $\text{tr } t^a t^b = \frac{1}{2} \delta^{ab}$. Note that in the two previous computations the terms involving α_0 all compensate and then vanish in the final Poisson brackets. Hence once quantized the parallel current leads to a current

algebra as in the previous models, with highest weight integrable representations as the building blocks of the Hilbert space.

However the behavior of the orthogonal part is not so simple: the Poisson brackets of such currents have to be computed by respecting the constraint (5.25), telling that the $J_{i,\ell}^\perp$ are not independent. It is still possible to compute them in the case where α_0 is fixed, but the result has no simple interpretation, even once quantized: the explicit algebraic structure has no canonically associated Hilbert space. Hence we must adopt another strategy to quantize the full system.

5.2 Equilibrium state

Although incomplete, the analysis of the symplectic structure shows that the parallel current associated to the diagonal subalgebra $\mathfrak{g}_{\text{diag}} \subset \mathfrak{g}^N$ is ruled by a current algebra that, once quantized, would lead to integrable representations $\widehat{V}_{Nk,\lambda}$. This current algebra induces itself a Virasoro algebra through the Sugawara construction. Roughly speaking, we have the decomposition $G^N \sim G^N/G_{\text{diag}} \times G_{\text{diag}}$, and the orthogonal part must in some sense carry the G^N/G_{diag} part of the theory. It is actually possible to give a precise meaning to such decomposition at the quantum level through the coset construction that we briefly present here.

5.2.1 Coset construction

For a Lie algebra \mathfrak{g} , denote by J^a its generators and by J_n^a the generators of the corresponding current algebra $\widehat{\mathfrak{g}}$. Consider the unitary highest weight representation $\widehat{V}_{k,\lambda}$ associated to the integrable weight λ (see Subsection 4.1.2 in the previous chapter for more details). Then consider a Lie subalgebra $\mathfrak{h} \subset \mathfrak{g}$, and denote by K^a its generator and K_n^a the generators of the corresponding current algebra $\widehat{\mathfrak{h}}$. As a subalgebra of $\widehat{\mathfrak{g}}$, current algebra $\widehat{\mathfrak{h}}$ also acts in $\widehat{V}_{k,\lambda}$, but the level k' associated to this action may be different from k , depending on the normalization of the generators K_n^a . We consider all the corresponding integrable weights λ' associated to unitary highest weight representations $\widehat{V}_{k',\lambda'}$ of the algebra $\widehat{\mathfrak{h}}$ at level k' . Now consider the following decomposition

$$\widehat{V}_{k,\lambda} = \bigoplus_{\lambda'} \left(\widehat{M}_{k,\lambda,\lambda'} \otimes \widehat{V}_{k',\lambda'} \right), \quad (5.29)$$

where $\widehat{M}_{k,\lambda,\lambda'}$ are called the multiplicity spaces and are complex vector spaces with dimension given by the number (possibly infinite) of occurrences of $\widehat{V}_{k',\lambda'}$ in the previous decomposition. Generators K_n^a of \mathfrak{h} act trivially on the multiplicity spaces and consequently every operator that commutes with all such generators acts trivially on $\widehat{V}_{k',\lambda'}$ and hence preserves the multiplicity spaces. In particular, consider the Virasoro generators L_n and L'_n associated, respectively, to the action of $\widehat{\mathfrak{g}}$ and $\widehat{\mathfrak{h}}$ through the Sugawara construction with respective central charge c_k and $c'_{k'}$. If we define

$$\tilde{L}_n = L_n - L'_n, \quad n \in \mathbb{Z}, \quad (5.30)$$

then a few lines of algebra shows that

$$[\tilde{L}_n, K_n^a] = 0 \quad (5.31)$$

$$[\tilde{L}_n, \tilde{L}_m] = (n-m)\tilde{L}_{n+m} + \frac{1}{12}\tilde{c}n(n^2-1)\delta_{n,-m} \quad (5.32)$$

for $\tilde{c} = c_k - c'_{k'}$, meaning that the \tilde{L}_n preserve the multiplicity spaces $\widehat{M}_{k,\lambda,\lambda'}$ and generate on them a Virasoro algebra representations of central charge $\tilde{c} = c_k - c'_{k'}$. Although abstract, such coset representations are unitary by construction, and were initially developed by Goddard, Kent and Olive in [89, 88] to prove unitarity of a representation appearing in a subclass of so called minimal models of CFT [13]. Through the characters of the representations, the multiplicity

spaces for the case $\mathfrak{g} = \mathfrak{su}(2) \oplus \mathfrak{su}(2)$ and the diagonal subalgebra $\mathfrak{h} = \mathfrak{su}(2)$, with levels $(k, 1)$ and $k' = k + 1$, respectively, were identified with the unitary irreducible Virasoro representations of central charge $\tilde{c} < 1$. Finally note that the coset construction can also be understood in the functional integral formalism [80] that will be discussed in some detail in the next part of the present manuscript.

5.2.2 Closed string picture

In order to apply the previous decomposition to our case and define the equilibrium state of the junction, consider the dual closed string picture instead of the initial junction. The corresponding worldsheet is a cylinder corresponding to periodic “space” of length β and infinite “time”, and we focus on the propagation of such closed string between 0 and L , for which we have to construct the corresponding boundary states. The closed string is described by currents $\mathcal{J}_{i,\ell}(t, x)$ and $\mathcal{J}_{i,r}(t, x)$ for $i = 1, \dots, N$ which are β -periodic in x and each one acting in an integrable representation of $\widehat{\mathfrak{g}}$ denoted respectively by $\widehat{V}_{k,\lambda_i}$ and $\widehat{V}_{k,\bar{\lambda}_i} \cong \overline{\widehat{V}_{k\lambda_i}}$, where the overline stands for the complex-conjugation of the representation space. The corresponding Hilbert space is

$$\mathcal{H} = \bigoplus_{\boldsymbol{\lambda}} \left[\left(\bigotimes_{i=1}^N \widehat{V}_{k,\lambda_i} \right) \otimes \left(\bigotimes_{i=1}^N \overline{\widehat{V}_{k,\lambda_i}} \right) \right] \quad (5.33)$$

where $\boldsymbol{\lambda} = (\lambda_1, \dots, \lambda_N)$. Remember from the symplectic structure of the junction that the subalgebra we consider here is the diagonal embedding of G into G^N , corresponding to the parallel current. Hence we apply the previous coset construction to algebra $\mathfrak{g} \oplus \dots \oplus \mathfrak{g}$ and diagonal subalgebra \mathfrak{g}

$$\bigoplus_{\boldsymbol{\lambda}} \left(\bigotimes_{i=1}^N \widehat{V}_{k,\lambda_i} \right) = \bigoplus_{\boldsymbol{\lambda}, \nu} \left(\widehat{M}_{k,\boldsymbol{\lambda},\nu} \otimes \widehat{V}_{Nk,\nu} \right). \quad (5.34)$$

It turns out [50] that such decomposition actually requires a supplementary condition on $\boldsymbol{\lambda}$, namely

$$\lambda_1 + \dots + \lambda_N - \nu \in Q^\vee(\mathfrak{g}) \quad (5.35)$$

where $Q^\vee(\mathfrak{g})$ is the coroot lattice of \mathfrak{g} . Such condition will be assumed for every sum written in the following. Finally the coset decomposition may be applied similarly to the antichiral part so that the Hilbert space may be written as

$$\mathcal{H} = \bigoplus_{\boldsymbol{\lambda}, \nu, \nu'} \left[\left(\widehat{M}_{k,\boldsymbol{\lambda},\nu} \otimes \widehat{V}_{Nk,\nu} \right) \otimes \left(\overline{\widehat{M}_{k,\boldsymbol{\lambda},\nu'}} \otimes \overline{\widehat{V}_{Nk,\nu'}} \right) \right], \quad (5.36)$$

where $\boldsymbol{\lambda}$ is common to both decompositions whereas ν and ν' may be different.

5.2.3 Boundary states

Consider respectively some abstract orthonormal bases $(e_r^{\lambda,\nu})_r$ and $(e_s^\nu)_s$ for multiplicity space $\widehat{M}_{k,\boldsymbol{\lambda},\nu}$ and integrable representation $\widehat{V}_{Nk,\nu}$, respectively, and similarly for the antichiral part by considering the complex conjugate vectors. Then consider the following boundary state

$$|\mathcal{D}_{\boldsymbol{\kappa},\sigma}\rangle = \sum_{\boldsymbol{\lambda},\nu} \left(\prod_{i=1}^N \frac{S_{\kappa_i,\lambda_i}}{\sqrt{S_{0,\lambda_i}}} \right) \frac{S_{\sigma,\nu}}{S_{0,\nu}} \sum_{r,s} \left| e_r^{\lambda,\nu} \otimes e_s^\nu \otimes \overline{e_r^{\lambda,\nu}} \otimes \overline{e_s^\nu} \right\rangle \quad (5.37)$$

where S is the modular matrix at level k and level Nk , respectively. Such boundary states, already considered in [145], couple the chiral and antichiral sector for each integrable weight ν and preserve the coset decomposition. To make them correspond to our boundary condition, we

set in the latter $\tau_i = \kappa_i/k$ and $\tau = \sigma/(Nk)$, where τ_i and τ were used in (5.4). Moreover, note that for $\kappa = 0$ and $\sigma = 0$, the corresponding brane is

$$|\mathcal{D}_0\rangle = \sum_{\lambda} \left(\prod_{i=1}^N \frac{S_{0,\lambda_i}}{\sqrt{S_{0,\lambda_i}}} \right) \sum_{r,s,\nu} |e_r^{\lambda,\nu} \otimes e_s^\nu \otimes \overline{e_r^{\lambda,\nu}} \otimes \overline{e_s^\nu}\rangle \quad (5.38)$$

which couples the left and right sector the same way for any ν . This is nothing but the symmetric brane corresponding to the Hilbert space decomposition (5.33), given before the coset construction. Such a state corresponds to the boundary condition that we impose at the free ends of the wires [77]. In particular, in the action on such a state, the left and right current will be identified.

5.2.4 Equilibrium state from the closed string picture

The equilibrium state is defined directly through the closed string picture here (we consider the case of vanishing chemical potential). Consider a general product of currents for non-coincident points $(x_{p_i}^i)$ and $(x_{q_i}^i)$ in the interval $[0, L]$,

$$A = \prod_{i=1}^N \left(\prod_{p_i=1}^{P_i} J_{i,\ell}^{a_{p_i}^i}(0, x_{p_i}^i) \prod_{q_i=1}^{Q_i} J_{i,r}^{a_{q_i}^i}(0, x_{q_i}^i) \right). \quad (5.39)$$

The thermal expectation of such product will be defined by the dual formula:

$$\omega_\beta^L(A) = (-i)^{P+Q} \frac{\langle \mathcal{D}_0 | e^{-\frac{2\pi}{\beta} \sum_i (L_{0i} + \bar{L}_{0i} - \frac{c}{12})L} A_{\text{c.s.}} | \mathcal{D}_{\lambda,\sigma} \rangle}{Z_\beta} \quad (5.40)$$

where P and Q are the respective sum over all P_i and Q_i . Such a formula was already appearing in the free bosonic model as a duality between open and closed string picture. Here only the last one has been quantized so that this equation must be seen as a definition. The denominator Z_β is the partition function:

$$Z_\beta = \langle \mathcal{D}_0 | e^{-\frac{2\pi}{\beta} \sum_i (L_{0i} + \bar{L}_{0i} - \frac{c}{12})L} | \mathcal{D}_{\lambda,\sigma} \rangle \quad (5.41)$$

and $A_{\text{c.s.}}$ is the translation of A into the closed string language, corresponding to the change of variable $z \mapsto -iz$ and leading to the i factors in the definition of ω_β . Explicitly,

$$A_{\text{c.s.}} = \prod_{i=1}^N \mathcal{T} \left(\prod_{p_i=1}^{P_i} \mathcal{J}_{i,\ell}^{a_{p_i}^i}(-ix_{p_i}^i) \prod_{q_i=1}^{Q_i} \mathcal{J}_{i,r}^{a_{q_i}^i}(ix_{q_i}^i) \right) \quad (5.42)$$

The equilibrium expectation, defined here by propagation between two boundary states, can be actually rewritten as a combination of traces. Using the explicit formula for the boundary states (5.37) and (5.38) in (5.40), the chiral and antichiral sector expectation can be factorized. Then we identify the action of left and right currents by

$$\mathcal{J}_{i,r}^a(z) = -(\mathcal{J}_{i,\ell}^a)^\dagger(\bar{z}) \quad (5.43)$$

since the mode decomposition is the same but just acting on $\widehat{V}_{k,\lambda_i}$ and its antichiral copy $\widehat{\overline{V}}_{k,\lambda_i}$. This allows to rewrite the expectation in terms of left movers only. After some algebra, we end up with the identity

$$\omega_\beta^L(A) = (-i)^{P+Q} Z_\beta^{-1} \sum_{\lambda,\nu} \prod_{i=1}^N S_{\kappa_i,\lambda_i} \frac{S_{\sigma,\nu}}{S_{0,\nu}} \text{Tr}_{\widehat{V}_{k,\lambda}} \left(e^{-\frac{2\pi}{\beta} \sum_i (L_{0i} - \frac{c}{24})2L} A_{\text{c.s.}}^\ell P_{\lambda,\nu} A_{\text{c.s.}}^r \right) \quad (5.44)$$

where, for a given A in the initial picture

$$A_{\text{c.s.}}^\ell = \prod_{i=1}^N \mathcal{T} \prod_{p_i=1}^{P_i} \mathcal{J}_{i,\ell}^{a_{p_i}}(-ix_{p_i}^i), \quad A_{\text{c.s.}}^r = \prod_{i=1}^N \mathcal{T} \prod_{q_i=1}^{q_i} \mathcal{J}_{i,\ell}^{a_{q_i}}(ix_{q_i}^i) \quad (5.45)$$

are the left and right parts of the closed string product, but with the right currents expressed in terms of the left ones. Between them appears the orthogonal projector

$$P_{\lambda,\nu} = \sum_{r,s} |e_r^{\lambda,\nu} \otimes e_s^{\lambda,\nu}\rangle \langle e_r^{\lambda,\nu} \otimes e_s^{\lambda,\nu}| \quad (5.46)$$

on the (λ, ν) -component in the coset decomposition (5.34).

5.2.5 Thermodynamic limit

As in the previous models, we expect the thermodynamic limit of the equilibrium to be simpler than the finite size case and corresponding to a more explicit formula for the expectations. In (5.44), the L -dependence of the system only appears in the exponential factor. As explained in the previous chapter, the dominant term in the trace will be the state with the lowest L_0 -eigenvalue, namely the vacuum state $|0\rangle$ belonging to the $\lambda = 0$ representation, and the contributions from all the other states will vanish in the limit $L \rightarrow \infty$ since they will be exponentially damped due to strictly positive eigenvalues of L_0 . In particular, only the term with $\lambda = 0$ remains in the thermodynamic limit.

The free energy of the full system reads

$$f_\beta = \lim_{L \rightarrow \infty} \frac{1}{\beta L} \ln Z_\beta = N \frac{\pi c_k}{6\beta^2} \quad (5.47)$$

corresponding to N disconnected wires and, assuming a normalized vacuum $\langle 0|0\rangle = 1$, we end up with the equilibrium current expectation of the form

$$\omega_\beta(A) = (-i)^{P+Q} \langle 0| A_{\text{c.s.}}^\ell \mathcal{S} A_{\text{c.s.}}^r |0\rangle, \quad \text{where} \quad \mathcal{S} = \sum_\nu \frac{S_{\sigma,\nu}}{S_{0,\nu}} P_{0,\nu}. \quad (5.48)$$

Thus in the thermodynamic limit the coset decomposition associated to the lowest weights $\lambda = 0$ remains, and seems to play the role of the scattering operator. First notice that if we take $\tau = 0$ in the initial boundary condition (5.4) then $\sigma = 0$ and \mathcal{S} becomes the identity operator on the $\lambda = 0$ factor of the coset decomposition (5.34), so that right currents become simply reflected to left currents and this corresponds to the result for the disconnected junction, the same we would get replacing $|\mathcal{D}_{\kappa,\sigma}\rangle$ by $|\mathcal{D}_{0,0}\rangle$. In the general case with arbitrary σ , any expectation of a product of current A^ℓ that contains left movers only is reduced in the closed string picture to a vacuum expectation

$$\omega_\beta(A^\ell) = (-i)^{P+Q} \langle 0| A_{\text{c.s.}}^\ell |0\rangle \quad (5.49)$$

since \mathcal{S} preserves the vacuum state $|0\rangle$, and similarly for a product containing only right movers. This is the expected factorization in the thermodynamic limit: the equilibrium correlations of currents of a single chiral nature (left or right only) become vacuum correlations and do not depend on the boundary condition. In particular they can be seen as disconnected junction expectations.

Finally, it is not quite true that the operator \mathcal{S} acts as a scattering operator for currents when computing mixed (left and right) current expectations. This would require that $\mathcal{S}\mathcal{J}\mathcal{S}^{-1}$ is a linear combination of currents, which is not necessarily true in general. Moreover, although powerful, the coset construction does not give any simple expression for the projector $P_{0,\nu}$ which can be computed only in specific models where an explicit representation of the multiplicity spaces is known.

5.3 The $SU(2)$ level 1 coset junction

Consider the simplest example with $N = 2$ wires and $G = SU(2)$ at level $k = 1$. The coset decomposition of the tensor product of two vacuum representations $\widehat{V}_{k,j}$ with spin $j = 0$ of $\widehat{\mathfrak{su}}(2)$ current algebra at level 1 takes the form [88]:

$$\widehat{V}_{1,0} \otimes \widehat{V}_{1,0} \cong (\widehat{M}_{\frac{1}{2},0} \otimes \widehat{V}_{2,0}) \oplus (\widehat{M}_{\frac{1}{2},\frac{1}{2}} \otimes \widehat{V}_{2,1}) \quad (5.50)$$

with $\widehat{M}_{c,\Delta}$ the irreducible module of the coset Virasoro algebra with central charge c and conformal weight Δ (we use such notation here instead of the previous one for multiplicity spaces since in this case the coset representations are known explicitly from [88], see below). We would like to understand how the currents $\mathcal{J}_{1,\ell}$ and $\mathcal{J}_{2,\ell}$, acting respectively on the first and second factor $\widehat{V}_{1,0}$ in the product of left hand side, behave under the action $P_{0,0}$ and $P_{0,1}$, the projectors on the first and second term of the right hand side direct sum.

In the case of $SU(2)$ the modular matrices have a simple form [50] so that we can compute the $S_{\sigma,\nu}$ appearing in operator \mathcal{S} given in (5.48). Remember that this modular matrix is associated to the diagonal part subalgebra in the coset decomposition (or to the parallel currents in our Lagrangian description) and then corresponds to level $k' = Nk = 2$ here. In that case σ can take values 0, 1/2 and 1 and

$$S_{0,0} = S_{0,1} = \frac{1}{2}, \quad S_{\frac{1}{2},0} = -S_{\frac{1}{2},1} = \frac{1}{\sqrt{2}}, \quad S_{1,0} = S_{1,1} = \frac{1}{2}. \quad (5.51)$$

Thus the operator \mathcal{S} is given by

$$\mathcal{S} = I \quad \text{for } \sigma = 0, 1, \quad \mathcal{S} = \frac{1}{\sqrt{2}}(P_{0,0} - P_{0,1}) \quad \text{for } \sigma = \frac{1}{2} \quad (5.52)$$

so that $\sigma = 0, 1$ correspond to the disconnected junction. Hence we focus on the case $\sigma = 1/2$ which might be nontrivial.

The idea is to identify both parts of (5.50) with a common Hilbert space where we can see explicitly the action of $P_{0,0}$ and $P_{0,1}$. Starting with left hand side we end up with a subspace of a tensor product of four Majorana fermionic space, that can be identified with left hand side using character formulae. To simplify the demonstration we defer all the explicit character formulae that we employ to Appendix 5.A.

5.3.1 Fermionization

Space $\widehat{V}_{1,0}$ may be realized as a sum of bosonic Fock spaces \mathcal{F}_α carrying irreducible unitary representation of the $\widehat{u}(1)$ algebra generated by the modes α_n , $n \in \mathbb{Z}$ satisfying canonical commutation relations $[\alpha_n, \alpha_m] = n\delta_{n,-m}$. Fock space \mathcal{F}_α is generated by action of the creators α_{-n} for $n > 0$ on the vacuum state $|\alpha\rangle$, where $\alpha \in \mathbb{R}$ is the α_0 -eigen value and $|\alpha\rangle$ is annihilated by the α_n for $n > 0$. One can construct a Virasoro algebra representation of central charge $c = 1$ from such Fock space. Then comparing the affine characters of the two theories (see 5.A), one has

$$\widehat{V}_{1,0} = \bigoplus_{m \in \mathbb{Z}} \mathcal{F}_{\sqrt{2}m} \quad (5.53)$$

such that the product appearing in the left hand side of (5.50) involve two families of Fock spaces, each one associated to modes α_n^1 and α_n^2 for $n \in \mathbb{Z}$, corresponding to the first and the second factor, and with arbitrary α_0 -eigenvalues $\sqrt{2}m^1$ and $\sqrt{2}m^2$ for $m_1, m_2 \in \mathbb{Z}$. Introducing the new modes

$$\alpha_n^\pm = \frac{1}{\sqrt{2}}(\alpha_n^1 \pm \alpha_n^2) \quad (5.54)$$

satisfying the canonical commutation relations and acting on the tensor product $\widehat{V}_{1,0} \otimes \widehat{V}_{1,0}$, we obtain new eigenvalues that become integer

$$\alpha_0^\pm |\sqrt{2}m^1, \sqrt{2}m^2\rangle = (m^1 \pm m^2) |\sqrt{2}m^1, \sqrt{2}m^2\rangle \quad (5.55)$$

and could be written $m^\pm = m^1 \pm m^2 \in \mathbb{Z}$ but with the constrain that m^+ and m^- must have the same parity. Hence we rewrite

$$\widehat{V}_{1,0} \otimes \widehat{V}_{1,0} = (P_e^- \otimes P_e^+ + P_o^- \otimes P_o^+) \left[\left(\bigoplus_{m^- \in \mathbb{Z}} \mathcal{F}_{m^-} \right) \otimes \left(\bigoplus_{m^+ \in \mathbb{Z}} \mathcal{F}_{m^+} \right) \right] \quad (5.56)$$

where we introduced the projectors ensuring the same parity of the α_0 eigenvalues in the two components

$$P_e^\mp = \frac{1 + (-1)^{\alpha_0^\mp}}{2}, \quad P_o^\mp = \frac{1 - (-1)^{\alpha_0^\mp}}{2} \quad (5.57)$$

Each of the two infinite sums of Fock spaces with integer eigenvalues appearing in the right hand side of (5.56) can be interpreted as the Fock space of Dirac fermions \mathcal{F}_D , generated by the Neveu-Schwarz fermionic operator $\{c_k, c_k^\dagger\}$ for $k \in \mathbb{Z} + 1/2$, satisfying canonical anticommutation relations $[c_k, c_{k'}^\dagger]_+ = \delta_{k,k'}$ with the other anticommutators vanishing. The space \mathcal{F}_D is generated by the c_k and c_{-k}^\dagger with $k < 0$ acting on a ground state $|D\rangle$ and annihilated by the same operators with $k > 0$. Then setting for $n \in \mathbb{Z}$

$$\alpha_n = \sum_{k \in \mathbb{Z} + 1/2} : c_{k-n}^\dagger c_k :, \quad L_n = \sum_{k \in \mathbb{Z} + 1/2} \left(k - \frac{n}{2} \right) : c_{k-n}^\dagger c_k : \quad (5.58)$$

with the fermionic normal ordering, we get back the canonical commutation relations for the α_n and L_n carry the Virasoro representation of central charge $c = 1$. Moreover in this picture α_0 is the charge operator, counting the number of particle minus the number of holes and hence has integer eigenvalues. Comparing the characters of the two Virasoro representations, see (5.80), one identifies

$$\mathcal{F}_D \cong \bigoplus_{m \in \mathbb{Z}} \mathcal{F}_m. \quad (5.59)$$

On top of that, the fermionic number operator defined as

$$F = \sum_{k>0} c_k^\dagger c_k + \sum_{k<0} c_k c_k^\dagger \quad (5.60)$$

is related to α_0 in such way that the parity of their eigenvalue is the same, namely

$$F - \alpha_0 = 2 \sum_{k<0} c_k c_k^\dagger, \quad \Rightarrow \quad (-1)^{\alpha_0} = (-1)^F. \quad (5.61)$$

The Fock space of Dirac fermions can then be decomposed in terms of two Majorana fermions, setting

$$d_k^1 = \frac{1}{\sqrt{2}}(c_k + c_{-k}^\dagger), \quad d_k^2 = \frac{1}{\sqrt{2}i}(c_k - c_{-k}^\dagger) \quad (5.62)$$

such that $(d_k^i)^\dagger = d_{-k}^i$ and $[d_k^i, d_{k'}^j]_+ = \delta^{ij} \delta_{kk'}$ are the canonical and independent anticommutation relations. Then one has:

$$\mathcal{F}_D = \mathcal{F}_M^1 \otimes \mathcal{F}_M^2 \quad (5.63)$$

where \mathcal{F}_M^i is generated by the d_{-k}^i acting on $|D\rangle$ for $k > 0$. By decomposing $L_n = L_n^1 + L_n^2$ one can show that each \mathcal{F}_M^i carries a Virasoro representation of central charge $c = 1/2$ and compute the corresponding character, see (5.81). Besides the fermionic number behaves simply with such decomposition: $F = F_1 + F_2$ where each F_i is the Majorana fermion number operator.

Consequently we have decomposition (5.56) in terms of four Majorana Fock spaces

$$\widehat{V}_{1,0} \otimes \widehat{V}_{1,0} = (P_e^- \otimes P_e^+ + P_o^- \otimes P_o^+) \left[\mathcal{F}_{M,1}^- \otimes \mathcal{F}_{M,2}^- \otimes \mathcal{F}_{M,1}^+ \otimes \mathcal{F}_{M,2}^+ \right] \quad (5.64)$$

and the projectors can be expressed as combinations of the parity of the Majorana fermion number:

$$P_e^{i\mp} = \frac{1}{2}(1 + (-1)^{F_i^\mp}), \quad P_o^{i\mp} = \frac{1}{2}(1 - (-1)^{F_i^\mp}) \quad (5.65)$$

since parity of α_0 is the same as the one of $F = F_1 + F_2$. Putting all together, we end up with the following decomposition

$$\widehat{V}_{1,0} \otimes \widehat{V}_{1,0} = P_e^{1-} \mathcal{F}_{M,1}^- \otimes [\mathcal{F}_{M,2}^- \otimes \mathcal{F}_{M,1}^+ \otimes \mathcal{F}_{M,2}^+]_e \oplus P_o^{1-} \mathcal{F}_{M,1}^- \otimes [\mathcal{F}_{M,2}^- \otimes \mathcal{F}_{M,1}^+ \otimes \mathcal{F}_{M,2}^+]_o \quad (5.66)$$

where the $[\mathcal{F}]_{e/o}$ denote the subspaces of \mathcal{F} with even or odd total fermion numbers (given by the sum over the three Majorana numbers of the tensor factors of \mathcal{F}).

5.3.2 Identification

We would like to identify the right hand side of the coset decomposition (5.50) with the one of (5.66). This is actually possible by comparing the character formulae for the different representations. The characters of the Verma modules $\widehat{M}_{\frac{1}{2},0}$ and $\widehat{M}_{\frac{1}{2},\frac{1}{2}}$ are known from the Ising model and can be expressed in terms of the Jacobi theta functions θ_3 and θ_4 and the Dedekind function η , see (5.82). Then it is simple to interpret such characters as the one for Majorana fermions with even or odd fermionic number, namely

$$\widehat{M}_{\frac{1}{2},0} \cong P_e \mathcal{F}_M, \quad \widehat{M}_{\frac{1}{2},\frac{1}{2}} \cong P_o \mathcal{F}_M \quad (5.67)$$

coinciding with the factors $P_e^{1-} \mathcal{F}_{M,1}^-$ in (5.66). Moreover the affine characters for the spaces $\widehat{V}_{2,0}$ and $\widehat{V}_{2,1}$ can be obtained through the Weyl-Kac character formula and are known explicitly, see (5.84). Rewriting

$$\mathcal{F}_{M,1} \otimes \mathcal{F}_{M,2} \otimes \mathcal{F}_{M,3} \cong \mathcal{F}_{M,1} \otimes \mathcal{F}_B \quad (5.68)$$

where we have partially bosonized two of the three fermionic spaces, we can show using Jacobi triple product identity that

$$\widehat{V}_{2,0} \cong [\mathcal{F}_{M,1} \otimes \mathcal{F}_{M,2} \otimes \mathcal{F}_{M,3}]_e, \quad \widehat{V}_{2,1} \cong [\mathcal{F}_{M,1} \otimes \mathcal{F}_{M,2} \otimes \mathcal{F}_{M,3}]_o \quad (5.69)$$

coinciding with $[\mathcal{F}_{M,2}^- \otimes \mathcal{F}_{M,1}^+ \otimes \mathcal{F}_{M,2}^+]_{o/e}$ factors in (5.66). In conclusion, we can identify the coset decomposition (5.50) with the fermionization (5.66) and consequently we may identify the projectors $P_{0,0}$ and $P_{0,1}$ with P_e^{1-} and P_o^{1-} respectively, acting on the first Majorana factor upon the identification (5.64).

The expression of the bosonic modes in terms of the Majorana modes reads

$$\alpha_n^\pm = i \sum_{k \in \mathbb{Z}} : d_{n-k}^{1\pm} d_k^{2\pm} : \quad (5.70)$$

so that the action of α_n^- inverts the parity on \mathcal{F}_{M1}^- by modifying the Fermionic number F_1^- by 1 or -1 , giving

$$P_e^{1-} \alpha_n^- = \alpha_n^- P_o^{1-}, \quad P_o^{1-} \alpha_n^- = \alpha_n^- P_e^{1-}, \quad (5.71)$$

whereas α_n^+ do not act on \mathcal{F}_{M1}^- , giving

$$[P_e^{1-}, \alpha_n^+] = 0 = [P_o^{1-}, \alpha_n^+]. \quad (5.72)$$

5.3.3 Scattering operator

We are now able to compute the action of the scattering operator \mathcal{S} on the closed string currents $\mathcal{J}_{1,\ell}$ and $\mathcal{J}_{2,\ell}$ on the two wires. We restrict to the Cartan component of such currents, denote by index 3 for $SU(2)$, since they are easily expressible in terms of the bosonic modes described above. Indeed we have the following mode decomposition

$$\mathcal{J}_{i,\ell}^3(z) = \frac{2\pi}{\beta} \sum_{n \in \mathbb{Z}} J_{i,n}^3 e^{-\frac{2\pi i n z}{\beta}} \quad (5.73)$$

where $J_{i,\ell}^3 = \alpha_n^i / \sqrt{2}$ or, upon identification (5.54)

$$J_{1,n}^3 = \frac{1}{2}(\alpha_n^+ + \alpha_n^-), \quad J_{2,n}^3 = \frac{1}{2}(\alpha_n^+ - \alpha_n^-). \quad (5.74)$$

Then using the actions (5.71) and (5.72) of P_e^{1-} and P_o^{1-} , identified with the one of $P_{0,0}$ and $P_{0,1}$, we deduce the action of \mathcal{S} in the nontrivial case (5.52) where $\sigma = 1/2$

$$\mathcal{S}\mathcal{J}_{1,\ell}^3(z) = \mathcal{J}_{2,\ell}^3\mathcal{S}, \quad \mathcal{S}\mathcal{J}_{2,\ell}^3(z) = \mathcal{J}_{1,\ell}^3\mathcal{S} \quad (5.75)$$

such that, for example, the two point function

$$\omega_\beta(J_{i,\ell}^3(x)J_{j,r}^3(x)) = \langle 0 | \mathcal{J}_{i,\ell}^3(-ix)\mathcal{J}_{j+1,\ell}^3(ix) | 0 \rangle \quad (5.76)$$

where $j+1$ has to be interpreted modulo 2. Hence the scattering operator send a right current to the left one on the other wire, which is nothing but the fully transmitting junction developed in the previous chapter but restricted to the case of two wires. It is then possible to construct the nonequilibrium stationary state, but we won't go further since it has already been done for the WZW permutation brane junction.

5.4 Conclusion

Although promising, the WZW junction with the coset brane leads to a scattering operator that is not known in general, since it involves the explicit expression (generally unknown) for the projectors on components of the coset space decomposition with respect to the diagonal action of the current algebra $\widehat{\mathfrak{g}}$ of the product of basic representations $\otimes_i \widehat{V}_{k,0}$. It was still possible to find such projectors in the simplest case with two wires, $G = SU(2)$ at level 1, but, unfortunately, this reproduced the fully transmitting junction already investigated previously. The scattering operator should, in principle, be calculable for other known models, but only a few have explicit representation for the coset decomposition and mostly only the coset characters are known, which is not enough to compute the projector appearing in the model. A junction with reflection and transmission that was proposed in [20], treating the example of parafermions and involving level 2 representation of $\widehat{\mathfrak{su}}(2)$, suggests that our computation at level 1 might be adaptable to higher levels. Also the case of 3 wires may be treatable. However such extensions would require a non-negligible amount of work.

5.A Character formulae

The affine character of the bosonic Fock space is computed via the Sugawara construction of L_0 from the α_n , and the corresponding spectrum. We end up with the massless free boson character

$$\mathrm{Tr}_{\mathcal{F}_\alpha} e^{2\pi i \tau (L_0 - \frac{1}{24})} e^{iu\alpha_0} = \frac{e^{\pi i \tau \alpha^2 + iu\alpha}}{\eta(\tau)} \quad (5.77)$$

where η is the Dedekind function already occurring in the bosonic junction, see(3.68). On the other hand the character formula for $\widehat{V}_{1,0}$ is given by the Weyl-Kac formula [100] and may be represented for $k = 1$ in the form

$$\mathrm{Tr}_{\widehat{V}_{1,0}} e^{2\pi i \tau (L_0 - \frac{1}{24})} e^{iuJ_0^3} = \frac{\sum_n e^{2\pi i \tau n^2 + iun}}{\eta(\tau)} \quad (5.78)$$

Hence identifying $J_n^3 = \alpha_n/\sqrt{2}$, we get (5.53) which was at the basis of the original works on the vertex operator representation of $\widehat{\mathfrak{su}}(2)$ at level 1.

The isomorphism (5.59) between fermionic and bosonic spaces comes from Jacobi triple product identity [50]

$$\prod_{n=1}^N (1 - x^{2n}) (1 + x^{2n-1}y^2) (1 + x^{2n-1}y^{-2}) = \sum_{n=-\infty}^{+\infty} x^{n^2} y^{2n} \quad (5.79)$$

leading to

$$\mathrm{Tr}_{\mathcal{F}_D} e^{2\pi i \tau (L_0 - \frac{1}{24})} = e^{-\pi i \tau / 12} \left(\prod_{k>0} (1 + e^{2\pi i k}) \right)^2 = \sum_{n \in \mathbb{Z}} \mathrm{Tr}_{\mathcal{F}_n} e^{2\pi i \tau (L_0 - \frac{1}{24})} \quad (5.80)$$

and the affine version also follows easily. The middle term of this equations reflects the decomposition (5.63) since the character for Majorana fermions is

$$\mathrm{Tr}_{\mathcal{F}_M} e^{2\pi i \tau (L_0 - \frac{1/2}{24})} = e^{-\pi i \tau / 24} \prod_{k>0} (1 + e^{2\pi i k}). \quad (5.81)$$

From the Ising model, we have the following formula [50]

$$\mathrm{Tr}_{\widehat{M}_{\frac{1}{2},0}} e^{2\pi i \tau (L_0 - \frac{1}{48})} = \frac{1}{2} \eta(\tau)^{-1/2} (\sqrt{\theta_3(0|\tau)} + \sqrt{\theta_4(0|\tau)}), \quad (5.82)$$

and similarly for $\widehat{M}_{\frac{1}{2},\frac{1}{2}}$ but with a minus sign. The Jacobi theta functions at $z = 0$ are given by

$$\theta_{3/4}(0|\tau) = \prod_{n=1}^{\infty} (1 - e^{2\pi i n}) \prod_{r \in \mathbb{N} + 1/2}^{\infty} (1 \pm e^{2\pi i \tau r})^2 \quad (5.83)$$

leading to (5.67).

Finally the affine characters for $\widehat{V}_{2,0}$ and $\widehat{V}_{2,1}$ follow from the Weyl-Kac character formula [100] and may be found in [118]. They read

$$\begin{aligned} \mathrm{Tr}_{\widehat{V}_{2,0/1}} e^{2\pi i \tau (L_0 - \frac{1}{16})} e^{iuJ_0} &= \frac{1}{2} e^{-\pi i \tau / 24} \left(\prod_{n=1}^{\infty} (1 + e^{2\pi i \tau (n - \frac{1}{2})}) \right) \frac{\sum_{n \in \mathbb{Z}} e^{\pi i \tau n^2 + iun}}{\eta(\tau)} \\ &\quad \pm \frac{1}{2} e^{-\pi i \tau / 24} \left(\prod_{n=1}^{\infty} (1 - e^{2\pi i \tau (n - \frac{1}{2})}) \right) \frac{\sum_{n \in \mathbb{Z}} (-1)^n e^{\pi i \tau n^2 + iun}}{\eta(\tau)}. \end{aligned} \quad (5.84)$$

Chapter 6

Conclusions and open questions

We have described in this part of the thesis three different models of conformal junctions of quantum wires, all based on the same scheme of construction, and, for the first two, studied them under nonequilibrium conditions. Depending on the conformal field theory chosen to describe the bulk of the wires, we found conformal boundary conditions that lead to various models of junctions. The free bosonic case led to a rich class of scattering matrices, allowing for both reflection and transmission at the junction. For the other cases, involving the Wess-Zumino-Witten models, we only managed to describe fully transmitting junctions, either because of the specific choice of boundary condition for the cyclic brane junction, or because this was the only case we managed to solve explicitly for the coset brane junction, although the classical theory indicates that more involved scattering at the latter junctions should occur.

In all the cases treated to the end, we constructed a nonequilibrium stationary state, driven by differences of temperature and electric or chemical potentials, where all the correlation functions were, in principle, calculable, although this was less obvious in the nonabelian case. The common features of the nonequilibrium states obtained are the following: the mean flux of current is linear in the difference of potential, and the mean flux of energy is driven by the differences of potentials and of squared temperatures, and the central charge of the theory appears as a proportionality coefficient for the latter contribution. On the top of that, we computed the full counting statistics of charge and energy transfer associated to a two-time measurement protocol. In the asymptotic large deviations regime, the corresponding probability density is always Gaussian for the charge transfers, whereas it has exponential tails for the energy transfers.

The possible generalizations of each specific model have been already suggested in the respective chapters. The most interesting would be the solution of the model with the coset brane junction for three wires described in the bulk by the $SU(2)$ WZW theory at level 1 or for two wires but at level 2 or higher. The already nontrivial calculation for two wires at level 1 suggests that such a solution may be far from straightforward. Another generalization would be to find another conformal boundary conditions with the difficulty in between the cyclic and the coset branes, but so far we have not found them. The problem of stability of the conformal junctions considered here could be also approached using the conformal field techniques and it was not addressed here.

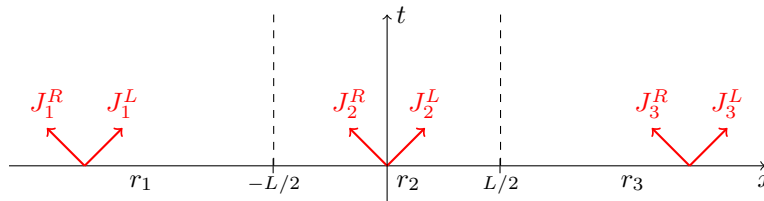


Figure 6.1: *The geometry with a finite wire between two semi-infinite ones.*

Finally, another direction would be to use the previous models but for a different geometry than the star graph configuration of a single junction. Consider for example the geometry of Figure 6.1 of one wire of finite size between two semi-infinite wires that will play the role of reservoirs.

Each wire is described e.g. by a free bosonic field, with Luttinger parameter r_i , and the two junctions at $\pm L/2$ are ruled by two S -matrices with reflection and transmission. When evolving with time, a current in the middle is partially transmitted in one of the reservoirs, and partially reflected, and so on. At asymptotically long time $t \rightarrow \infty$, the contribution from the region between the two reservoirs vanishes and preliminary results suggests that it is possible to compute the current fluxes in the outer wires. A detailed investigation of such a system, or of even more general geometries, seem to be a promising direction for the conformal field theory description of quantum wires in and out of equilibrium.

Part II

Global gauge anomaly in coset models

Chapter 7

Global gauge anomalies

The appearance of anomalies in quantum field theory yields a powerful selection principle in high energy physics: the breaking of a symmetry at the quantum level leads to inconsistent models, constraining the number of relevant theories and can even be used for the prediction of new particles [24]. Among the symmetries, gauge invariance plays a key role in particle physics since it describes the interactions between them. Although two dimensional conformal field theories are not all related to high energy physics, their mathematical coherence is still of crucial importance.

This part of the thesis deals with the question of the consistency of the gauged Wess-Zumino-Witten models that produce a large class of conformal field theories. Anomalies appear here as a breaking of gauge invariance because of nontrivial topological properties of the system. The first chapter summarizes the statements from [83]: the occurrence of global gauge anomalies in coset models and concludes with a no-anomaly condition that has to be satisfied for every consistent model. The second chapter presents the classification work of the anomalous models, testing the condition for a large class of models and based on the classification of Lie algebras and subalgebras. Such classification being rather complicated, we insist on the underlying ideas and techniques instead of giving a complete list of detailed results that can be found in [49].

7.1 Coset models as gauged WZW models

Instead of the algebraic construction proposed in [89, 88] and summarized in Subsection 5.2.1 of Part I, the coset models can be also realized via functional integral approach as gauged Wess-Zumino-Witten models [11, 103, 80, 30]. First, consider a WZW model describing the field

$$g : \Sigma \mapsto G \quad (7.1)$$

where Σ is a surface that, in the Euclidean approach that we adopt here, will be assumed to be compact, oriented, without boundaries and equipped with a complex structure, and G is a compact Lie group that is assumed to be simple, connected but not necessarily simply connected. Hence we write

$$G = \tilde{G}/Z, \quad Z \subset \tilde{Z} \equiv \mathcal{Z}(\tilde{G}), \quad (7.2)$$

where \tilde{G} is the universal covering group of G and $Z \subset \tilde{Z}$ is a subgroup of \tilde{Z} , the center of \tilde{G} (elements that commute with the whole group). Z is isomorphic with the fundamental group $\pi_1(G)$ of G so that non-trivial Z corresponds to non simply connected G .

We start from the Wess-Zumino-Witten action developed in Chapter 4 (except for the change to the Euclidean formalism). The Euclidean action functional is

$$S^E[g] = \frac{k}{4\pi} \int_{\Sigma} \text{tr}(g^{-1} \partial g) \wedge (g^{-1} \bar{\partial} g) + \frac{k}{4\pi} \int_{\tilde{\Sigma}} \tilde{g}^* \chi \equiv S_0^E + S_{\text{WZ}} \quad (7.3)$$

where $\partial = \partial_z dz$, $\bar{\partial} = \partial_{\bar{z}} d\bar{z}$, and tr is the Killing form on \mathfrak{g} normalized as before so that the longest roots have length squared equal to 2. The first (purely imaginary) term describes the nonlinear sigma model action and the second (real) one is the topological Wess-Zumino term where $\tilde{\Sigma}$ is a 3-dimensional manifold with boundary Σ and \tilde{g} is an extension of g to $\tilde{\Sigma}$. As before, χ is the closed 3-form on G given by

$$\chi = \frac{1}{3} \text{tr}(g^{-1} dg)^{\wedge 3}. \quad (7.4)$$

The theory must be independent of the choice of the extension \tilde{g} , at least as far as the Euclidean Feynman amplitudes $e^{iS^E(g)}$ are concerned, and this imposes restrictions on the “level” k , as already mentioned in Section 4.1 (note, that the contribution of the topological Wess-Zumino term to the Euclidean Feynman amplitudes e^{iS^E} is equal to $e^{iS_{\text{WZ}}}$ and coincides with the contribution to the Minkowskian amplitudes e^{iS}). For simply connected group, k has to be an integer, whereas for non-simply connected groups, further restrictions may appear [59] (e.g. k has to be even for $G = SO(3)$). Moreover it happens in some cases that no extension \tilde{g} of g to $\tilde{\Sigma}$ exists, and then the Wess-Zumino action should be defined using other techniques [59, 81], and there appear nonequivalent definitions leading to different theories, see below.

In the Euclidean setup, the classical equations of motions are

$$\partial(g^{-1}\bar{\partial}g) = 0 \quad \Leftrightarrow \quad \bar{\partial}(g\partial g^{-1}) = 0. \quad (7.5)$$

They have non-constant solutions only if we extend the possible values of fields to the complexified group $G^{\mathbb{C}}$. In that case, the general classical solutions have the form $g(z, \bar{z}) = g_{\ell}(z)g_r(\bar{z})$ that is preserved by the following chiral symmetry transformations:

$$g(z, \bar{z}) \mapsto h_{\ell}(z)g(z, \bar{z})h_r^{-1}(\bar{z}), \quad (7.6)$$

where h_{ℓ} (resp. h_r) is any holomorphic (resp. antiholomorphic) map with values in $G^{\mathbb{C}}$.

7.1.1 Gauging the chiral symmetry: local anomalies

We may attempt to render the chiral symmetry entirely local by gauging its rigid version $g(z, \bar{z}) \mapsto h_{\ell}g(z, \bar{z})h_r$ with fixed elements $h_{\ell}, h_r \in G$. Such a gauging of the sigma model term is possible using the minimal coupling. However, as was shown quite early, [51, 174, 63], for the topological term, only the (twisted) adjoint symmetry

$$g(z, \bar{z}) \mapsto h g(z, \bar{z}) \omega(h)^{-1}, \quad (7.7)$$

for ω a group automorphism of G , can be gauged. In the chiral case with general h_{ℓ} and h_r one cannot couple the WZW model to the corresponding gauge fields maintaining the complete infinitesimal gauge invariance. This is the phenomenon of the local gauge anomaly and only the nonchiral case where $h_r = \omega(h_{\ell})$ does not suffer from such problem.

For pedagogical reasons, we focus on the particular case where $\omega = I$, so that (7.7) is nothing but the adjoint action on G (the twisted case will be briefly discussed at the end, see Section 8.4 in the next chapter). The sigma model term $S_0^E[g]$ is then gauged by the minimal coupling to a gauge field A , a $\mathfrak{g}^{\mathbb{C}}$ -valued 1-form on Σ , by replacing $d = \partial_z dz + \partial_{\bar{z}} d\bar{z}$ by its covariant derivative D_A such that

$$g^{-1}dg \mapsto g^{-1}D_A g \equiv g^{-1}dg + [A, g]. \quad (7.8)$$

The resulting gauged sigma-model actions is $S_0^E[g, A]$. The Wess-Zumino term is not naturally given in terms of an integral over Σ so that the minimal prescription is ambiguous. Instead, we add to it the following term [51]

$$S_{\text{gauge}}[g, A] = \frac{k}{4\pi} \int \text{tr}((g^{-1}dg) \wedge A + (dg)g^{-1} \wedge A + g^{-1}Ag \wedge A). \quad (7.9)$$

The total gauged Euclidean Feynman amplitudes

$$e^{iS^E[g,A]} = e^{i(S_0^E[g,A] + S_{\text{WZ}}[g] + S_{\text{gauge}}[g,A])}, \quad (7.10)$$

depending on g and A , are then invariant under the infinitesimal version of the gauge transformations

$$g \mapsto g^h \equiv hgh^{-1}, \quad A \mapsto A^h \equiv hAh^{-1} + h^{-1}dh \quad (7.11)$$

where $h : \Sigma \mapsto G/Z = \tilde{G}/\tilde{Z}$ is a gauge transformation¹. The infinitesimal gauge transformations correspond to $h = e^{i\delta\Lambda}$ for $\delta\Lambda : \Sigma \rightarrow \mathfrak{g}$.

7.1.2 Coset models

In this approach, in order to construct the G/H coset theory, one restricts gauge fields A to \mathfrak{h} -valued 1-forms on Σ , where \mathfrak{h} is the Lie algebra of a closed connected subgroup H of G . Then one considers functional integrals

$$\int \dots e^{iS^E[g,A]} \mathcal{D}g \mathcal{D}A, \quad (7.12)$$

where $\mathcal{D}g$ stands for the formal local product of Haar measures on G and $\mathcal{D}A$ for the formal flat measure of the space of \mathfrak{h} -valued 1-forms. For insertions, one should take gauge invariant quantities, e.g. $\prod_i \text{tr } g(x_i)$ for $x_i \in \Sigma$. Although formal, such functional integrals may be exactly calculated in many cases (e.g. for simply connected G), and it was shown in [80] that they reproduce the coset G/H models constructed by the algebraic GKO construction [89, 88].

As was observed in [83], however, functional integrals (7.12) give a consistent theory only if the corresponding Feynman amplitudes are invariant under all gauge transformations (7.11) with $h : \Sigma \rightarrow H/(H \cap Z) = \tilde{H}/(\tilde{H} \cap \tilde{Z})$, not only under their infinitesimal versions (\tilde{H} denotes here the subgroup of \tilde{G} with Lie algebra \mathfrak{h} and is not necessarily simply connected). Otherwise, destructive interferences appear in (7.12) due to the breaking of gauge invariance leading to an inconsistent theory.

Geometrically, 1-forms A on Σ represent connections on trivial principal bundles over Σ . As was observed in [96], in general, one should also consider topologically nontrivial sectors of the coset theory obtained by coupling the WZW theory to gauge fields representing connections in nontrivial principal bundles. Ref. [83] showed, however, that all possible problems with the lack of gauge invariance arise already in the topologically trivial sector of the coset theories to which we shall limit our discussion.

7.1.3 Global gauge anomalies

The minimal coupling ensures that the sigma model amplitudes $e^{iS_0^E[g,A]}$ are invariant under all gauge transformation (7.11). This might not be the case, however, for the gauged Wess-Zumino amplitudes $e^{iS_{\text{top}}[g,A]} \equiv e^{i(S_{\text{WZ}}[g] + S_{\text{gauge}}[g,A])}$. One can show, see Appendix A of [49], that

$$e^{iS_{\text{top}}[g^h, A^h]} = e^{iS_{\text{top}}[g, A]} \quad \Leftrightarrow \quad \frac{e^{iS_{\text{WZ}}[g^h]}}{e^{iS_{\text{WZ}}[g]} e^{i\alpha[h,g]}} = 1, \quad (7.13)$$

where

$$\alpha[h, g] = \frac{k}{4\pi} \int_{\Sigma} \text{tr}(g^{-1}dg \wedge h^{-1}dh + (dg)g^{-1} \wedge h^{-1}dh + g^{-1}(h^{-1}dh) \wedge gh^{-1}dh). \quad (7.14)$$

¹Elements in the center \tilde{Z} of \tilde{G} have trivial adjoint action and the gauge transformation (7.11) are well defined for h with values in G/Z .

Eq. (7.13) is satisfied for infinitesimal gauge transformations, and, consequently, for all gauged transformations that can be deformed continuously to the unit gauge transformation that maps every point of Σ to the neutral element of G . Such transformations homotopic to unity are called small gauge transformations so that the gauge invariance is always ensured for them. However, large gauge transformations, which are not homotopic to unity, may violate condition (7.13) leading to the global gauge anomaly related to the nontrivial topology of the system, in particular the fact that G is not simply connected (there are no large gauge transformations for simply connected G).

This type of gauge anomaly was already noticed by Witten in [172] in the context of a four dimensional $SU(2)$ gauge theory with chiral fermions, where large gauge transformations also led to inconsistency of the model.

7.2 The no-anomaly condition

In order to investigate more in details the possible failure of gauge invariance in (7.13), we need to specify the Riemann surface Σ and the Lie group G .

7.2.1 Lie algebra classification

We briefly describe the ingredients from the theory of simple Lie algebras [73] that will be useful in the following. Consider the complex version $\mathfrak{g}^{\mathbb{C}}$ of a simple Lie algebra. The Cartan subalgebra $\mathfrak{t}^{\mathbb{C}}$ of $\mathfrak{g}^{\mathbb{C}}$ is defined as the maximal subalgebra of commuting elements. The dimension r of $\mathfrak{t}^{\mathbb{C}}$ is called the rank of $\mathfrak{g}^{\mathbb{C}}$. We then have the canonical decomposition

$$\mathfrak{g}^{\mathbb{C}} = \mathfrak{t}^{\mathbb{C}} \oplus \left(\bigoplus_{\alpha} \mathbb{C} E_{\alpha} \right) \quad (7.15)$$

where the E_{α} are eigenvectors of the adjoint action of $\mathfrak{t}^{\mathbb{C}}$ on $\mathfrak{g}^{\mathbb{C}}$, namely

$$\text{ad}_X E_{\alpha} \equiv [X, E_{\alpha}] = \alpha(X) E_{\alpha}, \quad \text{for} \quad X \in \mathfrak{t}^{\mathbb{C}} \quad (7.16)$$

The previous decomposition exists since all the elements in $\mathfrak{t}^{\mathbb{C}}$ commute and hence the corresponding adjoint actions on $\mathfrak{g}^{\mathbb{C}}$ can be diagonalized simultaneously for all $X \in \mathfrak{t}^{\mathbb{C}}$. The previous equation defines a linear form $\alpha \in (\mathfrak{t}^{\mathbb{C}})^*$, the dual space of $\mathfrak{t}^{\mathbb{C}}$ that can be identified with $\mathfrak{t}^{\mathbb{C}}$ through the Killing form tr normalized as before. We denote by $\alpha^{\vee} = \frac{2\alpha}{\text{tr}\alpha^2} \in \mathfrak{t}^{\mathbb{C}}$ the coroot associated to the root α . The roots α span all $\mathfrak{t}^{\mathbb{C}}$ and if α is a root, then so is $-\alpha$, allowing to split the set of roots into the positives and negative ones. Moreover, among the positive one, a subset of r roots denoted by α_i and called simple roots span all the positive roots with positive integer coefficients. We define the Chevalley-Serre basis for $\mathfrak{g}^{\mathbb{C}}$ as follows: to each simple root $\alpha_i \in (\mathfrak{t}^{\mathbb{C}})^*$ consider the corresponding simple coroot $\alpha_i^{\vee} \in \mathfrak{t}^{\mathbb{C}}$ and the eigenvectors E_i^+ and E_i^- associated to α_i and $-\alpha_i$. Then we have the relations

$$[\alpha_i^{\vee}, \alpha_j^{\vee}] = 0, \quad [\alpha_i^{\vee}, E_j^{\pm}] = \pm A_{ij} E_j^{\pm}, \quad [E_i^+, E_j^-] = \delta_{ij} \alpha_i^{\vee}, \quad \text{and} \quad \left(\text{ad}_{E_i^{\pm}} \right)^{(1-A_{ji})} E_j^{\pm} = 0 \quad (7.17)$$

which, via the Serre construction, are enough to reconstruct the full Lie algebra. This construction requires only the set of simple roots and their scalar products, encoded in the Cartan matrix

$$A_{ij} := 2 \frac{\text{tr} \alpha_i \alpha_j}{\text{tr} \alpha_j \alpha_j} \in \mathbb{Z} \quad (7.18)$$

so that the classification of simple Lie algebras, due to Élie Cartan (1984), is reduced to the combinatorial problem of classifying such Cartan matrices. In 1947, Dynkin proposed a diagrammatic representation of such matrices depicted in Figure 7.1, where each dot of the same color is

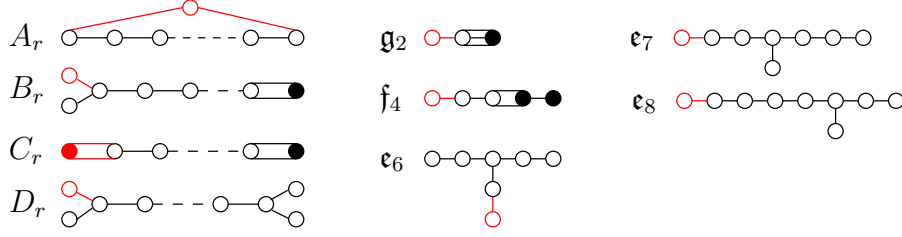


Figure 7.1: Dynkin diagrams of simple Lie algebras (the black part). Each dot is a simple positive root where the empty ones correspond to length 2. The number of link between two roots is the value of their scalar product: 0, -1, -2 or -3. The red part corresponds to the extended diagrams, discussed in Section 8.2 of the next chapter..

a root of same length and the type of the links between the dots indicate the value of the scalar product.

The classification ends up with four infinite series A_r, B_r, C_r and D_r called the classical algebras and five exceptional cases $\mathfrak{g}_2, \mathfrak{f}_4, \mathfrak{e}_6, \mathfrak{e}_7$ and \mathfrak{e}_8 . The above Lie algebras and the corresponding Lie groups will be described in more detail in the next chapter.

7.2.2 Coroots, coweights and center of the group

The center of the Lie group(s) corresponding to Lie algebra $\mathfrak{g}^{\mathbb{C}}$ can be related to the coroots α_i^{\vee} . First consider the set of simple coweights $\lambda_i^{\vee} \in \mathfrak{t}^{\mathbb{C}}$ for $i = 1, \dots, r$ defined by

$$\text{tr}(\lambda_i^{\vee} \alpha_j) = \delta_{ij}. \quad (7.19)$$

This definition ensures that the scalar product of a coroot with a coweight is always an integer number. Then consider the lattices of coroots and coweights

$$Q^{\vee} = \bigoplus_{i=1}^r \mathbb{Z} \alpha_i^{\vee}, \quad P^{\vee} = \bigoplus_{i=1}^r \mathbb{Z} \lambda_i^{\vee} \quad (7.20)$$

generated by the simple coroots and coweights with integral coefficients. Then we have [50]

$$\exp(2\pi i Q^{\vee}) = \{e\}, \quad \exp(2\pi i P^{\vee}) = \tilde{Z} = \mathcal{Z}(\tilde{G}) \quad (7.21)$$

Let $\tilde{G}^{\mathbb{C}}$ be the complex universal covering group associated to Lie algebra $\mathfrak{g}^{\mathbb{C}}$ and let \tilde{G} be its compact form. Both are simply connected and have the same center \tilde{Z} generated by the exponentiation of the coweight lattice, up to any element of the coroots lattice that the exponentiation sends to the neutral element. The center \tilde{Z} is a discrete group, and the other Lie groups having $\mathfrak{g}^{\mathbb{C}}$ as Lie algebra have the form $\tilde{G}^{\mathbb{C}}/Z$, where Z is any subgroup of \tilde{Z} . Their compact forms are $G = \tilde{G}/Z$. Since $\Pi_1(G) \cong Z$, the fundamental group of G becomes related to the coroot lattice of the corresponding Lie algebra $\mathfrak{g}^{\mathbb{C}}$.

7.2.3 Back to the Feynman amplitudes

The ratio on the left of (7.13), that always belongs to $U(1)$ may be easily shown to be constant under continuous deformation of fields (h, g) . It is then enough to compute it for special maps representing the homotopy classes of (h, g) .

Consider the Riemann surface Σ of genus γ with a given homology basis (a_i, b_i) for $i = 1, \dots, \gamma$, see Figure 7.2. The homotopy classes of maps g are in one-to-one correspondence with the elements of $Z^{2\gamma}$ given by the following winding numbers

$$z_{2j-1}(g) = \mathcal{P} \exp \left(\int_{a_j} g^{-1} dg \right), \quad z_{2j}(g) = \mathcal{P} \exp \left(\int_{b_j} g^{-1} dg \right) \quad (7.22)$$

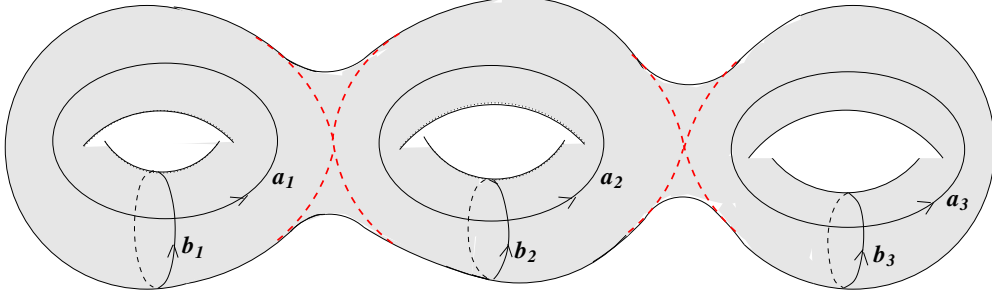


Figure 7.2: A Riemann surface of genus 3 with a marking. The evaluation of the gauge invariance condition can be factorized over each pair a_i, b_i , as if we have pinched and cut the surface along the red dashed lines, obtaining three independent tori.

and similarly for map h , whose homotopy classes are given by their winding numbers that take values in $\tilde{H} \cap \tilde{Z}$. It was shown in [83] that the equation (7.13) can be factorized as a product over tori with homology basis (a_i, b_i) by pinching the Riemann surface as illustrated on Figure 7.2, so that it is enough to restrict Σ to the torus $S^1 \times S^1$. Then, in order to cover the different homotopy classes of h and g defined on $S^1 \times S^1$, it is enough to consider the evaluation of (7.13) for the following maps

$$h(e^{i\sigma_1}, e^{i\sigma_2}) = e^{i\sigma_1 \tilde{M}}, \quad g(e^{i\sigma_1}, e^{i\sigma_2}) = e^{i\sigma_2 M} \quad (7.23)$$

where $\tilde{M}, M \in \mathfrak{t}^\mathbb{C}$ and are such that

$$e^{2\pi i \tilde{M}} \in \tilde{H} \cap \tilde{Z}, \quad e^{2\pi i M} \in Z. \quad (7.24)$$

In particular, M and \tilde{M} belongs to the coweight lattice P^\vee of the Lie algebra $\mathfrak{g}^\mathbb{C}$. The evaluation of (7.13) in that case is simple since we are dealing with commuting elements. The Wess-Zumino amplitudes compensate and we are left with the evaluation of $\alpha(g, h)$. The gauge invariance is finally reduced to the no-anomaly condition

$$\exp[-2\pi i k \operatorname{tr}(M\tilde{M})] = 1 \quad (7.25)$$

and what remains to do is to see in specific models when such condition is always satisfied, ensuring gauge invariance also for large gauge transformations. We shall see that if not, then in many coset models, the above condition restricts the values of possible levels k .

7.2.4 Reduction of the problem

The previous analysis has shown that the necessary and sufficient condition for the absence of global gauge anomalies requires that

$$k \operatorname{tr}(M\tilde{M}) \in \mathbb{Z}, \quad \forall M, \tilde{M} \in P^\vee(\mathfrak{g}), \quad \text{s.t.} \quad e^{2\pi i \tilde{M}} \in \tilde{Z} \cap \tilde{H}, \quad e^{2\pi i M} \in Z. \quad (7.26)$$

In the sequel we shall describe for each Lie algebra \mathfrak{g} the center \tilde{Z} of \tilde{G} and its subgroups Z in terms of coweights of \mathfrak{g} . Then choosing a Lie subalgebra $\mathfrak{h} \subset \mathfrak{g}$, we shall restrict elements \tilde{M} by requiring (7.24) and compute possible values of $k \operatorname{tr}(M\tilde{M})$ in each case. If a non-integer values appear for a given level k then the model will be anomalous.

The classification of anomalies can be reduced by eliminating some cases. First this is enough to check the above condition for \tilde{M} and M in different classes modulo the coroot lattice Q^\vee of G since the scalar product $\operatorname{tr} M\tilde{M}$ is always an integer if M or \tilde{M} belongs to Q^\vee . In particular, if $\tilde{Z} = \{1\}$ and $G = \tilde{G}$ is simply connected, then M is always a coroot and (7.25) is always satisfied. Hence there is no global gauge anomaly if G is simply connected, as already observed.

Note also that the no-anomaly condition for subalgebras related by an automorphism of \mathfrak{g} are identical or simply related, so that we only need to consider subalgebras up to such automorphisms.

Finally suppose that $\mathfrak{h}_1 \subset \mathfrak{h}_2 \subset \mathfrak{g}$ and assume that the model with \mathfrak{h}_2 is not anomalous. Consequently there will be no anomaly also for the model related to \mathfrak{h}_1 since \tilde{M} will be taken in a subset of the ones used to compute condition (7.26) for \mathfrak{h}_2 , already without anomaly. Thus this protection properties eliminates all the anomalies in smaller subalgebras and suggests to start the classification with maximal subalgebras.

Chapter 8

Classification of anomalous models

The no-anomaly condition given in the previous chapter tells us what quantity we need to compute in order to see if a given coset model is anomalous or not. What remains to do is to test such quantity for every known model G/H , and to give a classification of the anomalous (or, equivalently, non-anomalous) cases. In the first step of the classification, we shall use the fact that all simple Lie algebras are known. Thus choosing \mathfrak{g} among them, together with a subgroup $Z \subset \tilde{Z}$ specifies the group G .

A precise description of simple Lie algebras, in particular the simple roots and the coweight lattice, can be found in [29], see also [81]. Except in one case, the center \tilde{Z} of the corresponding Lie group \tilde{G} is cyclic and hence generated by one coweight. M and \tilde{M} are then chosen proportional to it, with supplementary restrictions in order to satisfy (7.24), once Z and the Lie subalgebra $\mathfrak{h} \subset \mathfrak{g}$ are specified. The subgroup $H \subset G$ is then determined by \mathfrak{h} . The levels k leading to anomalous theories will be given by computing the value of $k \operatorname{tr}(M\tilde{M})$, see (7.26). The most complicated point in this strategy is the choice of $\mathfrak{h} \subset \mathfrak{g}$. Here we shall use the classification of the Lie subalgebras of simple Lie algebras, due to Dynkin [55, 54], with few later developments.

8.1 Cases with $\mathfrak{h} = \mathfrak{g}$

As a first step, we shall consider the cases with arbitrary nontrivial subgroups $Z \subset \tilde{Z}$ and $\mathfrak{h} = \mathfrak{g}$, for all simple algebras \mathfrak{g} . This step is also the occasion to give a closer description of the simple algebras¹ associated to the Dynkin diagrams of Figure 7.1.

If there are no global gauge anomalies in that case, then the anomalies are absent also for strict subalgebras $\mathfrak{h} \subsetneq \mathfrak{g}$, according to the protection property discussed in of Subsection 7.2.4. In other words, upon restricting \mathfrak{h} to a smaller subalgebra, the anomalies may only disappear. In this way, a lot of trivial cases can be already treated without specifying \mathfrak{h} .

8.1.1 Case $\mathfrak{g} = A_r = \mathfrak{su}(r+1)$, $r \geq 1$

Lie algebra $\mathfrak{g} = A_r$, corresponding to the group $\tilde{G} = SU(r+1)$, is composed of traceless anti-Hermitian matrices of size $r+1$. Its Cartan subalgebra $\mathfrak{t}_{\mathfrak{g}}$ may be taken as the subalgebra of diagonal traceless matrices with imaginary entries. We define $e_i \in \mathfrak{it}_{\mathfrak{g}}$, $i = 1, \dots, r+1$, as a diagonal matrix with the j 's diagonal entry equal to δ_{ij} , so that $\operatorname{tr}(e_i e_j) = \delta_{ij}$. Roots (viewed as elements of $\mathfrak{it}_{\mathfrak{g}}$) and coroots of $\mathfrak{su}(r+1)$ have then the form $e_i - e_j$ for $i \neq j$ and the standard choice of simple roots is $\alpha_i = e_i - e_{i+1}$, $i = 1 \dots r$.

¹We consider here the compact real forms \mathfrak{g} of $\mathfrak{g}^{\mathbb{C}}$ that are in one-to-one correspondence with $\mathfrak{g}^{\mathbb{C}}$, and, unlike in the other parts of the thesis, use mathematicians' convention for \mathfrak{g} , differing by the imaginary unit from physicists' one.

The center $\tilde{Z} \cong \mathbb{Z}_{r+1}$ may be generated by

$$z = e^{2i\pi\theta} \quad \text{with} \quad \theta = \lambda_r^\vee = \frac{1}{r+1} \sum_{i=1}^{r+1} e_i - e_{r+1} \quad (8.1)$$

where λ_i^\vee denotes the i -th simple coweight satisfying $\text{tr}(\lambda_i^\vee \alpha_j) = \delta_{ij}$. Subgroups Z of \tilde{Z} are of the form $Z \cong \mathbb{Z}_p$ with p dividing $(r+1)$, and may be generated by $z^q = e^{2i\pi q\theta}$ for $r+1 = pq$.

The admissible levels, ensuring that the definition of the Feynman amplitudes $e^{-S_{\text{WZ}}[g]}$ is unambiguous for the WZW model based on group $G = \tilde{G}/\mathbb{Z}_p$ are:

$$k \in 2\mathbb{Z} \quad \text{if } p \text{ even and } q \text{ odd,} \quad \text{and} \quad k \in \mathbb{Z} \quad \text{otherwise,} \quad (8.2)$$

see [59, 81]. It will be convenient to represent M and \tilde{M} in the Euclidean space spanned by vectors e_i . Then

$$M = aq\theta = \left(\frac{a}{p}, \dots, \frac{a}{p}, -\frac{ar}{p} \right), \quad a \in \mathbb{Z}, \quad (8.3)$$

$$\tilde{M} = \tilde{a}\theta = \left(\frac{\tilde{a}}{r+1}, \dots, \frac{\tilde{a}}{r+1}, -\frac{\tilde{a}r}{r+1} \right), \quad \tilde{a} \in \mathbb{Z}, \quad (8.4)$$

where the condition for M in (7.26) is satisfied and $e^{2i\pi\tilde{M}} \in \tilde{Z}$. The global gauge invariance for $\mathfrak{h} = \mathfrak{g}$ is assured if

$$k \text{ tr}(M\tilde{M}) = k \frac{ra\tilde{a}}{p} \in \mathbb{Z}. \quad (8.5)$$

In particular, $k \in p\mathbb{Z}$ is a sufficient condition for the absence of global anomalies. Recall that p divides $r+1$. This implies that p and r are relatively prime. Hence $k \in p\mathbb{Z}$ is also a necessary condition for the absence of the anomalies if there are no further restrictions on the values of \tilde{a} , i.e. if $\mathfrak{h} = \mathfrak{g}$. Taking into account restrictions (8.2), this leads to the first result:

Proposition 8.1. *The coset models corresponding to Lie algebra $\mathfrak{g} = \mathfrak{su}(r+1)$, subgroups $Z \cong \mathbb{Z}_p$, $r+1 = pq$, and arbitrary subalgebras \mathfrak{h} do not have global gauge anomalies if $k \in p\mathbb{Z}$. The models with $\mathfrak{h} = \mathfrak{g}$ and with $k \notin p\mathbb{Z}$ for $p > 1$ odd or q even, or with $k \in 2\mathbb{Z} \setminus p\mathbb{Z}$ for $p > 2$ even and q odd are anomalous.*

Example 8.1

In the case where $r = 2$, $\tilde{G} = SU(3)$ and $\tilde{Z} = \mathbb{Z}_3$. The only nontrivial subgroup is $Z = \tilde{Z}$, with $p = 3$ and $q = 1$, so that every $k \in \mathbb{Z}$ is admissible according to (8.2). However, the coset model where $G = H = SU(3)/\mathbb{Z}_3$ has no anomaly if and only if $k \in 3\mathbb{Z}$, according to Proposition 8.1. It was shown in [83] that for the anomalous level $k = 1$, the coset partition function of the theory is

$$\mathcal{Z}^{G/G} = \frac{1}{3} \quad (8.6)$$

which is supposed to be the dimension of the Hilbert space for a consistent two-dimensional topological field theory and then cannot take a fractional value. This confirms the inconsistency of this G/G model at level one.

8.1.2 Case $\mathfrak{g} = B_r = \mathfrak{so}(2r+1)$, $r \geq 2$

Lie algebra $\mathfrak{g} = B_r$, corresponding to the group $\tilde{G} = Spin(2r+1)$, is composed of real antisymmetric matrices of size $2r+1$. The Cartan algebra $\mathfrak{t}_{\mathfrak{g}}$ may be taken as composed of r blocks

$$\begin{pmatrix} 0 & -t_i \\ t_i & 0 \end{pmatrix} \quad (8.7)$$

placed diagonally, with the last diagonal entry vanishing. Let $e_i \in \mathfrak{it}_{\mathfrak{g}}$ denote the matrix corresponding to $t_j = i\delta_{ij}$. With the normalization such that $\text{tr}(e_i e_j) = \delta_{ij}$, roots of \mathfrak{g} have the form $\pm e_i \pm e_j$ for $i \neq j$ and $\pm e_i$, and one may choose $\alpha_i = e_i - e_{i+1}$ for $i = 1 \dots r-1$ and $\alpha_r = e_r$ as the simple roots.

The center $\tilde{Z} \cong \mathbb{Z}_2$ is generated by $z = e^{2i\pi\theta}$ with $\theta = \lambda_1^\vee = e_1$, and the only nontrivial subgroup of the center is $Z = \tilde{Z}$. If we describe M and \tilde{M} in the Euclidean space spanned by vectors e_i , it is enough to take

$$M = a\theta = (a, 0, \dots, 0), \quad \tilde{M} = \tilde{a}\theta = (\tilde{a}, 0, \dots, 0), \quad a, \tilde{a} \in \mathbb{Z}. \quad (8.8)$$

The global gauge invariance is assured if $k \text{tr}(M\tilde{M}) = ka\tilde{a} \in \mathbb{Z}$ which is always the case leading to

Proposition 8.2. *The coset models corresponding to Lie algebra $\mathfrak{g} = \mathfrak{so}(2r+1)$ and any subalgebra \mathfrak{h} do not have global gauge anomalies.*

8.1.3 Case $\mathfrak{g} = C_r = \mathfrak{sp}(2r)$, $r \geq 3$

Lie algebra $\mathfrak{g} = C_r$, corresponding to the group $\tilde{G} = Sp(2r)$, is composed of antihermitian matrices X of size $2r$ such that ΩX is symmetric, with Ω built of r blocks

$$\omega = \begin{pmatrix} 0 & -1 \\ 1 & 0 \end{pmatrix} \quad (8.9)$$

placed diagonally. The Cartan algebra $\mathfrak{t}_{\mathfrak{g}}$ may be taken as composed of r blocks $t_i \omega$ placed diagonally. Let $e_i \in \mathfrak{it}_{\mathfrak{g}}$ denote the matrix corresponding to $t_j = i\delta_{ij}$. With the normalization $\text{tr}(e_i e_j) = 2\delta_{ij}$, roots of \mathfrak{g} have the form $(1/2)(\pm e_i \pm e_j)$ for $i \neq j$ and $\pm e_i$. The simple roots may be chosen as $\alpha_i = (1/2)(e_i - e_{i+1})$ for $i = 1, \dots, r-1$ and $\alpha_r = e_r$.

The center $\tilde{Z} \cong \mathbb{Z}_2$ is generated by $z = e^{2i\pi\theta}$ with $\theta = \lambda_r^\vee = (1/2)\sum_{i=1}^r e_i$, and its only nontrivial subgroup is $Z = \tilde{Z}$. We then take M and \tilde{M} in the Euclidean space spanned by vectors e_i to have the form

$$M = a\theta = \left(\frac{a}{2}, \dots, \frac{a}{2}\right) \quad \tilde{M} = \tilde{a}\theta = \left(\frac{\tilde{a}}{2}, \dots, \frac{\tilde{a}}{2}\right) \quad a, \tilde{a} \in \mathbb{Z}. \quad (8.10)$$

Taking into account the normalization of tr , we obtain:

$$k \text{tr}(M\tilde{M}) = k \frac{a\tilde{a}r}{2}, \quad (8.11)$$

ensuring the global gauge invariance if it is an integer. The admissible levels k are

$$k \in \mathbb{Z} \quad \text{if } r \text{ is even,} \quad k \in 2\mathbb{Z} \quad \text{if } r \text{ is odd,} \quad (8.12)$$

see [59, 81], so that the above condition is always satisfied leading to

Proposition 8.3. *The coset models corresponding to Lie algebra $\mathfrak{g} = \mathfrak{sp}(2r)$ and any subalgebra \mathfrak{h} do not have global gauge anomalies.*

8.1.4 Case $\mathfrak{g} = D_r = \mathfrak{so}(2r)$, $r \geq 4$

Lie algebra $\mathfrak{g} = D_r$, corresponding to the group $\tilde{G} = Spin(2r)$, is composed of real antisymmetric matrices of size $2r$. The Cartan algebra $\mathfrak{t}_{\mathfrak{g}}$ may be taken as composed of r blocks

$$\omega = \begin{pmatrix} 0 & -t_i \\ t_i & 0 \end{pmatrix} \quad (8.13)$$

placed diagonally. Let us denote by $e_i \in \mathfrak{it}_{\mathfrak{g}}$ the matrix corresponding to $t_j = i\delta_{ij}$. With the normalization $\text{tr}(e_i e_j) = \delta_{ij}$, roots of \mathfrak{g} have the form $\pm e_i \pm e_j$ for $i \neq j$, and the simple roots may be chosen as $\alpha_i = e_i - e_{i+1}$ for $i = 1 \dots r-1$ and $\alpha_r = e_{r-1} + e_r$. The center of the group associated to D_r depends on the parity of r .

Case of r odd. If r is odd, the center $\tilde{Z} \cong \mathbb{Z}_4$ is generated by $z = e^{2i\pi\theta}$ with $\theta = \lambda_r^\vee = (1/2) \sum_{i=1}^r e_i$. The possible nontrivial subgroups are $Z = \tilde{Z}$ and $Z \cong \mathbb{Z}_2$, generated by z^2 . In particular, $Spin(2r)/\mathbb{Z}_2 = SO(2r)$. Taking the general form of M and \tilde{M} in the Euclidean space spanned by vectors e_i ,

$$\begin{aligned} M &= a\theta = \left(\frac{a}{2}, \dots, \frac{a}{2}\right), & a \in \mathbb{Z} \text{ if } Z \cong \mathbb{Z}_4, \\ & & a \in 2\mathbb{Z} \text{ if } Z \cong \mathbb{Z}_2, \\ \tilde{M} &= \tilde{a}\theta = \left(\frac{\tilde{a}}{2}, \dots, \frac{\tilde{a}}{2}\right), & \tilde{a} \in \mathbb{Z}, \end{aligned} \quad (8.14)$$

the admissibility condition for the levels in the corresponding WZW models are:

$$k \in 2\mathbb{Z} \text{ if } Z \cong \mathbb{Z}_4, \quad \text{and} \quad k \in \mathbb{Z} \text{ if } Z \cong \mathbb{Z}_2. \quad (8.15)$$

The global gauge invariance is assured if the quantity

$$k \text{ tr}(M\tilde{M}) = k \frac{a\tilde{a}r}{4}, \quad (8.16)$$

is an integer. The latter holds for $k \in 4\mathbb{Z}$ if $Z \cong \mathbb{Z}_4$ and $k \in 2\mathbb{Z}$ if $Z \cong \mathbb{Z}_2$.

Comparing to the admissibility conditions (8.15), we deduce the following

Proposition 8.4. *The coset models corresponding to Lie algebra $\mathfrak{g} = \mathfrak{so}(2r)$, r odd, and any subalgebra \mathfrak{h} do not have global gauge anomalies for*

$$k \in 4\mathbb{Z} \text{ if } Z \cong \mathbb{Z}_4 \quad \text{and} \quad k \in 2\mathbb{Z} \text{ if } Z \cong \mathbb{Z}_2. \quad (8.17)$$

The models with $\mathfrak{h} = \mathfrak{g}$ and $k \in 2\mathbb{Z}$ with odd $k/2$ for $Z \cong \mathbb{Z}_4$ or with k odd for $Z \cong \mathbb{Z}_2$ are anomalous.

Case of r even. If r is even, the center $\tilde{Z} \cong \mathbb{Z}_2 \times \mathbb{Z}_2$ is generated by $z_1 = e^{2i\pi\theta_1}$ with $\theta_1 = \lambda_r^\vee = (1/2) \sum_{i=1}^r e_i$ and $z_2 = e^{2i\pi\theta_2}$ with $\theta_2 = \lambda_1^\vee = e_1$. The possible nontrivial subgroups are given in Table 8.1. Note that this is the only case of a simple group with a non cyclic center. It turns out that the extension \tilde{g} field g to a surface $\tilde{\Sigma}$ with $\partial\tilde{\Sigma} = \Sigma$, used to define the Wess-Zumino action (7.3), does not always exist in the case $G = Spin(2r)/\mathbb{Z}_2 \times \mathbb{Z}_2$. The Wess-Zumino amplitudes can still be defined and computed using other techniques [59, 81] for admissible levels k , see below, but two nonequivalent WZW theories exist in those cases. However, the anomaly condition is the same for both of them since we focus here only on the untwisted adjoint action where $\omega = I$, but it may depend on the theory in the twisted case, see Section 8.4 and [49].

The general form of M in the Euclidean space spanned by vectors e_i is

$$M = a_1\theta_1 + a_2\theta_2 = \left(\frac{a_1}{2} + a_2, \frac{a_1}{2}, \dots, \frac{a_1}{2}\right), \quad a_1, a_2 \in \mathbb{Z} \quad (8.18)$$

Subgroup Z	Type	Generator(s) z_i
\tilde{Z}	$\mathbb{Z}_2 \times \mathbb{Z}_2$	z_1, z_2
$Z_1 := \mathbb{Z}_2 \times \{1\}$	\mathbb{Z}_2	z_1
$Z_2 := \{1\} \times \mathbb{Z}_2$	\mathbb{Z}_2	z_2
Z_{diag}	\mathbb{Z}_2	$z_1 z_2$

Table 8.1: Subgroups of $\tilde{Z}(\text{Spin}(2r)) \cong \mathbb{Z}_2 \times \mathbb{Z}_2$, r even, and their generators.

and similarly for \tilde{M} with \tilde{a}_1, \tilde{a}_2 . Moreover we have $a_1 = 0$ (resp $a_2 = 0$) if $Z = Z_2$ (resp $Z = Z_1$) and $a_1 = a_2$ if $Z = Z_{\text{diag}}$. The corresponding conditions for admissible levels of the WZW model are :

$$\begin{aligned} k \in \mathbb{Z} & \quad \text{if} \quad \begin{aligned} & r/2 \text{ is even for any } Z, \\ & r/2 \text{ is odd for } Z = Z_2, \end{aligned} \\ k \in 2\mathbb{Z} & \quad \text{if} \quad r/2 \text{ is odd and } Z = \tilde{Z}, Z_1 \text{ or } Z_{\text{diag}}. \end{aligned} \quad (8.19)$$

The global gauge invariance is assured if

$$k \text{ tr}(M\tilde{M}) = k \left(\frac{a_1 \tilde{a}_1 r}{4} + \frac{a_1 \tilde{a}_2}{2} + \frac{a_2 \tilde{a}_1}{2} + a_2 \tilde{a}_2 \right), \quad (8.20)$$

is an integer. This holds for $k \in 2\mathbb{Z}$, whatever the subgroup considered. Comparing to the admissibility conditions (8.19), we deduce the following

Proposition 8.5. *The coset models corresponding to Lie algebra $\mathfrak{g} = \mathfrak{so}(2r)$, r even, and any subalgebra \mathfrak{h} do not have global gauge anomalies if $k \in 2\mathbb{Z}$. The models with $\mathfrak{h} = \mathfrak{g}$ and with k odd for $r/2$ even and any nontrivial Z , or with k odd for $r/2$ odd and $Z = Z_2$, are anomalous.*

8.1.5 Case $\mathfrak{g} = \mathfrak{e}_6$

The imaginary part $\text{it}_{\mathfrak{g}}$ of the complexification of the Cartan subalgebra $\mathfrak{t}_{\mathfrak{g}}$ of $\mathfrak{g} = \mathfrak{e}_6$ may be identified with the subspace of \mathbb{R}^7 orthogonal to the vector $(1, \dots, 1, 0)$, with the scalar product inherited from \mathbb{R}^7 . The simple roots may be taken as $\alpha_i = e_i - e_{i+1}$ for $i = 1 \dots 5$ and $\alpha_6 = (1/2)(-e_1 - e_2 - e_3 + e_4 + e_5 + e_6) + (1/\sqrt{2})e_7$, where e_i are the vectors of the canonical basis of \mathbb{R}^7 .

The center $\tilde{Z} \cong \mathbb{Z}_3$ is generated by $z = e^{2i\pi\theta}$ with $\theta = \lambda_5^\vee = (1/6)(e_1 + e_2 + e_3 + e_4 + e_5 - 5e_6) + (1/\sqrt{2})e_7$. The only nontrivial subgroup is $Z = \tilde{Z}$. The general form of M and \tilde{M} in the Euclidean space spanned by vectors e_i is

$$M = a\theta = \left(\frac{a}{6}, \dots, \frac{a}{6}, \frac{-5a}{6}, \frac{a}{\sqrt{2}} \right), \quad a \in \mathbb{Z}, \quad (8.21)$$

and similarly for \tilde{M} with $\tilde{a} \in \mathbb{Z}$. The global gauge invariance is assured if

$$k \text{ tr}(M\tilde{M}) = k \frac{4a\tilde{a}}{3}, \quad (8.22)$$

is an integer. This holds for $k \in 3\mathbb{Z}$. Since all integer levels $k \in \mathbb{Z}$ are admissible, we deduce

Proposition 8.6. *The coset models corresponding to Lie algebra $\mathfrak{g} = \mathfrak{e}_6$ and arbitrary subalgebra \mathfrak{h} do not have global gauge anomalies if $k \in 3\mathbb{Z}$. The models with $Z = \mathbb{Z}_3$, $\mathfrak{h} = \mathfrak{g}$ and $k \in \mathbb{Z} \setminus 3\mathbb{Z}$ are anomalous.*

8.1.6 Case $\mathfrak{g} = \mathfrak{e}_7$

The imaginary part $\text{it}_{\mathfrak{g}}$ of the complexification of the Cartan subalgebra $\mathfrak{t}_{\mathfrak{g}}$ of $\mathfrak{g} = \mathfrak{e}_7$ may be identified with the subspace of \mathbb{R}^8 orthogonal to the vector $(1, \dots, 1)$ with the simple roots $\alpha_i = e_i - e_{i+1}$ for $i = 1 \dots 6$ and $\alpha_7 = (1/2)(-e_1 - e_2 - e_3 - e_4 + e_5 + e_6 + e_7 + e_8)$, where e_i are the vectors of the canonical basis of \mathbb{R}^8 . The center $\tilde{Z} \cong \mathbb{Z}_2$ is generated by $z = e^{2i\pi\theta}$ with $\theta = \lambda_1^\vee = (1/4)(3, -1, \dots, -1, 3)$.

The only nontrivial subgroup is $Z = \tilde{Z}$. The general form of M and \tilde{M} in the Euclidean space generated by e_i is

$$\begin{aligned} M &= a\theta = \left(\frac{3a}{4}, \frac{-a}{4}, \dots, \frac{-a}{4}, \frac{3a}{4} \right), & a \in \mathbb{Z}, \\ \tilde{M} &= \tilde{a}\theta = \left(\frac{3\tilde{a}}{4}, \frac{-\tilde{a}}{4}, \dots, \frac{-\tilde{a}}{4}, \frac{3\tilde{a}}{4} \right), & \tilde{a} \in \mathbb{Z}. \end{aligned} \quad (8.23)$$

The global gauge invariance is then assured if the quantity

$$k \text{tr}(M\tilde{M}) = k \frac{3a\tilde{a}}{2}, \quad (8.24)$$

is an integer. This holds for $k \in 2\mathbb{Z}$. The condition for admissible levels also requires in this case that $k \in 2\mathbb{Z}$ so that we deduce:

Proposition 8.7. *The coset models corresponding to Lie algebra $\mathfrak{g} = \mathfrak{e}_7$ and any subalgebra \mathfrak{h} do not have global gauge anomalies.*

8.1.7 Cases $\mathfrak{g} = \mathfrak{g}_2$, $\mathfrak{g} = \mathfrak{f}_4$ and $\mathfrak{g} = \mathfrak{e}_8$

The center of the simply connected groups corresponding to Lie algebras $\mathfrak{g} = \mathfrak{g}_2, \mathfrak{f}_4$ or \mathfrak{e}_8 is trivial : $\tilde{Z} \cong \{1\}$ so that there are no nontrivial subgroups Z in that case and we infer:

Proposition 8.8. *The coset models corresponding to Lie algebras $\mathfrak{g} = \mathfrak{g}_2, \mathfrak{f}_4$ or \mathfrak{e}_8 and any subalgebra \mathfrak{h} do not have global gauge anomalies.*

8.1.8 What remains to be done?

The exhaustive treatment of the anomaly condition for $\mathfrak{h} = \mathfrak{g}$ allows a considerable simplification for the case of strict subalgebras $\mathfrak{h} \subsetneq \mathfrak{g}$. Summarizing the results, in the case where $\mathfrak{h} = \mathfrak{g}$, the anomalous models appear only for

- A_r , $Z \cong \mathbb{Z}_p$ with $r+1 = pq$: $k \notin p\mathbb{Z}$ for $p > 1$ odd and q even,
- A_r , $Z \cong \mathbb{Z}_p$ with $r+1 = pq$: $k \in 2\mathbb{Z} \setminus p\mathbb{Z}$ for $p > 2$ even and q odd,
- D_r , r odd, $Z \cong \mathbb{Z}_4$: k even with $k/2$ odd,
- D_r , r odd, $Z \cong \mathbb{Z}_2$: k odd,
- D_r , r even, $r/2$ even, $Z = Z_1, Z_2, Z_{\text{diag}}$ and \tilde{Z} : k odd,
- D_r , r odd, $r/2$ odd, $Z = Z_2$: k odd,
- \mathfrak{e}_6 , $Z \cong \mathbb{Z}_3$: $k \in 3\mathbb{Z}$.

The protection property discussed in Subsection 7.2.4 implies that the anomalous models with a strict subalgebra $\mathfrak{h} \subsetneq \mathfrak{g}$ can only appear in the cases from the above list, and all the other models are non anomalous also for a strict subalgebra. Thus we only focus on the simply laced algebra A_r, D_r and \mathfrak{e}_6 in the following.

8.2 Regular subalgebras

In order to investigate the remaining anomalous models, we need to specify the strict subalgebra $\mathfrak{h} \subsetneq \mathfrak{g}$, that we assume to be semisimple. A classification of semisimple Lie subalgebras of simple Lie algebras was achieved by Dynkin in [55]. The most natural ones are called the regular subalgebras, defined as follows: a Lie subalgebra \mathfrak{h} of an algebra \mathfrak{g} is called regular if, for a choice of the Cartan subalgebra $\mathfrak{t}_{\mathfrak{g}} \subset \mathfrak{g}$ (defined up to conjugation), its complexification is of the form

$$\mathfrak{h}^{\mathbb{C}} = \mathfrak{t}_{\mathfrak{h}}^{\mathbb{C}} \oplus \left(\bigoplus_{\alpha \in \Delta_{\mathfrak{h}} \subset \Delta_{\mathfrak{g}}} \mathbb{C} E_{\alpha} \right) \quad (8.25)$$

where $\mathfrak{t}_{\mathfrak{h}} \subset \mathfrak{t}_{\mathfrak{g}}$ is a Cartan subalgebra of \mathfrak{h} . Subalgebra \mathfrak{h} is semisimple if $\alpha \in \Delta_{\mathfrak{h}}$ implies that $-\alpha \in \Delta_{\mathfrak{h}}$ and if $\alpha \in \Delta_{\mathfrak{h}}$ span $\mathfrak{t}_{\mathfrak{h}}^{\mathbb{C}}$. $\Delta_{\mathfrak{h}}$ is then the set of roots of \mathfrak{h} .

Roughly speaking, a regular subalgebra \mathfrak{h} is constructed by choosing some simple roots among the roots of the ambient algebra and the rest of \mathfrak{h} is then obtained by the Serre construction. Consequently, there is a nice diagrammatic method to obtain all the regular semisimple subalgebras of a given simple algebra (up to conjugation), that was proposed by Dynkin in [55] and summarized in [122]. We briefly describe it here:

1. Take the Dynkin diagram of the ambient algebra \mathfrak{g} , and adjoin to it a node corresponding to the lowest root $\delta = -\phi$ (negative of the highest root ϕ) of \mathfrak{g} , obtaining the extended Dynkin diagram of \mathfrak{g} , see the red part of Figure 7.1 in the previous chapter.
2. Remove arbitrarily one root from this diagram, in order to obtain at most $r + 1$ different diagrams, which may split into orthogonal subdiagrams.
3. Reapply the first two steps to each connected subdiagram obtained above, until no new diagram appears. This way one gets all the regular subalgebras $\mathfrak{h} \subset \mathfrak{g}$ of maximal rank.
4. Remove again an arbitrarily root from each diagram, and apply the full procedure to each connected subdiagram obtained this way (including the last step).

The algorithm stops when no root can be removed, hence one will obtain all the regular subalgebras of \mathfrak{g} . We illustrated some steps in the case where $\mathfrak{g} = \mathfrak{e}_6$ in Figures 8.1 and 8.2.

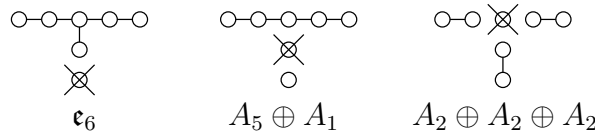


Figure 8.1: Subalgebras of \mathfrak{e}_6 of maximal rank obtained by steps one and two. If one extends again one of the subdiagrams and removes one of the roots, then no new diagram appears.

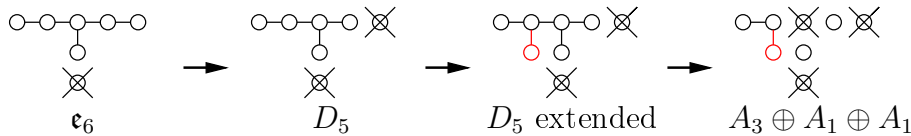


Figure 8.2: Subalgebras of \mathfrak{e}_6 of rank 5 obtained by removing two roots from the initial extended diagram. Repeating the procedure to the subdiagrams generates other subalgebras of rank 5.

8.2.1 Regular semisimple algebras of \mathfrak{e}_6

In this case with fixed rank $r = 6$, one can establish a complete list of regular semisimple subalgebras, and we shall only need the embedding of simple roots in the ambient algebra. The element M and \tilde{M} will be described employing the explicit realization of the coweight and coroot lattices of \mathfrak{e}_6 ,

$$P^\vee(\mathfrak{e}_6) = \left\{ \left(\frac{a}{6} + q_1, \dots, \frac{a}{6} + q_6, \frac{b}{\sqrt{2}} \right) \left| \begin{array}{l} a, b, q_1, \dots, q_6 \in \mathbb{Z} \\ a + q_1 + \dots + q_6 = 0 \\ a + b \in 2\mathbb{Z} \end{array} \right. \right\} \quad (8.26)$$

and the coroot lattice $Q^\vee(\mathfrak{e}_6)$ is defined the same way but adding the condition $a \in 3\mathbb{Z}$. Taking M and \tilde{M} in $P^\vee(\mathfrak{e}_6)$ with the corresponding coefficients, the quantity (8.22) becomes

$$k \operatorname{tr}(M\tilde{M}) = k \frac{a\tilde{a}}{3} + m, \quad \text{with } m \in \mathbb{Z} \quad (8.27)$$

Now, specifying a subalgebra $\mathfrak{h} \subset \mathfrak{e}_6$ and requiring that $e^{2i\pi\tilde{M}} \in \tilde{Z} \cap \tilde{H}$, two possibilities arise: if one can show that $\tilde{a} \in 3\mathbb{Z}$ then the previous quantity is an integer for every $k \in \mathbb{Z}$ and all the corresponding coset models are globally gauge invariant. Otherwise, if there exists an element \tilde{M} such that $\tilde{a} \notin 3\mathbb{Z}$, then we have to require $k \in 3\mathbb{Z}$ to have a globally gauge invariant coset model, and the other coset models are anomalous.

Invoking again the protection property (see 7.2.4), and the fact that the anomaly condition is invariant under automorphisms of the ambient algebra, the problem is reduced to only few cases: we look at the anomalies for subalgebras \mathfrak{h} with decreasing rank and only the ones coming from higher rank diagrams with anomalies, the other ones being protected. Moreover, if we get the same diagrams from two different paths in the algorithm, they are necessarily related by an automorphisms of \mathfrak{g} and it is enough to check the no anomaly condition for one of them. Finally, since $e^{2i\pi\tilde{M}} \in \tilde{Z} \cap \tilde{H}$ if and only if $\tilde{M} \in P^\vee(\mathfrak{g})$ and $\tilde{M} + q^\vee \in \mathfrak{it}_{\mathfrak{h}} \subset \mathfrak{it}_{\mathfrak{g}}$ for some $q^\vee \in Q^\vee(\mathfrak{e}_6)$, it is enough to check the no-anomaly condition (7.26) only for $\tilde{M} \in P^\vee(\mathfrak{g})$ perpendicular to the orthogonal complement $\mathfrak{it}_{\mathfrak{h}}^\perp$ (which is small for high rank) of $\mathfrak{it}_{\mathfrak{h}}$ in $\mathfrak{it}_{\mathfrak{g}}$.

The explicit computation is given in Table 8.1. The subalgebras of rank 6 are not represented because we have $\mathfrak{it}_{\mathfrak{h}}^\perp = \emptyset$, so there is no supplementary condition for \tilde{M} and there are always anomalies if $k \notin 3\mathbb{Z}$. At lower ranks, only subalgebras of rank 5 and 4 have potential anomalies, the ones of even lower ranks being protected by a possible inclusion into non-anomalous subalgebras.

\mathfrak{h}	simple roots of \mathfrak{h}	basis of $\mathfrak{it}_{\mathfrak{h}}^\perp$	\tilde{M}
D_5	$\alpha_1, \alpha_2, \alpha_3, \alpha_4, \alpha_6$	$(1, 1, 1, 1, 1, -5, 3\sqrt{2})$	$\tilde{a} \in 3\mathbb{Z}$
$A_3 \oplus 2A_1$	$\alpha_1, \alpha_2, \alpha_3 \oplus \delta \oplus \alpha_5$	$(1, 1, 1, 1, -2, -2, 0)$	$\tilde{a} \in 3\mathbb{Z}$
$A_4 \oplus A_1$	$\alpha_1, \alpha_2, \alpha_3, \alpha_4 \oplus \delta$	$(1, 1, 1, 1, 1, -5, 0)$	$\tilde{a} \in 3\mathbb{Z}$
A_5	$\alpha_1, \alpha_2, \alpha_3, \alpha_4, \alpha_5$	$(0, 0, 0, 0, 0, 0, 1)$	$\tilde{a} \in 2\mathbb{Z}$
$2A_2 \oplus A_1$	$\alpha_1, \alpha_2 \oplus \alpha_4, \alpha_5 \oplus \alpha_6$	$(1, 1, 1, -1, -1, -1, 3\sqrt{2})$	$\tilde{a} \in \mathbb{Z}$
$2A_2$	$\alpha_1, \alpha_2 \oplus \alpha_4, \alpha_5$	$(1, 1, 1, -1, -1, -1, 0)$ $(0, 0, 0, 0, 0, 0, 1)$	$\tilde{a} \in 2\mathbb{Z}$

Table 8.1: $\mathfrak{it}_{\mathfrak{h}}^\perp$ for the regular subalgebras of \mathfrak{e}_6 of rank 5 and 4 and consequences for \tilde{a} ; the simple roots α_i of \mathfrak{e}_6 and its lowest root δ are used to generate the regular subalgebras [122].

We are thus able to state

Proposition 8.9. *The coset models built with Lie algebra $\mathfrak{g} = \mathfrak{e}_6$ and any regular subalgebra \mathfrak{h} do not have global gauge anomalies for every $k \in \mathbb{Z}$, except for the cases $\mathfrak{h} = \mathfrak{e}_6, A_5 \oplus A_1, 3A_2$, of rank 6, $A_5, 2A_2 \oplus A_1$, of rank 5, and $2A_2$ of rank 4, where the only globally gauge invariant models are those with $k \in 3\mathbb{Z}$.*

8.2.2 Regular semisimple subalgebras of A_r and D_r

The semisimple regular subalgebras of A_r are given in [55] (Chapter II, Table 9) and have the form:

$$\mathfrak{h} = A_{r_1} \oplus \dots \oplus A_{r_m}, \quad r_1 + 1 + \dots + r_m + 1 \leq r + 1 \quad (8.28)$$

that can be easily seen from the extended diagram of A_r (see Figure 7.1) and the previous algorithm. The embedding of \mathfrak{h} in \mathfrak{g} realizing the ideals A_{r_i} as diagonal blocks in the matrices of A_r is unique up to an inner automorphism of A_r . Taking M and \tilde{M} as given in Equations (8.3) and (8.4) we must require that $\tilde{M} + q^\vee \in \text{it}_{\mathfrak{h}}$, for some $q^\vee \in Q^\vee(A_r)$. Looking block by block, we obtain the restrictions requiring that

$$\frac{\tilde{a}(r_i + 1)}{r + 1} \in \mathbb{Z} \quad \forall i = 1, \dots, m \quad \text{and} \quad \frac{\tilde{a}}{r + 1} \in \mathbb{Z} \quad (8.29)$$

if the inequality in (8.28) is strict. The latter condition implies that (8.5) holds eliminating possible global gauge anomalies. We may then limit ourselves to the case when the inequality in (8.28) is saturated. A careful study of the consistency of all these conditions, together with the ones given by (8.2) for the admissible levels, whose details we skip here, leads to the following result [49]:

Proposition 8.10. *The coset models built with Lie algebra $\mathfrak{g} = A_r$, subgroup $Z \cong \mathbb{Z}_p$ for $(r+1) = pq$ and any regular subalgebra $\mathfrak{h} = A_{r_1} \oplus \dots \oplus A_{r_m}$ do not have global gauge anomalies for*

$$\begin{aligned} \bullet \quad r_1 + 1 + \dots + r_m + 1 < r + 1 \quad & k \in \begin{cases} 2\mathbb{Z} \text{ if } p \text{ even and } q \text{ odd,} \\ \mathbb{Z} \text{ otherwise} \end{cases}, \\ \bullet \quad r_1 + 1 + \dots + r_m + 1 = r + 1 \quad & k \in \begin{cases} \frac{l}{q \wedge l} \mathbb{Z} \cap 2\mathbb{Z} \text{ if } p \text{ even and } q \text{ odd,} \\ \frac{l}{q \wedge l} \mathbb{Z} \text{ otherwise} \end{cases}, \end{aligned}$$

where $l = (r_1 + 1) \wedge \dots \wedge (r_m + 1)$. The other models with admissible levels are anomalous.

Example 8.2

$\mathfrak{g} = A_4 = \mathfrak{su}(5)$: the center $\tilde{Z} \cong \mathbb{Z}_5$ of the corresponding group has only one nontrivial subgroup, $Z = \tilde{Z}$, so with $p = 5$ odd and $q = 1$ odd in the previous notations. The admissible levels are $k \in \mathbb{Z}$, according to (8.2).

Following Proposition 8.1, the regular subalgebra $\mathfrak{h} = \mathfrak{g}$ leads to the condition $k \in 5\mathbb{Z}$ for non-anomalous models. Then, applying the last proposition above, the cases

$$\mathfrak{h} = A_1, A_1 \oplus A_1 \equiv 2A_1, A_2 \text{ and } A_3 \quad (8.30)$$

lead to non-anomalous models for every $k \in \mathbb{Z}$, because here we have $r_1 + 1 + \dots + r_m + 1 < r + 1 = 5$. For

$$\mathfrak{h} = A_2 \oplus A_1 \quad (8.31)$$

we have an equality. However, $l = (r_1 + 1) \wedge (r_2 + 1) = 3 \wedge 2 = 1$, so $l/(l \wedge q) = 1$ and the model has no anomalies for every $k \in \mathbb{Z}$. Consequently, the only anomalous models corresponding to $\mathfrak{g} = A_4$ and \mathfrak{h} regular are those with $\mathfrak{h} = \mathfrak{g}$, $Z = \tilde{Z}$ and $k \in \mathbb{Z} \setminus 5\mathbb{Z}$.

We see from the previous proposition that the nonanomalous models can be completely classified but that the conditions involve several cases that become somewhat complicated. Hence from now we shall not attempt to provide an exhaustive description of the classification since the

results are rather awkward to express. In the case of D_r , the semisimple regular subalgebras of D_r are given in [55] (Chapter II, Table 9) and have the form:

$$\mathfrak{h} = A_{r_1} \oplus \dots \oplus A_{r_m} \oplus D_{s_1} \oplus \dots \oplus D_{s_n} \quad (8.32)$$

where $r_1 + 1 + \dots + r_m + 1 + s_1 + \dots + s_n \leq r$. The same work can be done that for A_r , however we have to distinguish the case where r is odd or even as in the case $\mathfrak{h} = \mathfrak{g}$, and the possible subalgebras will be different. Moreover it happens in that case that \mathfrak{h} may have different nonequivalent embeddings in \mathfrak{g} that we have to be distinguished. One ends up with a full list of anomalous models taking into account all the different cases that appear. The result can be found in [49].

Since the other algebras lead to nonanomalous models already for $\mathfrak{h} = \mathfrak{g}$, this completes the classification for the semisimple regular subalgebras.

8.3 Nonregular subalgebras

The regular subalgebras are not the only possible Lie subalgebras for a given ambient Lie algebra. We can use them, however, to classify all the remaining ones. Let \mathfrak{h} be a semisimple subalgebra of \mathfrak{g} , and consider

$$\mathcal{R}(\mathfrak{h}) = \min_{\mathfrak{m}} \{ \mathfrak{m} \subset \mathfrak{g} \mid \mathfrak{h} \subset \mathfrak{m} \subset \mathfrak{g} \text{ and } \mathfrak{m} \text{ regular} \} \quad (8.33)$$

i.e. a minimal regular subalgebra of \mathfrak{g} containing \mathfrak{h} (up to conjugation). If $\mathcal{R}(\mathfrak{h}) = \mathfrak{g}$, then \mathfrak{h} is called an S-subalgebra. Otherwise, it is called an R-subalgebra, and consequently \mathfrak{h} is an S-subalgebra of $\mathcal{R}(\mathfrak{h})$.

For the exceptional simple algebras, the classification of R- and S-subalgebras has been achieved by Dynkin in [55]. The case of other simple algebras was discussed in [54] with less explicit results. Contrary to the regular subalgebras, where the embedding was obvious through the identification of the simple roots of \mathfrak{h} among those of \mathfrak{g} , the nonregular subalgebras are, by definition, embedded in a different way. In this case we need to know the embedding

$$\iota : \mathfrak{h} \rightarrow \mathfrak{g}. \quad (8.34)$$

Recall the compatibility condition for \tilde{M} in the anomaly problem

$$e^{2i\pi\tilde{M}} \in \tilde{H} \cap \tilde{Z} \subseteq \mathcal{Z}(\tilde{H}), \quad (8.35)$$

where $\mathcal{Z}(\tilde{H})$ is generated by exponentiation of one (eventually two if it is not cyclic) coweight $\lambda^\vee \in \mathfrak{h}$. Since $\exp 2i\pi\tilde{M}$ also belongs to \tilde{Z} the center of \tilde{G} , then the anomaly condition

$$k \operatorname{tr} M \tilde{M} \in \mathbb{Z} \quad (8.36)$$

must be checked for \tilde{M} that is proportional to λ^\vee and also belongs to the coweight lattice $P^\vee(\mathfrak{g})$ of the ambient algebra. Consequently three possibilities occur

1. If $\iota(\lambda^\vee) \notin P^\vee(\mathfrak{g})$ then $\tilde{Z} \cap \tilde{H} = \{1\}$ and \tilde{M} is a coroot of \mathfrak{g} , so the quantity (8.36) is always an integer and there are no anomalies for this model.
2. If $\iota(\lambda^\vee) \in Q^\vee(\mathfrak{g})$ then \tilde{M} is still only a coroot of \mathfrak{g} , and there are no anomalies too.
3. If $\iota(\lambda^\vee) \in P^\vee(\mathfrak{g}) \setminus Q^\vee(\mathfrak{g})$ then anomalies are possible and we have to check that the quantity (8.36) is an integer for $\tilde{M} = \iota(\lambda^\vee)$.

Thus the classification is reduced to the knowledge of such explicit embedding. It is then possible to compute the anomalous model for all the nonregular subalgebra of \mathfrak{e}_6 . For A_r and D_r the nonregular subalgebras can be constructed for a given fixed rank $r = r_0$ (this was actually done in [122] up to rank 6) but there is no general formula for any r such as in the regular case. In the following, we sum up the exhaustive results obtained for \mathfrak{e}_6 and discuss the other cases on a small rank example.

8.3.1 Nonregular subalgebras of \mathfrak{e}_6

The semi-simple S -subalgebras of \mathfrak{e}_6 (simple and semisimple) are given in Figure 8.1 with their inclusion relations and the explicit embedding is given in [55]. Applying the previous reasoning to each of them leads to only one anomalous case : $\mathfrak{h} = \mathfrak{g}_2 \oplus A_2$ for $k \in \mathbb{Z} \setminus 3\mathbb{Z}$, and all the other cases have no anomalies.

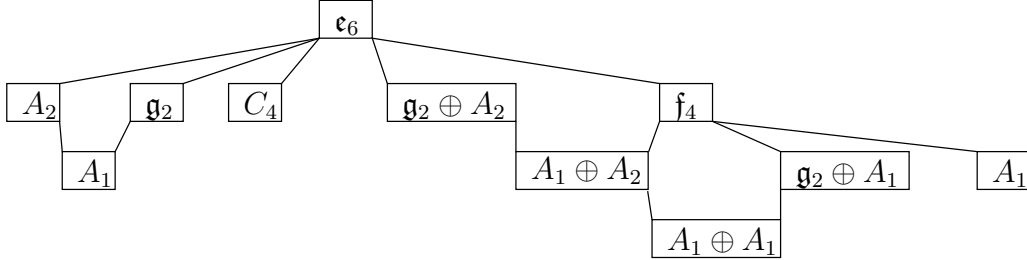


Figure 8.1: Simple and semisimple S -subalgebra of \mathfrak{e}_6 and their inclusion relations.

There exist a lot of semisimple R -subalgebras of \mathfrak{e}_6 , but again we use the protection property: since $\mathfrak{h} \subset \mathcal{R}(\mathfrak{h})$, anomalies can only occur when $\mathcal{R}(\mathfrak{h})$ corresponds to an anomalous case. This has been already treated previously since $\mathcal{R}(\mathfrak{h})$ is regular, hence only a few cases survive, namely $\mathcal{R}(\mathfrak{h}) = 2A_2, 3A_2, A_5$. Moreover such algebras can be seen as S -subalgebras in $\mathcal{R}(\mathfrak{h})$ instead of R -subalgebras in \mathfrak{e}_6 . The embedding can be found in [122, 125] since S -subalgebras of classical algebras of small rank have been classified. All the computations can be found in [49]. They led to several anomalous cases that we do not list here. We just point to one the particular case where $\mathfrak{h} = A_2$ and $\mathcal{R}(\mathfrak{h}) = A_2 \oplus A_2$ and where two nonequivalent embeddings appear. Denoting by $\tilde{\alpha}_1^\vee$ and $\tilde{\alpha}_2^\vee$ the simple coroots of A_2 , we have

$$\iota_1(\tilde{\alpha}_1^\vee) = \alpha_1^\vee + \alpha_5^\vee \quad \iota_2(\tilde{\alpha}_1^\vee) = \alpha_1^\vee + \alpha_4^\vee \quad (8.37)$$

$$\iota_1(\tilde{\alpha}_2^\vee) = \alpha_2^\vee + \alpha_4^\vee \quad \iota_2(\tilde{\alpha}_2^\vee) = \alpha_2^\vee + \alpha_5^\vee \quad (8.38)$$

where we have exchanged α_4^\vee and α_5^\vee . The other possible exchanges are equivalent to ι_1 or ι_2 [125]. It turns out that the embedding ι_1 leads to nonanomalous model for any $k \in \mathbb{Z}$ whereas ι_2 gives an anomalous models for $k \in \mathbb{Z} \setminus 3\mathbb{Z}$. This concludes our description of the anomaly problem for $\mathfrak{g} = \mathfrak{e}_6$, where a complete classification has been obtained for arbitrary semisimple subalgebras $\mathfrak{h} \subset \mathfrak{e}_6$ [49].

8.3.2 Nonregular subalgebras of A_r and D_r

The same work can be done for A_r or D_r , but only at a fixed rank: there is no general theorem giving all the nonregular subalgebras for any rank r , but such subalgebras may still be constructed when considering specific cases of low rank. This was done in [122] for semisimple subalgebras of simple algebras up to rank 6, and there is no technical difficulty to go further. Consequently the classification is reduced to the same problem: no theorem can be given for the anomalous models of any rank r , however the method works if we consider specific algebras.

Example 8.3

$\mathfrak{g} = A_4$: The coroot lattice is given by

$$P^\vee(A_4) = \left\{ \left(\frac{a}{5} + q_1, \dots, \frac{a}{5} + q_4, -\frac{4a}{5} - q_1 - \dots - q_4 \right) \mid a, q_1, \dots, q_4 \in \mathbb{Z} \right\} \quad (8.39)$$

and the coweight lattice $Q^\vee(A_4)$ is given by the same formula but with $a = 0$. According to [122], A_4 admits two S -subalgebras which are simple : A_1 and B_2 . For $\mathfrak{h} = A_1$, the embedding

of the generating element λ^\vee of the center of the corresponding group is given by

$$\iota(\lambda^\vee) = (2, 1, 0, -1, -2) \in Q^\vee(A_4) \quad (8.40)$$

so the quantity $k \operatorname{tr}(M\tilde{M})$ will be integral for every $k \in \mathbb{Z}$ and there will be no anomaly for this model. For $\mathfrak{h} = B_2$, one have

$$\iota(\lambda^\vee) = (1, 0, 0, 0, -1) \in Q^\vee(A_4) \quad (8.41)$$

which leads to the same conclusion. Recall from our previous discussion that all regular subalgebras of A_4 (except A_4 itself) lead to non-anomalous models. We immediately conclude that all the S -subalgebras of A_4 are protected by their regular $\mathcal{R}(\mathfrak{h})$, so there is also no anomaly for these models. Finally, the only anomalous models corresponding to $\mathfrak{g} = A_4$ and an arbitrary semisimple subalgebra \mathfrak{h} are those with $\mathfrak{h} = \mathfrak{g}$, $Z = \tilde{Z} \cong Z_5$ and $k \in \mathbb{Z} \setminus 5\mathbb{Z}$.

8.4 Twisted case

The twisted adjoint action (7.7) can also be gauged for ω an automorphism of \mathfrak{g} . By the minimal coupling on the sigma model term S_0 and adding an appropriate coupling term to S_{WZ} , we obtain the gauged action functional. The gauge transformations are described by the maps

$$h : \Sigma \rightarrow \tilde{H}/(\tilde{Z}^\omega \cap \tilde{H}), \quad \text{where} \quad \tilde{Z}^\omega = \{z \in \tilde{Z} \mid z\omega(z)^{-1} \in Z\} \quad (8.42)$$

is the subgroups of elements in \tilde{Z} that acts trivially on G . The gauged action is invariant under the local gauge transformations homotopic to unity, but the global gauge invariance requires (7.13) to be satisfied with

$$\alpha(h, g) = \frac{k}{4\pi} \int_{\Sigma} \operatorname{tr}(g^{-1}dg \wedge \omega(h^{-1}dh) + (dg)g^{-1} \wedge h^{-1}dh + g^{-1}(h^{-1}dh)g \wedge \omega(h^{-1}dh)). \quad (8.43)$$

As in the previous chapter, the problem can be reduced to the torus $\Sigma = S^1 \times S^1$ and g and h as in (7.23) with

$$\tilde{z} \equiv e^{2\pi i \tilde{M}} \in \tilde{H} \cap Z^\omega \quad \text{and} \quad z \equiv e^{2\pi i M} \in Z. \quad (8.44)$$

In particular M and \tilde{M} also belongs to the coweight lattice $P^\vee(\mathfrak{g})$ of the ambient algebra. The no anomaly condition (7.25) becomes in that case

$$c(\tilde{z}\omega(\tilde{z})^{-1}, z) \exp[-2\pi i k \operatorname{tr}(M\omega(\tilde{M}))] = 1, \quad (8.45)$$

where $c : Z^2 \rightarrow U(1)$ is a k -dependent bihomomorphism whose explicit form can be extracted from Appendix 2 of [59]. If ω is an inner automorphism then the twisted adjoint action may be reduced to the untwisted one by conjugating it with a right translation on G that is a rigid symmetry of the theory. Hence we consider only outer automorphism, modulo the inner one. Such classes are generated by automorphisms that preserve the set of simple roots of \mathfrak{g} , inducing a symmetry of the Dynkin diagram. Looking at Figure 7.1 (non-extended part only), we see that only the Dynkin diagrams of A_r , D_r and \mathfrak{e}_6 have symmetries, so that nontrivial twisted models appear only in such cases. The diagram symmetry group is always \mathbb{Z}_2 , so that there is only one nontrivial twisted model, except for D_4 where the symmetry group becomes the permutation group S_3 , see Figure 8.1

As in the untwisted case we take M and \tilde{M} in the coweight lattice of \mathfrak{g} , restrict them in order to satisfy (8.44) and compute the quantity (8.45) first in the case where $\mathfrak{h} = \mathfrak{g}$. It turns out that the twisted coset models with A_r and \mathfrak{e}_6 have no anomalies in that case and consequently for any

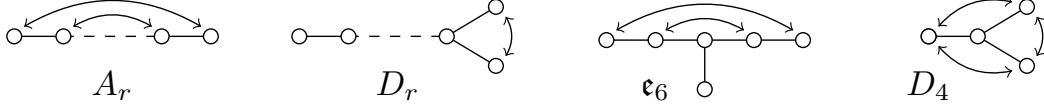


Figure 8.1: Nontrivial symmetry group of the Dynkin diagrams: always \mathbb{Z}_2 except for the case of D_4 where it is S_3 .

subalgebra \mathfrak{h} . Anomalies appear only for $\mathfrak{g} = D_r$ where a lot of cases must be distinguished. We sum up the results and refer to [49] for the details.

First for r odd, the anomalies are absent for twisted models for any subalgebra \mathfrak{h} . Then for $r > 4$ even, anomalies appear for $\mathfrak{h} = \mathfrak{g}$, depending on the subgroup Z considered. Moreover if $Z = \tilde{Z} = \mathbb{Z}_2 \times \mathbb{Z}_2$, two nonequivalent WZW theories exist and the no-anomaly condition (8.45) explicitly depends on the choice of a particular one through bihomomorphism c . It turns out that one of the theories leads to anomalous models whereas the other one does not. The case where $r = 4$ is particular since the diagram has the S_3 permutation group symmetry so that there are many different twisted models. Some models are anomalous and some other are not, and the nonequivalent WZW theories are also different with respect to the anomaly condition. Finally, a complete classification of the remaining anomalous models is done for $\mathfrak{g} = D_r$ and \mathfrak{h} any regular subalgebra, with the same arguments that the ones used in the untwisted case.

8.5 Conclusions

Global gauge anomalies appear in the context of coset models built as gauged Wess-Zumino-Witten models and correspond to a symmetry breaking under large gauge transformations that are not homotopic to unity. They may occur only in models with non simply connected target groups and arise as forbidden values for the level k that lead to inconsistent theories. The work described in this part of the thesis led to the classification of those forbidden levels for a coset model G/H , based on the classification of simple Lie algebras for \mathfrak{g} and their semisimple Lie subalgebra \mathfrak{h} . The classification obtained in the end was almost exhaustive: we obtained the explicit conditions for the absence of global gauge anomalies for any semisimple Lie algebra of any simple Lie algebra, except in the case of classical Lie algebras A_r and D_r , where the subalgebras were restricted to the regular case, except for low ranks. The anomalies appear only for A_r , D_r and \mathfrak{e}_6 in the untwisted case, and only for D_r in the twisted one.

There are several possible directions to generalize the global gauge anomalies to other systems. The first one would be to consider a different group target. Here we completely omitted the Abelian ideals since we focused on simple Lie algebras, but a particular symmetry called T-duality appears for WZW models with Abelian torus as group target, and the study of global gauge anomaly for T-dual models should be an interesting direction. Another natural generalization would be to study such anomaly for supersymmetric coset models. On the other hand one can also consider a more general worldsheet than a closed one. For example the global gauge anomalies for a worldsheet with a class of defects were already investigated in detail in [84]. The case of a worldsheet with boundaries was not treated in the complete generality, however, but the next part of the present manuscript may be seen as providing a particular example of a boundary gauge anomaly in the context of topological insulators.

Part III

Topological insulators with time reversal invariance

Chapter 9

Topological insulators

Topological insulators are, as quantum wires, devices where theory and experiment meet very nicely. Their main property is, that although insulators in the bulk, they support massless modes localized at the boundary that carry currents topologically protected against disorder or sufficiently weak perturbations. In this chapter we review the well-known facts about topological insulators, introducing step by step the different notions needed in the next chapters to define a geometric invariant for the time-reversal invariant two dimensional insulators.

9.1 Chern insulators

9.1.1 The quantum Hall effect

A century after the classical experiment of Hall, exhibiting the so-called Hall effect, von Klitzing and collaborators observed its quantum version: at very low temperature the Hall conductivity is quantized as an integer multiple of a universal constant [109]. This is the integer quantum Hall effect.

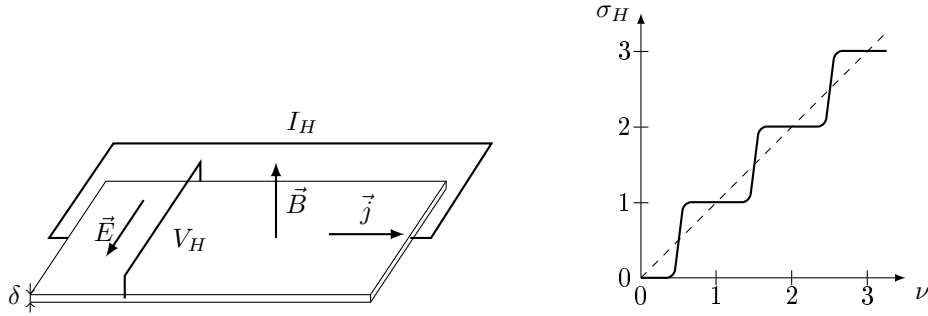


Figure 9.1: Schematic representation of the quantum Hall effect experiment and the corresponding observations. The Hall conductivity is quantized in plateaux instead of the linear classical effect (dashed line).

Consider a two-dimensional conductor placed in an intense transverse magnetic field \vec{B} , see Figure 9.1, and apply an electric field \vec{E} in the plane of the conductor via a difference of potential V_H . Because of the Lorentz force, the electrons move then in the direction perpendicular to \vec{E} , and the corresponding current I can be measured. It was observed that the corresponding Hall conductance is quantized

$$\sigma_H \equiv \frac{I}{V_H} = \frac{e^2}{h} n \quad \text{with} \quad n \in \mathbb{Z}, \quad (9.1)$$

where e is the electron charge and h is Planck's constant. On Figure 9.1 is plotted the evolution of σ_H with respect to the filling factor $\nu = h\rho\delta/Be$, where the product $\rho\delta$ is the carrier density per unit area. Instead of being proportional to it, as in the classical regime, σ_H increase by plateaux, and its value is an integer multiple of the universal constant $e^2/h \equiv 1/R_H$. Historically the motivation was to propose a very accurate measurement of the Hall resistance R_H , and it became the new standard of resistance in 1990 [161]. The theoretical understanding of such plateaux started the study of topological insulators.

Considering a gas of free electrons in a circular geometry with transverse magnetic field, Laughlin interpreted the quantization of the Hall conductance as a consequence of gauge invariance [117]: the consistence of wave functions along loops is ensured only for quantized vector potential, leading to relation (9.1). On the other hand, Thouless, Kohmoto, Nightingale and den Nijs proposed a model of free electrons on a lattice in a tight binding approximation with a transverse magnetic field [163]. Using the Kubo formula from linear response theory, they showed that the transverse conductivity (the local current response to an electric field) was quantized as in (9.1). Moreover such conductivity was related to a geometrical quantity associated to the projector on all the states below the Fermi level, the Chern number. On top of that Avron, Seiler and Simon showed in [9] that the quantum number obtained this way was the same for two homotopic systems, where one Hamiltonian could be deformed continuously to the other one. As long as the gap does not close, the conductivity is the same, leading to the idea of a topological number associated to the system.

Besides, it was argued in all those works that such topological invariant should persist in presence of perturbations such as interactions or disorder, since they only induce small deformations of the system. In the quantum Hall case, it turns out that disorder is actually necessary to define a fully rigorous mathematical invariant. This was done by Bellissard, van Elst and Schulz-Baldes in [15] in the context of noncommutative geometry.

9.1.2 Band insulators

Leaving the quantum Hall system that is somewhat specific, we now consider electrons on a d -dimensional crystal in a tight-binding approach. Neglecting interactions, the system is described by a one-particle Hamiltonian H , acting on a Hilbert space \mathcal{H} . Assume the invariance under crystalline lattice translations in all directions. The Bloch theorem states for such a system that the eigenstates of H are wave functions indexed by the quasi-momenta k [27, 71]. Nonequivalent k are restricted to the first Brillouin zone of the lattice, which has the topology of a d -dimensional torus \mathbb{T}^d since quasi-momenta are defined up to vectors in the reciprocal lattice. Hence we have

$$\mathcal{H} = \int_{k \in \mathbb{T}^d}^{\oplus} \mathcal{H}_k, \quad \text{with} \quad \mathcal{H}_k \cong \mathbb{C}^N, \quad (9.2)$$

where N counts the internal degrees of freedom of the electrons such as spin, orbitals or nonequivalent lattice sites. Hamiltonian H is partially diagonalized by such decomposition acting for each k as a Bloch Hamiltonian $H(k)$ in \mathcal{H}_k so that

$$H(k)\psi_\alpha(k) = E_\alpha(k)\psi_\alpha(k) \quad \text{for} \quad k \in \mathbb{T}^d \quad \text{and} \quad \alpha = 1, \dots, N. \quad (9.3)$$

As k goes along the Brillouin torus, real eigenvalues $E_\alpha(k)$ describe the so-called energy bands, see Figure 9.2, that in the ground state of the 2nd quantized theory, are progressively filled with available electrons in virtue of Pauli principle, in a way that minimizes the total energy. The crystal is called an insulator when there exists a gap separating the empty bands from the ones containing the filled states, called the valence bands. When the chemical potential lies in the gap, no electronic state is accessible to a small perturbation such as electric field and hence there is no

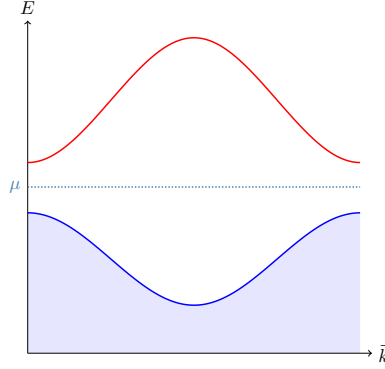


Figure 9.2: Typical dispersion relation over the Brillouin zone \mathbb{T}^d for an insulator. Conduction (red) and valence (blue) band are separated by a gap such that there is no accessible state to ensure conduction. A well defined gap is necessary for the definition of the topological invariants in the following.

current in that case. In the absence of such a gap, i.e. when the chemical potential cuts across the bands, the current can flow and the system is a conductor.

The eigenstates $\psi_\alpha(k)$ describe for each k a basis of \mathcal{H}_k . It turns out that one can always choose a family of bases $(\psi_\alpha(k))$ of \mathcal{H}_k (but not necessarily composed of eigenstates of $H(k)$) in a continuous way globally over \mathbb{T}^d , or, saying differently, the full Hilbert space may be viewed as a trivial fiber bundle over the Brillouin torus [158, 136], namely

$$\mathcal{H} \cong \mathbb{T}^d \times \mathbb{C}^N \quad (9.4)$$

However, in the case of an insulator the valence bands are well defined and describe its ground state properties since they contain all the filled single particle eigenstates. The nontrivial topology of the system is actually encoded in the valence bundle: the fiber bundle¹ over the Brillouin torus \mathbb{T}^d with fiber generated by the eigenstates of the valence bands only. Nontriviality of such a bundle would mean that we cannot choose a family of bases of such subspaces of \mathcal{H}_k in a continuous way over the whole of \mathbb{T}^d . In that case, the original system could not be deformed continuously to a one with a trivial valence bundle without closing the gap.

9.1.3 Chern number

Consider two-dimensional systems for a while, $d = 2$. The valence bundle can be seen as a subbundle of the trivial one (9.4) obtained by applying a family $P(k)$ for $k \in \mathbb{T}^d$ of orthogonal projectors in \mathbb{C}^N on the the subspaces of states spanned by the valence bands eigenstates.

In the theory of vector bundles over 2-dimensional compact spaces, (the torus \mathbb{T}^2 in our case), the simplest invariant associated to topological properties is the first Chern number C_1 [132]. There are several ways to compute it, but in the case of a projected subbundle of a trivial bundle, the formula reads

$$C_1 = \frac{i}{2\pi} \int_{\mathbb{T}^2} \text{tr}(P dP \wedge dP). \quad (9.5)$$

This integer is a topological invariant and will be the same for two homotopic systems, but different for those that cannot be deformed continuously one to the other without closing the gap. This way C_1 captures a ground state property of an insulator that is related to its nontrivial topology.

The Chern number can also be interpreted in terms of the so called Berry connection. The valence bundle is described by local sections $\psi_\alpha(k)$ up to a unitary transformations $U \in U(M)$

¹We recommend [10, 132] for a good introduction to the theory of fiber bundles in a physical context.

where M is the dimension of the valence fiber. Such freedom can be interpreted as gauge invariance, and is associated to a nontrivial connection, called Berry connection. The Chern number (9.5) is actually nothing but the integral of the corresponding Berry curvature over the Brillouin zone, given here by the 2-form $i \text{tr}(P dP \wedge dP)$ over \mathbb{T}^2 . For $M = 1$ such gauge invariance is just a $U(1)$ phase (the Berry phase), and a non vanishing Chern number corresponds to an obstruction in defining a global phase reference for the wave function ψ_1 over \mathbb{T}^2 .

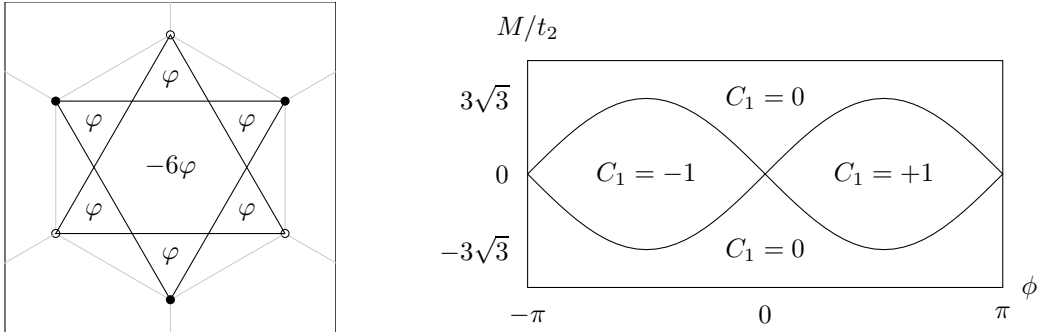
Example 9.1

The Haldane model:

It was realized by Haldane in [92] that for two-dimensional insulators a magnetic field was not necessary to produce models with non zero Chern numbers, but only the breaking of time-reversal symmetry. He then proposed a model of free spinless electrons on a honeycomb lattice with a local magnetic flux but a vanishing global magnetic field. The Hamiltonian consist in first and second nearest-neighbor hopping

$$H = t_1 \sum_{\langle i,j \rangle} \langle i | j \rangle + t_2 e^{i\phi} \sum_{\langle\langle i,j \rangle\rangle} \langle i | j \rangle + M \left(\sum_{i \in A} \langle i | i \rangle - \sum_{j \in B} \langle j | j \rangle \right) \quad (9.6)$$

with hopping coefficients t_1 and t_2 , and mass term M distinguishing the sites A, B of the bipartite triangular lattice. The Aharonov-Bohm phase ϕ acquired during second nearest-neighbor hopping corresponds to a local magnetic flux in a well chosen gauge. A possible choice for the corresponding flux is given in figure below (taken from [70], $\varphi = \phi/2$). This way the time-reversal symmetry is broken but the net magnetic flux per unit cell is zero. It is then possible to compute the Bloch Hamiltonians and the corresponding Chern number [92], the phase diagram is plotted in the figure below and presents three different phases with Chern number 0, 1 and -1. On the solid lines between the different phases, the gap of the system is explicitly closing, allowing for a continuous deformation from one class to another.



Because of the absence of a global transverse magnetic field, such system was associated to an anomalous quantum Hall effect and its experimental realization was recently achieved [46]. Finally it can be shown [92, 22] that in this model

$$\sigma_{xy} \equiv \frac{\partial j_x}{\partial E_y} = \frac{e^2}{h} C_1 \quad (9.7)$$

which is a version of relation (9.1).

9.1.4 Bulk-edge correspondence

Above, we spoke about quantized conductivity for insulators, i.e. for non-conducting systems, which might seem somewhat paradoxical. The paradox is solved by considering the boundaries of

the system. The Kubo formula allows to relate the Chern number with the transverse conductivity of the system. This quantity gives the linear-response current to an electric field. Both quantities are associated to the bulk properties of the system. In experiments, however, the insulators have finite size and boundaries, and moreover only the global conductance is measured, integrating the conductivity over the full sample. To understand better the role of the boundaries, consider the idealized case of an infinite interface between two topological insulators connected along a horizontal line (see Figure 9.3), and assume that their bulk versions correspond to distinct Chern numbers. The interface can be seen as a continuous deformation from one system to the other, but

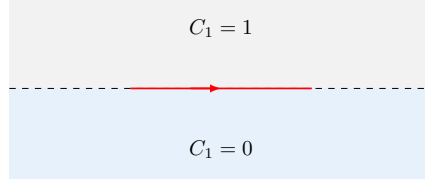


Figure 9.3: *Interface between two systems with different Chern numbers. The only way to have a continuous deformation from one to the other is to close the gap. Hence gapless edge states naturally appear at the boundary of a system.*

the only way to realize such a deformation is to close the gap. Then, near the interface, the system becomes a metal and a current can flow: conducting edge modes appear. Now, considering the vacuum as the most trivial insulator and using the same argument we conclude that edge modes should appear for a bounded system with nontrivial Chern number. These modes are localized at the edges and support all the current responsible for the nonvanishing conductance, since in the bulk the system is an insulator. The Chern numbers actually counts (algebraically) the number of modes localized at one edge. The quantum Hall effect also has this property although it is not rigorously an insulator: in that case there is no net current in the bulk because of the cyclotron orbits that trap electrons. Such orbits are broken at the boundaries and consequently the current can propagate along the edges.

The correspondence between the topological properties of a bulk system and the gapless edge modes of its bounded version was investigated in several models such as [95] for free electrons on a square lattice with magnetic field or [166] in a generalized version of quantum Hall effect called fractional [65]. A more mathematical approach to the problem of bulk-edge correspondence was more recently developed in [90, 8]. Finally, note that the edge gapless modes at the boundary of two dimensional topological insulators constitute good candidates to realize quantum wires analyzed in the first Part of the thesis. Indeed the propagation of edge modes is purely one dimensional and ballistic, although chiral in general, see below.

9.2 Time-reversal invariance

The key ingredient for the Chern insulators developed in the previous section was the symmetry breaking of time-reversal, using for example a magnetic flux. However it is possible to consider tight binding systems that are time-reversal invariant, and their topological properties are quite different.

Time-reversal operation, corresponding to time transformation $t \mapsto -t$, is described in quantum mechanics by an antiunitary (i.e. antilinear and unitary) operator Θ [155]. For systems with spin degrees of freedom, Θ can be written as a π -rotation in the spin space: $\Theta = \exp(-i\pi J_y/\hbar)C$ where J_y is the y -component of the spin operator and C is complex conjugation. Whether the spin is integer or half-integer then corresponds to two cases: $\Theta^2 = I$ or $\Theta^2 = -I$, respectively. A system will be called time-reversal invariant if its Hamiltonian H commutes with Θ .

Consider again the band theory of noninteracting electrons in crystals, still for $d = 2$. In that

case the spin of the particle is one half and Θ squares to $-\mathbb{I}$. Applying the Bloch decomposition to the system, and assuming the time-reversal invariance, we get for the family of Bloch Hamiltonians the relation

$$H(-k) = \Theta H(k) \Theta^{-1} \quad \forall k \in \mathbb{T}^2. \quad (9.8)$$

This equation has several consequences. First, on the Brillouin torus, the Bloch Hamiltonians are related by the involution $\vartheta(k) = -k$, so that only one half of them will be necessary to describe the full system. Hence we consider the effective Brillouin zone BZ_+ depicted in Figure 9.1, such that the full zone is generated by the action of ϑ on the effective one [130]. Note that there are many choices of effective Brillouin zones, but each one always contains four (nonequivalent) fixed points k^* such that $\vartheta k^* = k^*$. These point of higher symmetry, called the time reversal invariant momenta (TRIM), will be of crucial importance in the following.

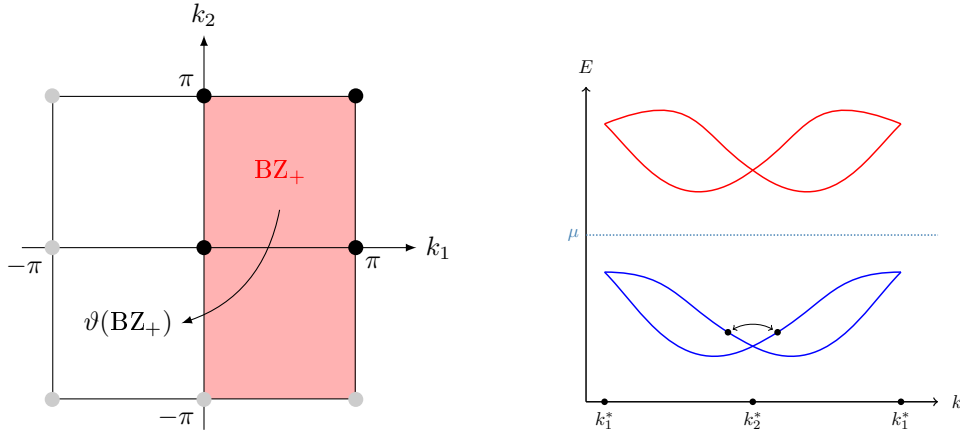


Figure 9.1: *Left: One possible effective Brillouin zone and its four nonequivalent TRIM (black dots, the gray ones are redundant). Right: Typical dispersion relation in direction k_1 of the Brillouin zone, k and $-k$ are related via the Kramers theorem, and at TRIM the energy eigenvalues are always degenerated.*

On the other hand equation (9.8) implies that if $\psi(k) \in \mathbb{C}^N$ is an eigenstate of $H(k)$ at k , then $\Theta\psi(k)$ is an eigenstate of $H(-k)$ at $-k$ with the same energy. For time-reversal invariant systems eigenstates always come in pairs, this is the Kramers theorem [155]. Note that such states correspond to different quasimomenta k and $-k$ that are different, except at the TRIM k^* . Moreover if $\Theta^2 = -\mathbb{I}$, then $\psi(k^*)$ and $\Theta\psi(k^*)$ are orthogonal. This implies that, for insulators, each valence band is always twice degenerated at any TRIM, and consequently the number of valence bands is even, see Figure 9.1.

Last but not least, the Kramers theorem implies that equation (9.8) is also satisfied when replacing $H(k)$ by the valence bands projector $P(k)$, so that the computation of the Chern number (9.5) can be decomposed in two parts (for example the previous effective Brillouin zone and its complementary) that compensate since the integrand is an odd function of k . Thus one always has $C_1 = 0$ for a time reversal topological insulator: the valence bundle is always topologically trivial.

9.2.1 \mathbb{Z}_2 invariants

Since the Chern number is vanishing in that case, there always exist a global continuous family of bases $(\psi_\alpha(k))$ of the valence bundle. However, there might not exist such a family that is composed of Kramers pairs, i.e. with $\psi_{2\alpha}(k) = \Theta\psi_{2\alpha-1}(-k)$. The existence or non-existence of such a family gives rise to two different classes of time-reversal topological insulators. Basically, for the nontrivial class, the valence bundle cannot be trivialized together with its time-reversal

invariant structure. Consider the sewing matrix, defined by Fu and Kane in [72]

$$w_{\alpha\beta}(k) = \langle \psi_\alpha(-k) | \Theta \psi_\beta(k) \rangle \quad (9.9)$$

which encodes how the Kramers partners of the states in the continuous family of bases $(\psi_\alpha(k))$ are related to the original states over the Brillouin torus. In particular, at each TRIM k^* , matrix w is antisymmetric, and one can define an invariant ν by the relation

$$(-1)^\nu = \prod_{k^*} \frac{\sqrt{\det(w(k^*))}}{\text{pf}(w(k^*))} \quad (9.10)$$

where “pf” stands for the Pfaffian of an antisymmetric matrix which squares to the determinant, so the left hand side squares to 1, and $\sqrt{\det(w(k))}$ is chosen continuously² over \mathbb{T}^2 . Note that the invariant ν is well defined modulo 2 only and hence corresponds to a \mathbb{Z}_2 valued quantity, instead of an integer as for the Chern number. It does not depend on the choice of the global family of states $(\psi_\alpha(k))$. Actually, it captures if it is possible ($\nu = 0 \bmod 2$) or not ($\nu = 1 \bmod 2$) to identify globally the Kramers partners over the Brillouin torus. For example, if $\Theta \psi_{2\alpha}(k) = \psi_{2\alpha-1}(-k)$, then $w(k)$ is a constant block diagonal matrix composed of blocks

$$\begin{pmatrix} 0 & -1 \\ 1 & 0 \end{pmatrix} \quad (9.11)$$

whose Pfaffian is -1 and determinant is 1, so that $\nu = 0 \bmod 2$. However if one cannot find a global continuous basis composed of Kramers pairs then such obstruction will lead to $\nu = 1 \bmod 2$.

The historically first proposal for the \mathbb{Z}_2 invariant was formulated by Kane and Mele in [102] also in terms of Pfaffians but of different quantities. However it appeared to coincide with the invariant ν proposed by Fu and Kane in (9.10), that we shall call the Kane-Mele invariant. Besides, Moore and Balents proposed an interpretation of this invariant based on the integral of the Berry curvature but restricted to the effective Brillouin zone [72, 130, 150], in analogy with the previous Chern number.

Example 9.2

The Kane-Mele model

The first model of time-reversal invariant topological insulator was proposed in [102]. The idea was to mix spin degrees of freedom with the two-site levels of a bipartite lattice. The Hamiltonian has the form [70]

$$H(k) = d_0(k)I_4 + \sum_{i=1}^5 d_i(k)\Gamma_i(k) \quad (9.12)$$

where Γ_i are 4×4 matrices that are of the form of tensor products $\sigma_j \otimes s_k$, of Pauli matrices σ_j and s_k : one family for the spin, and another one for the two-level lattice site. The model can be seen as two copies of the Haldane model with electrons of opposite spins, and the external magnetic flux replaced by the spin-orbit coupling, so that the two copies are not independent. The resulting four-band model leads to the \mathbb{Z}_2 invariant ν that can be either 0 or 1. Because of the construction, it was viewed as a model of quantum spin Hall effect.

Other models mixing internal degrees of freedom (e.g. orbitals) and spin were developed such as the Bernevig-Zhang-Hugues model [23] with an accessible realization of the nontrivial phase in HgTe quantum wells.

²This is always possible since $\det(w)$ has no winding numbers, see Appendix G of [70].

The nontrivial property of the time-reversal invariant bulk system captured by ν also corresponds to the appearance of edge states that appear in pairs of counter propagating gapless modes localized at each boundary of the system, with ν corresponding to the parity of the number of such pairs. The paired edge states were observed experimentally in [111], and the mathematical proof of the bulk-edge correspondence for time-reversal invariant topological insulators was achieved in [90].

9.3 The tenfold way and beyond

The previous cases of topological insulators are just few examples among a wide family of today's model and experiments [22, 94]. On one hand, topological insulators also appear in other dimensions than $d = 2$, and have corresponding topological invariants and edge states (that propagate on the surfaces of the sample for $d = 3$). On the other hand, one can also consider models with other symmetries than time-reversal, such as particle-hole symmetry for example.

Instead of looking at specific models, a systematical approach based on K -theory considerations or on homotopy theory allows to compute which kind of topological invariant is expected for given dimension and symmetries [106, 153, 94, 66, 162]. Such theory computes the isomorphism classes of vector bundles up to homotopy. Moreover such classes of vector bundles are considered up to an embedding into bigger bundles, which corresponds to the physical idea that topological insulators are equivalent when one adds supplementary valence bands with low energies. One obtain a full classification depending on the dimension d of the base space, and on the possible symmetries: time-reversal Θ and particle-hole exchange Ξ that are both antiunitary and can square to $+1$ or -1 , and the unitary chiral symmetry $\Pi = \Theta\Xi$. The corresponding invariants take values in the groups listed in Table 9.1.

AZ	Symmetry			d							
	Θ	Ξ	Π	1	2	3	4	5	6	7	8
A	0	0	0	0	\mathbb{Z}	0	\mathbb{Z}	0	\mathbb{Z}	0	\mathbb{Z}
AIII	0	0	1	\mathbb{Z}	0	\mathbb{Z}	0	\mathbb{Z}	0	\mathbb{Z}	0
AI	1	0	0	0	0	0	\mathbb{Z}	0	\mathbb{Z}_2	\mathbb{Z}_2	\mathbb{Z}
BDI	1	1	1	\mathbb{Z}	0	0	0	\mathbb{Z}	0	\mathbb{Z}_2	\mathbb{Z}_2
D	0	1	0	\mathbb{Z}_2	\mathbb{Z}	0	0	0	\mathbb{Z}	0	\mathbb{Z}_2
DIII	-1	1	1	\mathbb{Z}_2	\mathbb{Z}_2	\mathbb{Z}	0	0	0	\mathbb{Z}	0
AII	-1	0	0	0	\mathbb{Z}_2	\mathbb{Z}_2	\mathbb{Z}	0	0	0	\mathbb{Z}
CII	-1	-1	1	\mathbb{Z}	0	\mathbb{Z}_2	\mathbb{Z}_2	\mathbb{Z}	0	0	0
C	0	-1	0	0	\mathbb{Z}	0	\mathbb{Z}_2	\mathbb{Z}_2	\mathbb{Z}	0	0
CI	1	-1	1	0	0	\mathbb{Z}	0	\mathbb{Z}_2	\mathbb{Z}_2	\mathbb{Z}	0

Table 9.1: *Topological insulators classification in terms of K -theory groups, depending on the dimension of the base space and the symmetry involved, denoted by ± 1 when present. The sign is for the value of its square when relevant. (Taken from [94])*

The symmetries of the system are denoted by ± 1 , with the sign specifying the square of the antiunitary operators. When no symmetry or only chiral symmetry is involved, the corresponding K -theory is complex and the corresponding group is actually periodic modulo 2 in d , so that for the classes³ A and AIII, only the two first columns are sufficient, and the invariant takes values in either $\{0\}$ or \mathbb{Z} . The Chern insulators discussed in 9.1 correspond to A at $d = 2$. Conversely, an antiunitary symmetry imposes a real structure for the K -theory, leading to a periodicity modulo 8 in d . The time-reversal case discussed above corresponds to class AII, and one also sees on this table that the three-dimensional case is also associated to a \mathbb{Z}_2 invariant.

³The labels come from Atland and Zirnbauer classification using symmetric spaces, see [4].

Note that beyond this classification, topological invariants for periodically driven systems were recently discussed [97, 133, 151, 45], computed in terms of the unitary family of evolution operators instead of Hamiltonians. The initial idea was to change the topology of a static system by inducing a periodic exterior perturbation [121, 107]. Such Floquet systems are in some sense $d + 1$ topological insulators, but the role of time being specific, they do not enter in the previous classification. Such systems will be briefly described at the end of this part of the thesis, since they actually motivated our new definition of the Kane-Mele invariant in the static case. They are however not necessary to understand the upcoming construction, hence we chose to present them in Chapter 12 to avoid an overloading of this introduction and to focus on the main topic of this part of the manuscript.

9.4 Geometric interpretation of the Kane-Mele invariant

If the topological nature of insulator with no additional symmetry (class A) is well understood as a geometric obstruction to the topological triviality of the valence bundle that can be captured with a geometric quantity: the Chern number, the picture is not so clear in the context of time-reversal insulators (class AII). Although their topological nature is well understood as related to the obstruction to the existence of a time-reversal invariant trivialization of the valence bundle, the corresponding Kane-Mele invariant has no simple geometric interpretation. It is actually not obvious how to get a \mathbb{Z}_2 number from geometrical considerations. Several approaches have already proposed a geometric construction of Kane-Mele invariant, such as [130] and more recently [64], and we present in the following another one that is complementary.

We shall define and calculate a topological index for the two-dimensional time-reversal insulators that is related to a unitary family of operators, canonically associated to the family of projectors $P(k)$, $k \in \mathbb{T}^2$, on the valence states. This index was motivated from periodically driven system, but it turns out that it can be interpreted in terms of a Wess-Zumino amplitude, already introduced in the two previous parts of the thesis, in the context of Wess-Zumino-Witten models. This provides a new bridge between topological insulators and the conformal field theory approach, which should be also useful for studying the bulk-edge correspondence. The two following chapters are dedicated to the definition, the construction and the calculation of the new index, and to its matching with the Kane-Mele invariant. On the way, we also present the general ideas how to compute Wess-Zumino amplitudes in a local approach, by gluing expressions computed with the use of an open covering of the target space. Such approach was already used implicitly in the previous part for global gauge anomalies. It turns out that our topological index can be understood as a boundary gauge anomaly for Wess-Zumino amplitudes.

Note that conformal field theories were already successfully used to describe topological insulators, in particular the quantum Hall systems, integer and fractional [65, 34, 93, 160]. It turns out that some conformal field theories fit very well with the description of the spectrum and the states of such systems, both for the bulk and the edges. Here our approach is slightly different since we only use CFT techniques to define a bulk invariant, rather than a field content of a given model. We expect, however, that our approach will be also useful to make more direct the relation between the bulk properties and the conformal field theory description of the gapless edge modes.

Chapter 10

Geometric formulation of the Kane-Mele invariant

In order to construct a geometric invariant associated to a time-reversal invariant two dimensional insulator, we start from the family of orthogonal projectors $P(k)$ on the valence band states defined for k in the Brillouin torus \mathbb{T}^2 . We lift such a family to a family of unitary operators with one more parameter, with a map motivated by periodically driven systems, where the additional parameter is the evolution time. We first consider the homotopy invariant of such unitary families, that we call “degree”, which is, however, trivial in the presence of time reversal symmetry. In the latter case, we modify the unitary family on a half of the time-evolution interval and take the degree only afterwards. We end up with a formula involving a square root of the Wess-Zumino amplitude for unitary valued maps that we want to identify with the Kane-Mele invariant for time-reversal invariant insulators.

10.1 Invariants of 3d families of unitary matrices

10.1.1 The degree invariant

Consider the case of a band insulator in dimension $d = 2$. We take for initial datum of the model a smooth family of Bloch Hamiltonians $H(k)$ over the Brillouin Zone $BZ \cong \mathbb{T}^2$ that act in \mathbb{C}^N . Then consider the family over BZ of the orthogonal projectors $P(k)$ on the valence band states with energies below the gap. Let us associate to such a family the family $V(t, k)$ of unitary operators

$$V(t, k) = e^{\frac{2\pi i t}{T} P(k)} = e^{\frac{2\pi i t}{T}} P(k) + I - P(k) \quad (10.1)$$

that we shall consider for $t \in [0, T]$ and $k \in BZ$. As $V(0, k) = I = V(T, k)$, such a family may be viewed as periodic in t , and hence, as defined on a 3-torus¹ \mathbb{T}^3 . Here the period T does not have a physical meaning but since this formalism appeared in the context of periodically forced systems, we keep in the notation for coherence. Let us consider the integral

$$\frac{1}{8\pi^2} \int_{[0, T] \times BZ} V^* \chi \equiv \deg[V], \quad (10.2)$$

where $\chi = \frac{1}{3} \text{tr}(g^{-1} dg)^{\wedge 3}$ is the same closed 3-form on $U(N)$ that we considered before on compact groups. The above integral was normalized so that it takes values in \mathbb{Z} [28]. Somewhat abusively, we shall call in the “degree”² of V . $\deg[V]$ is a homotopy invariant of maps from \mathbb{T}^3 to $U(N)$. In

¹More properly, $V(t, k)$ may be viewed as defined on the suspension SBZ equal to $[0, T] \times BZ$ with $\{0\} \times BZ$ and $\{T\} \times BZ$ identified to points.

²The name comes from the case when V takes values in the 3-dimensional group $SU(2) \cong S^3$ where $\deg[V]$ counts how many times the image of V covers the 3-sphere.

particular, for V given by (10.1), it does not change if we continuously deform the family $P(k)$ of projectors and is directly connected to the Chern number of the valence bundle \mathcal{E} with fibers $P(k)\mathbb{C}^N$. Indeed, it may be easily shown by performing the integral over t in (10.2) that in that case,

$$\deg[V] = \frac{i}{2\pi} \int_{\text{BZ}} \text{tr}(P dP \wedge dP) = C_1, \quad (10.3)$$

see (9.5). The above relation may be viewed as a reflection of the Bott periodicity in the complex K -theory³.

10.1.2 The case with time-reversal invariance

Consider now the case of a time-reversal invariant two-dimensional topological insulator with property (9.8) for antiunitary Θ with $\Theta^2 = -I$. In this case necessarily N is even, $N = 2M$. Besides, the time reversal symmetry implies that

$$\Theta P(k) \Theta^{-1} = P(-k), \quad k \in \text{BZ} \quad (10.4)$$

and, consequently, that the Chern number of the valence bundle \mathcal{E} vanishes so that \mathcal{E} is also topologically trivial. Moreover the rank of \mathcal{E} , equal to the rank of all $P(k)$, is also even because of the Kramers theorem and will be denoted $2m$. The vanishing of C_1 implies that also $\deg[V] = 0$, which may be also seen as a consequence of the symmetry

$$\Theta V(t, k) \Theta^{-1} = V(T - t, -k). \quad (10.5)$$

In particular the operator at half-period $V(T/2, k) = I - 2P(k)$ satisfies

$$\Theta V(T/2, k) \Theta^{-1} = V(T/2, -k). \quad (10.6)$$

Note that $P \mapsto I - 2P$ is a canonical embedding of projectors into unitary operators. $V(T/2)$ will be the key ingredient from which the topological index of the time-reversal invariant insulator will be defined. For the time being, note that symmetry (10.5) shows that the second half of the period $[T/2, T]$ provides a redundant information about V so the idea is to modify that family on the that half-interval of time forgetting about that information, but not about the time reversal invariance. This will be done by considering a contraction

$$[0, 1] \times \text{BZ} \ni (r, k) \mapsto \tilde{V}(r, k) \in U(2M) \quad (10.7)$$

starting from $\tilde{V}(0, k) = I - 2P(k)$ and going to $\tilde{V}(1, k) = I$, but preserving time-reversal at each step of the contraction by requiring that

$$\Theta \tilde{V}(r, k) \Theta^{-1} = \tilde{V}(r, -k), \quad (10.8)$$

which should be compared with (10.5): here the parameter is the same on both sides of the equality. Assuming that such a contraction exist, consider finally the map

$$\hat{V}(t, k) = \begin{cases} V(t, k) & \text{for } 0 \leq t \leq T/2, \\ \tilde{V}((2t - T)/T, k) & \text{for } T/2 \leq t \leq T, \end{cases} \quad (10.9)$$

which is defined on $[0, T] \times \text{BZ}$ and periodic in t so that it can again be seen as a unitary family over the 3-torus $S^1 \times T^2$. Such family is illustrated in Figure 10.1.

³Application V allows to identify elements of $K^{-1}(SBZ)$, K -group of suspensions of BZ and $K^0(\text{BZ})$, that are necessarily identical due to Bott periodicity [149].

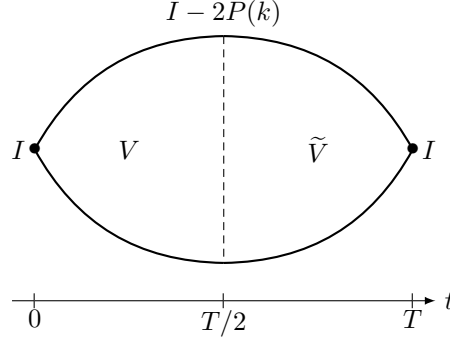


Figure 10.1: Schematic description of periodic family $\widehat{V}(t, k)$. From I to $I - 2P(k)$ then again contracted to I , with a different time reversal invariance for each step, since V satisfies (10.5) whereas \widetilde{V} satisfies (10.8).

We define a new topological index related to the family $P(k)$ and, consequently, to the valence bundle \mathcal{E} as

$$K[\mathcal{E}] \equiv \deg[\widehat{V}] \bmod 2. \quad (10.10)$$

We proved in [44] the following facts for a general family $V(t, k)$ over $[0, T] \times BZ$ with values in $U(2M)$ such that $V(0, k) = I = V(T, K)$ and satisfying the time-reversal invariance (10.5) the following facts:

1. A contraction \widetilde{V} of $V(T/2)$ to I preserving “constant time” time-reversal (10.8) always exists and can be constructed almost explicitly ([44], 3.2).
2. If \widetilde{V}_1 and \widetilde{V}_2 are two such contractions, then $\deg[\widehat{V}_1] - \deg[\widehat{V}_2] \in 2\mathbb{Z}$ for \widehat{V}_i related to the contractions \widetilde{V}_i by (10.9) ([44], 3.3).

This shows that the \mathbb{Z}_2 valued index $\deg[\widehat{V}] \bmod 2$ is well defined for general unitary families $V(t, k)$ with symmetry (10.5) starting and ending at I . In particular, index $K[\mathcal{E}]$ corresponding to the unitary family (10.1) is well defined. The more general result was used in the context of Floquet systems.

10.1.3 Relation to Wess-Zumino amplitudes

In the case where V is of the form (10.1), the expression (10.10) for index K may be simplified. Indeed because of the time-reversal invariance (10.5), using the fact that $V(T-t, k) = V(-t, k) = V^{-1}(t, k)$, one shows that the contribution from V (i.e. from $t \in [0, T/2]$ on the left part on Figure 10.1) vanishes in the computation of K . Indeed,

$$V^* \chi = (\Theta V \Theta^{-1})^* \chi = (V^{-1} \circ (\text{Id} \times \vartheta))^* \chi = (\text{Id} \times \vartheta)^* (V^{-1})^* \chi = -(\text{Id} \times \vartheta)^* \chi \quad (10.11)$$

because χ is real and $(V^{-1})^* \chi = -\chi$. Then since the map $\vartheta : k \mapsto -k$ does not change the orientation, we infer that the integral of $V^* \chi$ over $[0, T/2] \times BZ$ vanishes. We are left with the contribution of \widetilde{V} only

$$K[\mathcal{E}] = \frac{1}{8\pi^2} \int_{[0,1] \times BZ} \widetilde{V}^* \chi \bmod 2. \quad (10.12)$$

Note that the time variable has disappeared and what remains is only the contraction of $I - 2P$ to I while preserving time-reversal (10.8). This could have been directly the definition of the invariant K and the previous paragraph might look somewhat artificial, however it assures that expression (10.12) for K is an integer well defined modulo 2. Moreover if we set $\Sigma = BZ$ and

$\tilde{\Sigma} = [0, 1] \times \text{BZ}$, which has two boundaries but one where \tilde{V} is constant to I , then we recognize in K the expression of a Wess-Zumino action already presented in Sections 4.2 and 7.1. Namely

$$K[\mathcal{E}] = -\frac{1}{2\pi} S_{\text{WZ}}[U_P] \mod 2, \quad \text{with} \quad U_P = I - 2P \quad (10.13)$$

where the minus sign comes from orientation of boundary $\partial\tilde{\Sigma}$ but does not matter modulo 2. We know from [173] that $S_{\text{WZ}}[U_P]$ is defined modulo 2π because the corresponding Feynman amplitudes are $e^{iS_{\text{WZ}}}$ are well defined. This is not enough however to have a consistent right hand side of the previous equation, that would be well defined modulo 1 only. Since left hand-side is well-defined modulo 2, this means that when contractions of U_P are preserving time reversal (10.8) then the corresponding Wess-Zumino action is well defined modulo 4π rather than 2π . This is the essence of the second result of [44] mentioned at the end of the previous subsection. Note that since K is an integer then $S_{\text{WZ}}[U_P] \in 2\pi\mathbb{Z}$ according to (10.13), and its corresponding Feynman amplitude is always 1. Hence we may rewrite (10.13)

$$(-1)^{K[\mathcal{E}]} = \left(e^{iS_{\text{WZ}}[U_P]} \right)^{-1/2}, \quad (10.14)$$

where on the right hand side the square root of the Wess-Zumino is fixed by computing $S_{\text{WZ}}[U_P]$ with the use of a contraction \tilde{V} of U_P preserving the time-reversal invariance (10.8). This latter makes $S_{\text{WZ}}[U_P]$ well defined modulo 4π rather than 2π .

For more general families $V(t, k)$ satisfying the time-reversal symmetry (10.5) and such that $V(0, k) = I$, we may similarly write

$$(-1)^{\deg[\hat{V}]} = \frac{e^{\frac{i}{8\pi} \int_{[0, T/2] \times \text{BZ}} V^* \chi}}{\left(e^{iS_{\text{WZ}}[V(T/2)]} \right)^{1/2}}, \quad (10.15)$$

where the square root in the denominator is again defined by calculating $S_{\text{WZ}}[V(T/2)]$ with the use of a contraction \tilde{V} with symmetry (10.8) which makes it well defined modulo 4π . Here the numerator is, in general, different from 1 and is equal to the denominator modulo sign.

10.2 Towards the Kane-Mele invariant

Let us return to the expression (10.12) for the index K . We shall show that $K[\mathcal{E}]$ coincides with the Kane-Mele invariant given by (9.10). This will be done by constructing an explicit contraction \tilde{V} and computing $(-1)^K$. In the first step of the calculation, that will be described still in this chapter, the Wess-Zumino amplitudes will reappear again for fields localized at the boundary of the effective Brillouin zone, this time without square roots. In the next chapter, we shall calculate such amplitudes and will show that each of them localizes at two corresponding TRIM, giving at the end the expression on the right hand side of (9.10).

10.2.1 Introducing the sewing matrix

Before constructing the contraction \tilde{V} and in order to make $K[\mathcal{E}]$ explicitly dependent of the sewing matrix (9.9) that appears in the Kane-Mele invariant (9.10), we first show that \tilde{V} may be further restricted in a specific basis. First recall that the valence bundle \mathcal{E} , with fibers $P(k)\mathbb{C}^{2M}$ of dimension $2m$, is trivial because its Chern number vanishes. This is also the case for the conduction bundle, with fibers $(I - P(k))\mathbb{C}^{2M}$ of dimension $2(M - m)$. Thus there exist a continuous (even smooth) orthonormal basis $|e_i(k)\rangle$ for $i = 1, \dots, 2M$ such that

$$P(k) = \sum_{i=1}^{2m} |e_i(k)\rangle \langle e_i(k)| \quad (10.16)$$

and similarly for $I - P(k)$ with i summed from $2m + 1$ to $2M$. Besides consider the k -independent canonical basis $|f_i\rangle$ of \mathbb{C}^{2M} . Projector P becomes simpler in this basis:

$$R^{-1}(k)P(k)R(k) = \sum_{i=1}^{2m} |f_i\rangle \langle f_i| \equiv P_0, \quad \text{where} \quad R(k) = \sum_{i=1}^{2M} |e_i(k)\rangle \langle f_i| \quad (10.17)$$

is the operator describing the change of bases, and similarly for $I - P(k)$. The expression of \tilde{V} in the new basis, given by $\tilde{T}(r, k) \equiv R^{-1}(k)\tilde{V}(r, k)R(k)$, becomes a contraction of an initial map over BZ that is constant, namely

$$\tilde{T}(0, k) = I - 2P_0, \quad \tilde{T}(1, k) = I. \quad (10.18)$$

This will allow to reduce the problem to operators of size $2m$, see below. However the price to pay is that the time-reversal operator Θ becomes k dependent in the new basis. Property (10.8) for \tilde{V} becomes now

$$W(k)\overline{\tilde{T}(r, k)}W^{-1}(k) = \tilde{T}(r, -k), \quad (10.19)$$

where overlining is for the complex conjugation (remember that Θ is antilinear). Operator W is given by the matrix

$$W_{ij}(k) = \langle e_i(-k) | \Theta e_j(k) \rangle \quad (10.20)$$

in the canonical basis $|f_i\rangle$. This matrix is actually unitary, and block diagonal with two blocks of size $2m$ and $2(M - m)$ since valence and conduction bands are independent. In this new basis and up to some boundary terms that vanish because of dimensional reasons and properties of \tilde{T} , the index K can be computed simply by replacing \tilde{V} by \tilde{T} in (10.12).

On the top of that, due to the block diagonal structure of W and the fact that $\tilde{T}(0, k)$ is already equal to identity in its lower block part corresponding to $i = 2m + 1, \dots, 2(M - m)$, we may look for a contraction such that

$$\tilde{T}(r, k) = \tilde{t}(r, k) + (I - P_0), \quad (10.21)$$

where $\tilde{t}(r, k)$ acts in the space spanned by the $|f_i\rangle$ for $i = 1, \dots, 2m$. Such contraction satisfies

$$\tilde{t}(0, k) = -I, \quad \tilde{t}(1, k) = I, \quad w(k)\overline{\tilde{t}(r, k)}w(k)^{-1} = \tilde{t}(r, -k) \quad (10.22)$$

going from a constant map to another constant map, but preserving a k -dependent invariance encoded by unitary map $w(k)$ that is the $2m$ -dimensional block of $W(k)$, namely

$$w_{ij}(k) = \langle e_i(-k) | \Theta e_j(k) \rangle = -w_{ji}(-k) \quad (10.23)$$

which is nothing but the sewing matrix of the system, as introduced in (9.9). For such a contraction \tilde{t} , we obtain:

$$K[\mathcal{E}] = \frac{1}{8\pi^2} \int_{[0,1] \times \text{BZ}} \tilde{t}^* \chi \mod 2 \quad (10.24)$$

and the problem is reduced to linear maps in the $2m$ -dimensional subspace corresponding to the valence bands.

10.2.2 Modified sewing matrices

From now on we identify unitary operator $w(k)$ in \mathbb{C}^{2m} and its corresponding sewing matrix $w_{ij}(k)$. Due to relation (10.23) that implies that $\det w(k) = \det w(-k)$, function $\det w$ has no windings on BZ and hence it possesses a continuous $(2m)$ -th root, allowing to define

$$\tilde{w}(k) = \frac{w(k)}{(\det w(k))^{1/2m}} \quad (10.25)$$

that is uniquely determined only up to a global $(2m)$ -th root of 1, but this will not matter in the following. By construction $\det \tilde{w}(k) = 1$ so that $\tilde{w}(k) \in SU(2m)$. Finally, as for $w(k)$, one also has $\tilde{w}(k) = -\tilde{w}(-k)^T$.

In particular at a TRIM of BZ satisfying $k^* = -k^*$, \tilde{w} is antisymmetric and, consequently,

$$\tilde{w}_0 \equiv \tilde{w}(k^*) = u_0 \omega u_0^T \quad \text{with} \quad \omega = \begin{pmatrix} 0 & D_m \\ -D_m & 0 \end{pmatrix} \quad \text{and} \quad D_m = \begin{pmatrix} & & & 1 \\ & & & \\ & & \ddots & \\ & & & 1 \\ 1 & & & \end{pmatrix} \quad (10.26)$$

for some $u_0 \in U(2m)$. Necessarily, $\det u_0 = \pm 1$ and is equal to the Pfaffian $\text{pf}(\tilde{w}_0)$ of the antisymmetric matrix \tilde{w}_0 , giving on the way a method to compute it in this case. Moreover the fixed-point subgroup of $U(2m)$

$$Sp_{\tilde{w}_0}(2m) = \{u \in U(2m) \mid \tilde{w}_0 u \tilde{w}_0^{-1} = u\} \quad (10.27)$$

is conjugate to the symplectic group $Sp(2m) \subset U(2m)$. For $m = 1$ the situation is particularly simple since, necessarily, $\tilde{w}_0 = \pm \omega$ with the sign equal to $\text{pf}(\tilde{w}_0)$ and all the subgroups $Sp_{\tilde{w}_0}(2)$ coincide with $Sp(2) = SU(2)$.

10.2.3 Construction of the contraction

The general strategy to construct contraction \tilde{t} satisfying (10.22) is to look at half BZ_+ of the Brillouin zone only since \tilde{t} may be extended to the other half using the time reversal invariance, see the left part of Figure 9.1 from the previous chapter. However, unlike BZ, the effective Brillouin zone BZ_+ has boundaries that have to be treated carefully because the time-reversal invariance still imposes conditions on \tilde{t} there. Starting at the TRIM, which have the richest symmetry, we contract $-I$ to I while preserving time reversal invariance (10.22). Then we spread this contraction to the edges of BZ_+ , by mixing contraction parameter and momentum variable k , first on one half of an edge, then continuing to the full edge by time-reversal invariance. The contraction obtained on the edges is then extended to the interior of BZ_+ , and finally extended to BZ. All these steps are illustrated on Figure 10.1, then detailed in the following.

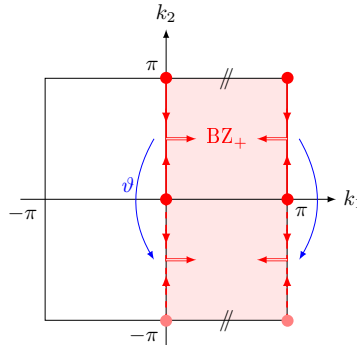


Figure 10.1: Schematic construction of the contraction over the effective Brillouin zone BZ_+ that is a cylinder with two edges $k_1 = 0$ and $k_1 = \pi$. Starting at the TRIM, we then expand to the upper edges, then to the lower ones related to the upper ones by ϑ , and finally into the interior of BZ_+ .

\tilde{t} at the TRIM. Denote the four nonequivalent TRIM k^* of BZ by (a, a') where a and a' are 0 or π . At such points, the time reversal invariance property reads

$$\tilde{w}(k^*) \overline{\tilde{t}(r, k^*)} \tilde{w}(k^*)^{-1} = \tilde{t}(r, k^*) \quad \Rightarrow \quad \tilde{t}(r, k^*) \in Sp_{\tilde{w}(k^*)}(2m) \quad (10.28)$$

as discussed in the previous subsection. Since $Sp_{\tilde{w}(k^*)}(2m)$ is conjugated to the symplectic group $Sp(2m)$, it is in particular connected, so that there exist a smooth path from $-I$ to I inside each $Sp_{\tilde{w}(k^*)}(2m)$. We denote such paths $t_{aa'}(r)$ for $r \in [0, 1/4]$. We take them as defining the contraction \tilde{t} restricted to the TRIM, since by construction they satisfy the time-reversal property.

\tilde{t} on the edges of \mathbf{BZ}_+ . The effective Brillouin zone has two edges delimited by $k_1 = 0$ and $k_1 = \pi$, whereas the lines $k_2 = \pi$ and $k_2 = -\pi$ are identified as by the periodicity remaining from the full torus. At $k_1 = 0$, consider the continuous map

$$t_0(r, k_2) = \begin{cases} t_{00}(r - k_2) & \text{for } 0 \leq k_2 \leq r \\ -I & \text{for } r \leq k_2 \leq \pi - r \\ t_{0\pi}(k_2 - (\pi - r)) & \text{for } \pi - r \leq k_2 \leq \pi \end{cases} \quad (10.29)$$

for $k_2 \in [0, \pi]$. At $r = 0$, this is the constant map equal to $-I$, continuously deformed to $r = 1/4$ where on the extremities $k_2 = 0$ and π the map is equal to I . Mixing parameter r with variable k_2 , we spread the contractions t_{00} and $t_{0\pi}$ inside the upper half of the left edge of \mathbf{BZ}_+ . In particular at $r = 1/4$ the map is a continuous loop starting and finishing at I , with a determinant fixed to 1 since $t_{0a} \in Sp_{\tilde{w}(0,a)}(2m)$ so that the loop $t_0(1/4, \cdot)$ may be contracted to the constant loop equal to I inside $SU(2m)$ which is simply connected. Use the latter contraction to extend t_0 to $r \in [1/4, 1/2]$. All the steps are illustrated on Figure 10.2. This gives contraction from $-I$

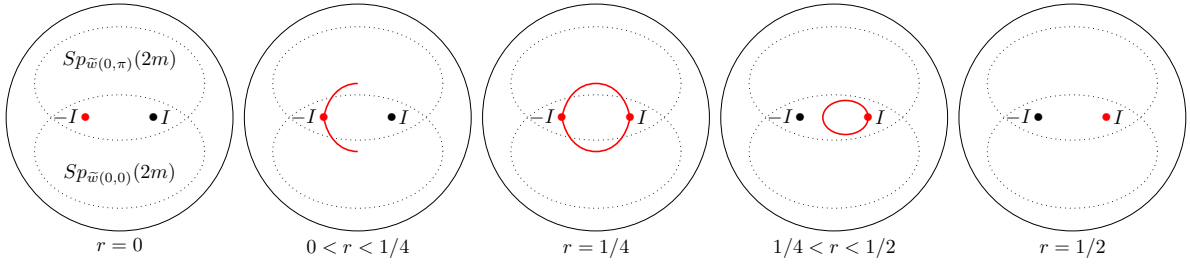


Figure 10.2: Different steps of construction of the contraction t_0 inside $U(2m)$ for $r \in [0, 1/2]$.

to I on upper half of the left edge of \mathbf{BZ}_+ for $0 \leq r \leq 1/2$ that we shall extend to $1/2 \leq r \leq 1$ by I and to the lower half of the left edge by setting

$$t_0(r, k_2) = \tilde{w}(0, -k_2) \overline{t_0(r, -k_2)} \tilde{w}(0, -k_2)^{-1} \quad (10.30)$$

for $r \in [0, 1]$ and $k_2 \in [-\pi, 0]$.

Similarly we construct $t_\pi(r, k_2)$ by spreading $t_{\pi 0}$ and $t_{\pi \pi}$ along the edge $k_1 = \pi$, contracting the loop to I and extending it to $k_2 < 0$ by the time reversal symmetry. This way we get the contraction \tilde{t} on each boundary edge of \mathbf{BZ}_+ defined for $r \in [0, 1]$ and that is equal to I for $r \in [1/2, 1]$.

\tilde{t} on the interior of \mathbf{BZ}_+ . We extend the contractions defined at the boundary edges of \mathbf{BZ}_+ to the interior of \mathbf{BZ}_+ by defining for $(r, k_1, k_2) \in [0, 1/2] \times \mathbf{BZ}_+$

$$\tilde{t}(r, k_1, k_2) = \begin{cases} t_0(r - k_1, k_2) & \text{for } 0 \leq k_1 \leq r \\ -I & \text{for } r \leq k_1 \leq \pi - r \\ t_\pi(k_1 - (\pi - r), k_2) & \text{for } \pi - r \leq k_1 \leq \pi \end{cases} \quad (10.31)$$

mixing this time parameter r with variable k_1 . At $r = 0$ this is nothing but the constant map $-I$ whereas at $r = 1/2$ the map \tilde{t} is I at the edges $k_1 = 0$ and $k_1 = \pi$. Because at all r the contraction the map is continuous and periodic in k_2 the map $\tilde{t}(1/2, \cdot)$ can be seen as a map

defined on the earring (or pinched torus), see Figure 10.3. Since all the building blocks of \tilde{t} take values in $SU(2m)$, there is no obstruction for $\tilde{t}(1/2, \cdot)$ to be contracted continuously to the constant map equal to I , keeping the values at $k_1 = 0, \pi$ equal to I . We use such a contraction by extend \tilde{t} to $r \in [1/2, 1]$. This way we get a time reversal invariant contraction from $-I$ to I on the full effective Brillouin zone BZ_+ .

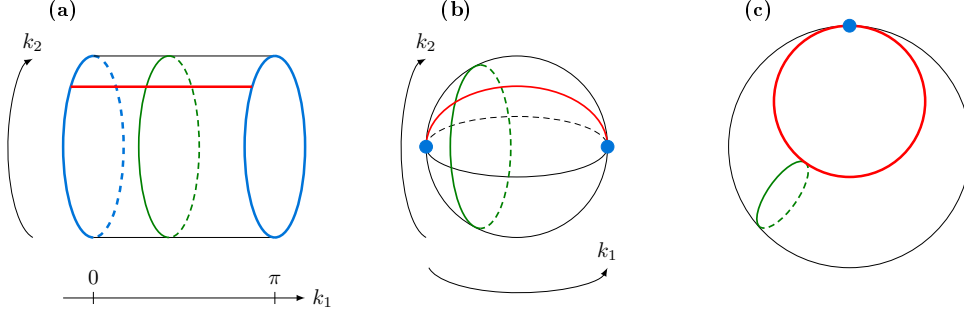


Figure 10.3: Effective Brillouin zone BZ_+ seen as a cylinder. The map $\tilde{t}(1/2, \cdot)$ being equal to I on both edges $k_1 = 0$ and π , it can be seen as a map on a 2-sphere first, then on an earring identifying the two edge points. Since $\tilde{t}(1/2, \cdot) \in SU(2m)$ it can be deformed to the constant map I keeping the value at the edges equal to I . This may be done by first contracting the red loop and then the resulting 2-sphere to I , which is possible since $\pi_1(SU(2m)) = 0 = \pi_2(SU(2m))$.

\tilde{t} on the full torus. Finally, we define for $k_1 \in [-\pi, 0]$

$$\tilde{t}(r, k_1, k_2) = \tilde{w}(-k_1, -k_2) \overline{\tilde{t}(r, -k_1, -k_2)} \tilde{w}(-k_1, -k_2)^{-1} \quad (10.32)$$

obtaining a continuous (or even a piecewise smooth) contraction well defined on $[0, 1] \times BZ$ and satisfying the required properties (10.22) which, besides, takes values in $SU(2m)$, which will simplify the calculation of the Wess-Zumino amplitudes that will reappear soon. Note that, by construction,

$$\tilde{t}(r, a, k_2) = t_a(r, k_2) \quad (10.33)$$

for $(r, k_2) \in [0, 1] \times [-\pi, \pi]$ and $a = 0, \pi$, i.e. t_a are indeed the values of \tilde{t} on the boundary edges of BZ_+ .

10.2.4 Back to the Wess-Zumino amplitudes

We now compute index K starting given by relation

$$K[\mathcal{E}] = \frac{1}{8\pi^2} \int_{[0,1] \times BZ} \tilde{t}^* \chi \mod 2, \quad (10.34)$$

see (10.24), using the just constructed contraction \tilde{t} and reducing the calculation to the edges of BZ_+ by going in the opposite direction than in the previous subsection. First we split the integral over BZ into two parts: over BZ_+ and over its complementary. Using the time-reversal property (10.22) over the latter, we obtain twice the same integral over BZ_+ up to the integral of an exact form that reduces to an integral over the boundary of $[0, 1] \times BZ_+$. Hence

$$\frac{1}{8\pi^2} \int_{[0,1] \times BZ} \tilde{t}^* \chi = \frac{1}{4\pi^2} \int_{[0,1] \times BZ_+} \tilde{t}^* \chi + \mathcal{B}(\tilde{t}), \quad (10.35)$$

where some simple algebra reduces the boundary term to

$$\mathcal{B}(\tilde{t}) = \frac{1}{8\pi^2} \left(\int_{[0,1] \times \{\pi\} \times [-\pi, \pi]} - \int_{[0,1] \times \{0\} \times [-\pi, \pi]} \right) \text{tr} \left(\tilde{w}^{-1} (d\tilde{w}) (\tilde{t}^{-1} (d\tilde{t}) + (d\tilde{t}) \tilde{t}^{-1}) \right) \quad (10.36)$$

with the integral localized at the boundaries of BZ_+ with $k_1 = a$ for $a = 0$ and π . On such boundaries, the explicit contraction (10.31) takes the form (10.33) so that the boundary term $\mathcal{B}(\tilde{t})$ depends only on t_0 and t_π , and only $r \in [0, 1/2]$ is relevant since otherwise the map is constant and the integral vanishes. Moreover t_0 and t_π also have time reversal invariance properties, see (10.30), so that in (10.36) the integral over $[-\pi, \pi]$ can be replaced by twice the same one over $[0, \pi]$ (using the property (10.23) of w). We finally end up with

$$\mathcal{B}(\tilde{t}) = \mathcal{B}(t_\pi) - \mathcal{B}(t_0) \quad (10.37)$$

where

$$\mathcal{B}(t_a) = \frac{1}{4\pi^2} \int_{[0, \frac{1}{2}] \times [0, \pi]} \text{tr} \left((\tilde{w}^{-1} d\tilde{w}) (\overline{t_a^{-1} (dt_a) + (dt_a) t_a^{-1}}) \right). \quad (10.38)$$

This boundary term \mathcal{B} does not vanish, but will actually be compensated by a term coming from the bulk integral over BZ_+ appearing in (10.35), that we shall elaborate upon now.

Since χ is a 3-form and for $r \in [0, 1/2]$ the contraction \tilde{t} actually depends only on 2 variables, see (10.31), the corresponding contribution to the bulk integral in (10.35) vanishes so that

$$\frac{1}{4\pi^2} \int_{[0,1] \times BZ_+} \tilde{t}^* \chi = \frac{1}{4\pi^2} \int_{[\frac{1}{2}, 1] \times BZ_+} \tilde{t}^* \chi \quad (10.39)$$

Then consider the map $\tilde{t}(1/2, \cdot)$ over BZ_+ . At the edges this is the constant map equal to I , and \tilde{t} is k_2 -periodic, so that it can be seen as a map defined on the sphere S^2 obtained by identifying $k_1 = 0$ and $k_1 = \pi$ to two points P_0 and P_π , see Figure 10.4. These boundary properties are preserved along the contraction, the map \tilde{t} restricted to $[1/2, 1] \times BZ_+$ may be seen as defined on $[1/2, 1] \times S^2$ and satisfies $\tilde{t}(1, \cdot) = 1$. Thus we can identify the previous integral of \tilde{t} as giving the Wess-Zumino action. More precisely

$$\frac{1}{4\pi^2} \int_{[\frac{1}{2}, 1] \times BZ_+} \tilde{t}^* \chi = -\frac{1}{\pi} S_{\text{WZ}} [\tilde{t}(\frac{1}{2}, \cdot)] \quad (10.40)$$

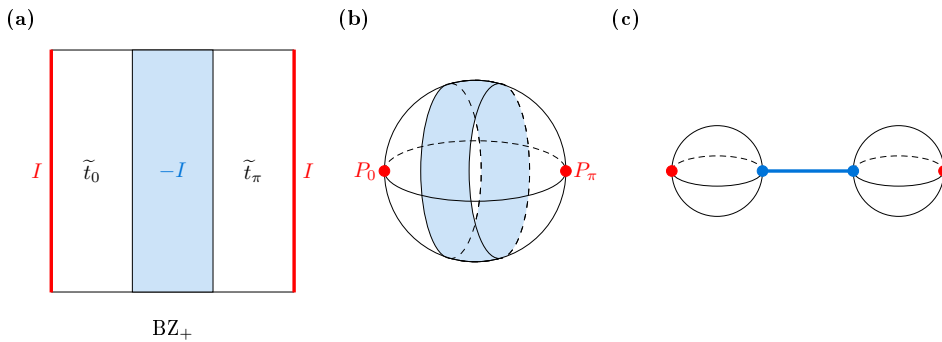


Figure 10.4: The effective Brillouin zone BZ_+ can be seen as a sphere for the map $\tilde{t}(1/2, \cdot)$ since it is k_2 -periodic and equal to I on the edges (a and b). As $\tilde{t}(1/2, \cdot)$ is also equal to $-I$ in an annulus in the interior of BZ_+ , it can even be decomposed in terms of t_0 and t_π seen as maps defined on effective spheres (b and c).

for the field $\tilde{t}(1/2, \cdot)$ viewed as defined on S^2 . Recall that Wess-Zumino action is defined modulo 2π so that the right hand side is well defined modulo 2 which is what is needed in the formula (10.34) for K . Here no further restriction on contraction of $\tilde{t}(1/2, \cdot)$ is required.

Finally, looking more precisely at this map, we observe in (10.31) that it is constant to $-I$ inside the bulk of BZ_+ . The previous Wess-Zumino action on the effective sphere S^2 can be split into two contributions coming from \tilde{t}_0 and \tilde{t}_π by identifying the points where $\tilde{t}(1/2, 1/2, k_2) = -I$ and $\tilde{t}(1/2, \pi - 1/2, k_2) = -I$, leading to two spheres illustrated on Figure 10.4, so that

$$S_{\text{WZ}}[\tilde{t}(1/2, \cdot)] \mod 2\pi = -S_{\text{WZ}}[t_0] + S_{\text{WZ}}[t_\pi] \mod 2\pi \quad (10.41)$$

The corresponding index K can be rewritten in the multiplicative form as

$$(-1)^{K[\mathcal{E}]} = e^{iS_{\text{WZ}}[t_0]} e^{-iS_{\text{WZ}}[t_\pi]} e^{i\pi\mathcal{B}(t_\pi) - i\pi\mathcal{B}(t_0)}, \quad (10.42)$$

where the factors on the right hand side are well defined. By computing K as twice an integral over BZ_+ , plus some boundary terms, we obtained by this tortuous construction an expression for the square root of the Wess-Zumino amplitude (10.14) that involves genuine Wess-Zumino amplitudes of fields t_0 and t_π , that still have to be computed in order to prove that $K[\mathcal{E}]$ coincides with the Kane-Mele invariant.

Chapter 11

Computation of the Wess-Zumino amplitudes

In the two previous parts, the Wess-Zumino amplitudes for a general field $g : \Sigma \mapsto G$ were defined in terms of an extension \tilde{g} over a 3-dimensional manifold $\tilde{\Sigma}$ and coinciding with g on $\partial\tilde{\Sigma} = \Sigma$. This is the original approach of Witten in the construction of Wess-Zumino-Witten models [173]. However such extensions do not make sense when Σ has boundaries. Another approach, based on local description of worldsheet Σ and target manifold M , was proposed in [5, 79]. Recall that if the closed g takes values in an (open) subset of G on which 3-form χ is exact then the Wess-Zumino amplitude is simply given by

$$e^{iS_{WZ}[g]} = \exp\left(\frac{i}{4\pi} \int_{\Sigma} g^* B\right) \quad \text{if} \quad \chi = dB \quad (11.1)$$

without requiring any extension of g . For more general g , it is possible to cover G by open subsets such that χ is exact on each one. Decomposing Σ in a way that g respects the covering, the Wess-Zumino amplitude would be naively the product of contributions (11.1) from different subsets. However the definition must be independent of the choices of the covering of M and decomposition of Σ , and extra terms should appear to ensure such independence.

Such an approach is presented and employed in this chapter in order to compute the Wess-Zumino amplitudes associated to maps t_0 and t_π , first in the case of $SU(2)$, where the construction is simpler, then in the general case.

11.1 Case with rank 2 valence bundle

The case of valence bundle with the smallest (nonzero) rank $2m = 2$ is particularly simple and the coincidence of K with the Kane-Mele invariant may be easily shown. First the structure at TRIM is much simpler than in general case, see Subsection 10.2.2. Indeed when $m = 1$ and at a TRIM (a, a') the only antisymmetric matrices of determinant 1 are

$$\tilde{w}(a, a') = \pm \begin{pmatrix} 0 & 1 \\ -1 & 0 \end{pmatrix} \quad \text{for} \quad a, a' = 0, \pi \quad (11.2)$$

and all subgroups $Sp_{\tilde{w}(a, a')}(2) = SU(2)$. Moreover we may use in this case a more explicit expression for edge contractions t_0 and t_π instead of (10.29). Consider for $(r, k_2) \in [0, 1/2] \times [-\pi, \pi]$ and $a = 0$ or π

$$t_a(r, k_2) = \begin{cases} e^{-2\pi i(1/2-r)\sigma_3} & \text{if } 0 \leq k_2 \leq \pi \\ \tilde{w}(a, k_2) e^{2\pi i(1/2-r)\sigma_3} \tilde{w}(a, k_2)^{-1} & \text{if } -\pi \leq k_2 \leq 0 \end{cases} \quad (11.3)$$

where σ_3 is the Pauli matrix $\text{diag}(1, -1)$. One can check that this formula is continuous at $k_2 = 0$ and k_2 -periodic using the commutation relations between σ_3 and $\tilde{w}(a, a')$. With this choices of t_a , the boundary terms (10.38) become

$$\mathcal{B}(t_a) = \frac{i}{2\pi} \int_0^\pi \text{tr}(\sigma_3(\tilde{w}^{-1}d\tilde{w})(a, k_2)) \quad (11.4)$$

and will be compensated by terms coming from Wess-Zumino amplitudes. The latter are easy to compute in the case of $SU(2)$ -valued maps. Instead of finding an extension of t_a on a 3-dimensional worldsheet, we cover $SU(2)$ by open sets where the 3-form χ is exact. Then the full amplitudes are obtained by gluing properly local expressions.

11.1.1 Covering of $SU(2)$

Consider the following parametrization of $SU(2)$

$$g = \gamma e^{2i\pi s \sigma_3} \gamma^{-1} \quad \text{for} \quad \gamma \in SU(2), \quad s \in [0, \frac{1}{2}] \quad (11.5)$$

in terms of conjugacy classes $\mathcal{C}_{s\sigma_3}$ of $SU(2)$, already used previously for the boundary conditions in the context of quantum wires, see (4.24) in Chapter 4. Note that this parametrization is redundant since γ and $\gamma e^{i\pi x \sigma_3}$ for $x \in \mathbb{R}$ describe the same element. When seeing $SU(2)$ as the 3-sphere S^3 , the parameter s describes the latitude on it, going from the north pole I to the south pole $-I$ when s cross from 0 to $1/2$, see Figure 11.1 right. Consequently, consider the open covering of $SU(2)$ given by

$$O_0 = SU(2) \setminus \{-I\}, \quad O_1 = SU(2) \setminus \{I\} \quad (11.6)$$

corresponding respectively to $0 \leq s < 1/2$ and $0 < s \leq 1/2$ in (11.5). These open subsets are obviously contractible, so that the restriction of 3-form χ must be exact on each one. Namely, one has $\chi|_{O_i} = dB_i$ with

$$B_0 = \text{tr}\left(\gamma^{-1}(d\gamma)e^{2\pi i s \sigma_3}\gamma^{-1}(d\gamma)e^{-\pi i s \sigma_3}\right) + 4\pi i s \text{tr}\left(\sigma_3(\gamma^{-1}(d\gamma))^2\right), \quad (11.7)$$

$$B_1 = \text{tr}\left(\gamma^{-1}(d\gamma)e^{\pi i (s-1)\sigma_3}\gamma^{-1}(d\gamma)e^{2\pi i (s-1)\sigma_3}\right) + 4\pi i (s - \frac{1}{2}) \text{tr}\left(\sigma_3(\gamma^{-1}(d\gamma))^2\right) \quad (11.8)$$

given consistently in terms of parametrization (11.5). Such expressions come from Poincaré Lemma and can be found in [82]. Finally note that on intersection $O_0 \cap O_1$, although not contractible, one has

$$B_0 - B_1 = 2\pi i \text{tr}(\sigma_3(\gamma^{-1}d\gamma)^2) = -2\pi i d \text{tr}(\sigma_3\gamma^{-1}d\gamma) \equiv d\alpha \quad (11.9)$$

which is a closed 2-form that becomes exact when described in the parametrization (11.5).

11.1.2 Rewriting the boundary maps t_a

Expression (11.3) for the maps t_0 and t_a almost respect parametrization (11.5) of $SU(2)$ in terms of conjugacy classes. Having in mind

$$t_a(r, k_2) = \gamma_a(k_2)e^{2\pi i s(r)\sigma_3}\gamma_a(k_2)^{-1} \quad (11.10)$$

we need to find functions $s(r)$ and $\gamma_a(k_2)$ that are continuous, and π -periodic for the latter. Remember that $\tilde{w}(a, a')$ can take only two values, see (11.2). Thus if we set $s(r) = (1/2 - r)$ and

$$\gamma_a(k_2) = \tilde{w}(a, 0) \quad \text{for} \quad 0 \leq k_2 \leq \pi \quad (11.11)$$

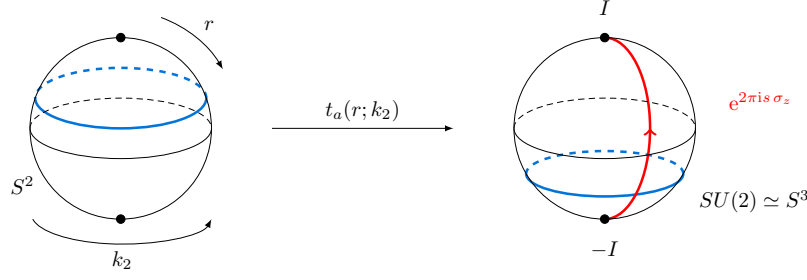


Figure 11.1: Maps t_a send parallels (circles) of S^2 into the parallels (2-spheres) of $SU(2) \cong S^3$ that corresponds to its conjugacy classes, reversing the latitude.

then expressions (11.3) and (11.10) for t_a coincide for the upper part $k_2 \geq 0$. The expression for γ_a when $k_2 \leq 0$ will actually depend on the value of $\tilde{w}(a, \pi)$. We set

$$\gamma_a(k_2) = \begin{cases} \tilde{w}(a, -k_2) & \text{for } -\pi \leq k_2 \leq 0 \quad \text{if } \tilde{w}(a, \pi) = \tilde{w}(a, 0) \\ \tilde{w}(a, -k_2)e^{-ik_2\sigma_3} & \text{for } -\pi \leq k_2 \leq 0 \quad \text{if } \tilde{w}(a, \pi) = -\tilde{w}(a, 0) \end{cases} \quad (11.12)$$

leading to a well defined parametrization (11.10) for t_0 and t_π . Moreover note that $t_a(r, k_2) \in O_0$ for $0 < r \leq 1/2$ and $t_a(r, k_2) \in O_1$ for $0 \leq r < 1/2$. Thus t_a are maps from the 2-sphere to the 3-sphere that reverse the latitude, as illustrated on Figure (11.1).

11.1.3 Computation of Wess-Zumino amplitude

We shall split the arguments (r, k_2) of t_a to $[0, 1/4] \times [-\pi, \pi]$ and $[1/4, 1/2] \times [-\pi, \pi]$. If we view the domain of definition of t_a as the 2-sphere S^2 , then this splits S^2 into the northern and southern hemispheres which are mapped by t_a to the open subsets O_1 and O_0 of $SU(2)$, respectively. The Wess-Zumino action of t_a may be represented in the local form by the expression

$$e^{iS_{WZ}[t_a]} = \exp \left[\frac{i}{4\pi} \int_{[0, \frac{1}{4}] \times [-\pi, \pi]} t_a^* B_1 + \frac{i}{4\pi} \int_{[\frac{1}{4}, \frac{1}{2}] \times [-\pi, \pi]} t_a^* B_0 \right] \text{Hol}_{\mathcal{L}}(t_a(\frac{1}{4}, \cdot)) \quad (11.13)$$

which ensures a consistent definition of Wess-Zumino amplitudes [82]. The first two terms in the right hand side are standard expression when the 3-form χ is exact, the last one ensures that the WZ-amplitude does not depend of the choice of covering of $SU(2)$, of forms B_i nor of the split S^2 . Over $O_1 \cap O_2$, the 2-form $B_0 - B_1$ is closed and defines a Hermitian line bundle \mathcal{L} with unitary connection, whose curvature is $\frac{1}{4\pi}(B_0 - B_1)$ (see next Subsection for a few details). The last term in the previous equation is the holonomy of that connection along the loop $t_a(1/4, k_2)$ for $k_2 \in [-\pi, \pi]$. In this case it has the simple form

$$\text{Hol}_{\mathcal{L}}(t_a(\frac{1}{4}, \cdot)) = \exp \left[\frac{i}{4\pi} \int_{[-\pi, \pi]} \gamma_a^* \alpha \right], \quad (11.14)$$

where 1-form α is given by (11.9).

Note that since γ_a only depends on one variable k_2 , the integrals of the 2-forms B_1 and B_0 in (11.13) vanish because of their explicit expressions (11.7) and (11.8). Only the holonomy term persists and is computed with the previous equation, depends on γ_a and hence of definition (11.12). We end up with

$$\text{Hol}_{\mathcal{L}}(t_a(\frac{1}{4}, \cdot)) = \exp \left[-\frac{1}{2} \int_0^\pi \text{tr} \sigma_3 (\tilde{w}^{-1} d\tilde{w}(a, k_2)) - \left\{ \begin{array}{ll} 0 & \text{if } \tilde{w}(a, \pi) = \tilde{w}(a, 0) \\ \pi i & \text{if } \tilde{w}(a, \pi) = -\tilde{w}(a, 0) \end{array} \right\} \right] \quad (11.15)$$

The first term in the exponential is nothing but the boundary term $i\pi\mathcal{B}(t_a)$ given by (11.4) in that case and will cancel the corresponding term appearing in the expression (10.42) for index K . Finally

$$(-1)^{K[\mathcal{E}]} = \left\{ \begin{array}{ll} 1 & \text{if } \tilde{w}(0, \pi) = \tilde{w}(0, 0) \\ -1 & \text{if } \tilde{w}(0, \pi) = -\tilde{w}(0, 0) \end{array} \right\} \times \left\{ \begin{array}{ll} 1 & \text{if } \tilde{w}(\pi, \pi) = \tilde{w}(\pi, 0) \\ -1 & \text{if } \tilde{w}(\pi, \pi) = -\tilde{w}(\pi, 0) \end{array} \right\} \quad (11.16)$$

In the case of $m = 1$, the Pfaffian $\text{pf}(\tilde{w}(a, a'))$ is just the sign appearing in equation (11.2). Hence the previous expression for $(-1)^K$ might be rewritten in the form

$$(-1)^{K[\mathcal{E}]} = \prod_{\text{TRIM}_{(a, a')}} \frac{1}{\text{pf}(\tilde{w}(a, a'))} = \prod_{\text{TRIM}_{(a, a')}} \frac{\sqrt{\det(w(a, a'))}}{\text{pf}(w(a, a'))} \quad (11.17)$$

with the products over the fours $\text{TRIM } k^* = (a, a')$ of BZ. The latter expression coincides with the multiplicative formula for the Kane-Mele invariant $(-1)^\nu$ obtained in [72] and presented in (9.10), ending the proof of the equality between the \mathbb{Z}_2 -valued indexes $K[\mathcal{E}]$ and ν for the valence bundles \mathcal{E} of rank 2.

11.1.4 Hermitian line bundles with connection

Before going to the general case of general rank, let us stop for a while on the line bundle with connection considered in the previous subsection. Such objects are the building blocks of the structure that will appear for general Wess-Zumino amplitudes. Given a closed 2-form B on a manifold M , one can associate a Hermitian line bundle with connection, whose curvature is $2\pi B$ if B has integral periods in M . This is a theorem established by Weil in [165], and used by Kostant in [112] in the context of geometric quantization (see also [157] for a more pedagogical introduction). We do not give the rigorous proof here but just show how the line bundle arises naturally.

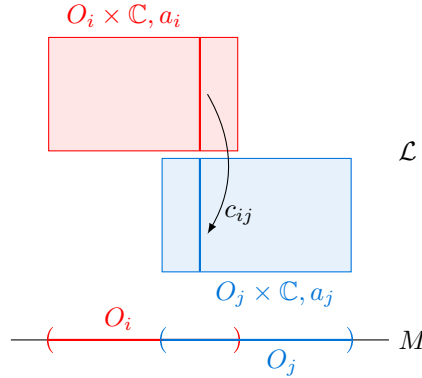


Figure 11.2: Schematic construction of a Hermitian line bundle \mathcal{L} over M from local data for the closed 2-form B .

Consider a manifold M and a closed 2-form $B \in \Omega^2(M)$. We assume that there exist a good open covering $\{O_i\}$ of M , namely such that sets O_i and their successive intersections are contractible. The 2-form B is not globally exact on M , but is exact on each O_i because of the Poincaré lemma, hence there exist a_i such that

$$B|_{O_i} = da_i, \quad a_i \in \Omega^1(O_i). \quad (11.18)$$

Then on each $O_i \cap O_j$ the 1-form $a_i - a_j$ is closed, hence it must be also exact for the same reason as before, so that

$$a_i - a_j = \frac{1}{2\pi i} c_{ij}^{-1} dc_{ij} \quad (11.19)$$

with $c_{ij} : O_i \cap O_j \mapsto \mathbb{C}^*$. Finally, the c_{ij} must be compatible on a triple intersection by satisfying the cocycle condition

$$c_{ij}c_{jk}c_{ki} = 1, \quad (11.20)$$

see below. From this set of data, one can actually build canonically a Hermitian line bundle \mathcal{L} with connection over M , as illustrated in Figure 11.2. Over O_i the line bundle is just the trivial one $O_i \times \mathbb{C}$, and the c_{ij} play the role of transition functions on the intersections $O_i \cap O_j$ that glue such local trivial bundles together to line bundle \mathcal{L} . The one forms a_i are interpreted as connections 1-forms on O_i which define a global connection on \mathcal{L} using the gluing property (11.19). Such a global connection allows for parallel transport in \mathcal{L} . Finally, the curvature of the connection is nothing but the initial closed 2-form B multiplied by 2π . The only additional assumption for this construction to work is that the periods

$$\int_{\mathcal{C}_2} B \in \mathbb{Z} \quad (11.21)$$

for any two-dimensional cycle \mathcal{C}_2 in M . This is actually the condition which guarantees the existence of the transition function c_{ij} satisfying the cocycle condition (11.20) and is also needed for the holonomies to be well defined [157]. It is automatically satisfied on contractible spaces. The Hermitian structure on the fibers of \mathcal{L} is inherited from the one of the trivial bundles $O_i \times \mathbb{C}$.

Hence we can associate to a closed 2-form and its local data a simple geometric structure: a line bundle \mathcal{L} with connection whose curvature is $2\pi B$. Such structure was used above to compute index K in the case $m = 1$. The general case will use the next level of such a construction starting with the 3-form χ . We shall construct a natural geometric structure which contains several line bundles related to 2-forms for χ that is only locally exact.

11.2 The general case

In the case of a valence bundle of dimension $n = 2m$ greater than 2, there is no simple explicit expression for t_0 and t_π such as (11.3) when $m = 1$, so that we need to adopt a more abstract strategy in order to compute the Wess-Zumino amplitudes appearing in (10.42). Forgetting about the sphere picture for the worldsheet developed in Figure 10.4, consider $t_0(r, k_2)$ and $t_\pi(r, k_2)$ as defined on $\Sigma = [0, 1/2] \times [-\pi, \pi]$. Recalling time-reversal property (10.30), we split Σ into two parts

$$\Sigma_+ = [0, 1/2] \times [0, \pi] \quad \text{and} \quad \Sigma_- = [0, 1/2] \times [-\pi, 0] \quad (11.22)$$

which are related by

$$t_a|_{\Sigma_-} = (\tilde{w}_a \bar{t}_a \tilde{w}_a^{-1})|_{\Sigma_+} \circ \vartheta_1 \quad (11.23)$$

where $\tilde{w}_a(r, k_2) \equiv \tilde{w}(a, k_2)$ is independent of r and $\vartheta_1(r, k_2) = (r, -k_2)$ is an orientation-changing diffeomorphism from Σ_+ to Σ_- , such that Wess-Zumino amplitudes of t_a over Σ_+ and Σ_- must be simply related. However these two surfaces have boundaries, that must be taken into account in the computation of the amplitudes. Furthermore, the maps satisfy the following invariance property on the boundary $\partial\Sigma_+$

$$\tilde{w}_a \bar{t}_a \tilde{w}_a^{-1} = t_a \quad (11.24)$$

so that we need to define and compute Wess-Zumino amplitudes for $SU(2m)$ -valued maps defined on surfaces with boundary on which they satisfying invariance property (11.24).

11.2.1 Local data on $SU(n)$

First we cover $SU(n)$ with open subset as in the case $n = 2$. Consider the simple coweights of Lie algebra $\mathfrak{su}(n) = A_{n-1}$, already mentioned in Chapter 8 in the previous part. They are given

by $n - 1$ diagonal $n \times n$ matrices [82]

$$\lambda_i^\vee = \text{diag}\left(\underbrace{\frac{n-i}{n}, \dots, \frac{n-i}{n}}_i, \underbrace{-\frac{i}{n}, \dots, -\frac{i}{n}}_{n-i}\right), \quad i = 1, \dots, n-1 \quad (11.25)$$

and we shall add to them the vanishing matrix $\lambda_0^\vee = 0$ for convenience. Consider a convex combination of such diagonal matrices (this is the positive Weyl alcove of $\mathfrak{su}(n)$)

$$\tau = \sum_{i=0}^{n-1} t_i \lambda_i^\vee, \quad 0 \leq t_i \leq 1 \quad \text{and} \quad \sum_{i=0}^{n-1} t_i = 1. \quad (11.26)$$

Group $SU(n)$ may be covered by n open subsets generated by conjugacy classes

$$O_i = \{g = \gamma e^{2\pi i \tau} \gamma^{-1} \mid \gamma \in SU(n), \tau \text{ such that } t_i > 0\} \quad (11.27)$$

Note that for $n = 2$ one has only $\lambda_1^\vee = 1/2 \sigma_3$ and O_0 and O_1 coincide with the sets given by (11.6). Subsets O_i are contractible so that 3-form χ is exact on each one, namely $\chi|_{O_i} = dB_i$ with smooth 2-forms [82]

$$B_i = \text{tr}\left(\gamma^{-1}(\text{d}\gamma)e^{2\pi i \tau}\gamma^{-1}(\text{d}\gamma)e^{-\pi i \tau}\right) + 4\pi i \text{tr}\left((\tau - \lambda_i^\vee)(\gamma^{-1}(\text{d}\gamma))^2\right), \quad (11.28)$$

for $i = 0, \dots, n$. On intersections $O_{ij} = O_i \cap O_j$, these 2-forms differ by

$$B_{ij} = B_j - B_i = -i \text{tr}\left[\lambda_{ij}^\vee (\gamma^{-1}(\text{d}\gamma))^2\right] \quad (11.29)$$

for $\lambda_{ij}^\vee = \lambda_j^\vee - \lambda_i^\vee$. 2-forms B_{ij} are closed and as explained in Subsection 11.1.4 there exist Hermitian line bundles \mathcal{L}_{ij} with unitary connection whose curvature is equal to $\frac{1}{4\pi} B_{ij}$. Since χ is exact, a Wess-Zumino amplitude can be computed locally on the subsets O_i , but then these local contribution must be glued consistently on their intersections O_{ij} through holonomies over line bundles \mathcal{L}_{ij} , as in (11.13) in the case $m = 1$, or more generally, using parallel transports in \mathcal{L}_{ij} . However this is not the end of the story here since on triple intersections $O_{ijk} = O_i \cap O_j \cap O_k$ that are not empty. The parallel transports in the bundles \mathcal{L}_{ij} , \mathcal{L}_{jk} and \mathcal{L}_{ik} must then be consistently related. We require the existence of isomorphisms of line bundles

$$t_{ijk} : \mathcal{L}_{ij} \otimes \mathcal{L}_{jk} \rightarrow \mathcal{L}_{ik} \quad (11.30)$$

on each O_{ijk} , that preserve the Hermitian structures and connections. Finally, the full picture also requires that such isomorphisms be associative over quadruple intersections O_{ijkl} so that the way to identify $\mathcal{L}_{ij} \otimes \mathcal{L}_{jk} \otimes \mathcal{L}_{kl}$ with \mathcal{L}_{il} does not matter, namely

$$t_{ikl} \circ (t_{ijk} \otimes id) = t_{ijl} \circ (id \otimes t_{jkl}) \quad (11.31)$$

All these properties are necessary to define consistent Wess-Zumino amplitudes [82]. Moreover in the case of $SU(n)$ an explicit construction of line bundles \mathcal{L}_{ij} and isomorphisms t_{ijk} exists from the Kiriliov-Kostant theory of quantization of coadjoint orbits [105, 112]. We do not describe these objects here, to avoid overloading the exposition, but they are implicitly present all along the computations.

Finally note that as announced, this construction is just the generalization of Subsection 11.1.4. Starting with a 3-form, we end up with several 2-forms and hence several line bundles that must be glued consistently. The underlying geometric structure is called a bundle gerbe, and was developed by [131] in a mathematical framework and in [82] in the context of WZW models.

11.2.2 Definition of general Wess-Zumino amplitudes

With the previous structure it is then possible to define properly the Wess-Zumino amplitudes for a field $g : \Sigma \mapsto SU(2m)$, starting with a closed and oriented surface Σ . First we need to triangulate Σ in terms of 2-cells (triangles) c that are glued along their edges e with each edge having two end-points (or vertices) denoted by v . 2-Cells are naturally oriented from the orientation on Σ and each $e \subset \partial c$ inherits orientation from c , as well as each $v \in e \subset c$. To such triangulation we associate a choice of indices i_c and i_e so that $g(c) \subset O_{i_c}$ and $g(e) \subset O_{i_e}$ (this choice is always possible when taking a fine enough triangulation), as illustrated on Figure 11.1.

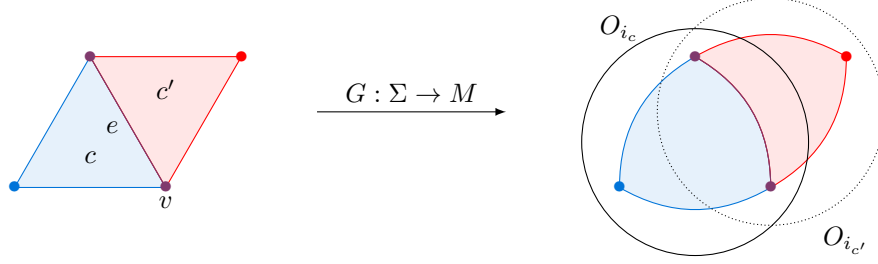


Figure 11.1: Image of the triangulation of Σ by g in the open covering of M . An edge e and a vertex v appear several times with different orientations in definition (11.32) when considering the boundary of all the cells.

The Wess-Zumino amplitudes may be expressed in the form [82]

$$e^{iS_{WZ}[g]} = \exp \left[\frac{i}{4\pi} \sum_c \int_c g^* B_{i_c} \right] \otimes_{e \subset c} \text{Hol}_{\mathcal{L}_{i_c i_e}}(g|_e), \quad (11.32)$$

where the tensor product runs over all the edges e of all the cells c of the triangulation. This is a generalization of (11.13). On each O_{i_c} the 3-form χ is exact so that we know the corresponding contributions to the amplitude and they must be glued consistently ensuring that the previous definition is independent of the triangulation and the choices of i_c , i_e and i_v [79]. Each factor

$$\text{Hol}_{\mathcal{L}_{ij}}(\mathcal{I}) \in (\mathcal{L}_{ij})_{\mathcal{I}_+} \otimes (\mathcal{L}_{ij})_{\mathcal{I}_-}^{-1} \quad (11.33)$$

denotes (somewhat misleadingly) the parallel transport in line bundle \mathcal{L}_{ij} along an oriented line $\mathcal{I} \subset O_{ij} \subset SU(2m)$ joining starting point \mathcal{I}_- to final point \mathcal{I}_+ . The inverse fiber is just the dual fiber and one actually has $\mathcal{L}_{ij}^{-1} = \mathcal{L}_{ji}^* = \mathcal{L}_{ji}$. Unlike in the formula for $SU(2)$, such amplitude takes values *a priori* in a tensor product of fibers of line bundles \mathcal{L}_{ij} over the vertices of the triangulation spaces rather than in complex numbers. However when Σ has no boundaries such tensor product may be canonically identified with \mathbb{C} . First notice that

$$\otimes_{e \subset c} \text{Hol}_{\mathcal{L}_{i_c i_e}}(g|_e) \in \otimes_{v \in e \subset c} (\mathcal{L}_{i_c i_e})_{g(v)}^{\pm 1}, \quad (11.34)$$

where v runs through all the vertices that are boundary points of all the edges in the boundary of all the 2-cells of the triangulation, and the sign of the fiber tells if v is the starting (−) or ending (+) point of edge $e \subset c$. The tensor product at a given vertex v as on the left of Figure 11.2 may be rewritten as the fiber

$$(\mathcal{L}_{i_{e_1} i_{c_1}} \otimes \mathcal{L}_{i_{c_1} i_{e_2}} \otimes \mathcal{L}_{i_{e_2} i_{c_2}} \otimes \mathcal{L}_{i_{c_2} i_{e_3}} \otimes \cdots \otimes \mathcal{L}_{i_{e_n} i_{c_n}} \otimes \mathcal{L}_{i_{c_n} i_{e_1}})_{g(v)} \quad (11.35)$$

of a tensor product of line bundles that can be canonically trivialized using consecutive isomorphisms t_{ijk} defined in (11.30). Note that the order in which we use t_{ijk} does not matter because of the associativity property (11.31), so that the trivialization is not ambiguous. Performing

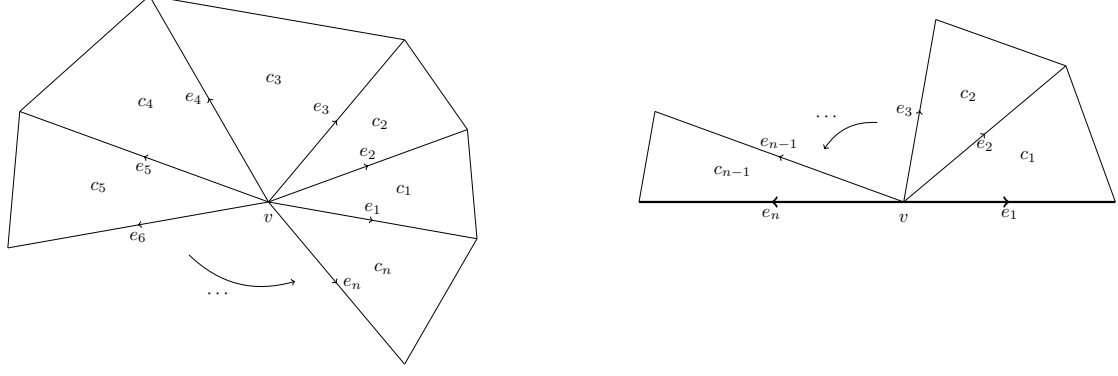


Figure 11.2: *Triangulation around a vertex. Left: when Σ is closed the vertex v appears always both as the end and the beginning of each edge e_i depending on the cell (c_i or c_{i-1}) considered, allowing to trivialize the tensor product of fibers. Right: this is not possible any more when Σ has boundaries since some edges appear only once.*

this trivialization around each vertex v , we end up with a complex number in the definition of Wess-Zumino amplitude (11.32). One can check that this amplitude is consistently defined when changing triangulation, or indices i_c and i_b [79].

In the case where Σ has a boundary composed of a circle \mathcal{C} , $\partial\Sigma = \mathcal{C}$, the previous trivialization at each vertex v still works except for the vertices belonging to \mathcal{C} , see Figure 11.2. In that case we may naturally identify

$$\bigotimes_{v \in b\mathcal{C}} (\mathcal{L}_{i_c i_b})_{g(v)}^{\pm 1} = (\mathbb{L})_{g|\mathcal{C}}, \quad (11.36)$$

where \mathbb{L} is a line bundle over the loop space $LSU(2m) = \{\varphi : S^1 \rightarrow SU(2m)\}$ and $g|_{\mathcal{C}}$ is a boundary loop of $LSU(2m)$. The fibers of \mathbb{L} over loops differing by an orientation-preserving reparametrization may be canonically identified, and those over loops differing by an orientation-changing reparametrization are canonically dual to each other. In that case the Wess-Zumino amplitude is not a complex number but takes values in the line (11.36) that is not canonically trivializable, in general.

Let $D : \Sigma_1 \rightarrow \Sigma_2$ be a diffeomorphism, then one can show that

$$e^{iS_{WZ}[g \circ D]} = \left(e^{iS_{WZ}[g]} \right)^{\pm 1} \quad (11.37)$$

where the inverse is taken if D is orientation changing. In the case of closed surface this is just an equality between complex numbers whereas for surfaces with boundaries the inverse of an element in $\mathbb{L}|\phi$ over a loop ϕ is interpreted as the element in the dual line bundle, that pairs with the original element to 1. Besides the line bundle \mathbb{L} inherits a Hermitian structure from line bundles \mathcal{L}_{ij} and may be equipped with a unitary connection allowing for parallel transport over the loop space.

11.2.3 Application to maps t_a

Each of the surfaces Σ_+ and Σ_- defined in (11.22) and seen as a rectangle has one boundary that is homeomorphic to a circle \mathcal{C} . Thus, according to the previous subsection, the amplitudes over Σ_{\pm}

$$e^{iS_{WZ}[t_a|_{\Sigma_{\pm}}]} \in (\mathbb{L})_{t_a|_{\partial\Sigma_{\pm}}} \quad (11.38)$$

are elements in fibers of \mathbb{L} over the boundary loops of maps t_a . However such boundary loops only differ by the orientation-changing reparametrization so that the corresponding fibers are canonically dual to each other. Thus the full Wess-Zumino amplitude

$$e^{iS_{WZ}[t_a]} = \left\langle e^{iS_{WZ}[t_a|_{\Sigma_-}], e^{iS_{WZ}[t_a|_{\Sigma_+}]} \right\rangle \quad (11.39)$$

remains a complex number. Moreover these two elements in dual fibers are related by the orientation-changing diffeomorphism ϑ_1 , since the maps t_a on Σ_{\pm} satisfy (11.23). Hence, according to (11.37),

$$e^{iS_{WZ}[t_a|_{\Sigma_-}]} = \left(e^{iS_{WZ}[(\tilde{w}_a \overline{t_a} \tilde{w}_a^{-1})|_{\Sigma_+}]} \right)^{-1} \quad (11.40)$$

What remains to do is to compare Wess-Zumino amplitudes for the fields t_a and $\tilde{w}_a \overline{t_a} \tilde{w}_a^{-1}$ on surface Σ_+ with one boundary circle, on which the two fields are equal because of (11.24). The latter field may be seen as a gauged version of t_a by the adjoint action of field \tilde{w}_a with additional complex conjugation. The corresponding amplitudes must be in some sense proportional. The proportionality factor could naively be expected to be given by the same (Polyakov-Wiegman [144]) formula as for surfaces without boundary. It appears, however, that there is an additional factor related to the boundary of Σ_+ which, in the spirit similar to the one discussed in Part 2 of this manuscript, will be later interpreted as the boundary gauge anomaly. We briefly describe the steps of the computation and refer to [44] for the detailed demonstrations.

1. *Local adjoint action.* Consider fields $h, g : \Sigma \rightarrow SU(n)$, with $\partial\Sigma = \mathcal{C}$. One has:

$$\mathbb{I} \left(e^{iS_{WZ}[hgh^{-1}]} \right) = \exp \left[i \int_{\Sigma} (h, g)^* \alpha \right] e^{iS_{WZ}[g]}, \quad (11.41)$$

where

$$\mathbb{I} : (\mathbb{L})_{hgh^{-1}|_{\mathcal{C}}} \rightarrow (\mathbb{L})_{g|_{\mathcal{C}}} \quad (11.42)$$

is an isomorphism between the fibers of \mathbb{L} over loops that are a priori different, allowing to see the previous amplitudes as elements in the same 1-dimensional complex space. The 2-form α over $SU(n) \times SU(n)$ is given by

$$\alpha(h, g) = \frac{k}{4\pi} \text{tr} (g^{-1} dg \wedge h^{-1} dh + (dg)g^{-1} \wedge h^{-1} dh + g^{-1}(h^{-1} dh)g \wedge (h^{-1} dh)), \quad (11.43)$$

compare to Eqs. (7.13) and (7.14) of Subsection 7.1.3 in Part II.

2. *Complex conjugation.* Consider only the field $g : \Sigma \rightarrow SU(n)$ and its complex conjugated \bar{g} . One has:

$$\mathbb{K} \left(e^{iS_{WZ}[\bar{g}]} \right) = e^{iS_{WZ}[g]} \quad \text{where} \quad \mathbb{K} : (\mathbb{L})_{\bar{g}|_{\mathcal{C}}} \rightarrow (\mathbb{L})_{g|_{\mathcal{C}}} \quad (11.44)$$

is an isomorphism between lines allowing to see both amplitudes in the same space.

3. *All together.* Combining the two previous steps, we end up with isomorphism

$$\mathbb{J} : (\mathbb{L})_{h\bar{g}h^{-1}|_{\mathcal{C}}} \rightarrow (\mathbb{L})_{g|_{\mathcal{C}}} \quad (11.45)$$

such that

$$\mathbb{J} \left(e^{iS_{WZ}[h\bar{g}h^{-1}]} \right) = \exp \left[i \int_{\Sigma} (h, g)^* \hat{\alpha} \right] e^{iS_{WZ}[g]}, \quad (11.46)$$

where $\hat{\alpha}(h, g) = \alpha(h, \bar{g})$.

At each step it is possible to compute explicitly isomorphisms \mathbb{I} , \mathbb{K} and \mathbb{J} in terms of local data over $SU(n)$, described in Subsection (11.2.1). Moreover, in the case of boundary maps t_a , the boundary loops $(h\bar{g}h^{-1})|_{\mathcal{C}}$ and $g|_{\mathcal{C}}$ are identical because of property (11.24), so that \mathbb{J} is just a multiplication by a phase in the same fiber. With explicit realization of the isomorphisms, this phase can be understood as follows. Consider the variety¹

$$F = \{(h, g) \in SU(n) \times SU(n) \mid h\bar{g}h^{-1} = h\} \quad (11.47)$$

¹This is not necessarily a manifold, but still the defined quantities are meaningful in our case.

Over the boundary $\partial\Sigma = \mathcal{C}$, our fields h and g take values in F . From the local data \mathcal{L}_{ij} over $SU(2m)$ and the corresponding line bundle \mathbb{L} over its loop space, it is actually possible to construct a Hermitian line bundle $\widehat{\mathcal{J}}$ over F with a unitary connection of curvature $\widehat{\alpha}$, so that the action of \mathbb{J} is just a multiplication by the holonomy of this connection along the loop $(h, g)|_{\mathcal{C}}$. Hence (11.46) finally becomes

$$\text{Hol}_{\widehat{\mathcal{J}}}((h, g)|_{\mathcal{C}}) e^{iS_{\text{WZ}}[h\bar{g}h^{-1}]} = \exp \left[i \int_{\Sigma} (h, g)^* \widehat{\alpha} \right] e^{iS_{\text{WZ}}[g]}, \quad (11.48)$$

where both amplitudes are considered as elements in the fiber $\mathbb{L}_{g|_{\mathcal{C}}}$. Applying to the case where $g = t_a$ and $h = \widetilde{w}_a$, we get

$$e^{iS_{\text{WZ}}[(\widetilde{w}_a \bar{t}_a \widetilde{w}_a^{-1})|_{\Sigma_+}]} = \left(\text{Hol}_{\widehat{\mathcal{J}}}((\widetilde{w}_a, t_a)|_{\partial\Sigma_+}) \right)^{-1} \exp \left[i \int_{\Sigma_+} (\widetilde{w}_a, t_a)^* \widehat{\alpha} \right] e^{iS_{\text{WZ}}[(t_a)|_{\Sigma_+}]} \quad (11.49)$$

Remembering that $\widetilde{w}_a(k_2) = \widetilde{w}(a, k_2)$ is a one variable field, the contribution from the last part of $\widehat{\alpha}$, see (11.43), vanishes so that the integral of $\widehat{\beta}$ over Σ^+ in the previous equation is nothing but $\exp(-i\pi\mathcal{B}(t_a))$ of the boundary term (10.38) appearing in the final expression (10.42) for $K[\mathcal{E}]$. Putting all together, we inject the previous equation into (11.40), and with the fact that $\langle (e^{iS_{\text{WZ}}[t_a]_{\Sigma_+}})^{-1}, e^{iS_{\text{WZ}}[t_a]_{\Sigma_+}} \rangle = 1$ we end up with a final expression for Wess-Zumino amplitude (11.39) of field t_a

$$e^{iS_{\text{WZ}}[t_a]} = \text{Hol}_{\widehat{\mathcal{J}}}((\widetilde{w}_a, t_a)|_{\partial\Sigma_+}) e^{i\pi\mathcal{B}(t_a)} \quad (11.50)$$

such that in expression (10.42) the boundary terms compensate, and $K[\mathcal{E}]$ is reduced to the computation of the holonomies in $\widehat{\mathcal{J}}$ of fields t_0 and t_π over $\partial\Sigma_+$

$$(-1)^{K[\mathcal{E}]} = \frac{\text{Hol}_{\widehat{\mathcal{J}}}((\widetilde{w}_0, t_0)|_{\partial\Sigma_+})}{\text{Hol}_{\widehat{\mathcal{J}}}((\widetilde{w}_\pi, t_\pi)|_{\partial\Sigma_+})}. \quad (11.51)$$

11.2.4 Boundary gauge anomaly interpretation

Upon introducing a coupling to the gauge fields A as in Section 7.1, identity (11.48) may be rewritten in a more suggestive form as

$$\text{Hol}_{\widehat{\mathcal{J}}}((h, g)|_{\mathcal{C}}) e^{iS_{\text{WZ}}[\bar{g}^h, \bar{A}^h]} = e^{iS_{\text{WZ}}[g, A]}, \quad (11.52)$$

where the gauge transformations were defined in (7.11) and 1-form A was supposed to take values in $\mathfrak{su}(N)$ (i.e. in anti-Hermitian matrices). In this form, the holonomy term has a clear interpretation of the “boundary gauge anomaly”, (there exists also a similar version of the above relation without complex conjugations but assuming that $g^h|_{\mathcal{C}} = g|_{\mathcal{C}}$). This provides a link between the themes developed in this part of the thesis and the preceding one.

11.2.5 Calculation of the loop holonomy

The computation of the previous holonomies requires the explicit expressions for local data of line bundle $\widehat{\mathcal{J}}$ over F , that can be found in [44]. Again we just give here the general ideas. First we triangulate the boundary of Σ_+ as illustrated on Figure 11.3 with the four edges $e_0, e_{1/2}, \ell_0$ and ℓ_π of the rectangle.

The holonomies appearing in (11.51) will be computed as a product of local parallel transports along (\widetilde{w}_a, t_a) restricted to those edges, using a local expression for $\widehat{\mathcal{J}}$, and glued together at their intersection using corresponding local isomorphisms. First notice that $t_a|_{e_0} = -I$ and $t_a|_{e_\pi} = I$, so that the corresponding parallel transport in \mathcal{J} along these edges does not contribute, and

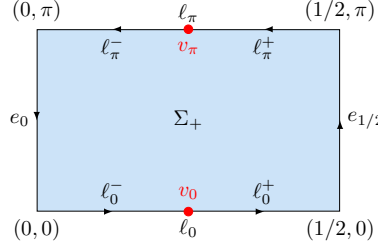


Figure 11.3: Surface Σ_+ and a triangulation of its boundary.

we are left with contribution from ℓ_0 and ℓ_π , where $k_2 = 0$ and π respectively. On such edges, denoted $\ell_{a'}$, maps t_a satisfy

$$t_a(0, a') = -I, \quad t_a(\frac{1}{2}, a') = I, \quad \tilde{w}(a, a') \overline{t_a(r, a')} \tilde{w}(a, a')^{-1} = t_a(r, a'). \quad (11.53)$$

In particular maps $t_a|_{\ell_{a'}}$ take value in the subgroup $Sp_{\tilde{w}(a, a')}(2m)$ defined in (10.27), that is simply connected. Besides, the key point is that curvature $\hat{\alpha}$ of bundle \mathcal{J} vanishes when restricted to $\{\tilde{w}_{a, a'}\} \times Sp_{\tilde{w}(a, a')}(2m)$, so that the holonomies do not depend on the choice of maps $t_a|_{\ell_{a'}}$, provided that they respect the previous constrains. Thus we can use this freedom to choose maps t_a over each boundary $\ell_{a'}$, without bothering how to extend such restriction inside Σ_+ , so that we are able to give explicit expressions as in the $m = 1$ -case. Remember from (10.26) that at each TRIM $k^* = (a, a')$ one has $\tilde{w}(k^*) = u_0 \omega u_0^{-1}$ with a unitary matrix u_0 such that $\det u_0 = \text{pf}(\tilde{w}(k^*))$. Hence we set on each edge $\ell_{a'}$

$$t_a(r, a') = u(a, a') e^{4\pi i(1/2-r)\lambda_m^\vee} u(a, a')^{-1}, \quad (11.54)$$

where

$$u(a, a') = \begin{cases} u_0(a, a') & \text{if } \text{pf}(\tilde{w}(a, a')) = 1 \\ e^{\frac{\pi i}{2m}} u_0(a, a') & \text{if } \text{pf}(\tilde{w}(a, a')) = -1 \end{cases}, \quad (11.55)$$

which is the generalization of the case $m = 1$ where the t_a were given by (11.10), (11.11) and (11.11), but restricted to $k_2 = a'$ here. One can check that such maps satisfy constraints (11.53) (in particular note that whatever m , we always have $\lambda_m^\vee = \text{diag}(1/2, \dots, 1/2, -1/2, \dots, -1/2)$, see (11.25)).

Finally for $r \in [1/4, 1/2]$ one has $t_a \in O_0$ and $r \in [0, 1/4]$ one has $t_a \in O_m$, where the open subsets were defined in (11.27). This structure is transported into F , through open subset \hat{O}_i , such that if we split the edges $\ell_{a'} = \ell_{a'}^+ \cup \ell_{a'}^-$ as in Figure 11.3, and the local parallel transports in \mathcal{J} is trivial along $t_a|_{\ell_{a'}^\pm}$ and we are left only with the gluing isomorphisms at vertices $t_a(v_0)$ and $t_a(v_\pi)$ in the computation of the holonomies. We end up with [44]

$$\text{Hol}_{\hat{\mathcal{J}}}(t_a|_{\Sigma_+}) = \frac{\text{pf}(\tilde{w}(a, \pi))}{\text{pf}(\tilde{w}(a, 0))} \quad (11.56)$$

and index K is given by

$$(-1)^{K[\mathcal{E}]} = \frac{\text{pf}(\tilde{w}(0, \pi)) \text{pf}(\tilde{w}(\pi, 0))}{\text{pf}(\tilde{w}(0, 0)) \text{pf}(\tilde{w}(\pi, \pi))}. \quad (11.57)$$

Since the Pfaffians in the right hand side are ± 1 -valued, this product can be rewritten as in (11.17), i.e. as the Kane-Mele invariant. This concludes the proof.

Chapter 12

Conclusions and perspectives

We have shown in the two previous chapters that the geometric index K coincides with the Kane-Mele invariant. Our construction provides a new geometric interpretation of the Kane-Mele invariant, computed in terms of Wess-Zumino amplitudes requiring advanced techniques developed first for WZW conformal field theory models. The proof was somewhat sinuous and even the initial definition of K might look somewhat artificial. We conclude this part by justifying the natural appearance of index K in the context of periodically driven system, presenting on the way their interesting topological properties. At the end we make some comments on the geometry underlying our constructions and the related open problems.

12.1 Floquet systems

12.1.1 Topological invariant for periodically driven systems

Consider a system with a Hamiltonian $H(t)$ that is time-dependent but periodic, $H(t+T) = H(t)$. For space-periodic crystals, the Bloch decomposition still applies, leading to a family of time-periodic Bloch Hamiltonian $H(t, k)$ over $[0, T] \times \text{BZ}$. Because of time-dependence, energy is not conserved in the system, so that a better family to consider than the Hamiltonians is actually the one of evolution operators $U(t, k)$ solving the equation

$$i\dot{U}(t, k) = H(t, k)U(t, k) \quad \text{and} \quad U(0, k) = I, \quad (12.1)$$

where dot denotes the time derivative. This is a smooth family of unitary operators over $[0, T] \times \text{BZ}$ which, however, is not time-periodic, but satisfies instead $U(t+T, k) = U(t, k)U(T, k)$. Thus the whole information about the evolution is still contained in the time-interval $[0, T]$. Since $[0, T]$ is contractible and U is a smoothly deformable to its constant $t = 0$ value, the homotopy class for this family is trivial. A family of unitaries over $S^1 \times \text{BZ}$ could have instead a nontrivial homotopy class. Hence we construct a periodized version of U , using the Floquet theory [44].

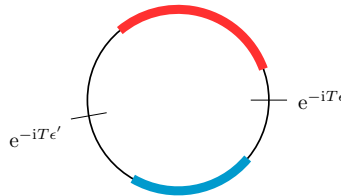


Figure 12.1: Full spectrum of the unitary family $U(T, k)$ for $k \in \text{BZ}$. For each k we have a discrete set of $U(1)$ -valued eigenvalues that describe continuous bands when k moves. We assume such bands to be separated by gaps, in analogy with static insulators.

Assume that at the end of one period, family $U(T, k)$ has at least one common spectral gap, as in Figure 12.1. The eigenvalue of $U(T, k)$ are phases $\lambda(k) \in U(1)$, that are usually written in terms of quasi-energies $\epsilon(k)$ such that $\lambda(k) = e^{-iT\epsilon(k)}$. The quasi-energies are defined modulo $2\pi/T$ so that the corresponding spectrum repeats itself when unrolled. If there exist an ϵ in the gap of the quasi-energy spectrum of the whole family $U(k, T)$, then it is possible to define an effective Hamiltonian H_ϵ^{eff} smoothly depending on k such that

$$U(T, k) = e^{-iT H_\epsilon^{\text{eff}}(k)} \quad (12.2)$$

using the spectral decomposition. H_ϵ^{eff} is, up to the factor $\frac{i}{T}$, given by the logarithm of U with the branch cut at $-T\epsilon$. This allows to define a periodized version of the full family $U(t, k)$ by introducing

$$V_\epsilon(t, k) = U(t, k) e^{it H_\epsilon^{\text{eff}}(k)}. \quad (12.3)$$

The new family is T -periodic, hence it is defined on the 3-torus $S^1 \times \text{BZ}$, and also satisfies $V_\epsilon(0, k) = I = V_\epsilon(T, k)$. It might have a nontrivial homotopy class represented by the degree

$$\deg(V_\epsilon) = \frac{1}{24\pi^2} \int_{[0, T] \times \text{BZ}} \text{tr}(V_\epsilon^{-1} dV_\epsilon)^{\wedge 3} \quad (12.4)$$

already used previously, see (10.2). This is an integer number, called $W_\epsilon[U]$ in [151] in the context of time-periodic systems, and shown there to be a topological invariant analogous to the Chern number. Note, however, that, in contrast to static systems, such invariant is associated to a gap rather than to a band, hence its ϵ -dependence.

It is also possible to impose the time-reversal symmetry on such periodically forced systems by demanding that

$$\Theta H(t, k) \Theta^{-1} = H(-t, -k) \quad \Rightarrow \quad \Theta V_\epsilon(t, k) \Theta^{-1} = V_\epsilon(T - t, -k), \quad (12.5)$$

so that, in that case, family $V_\epsilon(t, k)$ is redundant for $t \in [T/2, T]$. Besides, the previous invariant always vanishes in that case: $\deg(V_\epsilon) = 0$. Another topological invariant was proposed in [45] for time-reversal periodically driven system, by artificially modifying the evolution for V after $T/2$. Consider the map

$$\widehat{V}_\epsilon(t, k) = \begin{cases} V_\epsilon(t, k) & \text{if } 0 \leq t \leq T/2 \\ \widetilde{V}_\epsilon(t, k) & \text{if } T/2 \leq t \leq T \end{cases} \quad (12.6)$$

with $\widetilde{V}_\epsilon(T/2, k) = V_\epsilon(T/2, k)$ and $\widetilde{V}_\epsilon(T, k) = I$ and satisfying

$$\Theta \widetilde{V}_\epsilon(t, k) \Theta^{-1} = \widetilde{V}_\epsilon(t, -k) \quad (12.7)$$

instead of (12.5) for V_ϵ (note that the two relations are compatible at $T/2$). The family $\widehat{V}_\epsilon(t, k)$ is still defined on the 3-torus $S^1 \times \text{BZ}$, and we proved in [44] that

$$K_\epsilon[U] = \deg(\widehat{V}_\epsilon) \mod 2 \quad (12.8)$$

is a well defined topological invariant for such systems that is associated to a quasienergy gap ϵ . In analogy with the Kane-Mele invariant, this quantity is \mathbb{Z}_2 valued. It captures the obstruction of the evolution family U to preserve the corresponding (time evolving) Kramers pairs [45].

Expression (12.8) for $K_\epsilon[U]$ may be also rewritten with the use of the square root of the Wess-Zumino amplitude as

$$(-1)^{K_\epsilon[U]} = \frac{e^{\frac{i}{8\pi} \int_{[0, T/2] \times \text{BZ}} V_\epsilon^* \chi}}{\left(e^{S_{\text{WZ}}[V_\epsilon(T/2)]} \right)^{1/2}}, \quad (12.9)$$

see (10.15).

12.1.2 Relation to the static case

The previous invariants $W_\epsilon[U]$ and $K_\epsilon[U]$ are associated to quasi-energy ϵ that lies in a gap of the family $U(t, k)$ of the evolution operators. A natural question to ask is how they change when taking a different ϵ . In the first case where time-reversal symmetry is broken, it was shown in [151] that, for two quasi-energies ϵ and ϵ' , the difference

$$W_{\epsilon'}[U] - W_\epsilon[U] = C_1[\mathcal{E}_{\epsilon, \epsilon'}] \quad (12.10)$$

is the Chern number associated to the vector bundle $\mathcal{E}_{\epsilon, \epsilon'}$ generated by the eigenstates of operator $U(T, k)$ corresponding to quasi-energies between ϵ and ϵ' . In particular, if the quasi-energy belongs to the same gap, then W is the same, confirming that this invariant is associated to gaps. In the time-reversal case both part of the previous equation vanish, but

$$K_{\epsilon'}[U] - K_\epsilon[U] = K[\mathcal{E}_{\epsilon, \epsilon'}] \quad (12.11)$$

where K on the right hand side is the index defined previously in (10.10), which coincides with the Kane-Mele invariant according to the two previous chapters. Indeed, one can show that operators V_ϵ for different quasi-energies differ by

$$V_{\epsilon'}(t, k) = V_\epsilon(t, k) e^{\frac{2\pi i t}{T} P_{\epsilon, \epsilon'}(k)} \quad (12.12)$$

where $P_{\epsilon, \epsilon'}(k)$ is the family of projectors onto the fibers of $\mathcal{E}_{\epsilon, \epsilon'}$. Thus when taking the difference of K_ϵ , we end up with index K . Conversely, a family of projector $P(k)$ for a static system can be seen as a trivial evolution operator $U = \exp(\frac{2\pi i t}{T} P(k))$, which motivates the definition (10.10) of K .

Topological invariants for periodic systems are naturally defined for a given gap in the quasi-energy instead of a given band for static systems. However the two cases are related: when taking a difference of gap invariants for a periodic system, one obtains a band invariant that can be compared with the corresponding static one.

12.1.3 Possible generalizations

Our expressions for topological indices like (10.13) or (12.9) involve square roots of Wess-Zumino amplitudes. The geometric structure underlying the Wess-Zumino amplitudes involves the theory of bundle gerbes, presented informally in Section 11.2 as consistent collections of local line bundle \mathcal{L}_{ij} over $SU(2m)$. Such theory allows to treat Wess-Zumino amplitudes in more general situations [82]. In such cases, handling square roots of Wess-Zumino amplitudes requires an introduction of a time-reversal equivariant structures on gerbes, roughly exhibiting their consistent behavior under the action of Θ . The geometry of time-reversal equivariant gerbes is still under construction.

Once such theory developed, it could be used to tackle topological problems of various kind involving time-reversal invariance. An extension to 3-dimensional system seems for example accessible and related to square roots of Wess-Zumino amplitude for fields restricted to the boundaries of the effective Brillouin zone. In particular, the relation between strong and weak index for 3-dimensional Kane-Mele invariant, as well as its Floquet version, may be understood in this approach. Another possible generalization would be to consider amplitudes for field valued in other groups than $U(N)$ (the bundle gerbes have been constructed for any simple Lie group, even not simply connected [81]). It could describe systems with additional symmetries, for example of the initial lattice. Moreover, the equivariant structures relative to the time-reversal can in principle be adapted to the other symmetries appearing in the classification of topological insulators from Table 9.1. Finally, systems with boundaries are a interesting direction for investigation in terms of Wess-Zumino amplitudes. Such an investigation could contribute to a better understanding of the bulk-edge correspondence and of the conformal field theory description of the edge modes.

12.2 Conclusions

We have shown in the present part of the thesis that the Kane-Mele invariant, for time-reversal invariant topological insulators in dimension two coincides with a geometric quantity $K[\mathcal{E}]$ associated to a contraction to identity of a family of unitary operator U_P preserving the time-reversal structure all along the contraction. Such unitary families are canonically related to families of projectors associated to the valence band of the system. Definition of index $K[\mathcal{E}]$ came from the context of periodically driven systems, where the physical time plays the role of contraction parameter, which is then replaced by a formal parameter for the static case.

Index $K[\mathcal{E}]$ naturally involves Wess-Zumino amplitudes in its computation. More exactly, $K[\mathcal{E}]$ may be directly interpreted as a square root of Wess-Zumino amplitude for the field U_P . Although nontrivial, the underlying structure of bundle gerbes needed to compute such square roots seems a powerful tool that, once fully developed, suggests various interesting perspectives for other topological problems that could be tackled with such conformal field theory related techniques.

Chapter 13

General conclusion

This work has shown the ubiquitous aspect of conformal field theory and its geometric formalism relating systems, models and problems *a priori* independent. From nonequilibrium junctions of quantum wires to two-dimensional topological insulators, passing by global gauge anomalies in coset models, the power of the approach showed in the mathematical constructions well under control at each step from the Lagrangian formulation to the quantum description, with the functional integral often helpful or even necessary to understand specifics aspects.

If the nonequilibrium transport properties for junctions of quantum wires were well understood for few different models, in particular in the asymptotic regime of large scales and long times, the formalism has also shown its limits in the promising case of the coset-brane junction mixing nonabelian theories at a contact point with nontrivial scattering. Although the underlying conformal field theory is, in principle, exactly solvable, some explicit quantities are still unknown, and an indirect approach might be needed to circumvent this difficulty. The bosonic junction, easier to handle, opened some interesting perspectives for extracting nonequilibrium properties of more complicated networks of quantum wires. This direction seems more accessible.

My contribution to the classification of global gauge anomalies described here came mainly at the end of the story, providing a definite answer to the question: which coset models suffer from such anomalies for a closed worldsheet and a simple Lie groups? It was the first task that I tackled in my thesis work and a good opportunity to learn both the basics of conformal field theory and the subtle structure of semi-simple Lie algebras and subalgebras that play an important role in many physical theories. Generalizations of the work presented here to supersymmetric or T-dual models seems possible, but another direction on the crossroads between anomalies and conformal field theory suggested by the problems discussed in the third part of the thesis may be more attractive.

The calculation of the index that we have defined for time-reversal invariant two-dimensional topological insulators and which, at the end, was shown to give the Kane-Mele invariant, involved the appearance of a gauge anomaly on worldsheet with boundaries. This part was in some sense a preliminary work, leading to various open questions. The study of geometric structures underlying our approach should lead to a better understanding of relations between anomalies and topological torsion invariants for insulators, as e.g. the ones discussed in [154] or [153]. As already mentioned, refining such structures to capture the case of systems with boundaries should provide a better understanding of the bulk-edge correspondence and the conformal field theory content of edge modes. Since the edges of topological insulators can be viewed as realizations of quantum wires, this would provide a step further in building links between the three different aspects of my thesis work.

Bibliography

- [1] I. AFFLECK and A.W.W. LUDWIG. “Critical theory of overscreened Kondo fixed points”. In: *Nucl. Phys. B* 360.2-3 (1991), pp. 641–696. DOI: [10.1016/0550-3213\(91\)90419-X](https://doi.org/10.1016/0550-3213(91)90419-X).
- [2] A. ALEKSEEV and V. SCHOMERUS. “D-branes in the WZW model”. In: *Phys. Rev. D* 60.6 (1999), p. 061901. DOI: [10.1103/PhysRevD.60.061901](https://doi.org/10.1103/PhysRevD.60.061901).
- [3] A. ALTLAND and B. SIMONS. *Condensed Matter Field Theory*. Cambridge University Press, 2006. ISBN: 9780521845083. DOI: [10.1017/CB09780511804236](https://doi.org/10.1017/CB09780511804236).
- [4] A. ALTLAND and M.R. ZIRNBAUER. “Nonstandard symmetry classes in mesoscopic normal-superconducting hybrid structures”. In: *Phys. Rev. B* 55 (2 1997), pp. 1142–1161. DOI: [10.1103/PhysRevB.55.1142](https://doi.org/10.1103/PhysRevB.55.1142).
- [5] O. ALVAREZ. “Topological quantization and cohomology”. In: *Comm. Math. Phys.* 100 (1985), pp. 279–309. DOI: [10.1007/BF01212452](https://doi.org/10.1007/BF01212452).
- [6] D. ANDRIEUX et al. “The fluctuation theorem for currents in open quantum systems”. In: *New J. Phys.* 11.4 (2009), p. 043014. DOI: [10.1088/1367-2630/11/4/043014](https://doi.org/10.1088/1367-2630/11/4/043014).
- [7] H. ARAKI and E. J. WOODS. “Representations of the Canonical Commutation Relations Describing a Nonrelativistic Infinite Free Bose Gas”. In: *J. Math. Phys.* 4 (1963), pp. 637–662. DOI: [10.1063/1.1704002](https://doi.org/10.1063/1.1704002).
- [8] J.C. AVILA, H. SCHULZ-BALDES, and C. VILLEGAS-BLAS. “Topological Invariants of Edge States for Periodic Two-Dimensional Models”. In: *Mathematical Physics, Analysis and Geometry* 16.2 (2013), pp. 137–170. DOI: [10.1007/s11040-012-9123-9](https://doi.org/10.1007/s11040-012-9123-9).
- [9] J.E. AVRON, R. SEILER, and B. SIMON. “Homotopy and quantization in condensed matter physics”. In: *Phys. Rev. Lett.* 51.1 (1983), p. 51. DOI: [10.1103/PhysRevLett.51.51](https://doi.org/10.1103/PhysRevLett.51.51).
- [10] J.C. BAEZ and J.P. MUNIAIN. *Gauge Fields, Knots, and Gravity*. K & E series on knots and everything. World Scientific, 1994. ISBN: 9789810217297. DOI: [10.1142/2324](https://doi.org/10.1142/2324).
- [11] K. BARDAKCI, E. RABINOVICI, and B. SÄRING. “String models with $c < 1$ components”. In: *Nucl. Phys. B* 299.1 (1988), pp. 151–182. DOI: [10.1016/0550-3213\(88\)90470-1](https://doi.org/10.1016/0550-3213(88)90470-1).
- [12] M. BAUER and D. BERNARD. “2D growth processes: SLE and Loewner chains”. In: *Physics Reports* 432 (2006), pp. 115–221. DOI: [10.1016/j.physrep.2006.06.002](https://doi.org/10.1016/j.physrep.2006.06.002).
- [13] A.A. BELAVIN, A.M. POLYAKOV, and A.B. ZAMOLODCHIKOV. “Infinite conformal symmetry in two-dimensional quantum field theory”. In: *Nucl. Phys. B* 241.2 (1984), pp. 333–380. DOI: [10.1016/0550-3213\(84\)90052-X](https://doi.org/10.1016/0550-3213(84)90052-X).
- [14] B. BELLAZZINI, M. MINTCHEV, and P. SORBA. “Bosonization and scale invariance on quantum wires”. In: *J. Phys. A* 40.10 (2007), p. 2485. DOI: [10.1088/1751-8113/40/10/017](https://doi.org/10.1088/1751-8113/40/10/017).

- [15] J. BELLISSARD, A. v. ELST, and H. SCHULZ-BALDES. “The noncommutative geometry of the quantum Hall effect”. In: *J. Math. Phys.* 35.10 (1994), pp. 5373–5451. DOI: [10.1063/1.530758](https://doi.org/10.1063/1.530758).
- [16] D. BERNARD and B. DOYON. “A hydrodynamic approach to non-equilibrium conformal field theories”. In: *ArXiv eprints* (2015). arXiv: [1507.07474](https://arxiv.org/abs/1507.07474).
- [17] D. BERNARD and B. DOYON. “Energy flow in non-equilibrium conformal field theory”. In: *J. Phys. A* 45.36 (2012), p. 362001. DOI: [10.1088/1751-8113/45/36/362001](https://doi.org/10.1088/1751-8113/45/36/362001).
- [18] D. BERNARD and B. DOYON. “Non-Equilibrium Steady States in Conformal Field Theory”. In: *Annales Henri Poincaré* 16.1 (2015), pp. 113–161. DOI: [10.1007/s00023-014-0314-8](https://doi.org/10.1007/s00023-014-0314-8).
- [19] D. BERNARD and B. DOYON. “Time-reversal symmetry and fluctuation relations in non-equilibrium quantum steady states”. In: *J. Phys. A* 46.37 (2013), p. 372001. DOI: [10.1088/1751-8113/46/37/372001](https://doi.org/10.1088/1751-8113/46/37/372001).
- [20] D. BERNARD, B. DOYON, and J. VITI. “Non-equilibrium conformal field theories with impurities”. In: *J. Phys. A* 48.5 (2015), 05FT01. DOI: [10.1088/1751-8113/48/5/05FT01](https://doi.org/10.1088/1751-8113/48/5/05FT01).
- [21] D. BERNARD et al. “Conformal invariance in two-dimensional turbulence”. In: *Nature Physics* 2.2 (2006), pp. 124–128. DOI: [10.1038/nphys217](https://doi.org/10.1038/nphys217).
- [22] B.A. BERNEVIG and T.L. HUGHES. *Topological insulators and topological superconductors*. Princeton University Press, 2013. ISBN: 9781400846733. URL: <http://books.google.fr/books?id=wOn7JHSSxrsC>.
- [23] B.A. BERNEVIG, T.L. HUGHES, and S.-C. ZHANG. “Quantum spin Hall effect and topological phase transition in HgTe quantum wells”. In: *Science* 314.5806 (2006), pp. 1757–1761. DOI: [10.1126/science.1133734](https://doi.org/10.1126/science.1133734).
- [24] R.A. BERTLMANN. *Anomalies in quantum field theory*. Vol. 91. Oxford University Press, 2000. ISBN: 9780198507628. DOI: [10.1093/acprof:oso/9780198507628.001.0001](https://doi.org/10.1093/acprof:oso/9780198507628.001.0001).
- [25] M. J. BHASEEN et al. “Energy flow in quantum critical systems far from equilibrium”. In: *Nature Physics* 11 (6 2015). DOI: [10.1038/nphys3220](https://doi.org/10.1038/nphys3220).
- [26] Y. M. BLANTER and M. BÜTTIKER. “Shot Noise in Mesoscopic Conductors”. In: *Physics Reports* 336 (2000), pp. 1–166. DOI: [10.1016/S0370-1573\(99\)00123-4](https://doi.org/10.1016/S0370-1573(99)00123-4).
- [27] F. BLOCH. “Über die quantenmechanik der elektronen in kristallgittern [About the quantum mechanics of electrons in crystal lattices]”. German. In: *Z. Phys* 52 (1927), pp. 555–600. DOI: [10.1007/BF01339455](https://doi.org/10.1007/BF01339455).
- [28] R. BOTT and J.R. SEELEY. “Some remarks on the paper of Callias: “Axial anomalies and index theorems on open spaces””. In: *Comm. Math. Phys.* 62 (1978), pp. 235–245. URL: <http://projecteuclid.org/euclid.cmp/1103904396>.
- [29] N. BOURBAKI. *Groupes et Algebres de Lie, Chapitres 4, 5 et 6*. French. Hermann, Paris, 1968. ISBN: 9783540344919. URL: <https://books.google.fr/books?id=4NpGP9BbdygC>.
- [30] P. BOWCOCK. “Canonical quantisation of the gauged Wess-Zumino model”. In: *Nucl. Phys. B* 316 (1989), pp. 80–100. DOI: [10.1016/0550-3213\(89\)90387-8](https://doi.org/10.1016/0550-3213(89)90387-8).
- [31] M. BÜTTIKER. “Four-terminal phase-coherent conductance”. In: *Phys. Rev. Lett.* 57.14 (1986), p. 1761. DOI: [10.1103/PhysRevLett.57.1761](https://doi.org/10.1103/PhysRevLett.57.1761).
- [32] M. BÜTTIKER. “Scattering theory of thermal and excess noise in open conductors”. In: *Phys. Rev. Lett.* 65.23 (1990), p. 2901. DOI: [10.1103/PhysRevLett.65.2901](https://doi.org/10.1103/PhysRevLett.65.2901).
- [33] M. BÜTTIKER et al. “Generalized many-channel conductance formula with application to small rings”. In: *Phys. Rev. B* 31 (10 1985), pp. 6207–6215. DOI: [10.1103/PhysRevB.31.6207](https://doi.org/10.1103/PhysRevB.31.6207).

- [34] A. CAPPELLI, L.S. GEORGIEV, and I.T. TODOROV. “A Unified Conformal Field Theory Description of Paired Quantum Hall States”. In: *Comm. Math. Phys.* 205 (1999), pp. 657–689. DOI: [10.1007/s002200050693](https://doi.org/10.1007/s002200050693).
- [35] A. CAPPELLI, C. ITZYKSON, and J.-B. ZUBER. “Modular invariant partition functions in two dimensions”. In: *Nucl. Phys. B* 280 (1987), pp. 445–465. DOI: [10.1016/0550-3213\(87\)90155-6](https://doi.org/10.1016/0550-3213(87)90155-6).
- [36] A. CAPPELLI, C. ITZYKSON, and J.-B. ZUBER. “The ADE classification of minimal and A1 (1) conformal invariant theories”. In: *Comm. Math. Phys.* 113.1 (1987), pp. 1–26. DOI: [10.1007/BF01221394](https://doi.org/10.1007/BF01221394).
- [37] J.L. CARDY. “Boundary conditions, fusion rules and the Verlinde formula”. In: *Nucl. Phys. B* 324.3 (1989), pp. 581–596. DOI: [10.1016/0550-3213\(89\)90521-X](https://doi.org/10.1016/0550-3213(89)90521-X).
- [38] J.L. CARDY. “Conformal field theory comes of age”. In: *Phys. World* 6N12 (1993), pp. 29–33.
- [39] J.L. CARDY. “Conformal invariance and surface critical behavior”. In: *Nucl. Phys. B* 240.4 (1984), pp. 514–532. DOI: [10.1016/0550-3213\(84\)90241-4](https://doi.org/10.1016/0550-3213(84)90241-4).
- [40] J.L. CARDY. “Effect of boundary conditions on the operator content of two-dimensional conformally invariant theories”. In: *Nucl. Phys. B* 275.2 (1986), pp. 200–218. DOI: [10.1016/0550-3213\(86\)90596-1](https://doi.org/10.1016/0550-3213(86)90596-1).
- [41] J.L. CARDY. “Operator Content of Two-Dimensional Conformally Invariant Theories”. In: *Nucl. Phys. B* 270 (1986), pp. 186–204. DOI: [10.1016/0550-3213\(86\)90552-3](https://doi.org/10.1016/0550-3213(86)90552-3).
- [42] J.L. CARDY. “SLE for theoretical physicists”. In: *Annals of Physics* 318 (2005), pp. 81–118. DOI: [10.1016/j.aop.2005.04.001](https://doi.org/10.1016/j.aop.2005.04.001).
- [43] J.L. CARDY. “The ubiquitous ‘c’: from the Stefan-Boltzmann law to quantum information”. In: *J. Stat. Mech.* 2010.10 (2010), P10004. DOI: [10.1088/1742-5468/2010/10/P10004](https://doi.org/10.1088/1742-5468/2010/10/P10004).
- [44] D. CARPENTIER et al. “Construction and properties of a topological index for periodically driven time-reversal invariant 2D crystals”. In: *Nucl. Phys. B* 896 (2015), pp. 779–834. DOI: [10.1016/j.nuclphysb.2015.05.009](https://doi.org/10.1016/j.nuclphysb.2015.05.009).
- [45] D. CARPENTIER et al. “Topological index for periodically driven time-reversal invariant 2d systems”. In: *Phys. Rev. Lett.* 114.10 (2015), p. 106806. DOI: [10.1103/PhysRevLett.114.106806](https://doi.org/10.1103/PhysRevLett.114.106806).
- [46] C.-Z. CHANG et al. “Experimental observation of the quantum anomalous Hall effect in a magnetic topological insulator”. In: *Science* 340.6129 (2013), pp. 167–170. DOI: [10.1126/science.1234414](https://doi.org/10.1126/science.1234414).
- [47] E. CHARPENTIER and K. GAWĘDZKI. “Wess-Zumino-Witten conformal field theory for simply laced groups at level one”. In: *Annals of Physics* 213.2 (1992), pp. 233–294. DOI: [10.1016/0003-4916\(92\)90047-P](https://doi.org/10.1016/0003-4916(92)90047-P).
- [48] S. DATTA. *Electronic transport in mesoscopic systems*. Cambridge University Press, 1997. ISBN: 9780521599436. DOI: [10.1017/CB09780511805776](https://doi.org/10.1017/CB09780511805776).
- [49] P. DE FROMONT, K. GAWĘDZKI, and C. TAUBER. “Global gauge anomalies in coset models of conformal field theory”. In: *Comm. Math. Phys.* 328.3 (2014), pp. 1371–1400. DOI: [10.1007/s00220-014-1995-z](https://doi.org/10.1007/s00220-014-1995-z).
- [50] P. DI FRANCESCO, P. MATHIEU, and D. SÉNÉCHAL. *Conformal field theory*. Springer, 1997. DOI: [10.1007/978-1-4612-2256-9](https://doi.org/10.1007/978-1-4612-2256-9).

- [51] P. DI VECCHIA, B. DURHUUS, and J. L. PETERSEN. “The Wess-Zumino action in two dimensions and non-abelian bosonization”. In: *Phys. Lett. B* 144 (1984), pp. 245–249. DOI: [10.1142/S0217751X95000772](https://doi.org/10.1142/S0217751X95000772).
- [52] B. DOYON, M. HOOGEVEEN, and D. BERNARD. “Energy flow and fluctuations in non-equilibrium conformal field theory on star graphs”. In: *J. Stat. Mech.* 2014 (2014), P03002. DOI: [10.1088/1742-5468/2014/03/P03002](https://doi.org/10.1088/1742-5468/2014/03/P03002).
- [53] Benjamin DOYON. “Lower bounds for ballistic current and noise in non-equilibrium quantum steady states”. In: *Nucl. Phys. B* 892 (2015), pp. 190–210. DOI: [10.1016/j.nuclphysb.2015.01.007](https://doi.org/10.1016/j.nuclphysb.2015.01.007).
- [54] E.B. DYNKIN. “Maximal subgroups of the classical groups”. In: *Trudy Moskovskogo Matematicheskogo Obshchestva* 1 (1952), pp. 39–166. DOI: [10.1007/BF01388470](https://doi.org/10.1007/BF01388470).
- [55] E.B. DYNKIN. “Semisimple subalgebras of semisimple Lie algebras”. In: *Matematicheskii Sbornik* 72.2 (1952), pp. 349–462. DOI: [10.1090/S0077-1554-06-00156-7](https://doi.org/10.1090/S0077-1554-06-00156-7).
- [56] S. ELITZUR and G. SARKISSIAN. “D-branes on a gauged WZW model”. In: *Nucl. Phys. B* 625.1 (2002), pp. 166–178. DOI: [10.1016/S0550-3213\(02\)00010-X](https://doi.org/10.1016/S0550-3213(02)00010-X).
- [57] W. EUGENE and I. AFFLECK. “Tunneling in quantum wires: A boundary conformal field theory approach”. In: *Nucl. Phys. B* 417.3 (1994), pp. 403–438. DOI: [10.1016/0550-3213\(94\)90479-0](https://doi.org/10.1016/0550-3213(94)90479-0).
- [58] B.L. FEIGIN and D.B. FUKS. “Verma modules over the virasoro algebra”. In: *Functional Analysis and Its Applications* 17.3 (1983), pp. 241–242. DOI: [10.1007/BF01078118](https://doi.org/10.1007/BF01078118).
- [59] G. FELDER, K. GAWĘDZKI, and A. KUPIAINEN. “Spectra of Wess-Zumino-Witten models with arbitrary simple groups”. In: *Comm. Math. Phys.* 117.1 (1988), pp. 127–158. DOI: [10.1007/BF01228414](https://doi.org/10.1007/BF01228414).
- [60] G. FELDER et al. “The geometry of WZW branes”. In: *J. Geom. Phys.* 34.2 (2000), pp. 162–190. DOI: [10.1016/S0393-0440\(99\)00061-3](https://doi.org/10.1016/S0393-0440(99)00061-3).
- [61] P. FENDLEY, A.W.W. LUDWIG, and H. SALEUR. “Exact nonequilibrium transport through point contacts in quantum wires and fractional quantum Hall devices”. In: *Phys. Rev. B* 52 (12 1995), pp. 8934–8950. DOI: [10.1103/PhysRevB.52.8934](https://doi.org/10.1103/PhysRevB.52.8934).
- [62] D. FERRARO et al. “Real-Time Decoherence of Landau and Levitov Quasiparticles in Quantum Hall Edge Channels”. In: *Phys. Rev. Lett.* 113 (16 2014), p. 166403. DOI: [10.1103/PhysRevLett.113.166403](https://doi.org/10.1103/PhysRevLett.113.166403).
- [63] J. FIGUEROA-O’FARRILL and S. STANCIU. “Gauged Wess-Zumino terms and equivariant cohomology”. In: *Phys. Lett. B* 341.2 (1994), pp. 153–159. DOI: [10.1016/0370-2693\(94\)90304-2](https://doi.org/10.1016/0370-2693(94)90304-2).
- [64] D. FIORENZA, D. MONACO, and G. PANATI. “ Z_2 invariants of topological insulators as geometric obstructions”. In: *arXiv preprint* (2014). arXiv: [1408.1030](https://arxiv.org/abs/1408.1030).
- [65] E. FRADKIN. *Field Theories of Condensed Matter Physics*. Cambridge University Press, 2013. ISBN: 9781139015509. DOI: [10.1017/CB09781139015509](https://doi.org/10.1017/CB09781139015509).
- [66] D.S. FREED and G.W. MOORE. “Twisted equivariant matter”. In: *Annales Henri Poincaré* 14.8 (2013), pp. 1927–2023. DOI: [10.1007/s00023-013-0236-x](https://doi.org/10.1007/s00023-013-0236-x).
- [67] E. FRENKEL and D. BEN-ZVI. *Vertex Algebras and Algebraic Curves: Second Edition*. American Mathematical Society, 2004. ISBN: 978-0-8218-3674-3. URL: <http://books.google.fr/books?id=r82mAgAAQBAJ>.
- [68] I. FRENKEL, J. LEPOWSKY, and A. MEURMAN. *Vertex Operator Algebras and the Monster*. Pure and Applied Mathematics. Elsevier, 1989. ISBN: 9780080874548. URL: <http://books.google.com/books?id=y0C90FC1YSUC>.

- [69] D. FRIEDAN, Z. QIU, and S. SHENKER. “Conformal Invariance, Unitarity, and Critical Exponents in Two Dimensions”. In: *Phys. Rev. Lett.* 52 (18 1984), pp. 1575–1578. DOI: [10.1103/PhysRevLett.52.1575](https://doi.org/10.1103/PhysRevLett.52.1575).
- [70] M. FRUCHART and D. CARPENTIER. “An introduction to topological insulators”. In: *Comptes Rendus Physique* 14.9 (2013), pp. 779–815. DOI: [10.1016/j.crhy.2013.09.013](https://doi.org/10.1016/j.crhy.2013.09.013).
- [71] M. FRUCHART, D. CARPENTIER, and K. GAWĘDZKI. “Parallel transport and band theory in crystals”. In: *Europhysics Letters* 106.6 (2014), p. 60002. DOI: [10.1209/0295-5075/106/60002](https://doi.org/10.1209/0295-5075/106/60002).
- [72] L. FU and C.L. KANE. “Time reversal polarization and a Z_2 adiabatic spin pump”. In: *Phys. Rev. B* 74.19 (2006), p. 195312. DOI: [10.1103/PhysRevB.74.195312](https://doi.org/10.1103/PhysRevB.74.195312).
- [73] J. FUCHS and C. SCHWEIGERT. *Symmetries, Lie algebras and representations: A graduate course for physicists*. Cambridge University Press, 2003. URL: https://books.google.fr/books?id=B_JQryjNYyAC.
- [74] M. GABERDIEL. “Boundary conformal field theory and D-branes”. In: *TMR network school, Budapest* (2003). URL: <http://www.phys.ethz.ch/~mrg/lectures2.pdf>.
- [75] M.R. GABERDIEL and H.G. KAUSCH. “A Local logarithmic conformal field theory”. In: *Nucl. Phys. B* 538 (1999), pp. 631–658. DOI: [10.1016/S0550-3213\(98\)00701-9](https://doi.org/10.1016/S0550-3213(98)00701-9).
- [76] K. GAWĘDZKI. “Boundary WZW, G/H , G/G and CS theories”. In: *Annales Henri Poincaré* 3 (2002), pp. 847–881. DOI: [10.1007/s00023-002-8639-0](https://doi.org/10.1007/s00023-002-8639-0).
- [77] K. GAWĘDZKI. “Conformal field theory: a case study”. In: *arXiv preprint* (1999). arXiv: [hep-th/9904145](https://arxiv.org/abs/hep-th/9904145).
- [78] K. GAWĘDZKI. “Constructive conformal field theory”. In: *Functional Integration, Geometry and Strings, Birkhauser, Basel* (1989).
- [79] K. GAWĘDZKI. “Topological actions in two-dimensional quantum field theories”. In: *Non-perturbative quantum field theory*. Springer, 1988, pp. 101–141. ISBN: 978-1-4612-8053-8. DOI: [10.1007/978-1-4613-0729-7_5](https://doi.org/10.1007/978-1-4613-0729-7_5).
- [80] K. GAWĘDZKI and A. KUPIAINEN. “Coset construction from functional integrals”. In: *Nucl. Phys. B* 320.3 (1989), pp. 625–668. DOI: [10.1016/0550-3213\(89\)90015-1](https://doi.org/10.1016/0550-3213(89)90015-1).
- [81] K. GAWĘDZKI and N. REIS. “Basic gerbe over non-simply connected compact groups”. In: *J. Geom. Phys.* 50.1 (2004), pp. 28–55. DOI: [10.1016/j.geomphys.2003.11.004](https://doi.org/10.1016/j.geomphys.2003.11.004).
- [82] K. GAWĘDZKI and N. REIS. “WZW branes and gerbes”. In: *Rev. Math. Phys.* 14.12 (2002), pp. 1281–1334. DOI: [10.1142/S0129055X02001557](https://doi.org/10.1142/S0129055X02001557).
- [83] K. GAWĘDZKI, R.R. SUSZEK, and K. WALDORF. “Global gauge anomalies in two-dimensional bosonic sigma models”. In: *Comm. Math. Phys.* 302.2 (2011), pp. 513–580. DOI: [10.1007/s00220-010-1162-0](https://doi.org/10.1007/s00220-010-1162-0).
- [84] K. GAWĘDZKI, R.R. SUSZEK, and K. WALDORF. “The gauging of two dimensional bosonic sigma models on world-sheets with defects”. In: *Rev. Math. Phys.* 25.06 (2013), p. 1350010. DOI: [10.1142/S0129055X13500104](https://doi.org/10.1142/S0129055X13500104).
- [85] K. GAWĘDZKI and C. TAUBER. “Nonequilibrium transport through quantum-wire junctions and boundary defects for free massless bosonic fields”. In: *Nucl. Phys. B* 896 (2015), pp. 138–199. DOI: [10.1016/j.nuclphysb.2015.04.014](https://doi.org/10.1016/j.nuclphysb.2015.04.014).
- [86] K. GAWĘDZKI, I. TODOROV, and P. TRAN-NGOC-BICH. “Canonical quantization of the boundary Wess-Zumino-Witten model”. In: *Comm. Math. Phys.* 248 (2004), pp. 217–254. DOI: [10.1007/s00220-004-1107-6](https://doi.org/10.1007/s00220-004-1107-6).

- [87] T. GIAMARCHI. *Quantum physics in one dimension*. Oxford University Press, 2004. ISBN: 9780198525004. DOI: [10.1093/acprof:oso/9780198525004.001.0001](https://doi.org/10.1093/acprof:oso/9780198525004.001.0001).
- [88] P. GODDARD, A. KENT, and D. OLIVE. “Unitary representations of the Virasoro and super-Virasoro algebras”. In: *Comm. Math. Phys.* 103.1 (1986), pp. 105–119. DOI: [10.1007/BF01464283](https://doi.org/10.1007/BF01464283).
- [89] P. GODDARD, A. KENT, and D. OLIVE. “Virasoro algebras and coset space models”. In: *Phys. Lett. B* 152.1 (1985), pp. 88–92. DOI: [10.1016/0370-2693\(85\)91145-1](https://doi.org/10.1016/0370-2693(85)91145-1).
- [90] G.M. GRAF and M. PORTA. “Bulk-edge correspondence for two dimensional topological insulators”. In: *Comm. Math. Phys.* 324.3 (2013), pp. 851–895. DOI: [10.1007/s00220-013-1819-6](https://doi.org/10.1007/s00220-013-1819-6).
- [91] M.B. GREEN, J.H. SCHWARZ, and E. WITTEN. *Superstring theory*. Cambridge University Press, 1987. ISBN: 9781107029118. DOI: [10.1017/CB09781139248563](https://doi.org/10.1017/CB09781139248563).
- [92] F.D.M. HALDANE. “Model for a quantum Hall effect without Landau levels: Condensed-matter realization of the "parity anomaly"”. In: *Phys. Rev. Lett.* 61.18 (1988), p. 2015. DOI: [10.1103/PhysRevLett.61.2015](https://doi.org/10.1103/PhysRevLett.61.2015).
- [93] T.H. HANSSON et al. “Composite-fermion wave functions as correlators in conformal field theory”. In: *Phys. Rev. B* 76.7 (2007), p. 075347. DOI: [10.1103/PhysRevB.76.075347](https://doi.org/10.1103/PhysRevB.76.075347).
- [94] M.Z. HASAN and C.L. KANE. “Colloquium: topological insulators”. In: *Reviews of Modern Physics* 82.4 (2010), p. 3045. DOI: [10.1103/RevModPhys.82.3045](https://doi.org/10.1103/RevModPhys.82.3045).
- [95] Y. HATSUGAI. “Chern number and edge states in the integer quantum Hall effect”. In: *Phys. Rev. Lett.* 71.22 (1993), p. 3697. DOI: [10.1103/PhysRevLett.71.3697](https://doi.org/10.1103/PhysRevLett.71.3697).
- [96] K. HORI. “Global aspects of gauged Wess-Zumino-Witten models”. In: *Comm. Math. Phys.* 182 (1996), pp. 1–32. DOI: [10.1007/BF02506384](https://doi.org/10.1007/BF02506384).
- [97] J.-I. INOUE and A. TANAKA. “Photoinduced Transition between Conventional and Topological Insulators in Two-Dimensional Electronic Systems”. In: *Phys. Rev. Lett.* 105 (1 2010), p. 017401. DOI: [10.1103/PhysRevLett.105.017401](https://doi.org/10.1103/PhysRevLett.105.017401).
- [98] E. ISING. “Beitrag zur theorie des ferromagnetismus”. German. In: *Zeitschrift für Physik A Hadrons and Nuclei* 31.1 (1925), pp. 253–258. DOI: [10.1007/BF02980577](https://doi.org/10.1007/BF02980577).
- [99] V.G. KAC. “Contravariant form for infinite-dimensional Lie algebras and superalgebras”. In: *Group Theoretical Methods in Physics*. Springer, 1979, pp. 441–445. DOI: [10.1007/3-540-09238-2_102](https://doi.org/10.1007/3-540-09238-2_102).
- [100] V.G. KAC. *Infinite-dimensional Lie algebras*. Vol. 44. Cambridge University Press, 1994. ISBN: 9780521466936. DOI: [10.1017/CB09780511626234](https://doi.org/10.1017/CB09780511626234).
- [101] V.G. KAC. *Vertex algebras for beginners*. American Mathematical Society, 1998. ISBN: 978-0-8218-1396-6. URL: <http://books.google.fr/books?id=e-jxBwAAQBAJ>.
- [102] C.L. KANE and E.J. MELE. “ Z_2 topological order and the quantum spin Hall effect”. In: *Phys. Rev. Lett.* 95.14 (2005), p. 146802. DOI: [10.1103/PhysRevLett.95.146802](https://doi.org/10.1103/PhysRevLett.95.146802).
- [103] D. KARABALI et al. “A GKO construction based on a path integral formulation of gauged Wess-Zumino-Witten actions”. In: *Phys. Lett. B* 216 (1989), pp. 307–312. DOI: [10.1016/0370-2693\(89\)91120-9](https://doi.org/10.1016/0370-2693(89)91120-9).
- [104] O.D. KELLOGG. *Foundations of potential theory*. Verlag Julius Springer, 1929.
- [105] A. KIRILLOV and E. HEWITT. *Elements of the Theory of Representations*. Vol. 145. Springer, 1976. ISBN: 978-3-642-66245-4. DOI: [10.1007/978-3-642-66243-0](https://doi.org/10.1007/978-3-642-66243-0).
- [106] A. KITAEV. “Periodic table for topological insulators and superconductors”. In: *AIP Conf. Proc.* 1134 (2009), pp. 22–30. DOI: [10.1063/1.3149495](https://doi.org/10.1063/1.3149495).

- [107] T. KITAGAWA et al. “Transport properties of nonequilibrium systems under the application of light: Photoinduced quantum Hall insulators without Landau levels”. In: *Phys. Rev. B* 84 (23 2011), p. 235108. DOI: [10.1103/PhysRevB.84.235108](https://doi.org/10.1103/PhysRevB.84.235108).
- [108] I. KLICH. “Full Counting Statistics: An elementary derivation of Levitov’s formula”. In: *Quantum noise in mesoscopic physics*. Yu. V. Nazarov, Springer, 2003, pp. 397–402. DOI: [10.1007/978-94-010-0089-5](https://doi.org/10.1007/978-94-010-0089-5).
- [109] K. v. KLITZING, G. DORDA, and M. PEPPER. “New Method for High-Accuracy Determination of the Fine-Structure Constant Based on Quantized Hall Resistance”. In: *Phys. Rev. Lett.* 45 (6 1980), pp. 494–497. DOI: [10.1103/PhysRevLett.45.494](https://doi.org/10.1103/PhysRevLett.45.494).
- [110] V. KNIZHNIK and A.B. ZAMOLODCHIKOV. “Current algebra and Wess-Zumino model in two dimensions”. In: *Nucl. Phys. B* 247 (1984), pp. 83–103. DOI: [10.1016/0550-3213\(84\)90374-2](https://doi.org/10.1016/0550-3213(84)90374-2).
- [111] M. KÖNIG et al. “Quantum spin Hall insulator state in HgTe quantum wells”. In: *Science* 318.5851 (2007), pp. 766–770. DOI: [10.1126/science.1148047](https://doi.org/10.1126/science.1148047).
- [112] B. KOSTANT. “Quantization and unitary representations”. In: *Lectures in Modern Analysis and Applications III*. Ed. by C.T. TAAM. Vol. 170. Lecture Notes in Mathematics. Springer Berlin Heidelberg, 1970, pp. 87–208. ISBN: 978-3-540-05284-5. DOI: [10.1007/BFb0079068](https://doi.org/10.1007/BFb0079068).
- [113] R. LANDAUER. “Conductance determined by transmission: probes and quantised constriction resistance”. In: *Journal of Physics: Condensed Matter* 1.43 (1989), p. 8099. DOI: [10.1088/0953-8984/1/43/011](https://doi.org/10.1088/0953-8984/1/43/011).
- [114] R. LANDAUER. “Electrical resistance of disordered one-dimensional lattices”. In: *Philosophical Magazine* 21.172 (1970), pp. 863–867. DOI: [10.1080/14786437008238472](https://doi.org/10.1080/14786437008238472).
- [115] R. LANDAUER. “Spatial Variation of Currents and Fields Due to Localized Scatterers in Metallic Conduction”. In: *IBM Journal of Research and Development* 1 (3 1957), pp. 223–231. DOI: [10.1147/rd.13.0223](https://doi.org/10.1147/rd.13.0223).
- [116] S. LANG. *Introduction to algebraic and abelian functions*. Springer, 1972. ISBN: 9781461257424. DOI: [10.1007/978-1-4612-5740-0](https://doi.org/10.1007/978-1-4612-5740-0).
- [117] R.B. LAUGHLIN. “Quantized Hall conductivity in two dimensions”. In: *Phys. Rev. B* 23.10 (1981), p. 5632. DOI: [10.1103/PhysRevB.23.5632](https://doi.org/10.1103/PhysRevB.23.5632).
- [118] J. LEPOWSKY and S. MILNE. “Lie algebras and classical partition identities”. In: *Proceedings of the National Academy of Sciences* 75.2 (1978), pp. 578–579. DOI: [10.1016/0001-8708\(78\)90004-X](https://doi.org/10.1016/0001-8708(78)90004-X).
- [119] L.S. LEVITOV, H. LEE, and G.B. LESOVIK. “Electron counting statistics and coherent states of electric current”. In: *J. Math. Phys.* 37 (1996), pp. 4845–4866. DOI: [10.1063/1.531672](https://doi.org/10.1063/1.531672).
- [120] L.S. LEVITOV and G.B. LESOVIK. “Charge distribution in quantum shot noise”. In: *JETP Letters* 58 (3 1993), pp. 230–235. URL: http://www.jetpletters.ac.ru/ps/1186/article_17907.pdf.
- [121] N.H. LINDNER, G. REFAEL, and V. GALITSKI. “Floquet topological insulator in semiconductor quantum wells”. In: *Nature Physics* 7 (2011), pp. 490–495. DOI: [10.1038/nphys1926](https://doi.org/10.1038/nphys1926).
- [122] M. LORENTE and B. GRUBER. “Classification of semisimple subalgebras of simple Lie algebras”. In: *J. Math. Phys.* 13.10 (1972), pp. 1639–1663. DOI: [10.1063/1.1665888](https://doi.org/10.1063/1.1665888).
- [123] J.M. MALDACENA. “TASI 2003 lectures on AdS / CFT”. In: *Progress in string theory. Proceedings, Summer School, TASI 2003, Boulder*. 2003, pp. 155–203. arXiv: [hep-th/0309246](https://arxiv.org/abs/hep-th/0309246).

- [124] L.M. MILNE-THOMSON. *Theoretical Aerodynamics*. Dover Books on Aeronautical Engineering Series. Dover Publications, 1966. ISBN: 9780486619804.
- [125] A. MINCHENKO. “The semisimple subalgebras of exceptional Lie algebras”. In: *Transactions of the Moscow Mathematical Society* 67 (2006), pp. 225–259. DOI: [10.1090/S0077-1554-06-00156-7](https://doi.org/10.1090/S0077-1554-06-00156-7).
- [126] M. MINTCHEV, S. SANTONI, and P. SORBA. “Non-linear quantum noise effects in scale invariant junctions”. In: *J.Phys. A* 48.28 (2015), p. 285002. DOI: [10.1088/1751-8113/48/28/285002](https://doi.org/10.1088/1751-8113/48/28/285002).
- [127] M. MINTCHEV and P. SORBA. “Luttinger Liquid in Non-equilibrium Steady State”. In: *J. Phys. A* 46 (2013), p. 095006. DOI: [10.1088/1751-8113/46/9/095006](https://doi.org/10.1088/1751-8113/46/9/095006).
- [128] R.V. MOODY. “Lie algebras associated with generalized Cartan matrices”. In: *Bull. Amer. Math. Soc.* 73.2 (1967), pp. 217–221. URL: <http://projecteuclid.org/euclid.bams/1183528782>.
- [129] G. MOORE and N. READ. “Nonabelions in the fractional quantum Hall effect”. In: *Nucl. Phys. B* 360.2 (1991), pp. 362–396. DOI: [10.1016/0550-3213\(91\)90407-0](https://doi.org/10.1016/0550-3213(91)90407-0).
- [130] J.E. MOORE and L. BALENTS. “Topological invariants of time-reversal-invariant band structures”. In: *Phys. Rev. B* 75.12 (2007), p. 121306. DOI: [10.1103/PhysRevB.75.121306](https://doi.org/10.1103/PhysRevB.75.121306).
- [131] M.K. MURRAY. “Bundle gerbes”. In: *Journal of the London Mathematical Society* 54.2 (1996), pp. 403–416. arXiv: [dg-ga/9407015](https://arxiv.org/abs/dg-ga/9407015).
- [132] M. NAKAHARA. *Geometry, Topology and Physics, Second Edition*. Graduate student series in physics. Taylor & Francis, 2003. ISBN: 9780750306065. URL: <http://books.google.fr/books?id=cH-XQB0Ex5wC>.
- [133] T. OKA and H. AOKI. “Photovoltaic Hall effect in graphene”. In: *Phys. Rev. B* 79.8 (2009), p. 081406. DOI: [10.1103/PhysRevB.79.169901](https://doi.org/10.1103/PhysRevB.79.169901).
- [134] L. ONSAGER. “Crystal Statistics. I. A Two-Dimensional Model with an Order-Disorder Transition”. In: *Phys. Rev.* 65 (3-4 1944), pp. 117–149. DOI: [10.1103/PhysRev.65.117](https://doi.org/10.1103/PhysRev.65.117).
- [135] M. OSHIKAWA, C. CHAMON, and I. AFFLECK. “Junctions of three quantum wires”. In: *J. Stat. Mech.* 2006.02 (2006), P02008. DOI: [10.1088/1742-5468/2006/02/P02008](https://doi.org/10.1088/1742-5468/2006/02/P02008).
- [136] G. PANATI. “Triviality of Bloch and Bloch-Dirac bundles”. In: *Annales Henri Poincaré*. Vol. 8. 5. Springer, 2007, pp. 995–1011. DOI: [10.1007/s00023-007-0326-8](https://doi.org/10.1007/s00023-007-0326-8).
- [137] P.A. PEARCE, J. RASMUSSEN, and J.-B. ZUBER. “Logarithmic minimal models”. In: *J. Stat. Mech.* 0611 (2006), P11017. DOI: [10.1088/1742-5468/2006/11/P11017](https://doi.org/10.1088/1742-5468/2006/11/P11017).
- [138] J. POLCHINSKI. “Dirichlet Branes and Ramond-Ramond Charges”. In: *Phys. Rev. Lett.* 75 (1995), pp. 4724–4727. DOI: [10.1103/PhysRevLett.75.4724](https://doi.org/10.1103/PhysRevLett.75.4724).
- [139] J. POLCHINSKI. *String Theory*. Cambridge Monographs in Mathematical Physics. Cambridge University Press, 1998. ISBN: 9780521672276. DOI: [10.1017/CB09780511816079](https://doi.org/10.1017/CB09780511816079).
- [140] A.M. POLYAKOV. “Conformal symmetry of critical fluctuations”. In: *JETP Lett.* 12 (1970), pp. 381–383. URL: http://www.jetpletters.ac.ru/ps/1737/article_26381.pdf.
- [141] A.M. POLYAKOV. “Nonhamiltonian approach to conformal quantum field theory”. In: *Zh. Eksp. Teor. Fiz* 66.1 (1974), pp. 23–42. URL: http://www.jetp.ac.ru/cgi-bin/dn/e_039_01_0010.pdf.
- [142] A.M. POLYAKOV. “Quantum geometry of bosonic strings”. In: *Phys. Lett. B* 103.3 (1981), pp. 207–210. DOI: [10.1016/0370-2693\(81\)90743-7](https://doi.org/10.1016/0370-2693(81)90743-7).
- [143] A.M. POLYAKOV. “Quantum geometry of fermionic strings”. In: *Phys. Lett. B* 103.3 (1981), pp. 211–213. DOI: [10.1016/0370-2693\(81\)90744-9](https://doi.org/10.1016/0370-2693(81)90744-9).

- [144] A.M. POLYAKOV and P.B. WIEGMANN. “Goldstone fields in two dimensions with multi-valued actions”. In: *Phys. Lett. B* 141 (1984), pp. 223–228. DOI: [10.1016/0370-2693\(84\)90206-5](https://doi.org/10.1016/0370-2693(84)90206-5).
- [145] T. QUELLA and V. SCHOMERUS. “Symmetry breaking boundary states and defect lines”. In: *Journal of High Energy Physics* 2002.06 (2002), p. 028. DOI: [10.1088/1126-6708/2002/06/028](https://doi.org/10.1088/1126-6708/2002/06/028).
- [146] A. RAHMANI et al. “General method for calculating the universal conductance of strongly correlated junctions of multiple quantum wires”. In: *Phys. Rev. B* 85 (4 2012), p. 045120. DOI: [10.1103/PhysRevB.85.045120](https://doi.org/10.1103/PhysRevB.85.045120).
- [147] A. RAHMANI et al. “How to Find Conductance Tensors of Quantum Multiwire Junctions through Static Calculations: Application to an Interacting Y Junction”. In: *Phys. Rev. Lett.* 105 (22 2010), p. 226803. DOI: [10.1103/PhysRevLett.105.226803](https://doi.org/10.1103/PhysRevLett.105.226803).
- [148] A. RECKNAGEL. “On permutation branes”. In: *Fortschritte der Physik* 51 (2003), pp. 824–829. DOI: [10.1002/prop.200310103](https://doi.org/10.1002/prop.200310103).
- [149] M. RØRDAM, F. LARSEN, and N. LAUSTSEN. *An Introduction to K-Theory for C*-Algebras*. Cambridge University Press, 2000. ISBN: 9780511623806. DOI: [10.1017/CB09780511623806](https://doi.org/10.1017/CB09780511623806).
- [150] R. ROY. “ \mathbb{Z}_2 classification of quantum spin Hall systems: An approach using time-reversal invariance”. In: *Phys. Rev. B* 79.19 (2009), p. 195321. DOI: [10.1103/PhysRevB.79.195321](https://doi.org/10.1103/PhysRevB.79.195321).
- [151] M.S. RUDNER et al. “Anomalous edge states and the bulk-edge correspondence for periodically driven two-dimensional systems”. In: *Phys. Rev. X* 3.3 (2013), p. 031005. DOI: [10.1103/PhysRevX.3.031005](https://doi.org/10.1103/PhysRevX.3.031005).
- [152] D. RUELE. “Natural nonequilibrium states in quantum statistical mechanics”. In: *J. Stat. Phys.* 98.1-2 (2000), pp. 57–75. DOI: [10.1023/A:1018618704438](https://doi.org/10.1023/A:1018618704438).
- [153] S. RYU et al. “Topological insulators and superconductors: tenfold way and dimensional hierarchy”. In: *New J. Phys.* 12.6 (2010), p. 065010. DOI: [10.1088/1367-2630/12/6/065010](https://doi.org/10.1088/1367-2630/12/6/065010).
- [154] S. RYU et al. “ \mathbb{Z}_2 Topological Term, the Global Anomaly, and the Two-Dimensional Symplectic Symmetry Class of Anderson Localization”. In: *Phys. Rev. Lett.* 99 (11 2007), p. 116601. DOI: [10.1103/PhysRevLett.99.116601](https://doi.org/10.1103/PhysRevLett.99.116601).
- [155] J.J. SAKURAI and J. NAPOLITANO. *Modern Quantum Mechanics*. Addison-Wesley, 2011. ISBN: 9780805382914. URL: <https://books.google.fr/books?id=N4I-AQAACAAJ>.
- [156] S. EL-SHOWK et al. “Solving the 3D Ising Model with the Conformal Bootstrap”. In: *Phys. Rev. D* 86 (2012), p. 025022. DOI: [10.1103/PhysRevD.86.025022](https://doi.org/10.1103/PhysRevD.86.025022).
- [157] D.J. SIMMS and N.M.J. WOODHOUSE. *Lectures on geometric quantization*. Lecture notes in physics. Springer-Verlag, 1976. ISBN: 978-3-540-07860-9. DOI: [10.1007/3-540-07860-6](https://doi.org/10.1007/3-540-07860-6).
- [158] B. SIMON. “Holonomy, the quantum adiabatic theorem, and Berry’s phase”. In: *Phys. Rev. Lett.* 51.24 (1983), p. 2167. DOI: [10.1103/PhysRevLett.51.2167](https://doi.org/10.1103/PhysRevLett.51.2167).
- [159] C.C. SIMS. *Computation with Finitely Presented Groups*. Encyclopedia of Mathematics and its Applications. Cambridge University Press, 1994. ISBN: 9780521432139. DOI: [10.1017/CB09780511574702](https://doi.org/10.1017/CB09780511574702).
- [160] A. STERN. “Non-Abelian states of matter”. In: *Nature* 464.7286 (2010), pp. 187–193. DOI: [10.1038/nature08915](https://doi.org/10.1038/nature08915).
- [161] M. STONE. *Quantum Hall Effect*. World Scientific, 1992. ISBN: 9789810208844. URL: <http://books.google.fr/books?id=kZDwKcH4E04C>.

- [162] G.C. THIANG. “On the K-Theoretic Classification of Topological Phases of Matter”. In: *Annales Henri Poincaré* online first (2015). DOI: [10.1007/s00023-015-0418-9](https://doi.org/10.1007/s00023-015-0418-9).
- [163] D.J. THOULESS et al. “Quantized Hall conductance in a two-dimensional periodic potential”. In: *Phys. Rev. Lett.* 49.6 (1982), p. 405. DOI: [10.1103/PhysRevLett.49.405](https://doi.org/10.1103/PhysRevLett.49.405).
- [164] J. VOIT. “One-dimensional Fermi liquids”. In: *Reports on Progress in Physics* 58.9 (1995), p. 977. DOI: [10.1088/0034-4885/58/9/002](https://doi.org/10.1088/0034-4885/58/9/002).
- [165] A. WEIL. *Introduction à l’étude des variétés kählériennes*. French. Actualités scientifiques et industrielles. Hermann, 1971.
- [166] X.G. WEN. “Chiral Luttinger liquid and the edge excitations in the fractional quantum Hall states”. In: *Phys. Rev. B* 41 (18 1990), pp. 12838–12844. DOI: [10.1103/PhysRevB.41.12838](https://doi.org/10.1103/PhysRevB.41.12838).
- [167] J. WESS and B. ZUMINO. “Consequences of anomalous ward identities”. In: *Phys. Lett. B* 37.1 (1971), pp. 95–97. DOI: [10.1016/0370-2693\(71\)90582-X](https://doi.org/10.1016/0370-2693(71)90582-X).
- [168] H. WEYL. “Gravitation und elektrizität”. German. In: *Sitzungsberichte der Königlich Preußischen Akademie der Wissenschaften (Berlin)* 1 (1918), pp. 465–478.
- [169] E.T. WHITTAKER and G.N. WATSON. *A course of modern analysis*. Cambridge University Press, 1996. ISBN: 9780521588072. DOI: [10.1017/CB09780511608759](https://doi.org/10.1017/CB09780511608759).
- [170] R.L. WILLETT et al. “Magnetic-field-tuned Aharonov-Bohm oscillations and evidence for non-abelian anyons at $\nu = 5/2$ ”. In: *Phys. Rev. Lett.* 111.18 (2013), p. 186401. DOI: [10.1103/PhysRevLett.111.186401](https://doi.org/10.1103/PhysRevLett.111.186401).
- [171] K.G. WILSON. “Non-Lagrangian Models of Current Algebra”. In: *Phys. Rev.* 179 (5 1969), pp. 1499–1512. DOI: [10.1103/PhysRev.179.1499](https://doi.org/10.1103/PhysRev.179.1499).
- [172] E. WITTEN. “An SU (2) anomaly”. In: *Phys. Lett. B* 117.5 (1982), pp. 324–328. DOI: [10.1016/0370-2693\(82\)90728-6](https://doi.org/10.1016/0370-2693(82)90728-6).
- [173] E. WITTEN. “Nonabelian bosonization in two dimensions”. In: *Comm. Math. Phys.* 92 (1984), pp. 455–472. DOI: [10.1007/BF01215276](https://doi.org/10.1007/BF01215276).
- [174] E. WITTEN. “On holomorphic factorization of WZW and coset models”. In: *Comm. Math. Phys.* 144 (1992), pp. 189–212. DOI: [10.1007/BF02099196](https://doi.org/10.1007/BF02099196).
- [175] E. WITTEN. “Quantum field theory and the Jones polynomial”. In: *Comm. Math. Phys.* 121 (1989), pp. 351–399. DOI: [10.1007/BF01217730](https://doi.org/10.1007/BF01217730).
- [176] A.B. ZAMOŁODCHIKOV. “Integrable field theory from conformal field theory”. In: *Adv. Stud. Pure Math.* 19 (1989), pp. 641–674.
- [177] J.-B. ZUBER. “L’invariance conforme et la physique à deux dimensions”. French. In: *La Recherche* (1993), pp. 142–151. URL: <http://www.lpthe.jussieu.fr/~zuber/MesPapiers/LaRecherche92.pdf>.